universität wien

DISSERTATION

Titel der Dissertation

Functions of plectin and its isoforms assessed in mouse stratified epithelia and keratinocyte cell cultures

angestrebter akademischer Grad

Doktor der Naturwissenschaften (Dr. rer.nat.)

Verfasserin / Verfasser:	Mag. Gernot Walko
Matrikel-Nummer:	9607581
Dissertationsgebiet (lt. Studienblatt):	Molekulare Biologie
Betreuerin / Betreuer:	Univ.-Prof. Dr. Gerhard Wiche

Wien, am 10.12.2007

In der Wissenschaft gleichen wir alle nur den Kindern, die am Rande des Wissens hie und da einen Kiesel aufheben, während sich der weite Ozean des Unbekannten vor unseren Augen erstreckt.

Isaac Newton (1643-1727), engl. Physiker,
Mathematiker u. Astronom

DANKSAGUNG

Auf fast 200 Seiten – prallvoll mit Wissen und Wissenschaft – sollte man die Einflüsse vieler kluger Leute erwarten, und so ist es auch. Im Einzelnen danke ich:

Prof. Dr. Gerhard Wiche für ein spannendes Dissertationsgebiet, viele interessante Diskussionen und viel Freiheit beim Forschen.

Dr. Kerstin Andrä-Marobela für das Lehren von Allem was für die Wissenschaft von Bedeutung ist, inklusive dem Durchsetzen des eigenen Sturkopfes.

Prof. Dr. Roland Foisner und Prof. Dr. Milos Pekny für das Lesen und Beurteilen einer sehr dicken Dissertation.

Prof. Dr. Fritz Propst und Dr. Christina Abrahamsberg für ihr Mentoring, inklusive Schulterklopfen, Aufmuntern und vieler langer Gespräche bei vielen Tassen Kaffee.

Prof. Dr. Fritz Pittner für so manch aufmunterndes Wort.

Prof. Dr. Matthias Schmuth für das weltumspannende Verschicken kostbarer Messgeräte und das Beisteuern guter Ideen.

Prof. Dr. Thomas Marlovits und Dr. Philip Zeller für die Benützung einer wunderbaren Maschine zum Auseinanderdehnen von Zellen.

Prof. Dr. Milos Pekny für aufmunternde Worte wann und wo wir uns auch immer begegnet sind.

Dr. Peter Fuchs für das Lehren vom richtigen Umgang mit kleinen (bissigen) Nagetieren.

Irmgard Fischer für die Herstellung unzähliger großartiger Mikroskoppräparate.

Elisabeth Jursa für prompte Hilfestellungen in Zellkulturfragen.

Dr. Lubomir Janda and Mag. Julius Kostan für ihr Fachwissen rund ums Exprimieren und Aufreinigen von Proteinen.

Dr. Reinhard Ackerl, Dr. Selma Osmanagic-Myers, Dr. Martin Gregor und Dr. Gerald Burgstaller für das Teilen von Freud und Leid beim Publizieren.

Dr. Reinhard Ackerl, Dr. Selma Osmanagic-Myers, Mag. Nevena Vukasinovic, Dr. Günter Rezniczek, Dr. Siegfried Reipert und Dr. Anikó Zeold für eine wahnsinning tolle Zeit im Labor 2.

Gerlinde Aschauer für das Verkörpern des „Guten Geistes“ unseres Institutes und für ihr großes Verständnis studentischer Probleme.

Meinen Freunden Wolfi, Steffi, Christine, Sandra, Thomas und Alex für ihre wunderbare Freundschaft.

Meinen drei Familien im Süden und Westen dieses Landes für alles wofür man Familie hat und braucht.

Meinen Eltern für ihre bedingungslose Unterstützung des armen Studenten, viel Verständnis und für das frühe Erwecken von wissenschaftlichem Interesse.

Im großen Kreislauf der Natur ist Ende gleich Anfang. Dieser schönen Logik zufolge beginnt eine Danksagung eigentlich erst so richtig mit dem Ende.

So, wie auch alle meine Tage beginnen und enden mit dem Schönsten, das man sich wünschen kann, nämlich der großen Liebe. Dir, mein Schatz, danke ich einfach für Alles!

TABLE OF CONTENTS

TABLE OF FIGURES

ABBREVIATIONS

ABD	actin-binding domain
AJ	adherens junction
Amp	ampicillin
AP	alkaline phosphatase
BCIP	5-bromo-4-chloro-3-indolylphosphate
BSA	bovine serum albumin
CBB	Coomassie brilliant blue
cDNA	complementary DNA
CH, CH1, CH2	calponin homology (domain 1, 2)
DB	DNA-binding domain
DMF	dimethyl-formamide
DNA	deoxy ribonucleic acid
DTT	dithiothreitole
EB-PA	epidermolysis bullosa-pyloric atresia
EBS-MD	epidermolysis bullosa simplex-muscular dystrophy
EDTA	ethylene-diamine tetra-acetic acid
EGTA	ethylene glycole-bis(β-aminoethyl ether)-N,N,N',N'-tetra-acetic acid
ER	estrogen receptor
Erk	Extracellular-signal Regulated Kinase
ES cells	embryonic stem cells
HMW	high molecular weight
IFs	intermediate filament
IFBD	intermediate filament binding site
i.p.	intraperitoneal
IPTG	isopropyl-β,D-thiogalactopyranoside
K	keratin
Kan	kanamycine
KGM	keratinocyte growth medium
LB	Luria broth
MBP	maltose-binding protein
MAP	microtubule associated protein
MAPK	Map kinase
MFs	microfilaments
MTs	microtubules
OD	optical density
OHT	4-hydroxy-tamoxifen

PBS	phosphate-buffered saline
PEG	polyethylene glycol
PKC	protein kinase C
PMSF	phenyl-methyl-sulfonyl-fluorid
RACK1	Receptor of activated C-kinase 1
RT	room temperature
SAC	stable anchoring contact
SDS	sodium dodecyl sulfate
SDS-PAGE	SDS-polyacrylamide gel electrophoresis
SH3	Src homology 3
Src	v-src sarcoma (Schmidt-Ruppin A-2) viral oncogene
TAE	Tris/acetic acid/EDTA
TB	terrific broth
TE	Tris/EDTA
Tris	Tris-(hydroxymethyl)aminomethane
UTR	untranslated region
X-Gal	5-bromo-4-chloro-3-indolyl-β,D-galactopyranoside
YPD	yeast extract/peptone/dextrose

SUMMARY

Plectin is a major intermediate filament (IF)–based cytolinker protein that stabilizes cells and tissues mechanically, regulates actin filament dynamics, and serves as a scaffolding platform for signaling molecules. The importance of plectin for tissue integrity was demonstrated in plectin knockout mice which die early after birth, exhibiting severe skin blistering defects and abnormalities in skeletal and heart muscle, similar to the disorders found in patients suffering from epidermolysis bullosa simplex with muscular dystrophy (EBS-MD), which is caused by various mutations in the plectin gene. In the 5´-prime region of the plectin gene complex splicing takes place, giving rise to several alternatively spliced transcripts containing different first exons. It has been proposed that plectin fulfils a variety of distinct functions presumably mediated by different isoforms.

In the first part of this thesis, I present the phenotypic characterization of a mouse line with a specific deletion of plectin in stratified epithelia. Conditional targeting of plectin enabled me to study the consequences of plectin deficiency in this particular type of tissues in the context of the whole organism without plectin loss affecting other tissues. Conditional knockout mice died early after birth, showing signs of starvation and growth retardation. Blistering was observed on their extremities and on the oral epithelium after initial nursing, impairing food uptake. Knockout epidermis was very fragile and showed focal epidermal barrier defects caused by the presence of small skin lesions. Stratification, proliferation and differentiation of knockout skin seemed unaffected by epidermis-restricted plectin deficiency. In an additionally generated mouse model, tamoxifen-induced Cre-ER^{T}-mediated recombination led to mice with a mosaic plectin deletion pattern in adult epidermis, combined with microblister formation. This study explains the early lethality of plectin-deficient mice and provides a model to ablate plectin in adult animals which could be used for developing gene or pharmacological therapies.

In the second part of my thesis it is shown that plectin deficiency in cultured keratinocytes is a cause of aberrant keratin cytoskeleton organization caused by a lack of orthogonal IF cross-linking. Keratin association of the hemidesmosomal integrin $\alpha6\beta4$ is lost in plectin-deficient keratinocytes, and the integrin relocates to lamellipodia. Basal activities of the MAP kinase Erk1/2 and of membrane-associated upstream protein kinases PKCδ and Src-

family kinases were significantly elevated in plectin-deficient keratinocytes, and increased migration rates, as assessed by in vitro wound-closure assays and time-lapse microscopy, were observed. These data establish a link between cytolinker-controlled cytoarchitecture/scaffolding functions of keratin IFs and specific MAP kinase cascades mediating distinct cellular responses.

In the third part, the interaction of plectin isoform 1c with microtubules is addressed on functional and mechanistic levels. Plectin 1c is localized at the cortical submembrane cytoskeleton of polarized neuronal cells and keratinocytes, and in addition, distributes along microtubules. Microtubule binding depends on plectin 1c-specific N-terminal sequences, since plectin 1a, the major isoform found in keratinocytes, did associate with microtubules neither in vivo nor in vitro. It is demonstrated that a putative SH3 domain residing within plectin`s plakin domain is able to mediate binding to members of the MAP2/tau family of microtubule-associated proteins in vitro. Because of the importance of plectin for maintaining epithelial tissue integrity, the role of plectin-microtubule interaction during Ca^{2+}-induced differentiation of cultured keratinocytes was investigated. Interestingly, I found that the absence of plectin led to abnormally dense packing and increased stability of microtubules. Based on these results, I propose a model where plectin 1c is targeted to microtubules via different N-terminal sequences and regulates MT dynamics by modulating MT-binding of microtubule associated proteins of the MAP2/tau family.

Studies described in the final part give insight into the molecular mechanism causing the reduced migration potential of plectin-deficient fibroblasts. I found that the PKC regulatory protein RACK1 (receptor for activated C kinase 1) was strongly accumulated at lamellipodial edges of migrating plectin-deficient fibroblasts. Concomitantly, elevated enzymatic activity of PKCδ was observed in these cells. These data show that plectin-deficiency has similar consequences on RACK1/PKCδ signaling in keratinocytes and fibroblasts, but hyperactivation of RACK1/PKCδ appears to affect cell migration in a cell type specific manner.

ZUSAMMENFASSUNG

Plectin, ein Mitglied der Plakin-Proteinfamilie, ist ein großes und überaus vielseitiges Protein, das an der Bildung von zytoskelettären Strukturen und deren Verankerung an Zellmembranen entscheidend beteiligt ist. Es fungiert als Regulator der Aktin-Dynamik und spielt eine wesentliche Rolle in Epithelial-, Muskel- und Nervengeweben, was durch ausgeprägte Hautablösung auf hemidesmosomaler Ebene und pathologische Muskelveränderungen in Mäusen mit inaktiviertem Plectingen verdeutlicht wird. Ein ähnliches Erscheinungsbild tritt in Patienten auf, die an durch Defekte im Plectingen verursachter bullöser Epidermolysis mit muskulärer Dystrophie (EBS-MD) leiden. Plectin wird in Form einer Vielzahl von unterschiedlichen Isoformen exprimiert, die wahrscheinlich unterschiedliche Aufgaben erfüllen.

Im ersten Teil meiner Dissertation präsentiere ich die phänotypische Charakterisierung einer Mauslinie mit einer spezifischen Deletion von Plectin in mehrschichtigen Epithelgeweben. Konditionelle Deletion von Plectin erlaubte es mir, die Konsequenzen von Plectin-Defizienz in diesem speziellen Gewebstyp im Kontext des gesamten Organismus zu studieren. Die konditionellen knockout Mäuse starben früh nach ihrer Geburt, mit Anzeichen von Entkräftung und Wachstumsverzögerung. Blasenbildung konnte an ihren Extremitäten sowie auch am Schleimhautepithel der Mundhöhle nach initialem Säugen beobachtet werden. Die Ablösung des oralen Schleimhautepithels führte zu einer Beeinträchtigung der Nahrungsaufnahme. Die Epidermis der knockout Tiere war äußerst fragil und zeigte lokale Defekte in der Funktion der epidermalen Barriere. Diese Studie gibt eine Erklärung für die frühe Sterblichkeit von plectin-defizienten Mäusen und beinhaltet erste Daten über die induzierbare Deletion von Plectin in mehrschichtigen Epithelien von adulten Mäusen.

Im zweiten Teil zeige ich, dass Plectin-Defizienz zu einer anomalen Organisation des Keratinfilamentzytoskeletts, verursacht durch fehlende orthogonale Quervernetzung von Keratinintermediärfilamenten, in kultivierten Keratinozyten führt. Das hemidesmosomale Integrin $\alpha 6\beta 4$ Heterodimer war in Plectin-defizienten Keratinozyten nicht mit Keratinfilamenten assoziiert, sondern in Lamellipodien umgelagert. Die basale Aktivität der MAP Kinasen Erk1/2, der membranassoziierten upstream Proteinkinase PKCδ, sowie von

Kinasen der Src-Familien Kinasen waren in Plectin-defizienten Keratinozyten signifikant erhöht. Des Weiteren beobachtete ich erhöhte Migrationsraten von Plectin-defizienten Keratinozyten mittels in vitro Wundheilungsassays und time-lapse Videomikroskopie. Diese Daten offenbaren eine Verbindung zwischen Zytolinker-kontrollierter Zytoarchitektur und der Gerüstfunktion von Keratin-Intermediärfilamenten mit spezifischen MAP Signalkaskaden.

Im dritten Teil meiner Dissertation charakterisiere ich die Interaktion der Plectin Isoform 1c mit Mikrotubuli auf funktioneller und mechanistischer Ebene. Plectin 1c war am kortikalen submembranen Zytoskelett von polarisierten neuronalen Zellen und Keratinozyten, sowie auch an Mikrotubuli lokalisiert. Die Bindung an Mikrotubuli hing von Plectin 1c-spezifischen N-terminalen Sequenzen ab. Die Hauptisoform in Keratinozyten, Plectin 1a, welche keine Plectin 1c-spezifischen Sequenzen enthielt, interagierte weder in vivo noch in vitro mit Mikrotubuli. Weiters zeigte ich, dass eine mutmaßliche SH3 Domäne, welche sich innerhalb von Plectins Plakin-Domäne befindet, in vitro an Mitglieder der MAP2/tau Familie von mikrotubuliassoziierten Proteinen binden konnte. Aufgrund der Wichtigkeit von Plectin für die Aufrechterhaltung der Integrität von epithelialen Geweben wurde die Rolle von Plectin während der kalziuminduzierten Differenzierung von Keratinozyten analysiert. Interessanterweise fand ich, dass das Fehlen von Plectin zu einer abnormalen dichten Bündelung sowie einer Zunahme der Stabilität von Mikrotubuli führte. Basierend auf diesen Ergebnissen schlage ich ein Modell vor, in welchem Plectin 1c mittels unterschiedlicher N-terminaler Sequenzen an Mikrotubuli lokalisiert und deren Dynamik durch Modulation der Mikrotubuli-Bindung von mikrotubuliassoziierten Proteinen der MAP2/tau Familie beeinflusst.

Im vierten Teil analysiere ich den Mechanismus des reduzierten Migrationspotentials von Plectin-defizienten Fibroblasten. Ich fand, dass das PKC-regulatorische Protein RACK1 stark am Lamellipodiensaum von Plectin-defizienten Fibroblasten lokalisiert war. Damit einhergehend beobachtete ich erhöhte Enzymaktivität von PKCδ in diesen Zellen. Diese Daten zeigen, dass Plectin-Defizienz ähnliche Auswirkungen auf die PKCδ/RACK1 Signaltransduktion in Keratinozyten und in Fibroblasten hat. Gleichzeitig scheint aber die Hyperaktivierung von PKCδ/RACK1 die Zellmigration in einer, dem Zelltyp entsprechenden Art und Weise, zu beeinflussen.

INTRODUCTION

The cytoskeleton

Eukaryotic cells depend on a dense filamentous network system, the cytoskeleton, which is important for the organization of their nucleus and cytoplasm. The cytoskeleton is composed of three major filament classes: actin (micro) filaments, microtubules, and intermediate filaments (IFs), which are briefly discussed below:

Actin (micro) filaments

The ability of eukaryotic cells to maintain or change their shape and their degree of attachment in response to extracellular stimuli is for the most part dependent on rearrangements of the actin cytoskeleton (Van Aelst and D'Souza-Schorey, 1997). The actin cytoskeleton plays an important role in many diverse intracellular processes, including endocytosis, vesicle trafficking, cytokinesis, and cell migration (Goley and Welch, 2006). Many of these processes are essential for the survival of the cell. Actin is a highly conserved ATPase that can spontaneously self-assemble into filamentous (F)-actin (Goley and Welch, 2006) (Fig. 1). Actin filaments consist of an ~8 nm wide tight helix of globular actin monomers (G-actin) (Alberts et al., 2002). They are polar structures possessing a fast growing plus end (also referred to as the barbed end) and a slow growing minus end (also called the pointed end) that can be distinguished by their structural characteristics and kinetic properties (Goley and Welch, 2006; Ono, 2007; Pollard and Borisy, 2003). ATP hydrolysis in the actin filament is tightly coupled to polymerization and regulates the kinetics of assembly and disassembly, as well as the association of interacting proteins (Goley and Welch, 2006). A multitude of actin-binding proteins control the dynamic assembly and disassembly of actin filaments (Goley and Welch, 2006; Ono, 2007; Pollard and Borisy, 2003). These proteins bind directly to actin filaments or monomers and control actin structure and dynamics by nucleating, capping, stabilizing, severing, depolymerizing, crosslinking, bundling, sequestering, or delivering monomers, or by promoting monomer nucleotide exchange (Goley and Welch, 2006). The coordinated actions of specific subsets of actin-binding proteins

regulate the dynamics of distinct arrays of actin filaments at specific times and places within the cell (Goley and Welch, 2006; Pollard and Borisy, 2003). In the cellular cortex, actin molecules polymerize and depolymerize continually and are organized into three general types of arrays (Alberts et al., 2002). In contractile bundles such as are found in stress fibers and in the contractile ring during mitosis, the filaments are arranged with opposite polarities and contain the motorprotein myosin II (Alberts et al., 2002). In the gel-like networks of the cell cortex, actin filaments are loosely arranged. The best-characterized protrusive structure is the lamellipodium, which is built of a dense two-dimensional network of branched or crosslinked actin filaments (Faix and Rottner, 2006; Revenu et al., 2004; Small, 1994). Continuous lamellipodium protrusion and ruffling is frequently accompanied by the formation of filopodia (Faix and Rottner, 2006; Small et al., 2002; Wood and Martin, 2002), in which actin filaments exist as crosslinked parallel bundles orientated with the same polarity. Filopodia are particularly prominent in individual cells such as fibroblasts or axonal growth cones (Faix and Rottner, 2006).

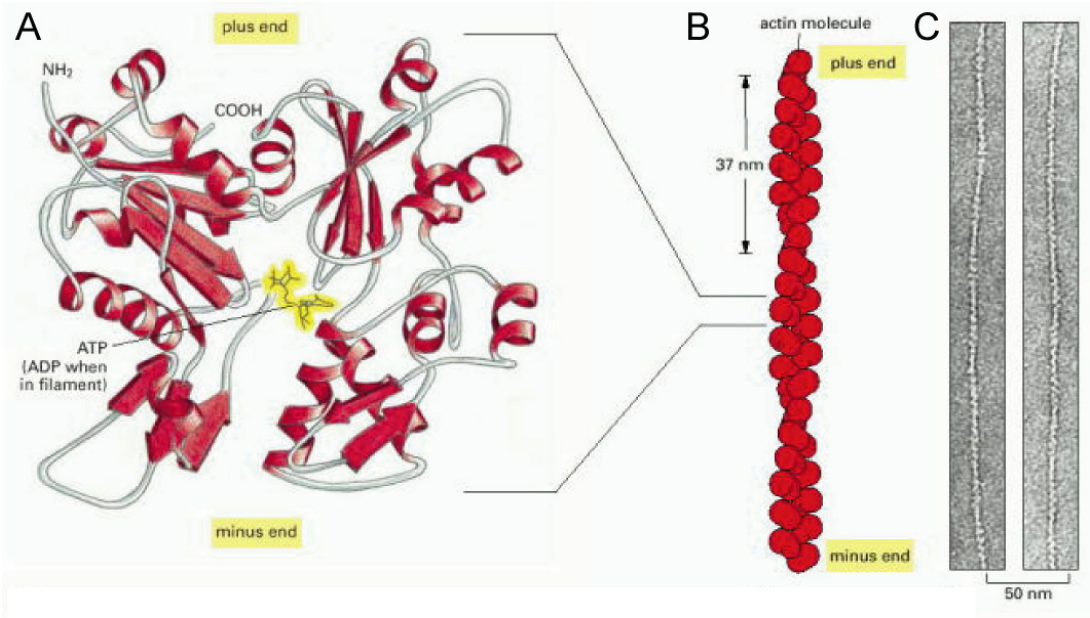

Figure 1. The structures of an actin monomer and actin filament. (A) The actin monomer has a nucleotide (either ATP or ADP) bound in a deep cleft in the center of the molecule. The nucleotide is shown in *yellow*. (B) Arrangement of monomers in an actin filament. Although the filament is often described as a single helix of monomers, it can also be thought of as consisting of two protofilaments, held together by lateral contacts, which wind around each other as two parallel strands of a helix, with a twist repeating every 37 nm. All the subunits within the filament have the same orientation. (C) Electron micrographs of negatively stained actin filaments. (Adapted from (Alberts et al., 2002)).

Microtubules

Microtubules (MTs) are dynamic biological polymers. They are involved in cell morphogenesis, organization and movement of organelles in the cytoplasm, chromosome segregation, and polarized cell migration (Alberts et al., 2002). MTs are assembled from heterodimers of α–β tubulin, which endows them with intrinsic polarity (Morrison, 2007) (Fig. 2). MTs assembled from purified tubulin in vitro grow faster at one end than the other; this is the end terminated by β-tubulin and it is referred to as the MT plus end (Desai and Mitchison, 1997; Morrison, 2007). The slower growing end which is terminated by α-tubulin is called the minus end (Morrison, 2007).

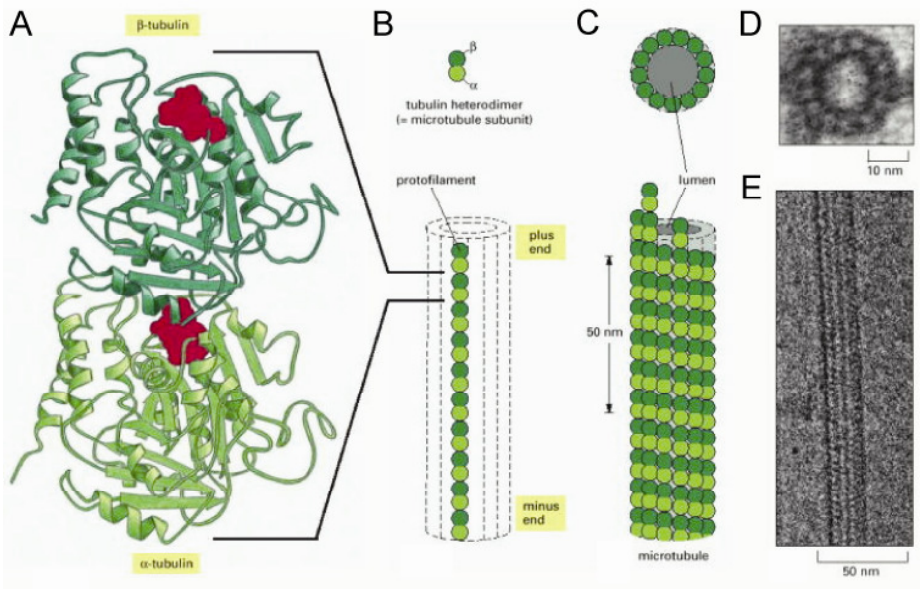

Figure 2. The structure of a microtubule and its subunit. (A) The subunit of each protofilament is a tubulin heterodimer, formed from a tightly linked pair of α- and β-tubulin monomers. The GTP molecule in the α-tubulin monomer is tightly bound so that it is an integral part of the protein, whereas the GTP molecule in the β-tubulin monomer, is less tightly bound and has an important role in filament dynamics. Both nucleotides are shown in *red*. (B) One tubulin subunit (α-β heterodimer) and one protofilament are shown schematically. Each protofilament consists of many adjacent subunits with the same orientation. (C) The microtubule is a stiff hollow tube formed from 13 protofilaments aligned in parallel. (D) Electron micrograph of a cross section of a microtubule showing a ring of 13 distinct protofilaments. (E) A short segment of a microtubule viewed in an electron microscope. (Modified from (Alberts et al., 2002)).

In MT-organizing centers, such as centrosomes, the minus ends of the MTs are anchored and stabilized, while the plus ends are free to add tubulin molecules (Alberts et al., 2002). Individual MT plus ends can alternate between periods of slow growth and rapid disassembly, a phenomenon called dynamic instability, for which GTP hydrolysis is responsible (Desai and Mitchison, 1997). Dynamic instability is an intrinsic feature of MTs and can also be observed in purified tubulin preparations in vitro (Morrison, 2007). Rapid and direct transition from growth to shrinkage is called catastrophe, and direct transition from shrinkage to growth is called rescue (Desai and Mitchison, 1997). The binding of specific microtubule associated proteins (MAPs) regulates MT dynamics and mediates interaction of MTs with other cell compartments (Amos and Schlieper, 2005).

Intermediate filaments

Structure of intermediate filament proteins

IF type	Protein name	Number of genes	Tissue distribution
I	Keratins (acidic)	>25	K9-K20, soft epithelia
			Ha1-Ha8, hard epithelia
			Irs1-4, inner root sheath
II	Keratins (basic)	>24	K1-K8, soft epithelia
			Hb1-Hb6, hard epithelia
			K6irs1-4, inner root sheath
III	Vimentin	1	Mesenchymal
	Desmin	1	Muscle
	GFAP	1	Astrocytes/Glia
	Peripherin	1	PNS neurons
	Syncoillin	1	Muscle
IV	NF-L	1	CNS neurons
	NF-M	1	CNS neurons
	NF-H	1	CNS neurons
	Nestin	1	Heterogeneous
	Synemin	1	Muscle
	Desmuslin	1	Muscle
V	Lamin A/C	1	Differentiated tissues (nucleus)
	Lamin B1	1	Ubiquitous (nucleus)
	Lamin B2	1	Ubiquitous (nucleus)

Table 1. The intermediate filament family (according to Kim and Coulombe, 2007)**.**

Intermediate filament (IF) proteins have been grouped into five types on the basis of amino acid identity (Fuchs and Weber, 1994; Herrmann et al., 2007). The acidic and basic keratins are grouped into type 1 and 2, respectively. Vimentin, desmin, GFAP, peripherin and syncoilin are designated as type 3, the neurofilament proteins, nestin, synemin, and desmuslin as type 4, and the nuclear lamins as type 5 (Coulombe and Wong, 2004; Herrmann et al., 2007). Alternatively, IF proteins can be subdivided into three independent groups in accordance with their mode of assembly, namely the keratins, vimentin-like proteins, and lamins (Herrmann et al., 2007). In spite of the large diversity among IF proteins, they all share a similar structural building plan, with an ~45-nm-long central α-helical "rod" domain that is flanked by non-α-helical N- and C-terminal end domains (Herrmann et al., 2007) (Fig. 4).

Cellular organization of IFs

Whereas both MTs and MFs are restricted to the cytoplasm, most metazoan cells contain two principally different IF systems. One resides inside the nucleus and is attached to the inner nuclear membrane, the nuclear pores and chromatin, and the other is cytoplasmic, which connects intercellular junctional complexes located at the plasma membrane with the outer nuclear membrane (Herrmann et al., 2007). Cytoplasmic IFs are integrated with many other key elements of the cell`s interior (Herrmann et al., 2007). They interact with MTs, MFs, and various types of junctional adhesive complexes spanning the outer cell membrane, inluding desmosomal (cell-cell) and hemidesmosomal (cell-matrix) attachments (Fuchs and Cleveland, 1998; Herrmann et al., 2007; Jefferson et al., 2004; Svitkina et al., 1996) (Fig. 3). The interactions of MFs and MTs with IFs and that of IFs with attachment sites at plasma and nuclear membranes is mediated by a specialized group of proteins termed "plakins" (see below). IFs also interact with organelles, including the Golgi apparatus, mitochondria, endosomes and lysosomes (Kim and Coulombe, 2007; Toivola et al., 2005). In vivo, the cytoplasmic IF network architecture varies according to cell type and tissue context (Kim and Coulombe, 2007). In the stratified keratinocytes of the epidermis, keratin IFs form a dense, cytoplasmic network that is anchored at desmosomes and hemidesmosomes (HDs), whereas in simple epithelia, IFs are sparser and often concentrated near the apical pole of the cell (Coulombe and Omary, 2002; Kim and Coulombe, 2007). In fibroblasts, IFs extend through

much of the cytoplasm, and are often found in close juxtaposition to microtubules (Ball and Singer, 1981; Kim and Coulombe, 2007).

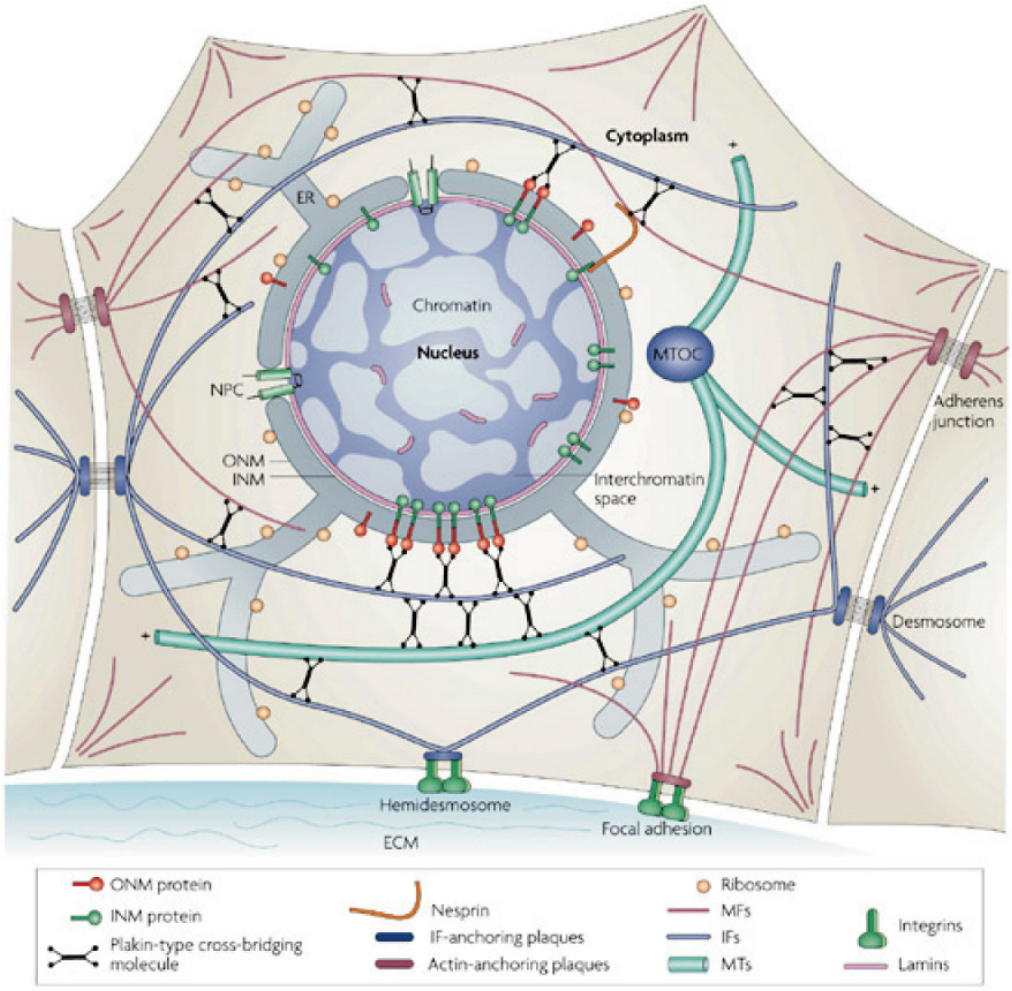

Figure 3. Cellular organization of IFs. The three cytoskeletal filament systems, actin (micro) filaments (MFs), microtubules (MTs) and intermediate filaments (IFs), are connected to each other by dimeric (or multimeric) complexes of plakin-family proteins such as plectin and BPAG1. In addition, various MT-associated proteins and actin-binding proteins are thought to increase the complexity of these interactions. IFs are attached to IF-anchoring plaques of cell–cell junctions (desmosomes) by desmoplakin, and to those of cell–matrix junctions (hemidesmosomes) by plectin and BPAG1. Desmosomal cadherins and integrins mediate the contact with the neighbouring cells and with the extracellular matrix (ECM), respectively. IFs are furthermore coupled to the outer nuclear membrane (ONM) by plectin and nesprin-3, whereas nesprin-2 anchors the MF system to the nucleus. On the inner side of the nuclear envelope, a layer of nuclear IF proteins (lamins) is attached to pores and inner nuclear membrane (INM) proteins as well as to chromatin. The membrane proteins of the INM are

linked to those of the ONM and thereby provide a mechanical continuum reaching from the ECM to chromatin. ER, endoplasmic reticulum; MTOC, microtubule-organizing centre; NPC, nuclear pore complex. (Modified from (Herrmann et al., 2007)).

Filament assembly and dynamics

IF assembly starts with the association of two individual polypeptide chains in parallel and in register, forming a coiled-coil (Herrmann et al., 2007). These coiled-coil dimers are the basic building block of IF assembly (Herrmann et al., 2007). Subsequently, at low ionic strength and physiological pH values, cytoplasmic IF proteins form anti-parallel, half-staggered tetramers (Hermann et al., 2007) (Fig. 4). Ultimately, these tetramers align in a helical array along the filament axis (Hermann et al., 2007) (Fig. 4). As a consequence of the anti-parallel association of the polar dimers, IFs exhibit no polarity, in contrast to both MTs and MFs (Herrmann et al., 2007) (Fig. 4). Moreover, IFs do not depend on nucleotide hydrolysis for filament assembly (Herrmann et al., 2007). However, in vivo, IF remodeling and structural performance of IFs is functionally dependent on the combined action of kinases, phosphatases and chaperones (Green et al., 2005; Herrmann et al., 2007; Izawa and Inagaki, 2006). Once IF proteins have been synthesized, they are very stable and exhibit long half-lives, although they can be turned over rapidly by the proteasome in a phosphorylation- and ubiquitination-dependent manner (Kim and Coulombe, 2007; Ku and Omary, 2000). In various types of epithelial cells in culture, keratin IF precursors form in the peripheral cytoplasm, proximal to the subcortical F-actin network and in close proximity to focal adhesion contacts (Gu and Coulombe, 2007; Windoffer et al., 2006; Windoffer and Leube, 1999; Windoffer and Leube, 2004; Windoffer et al., 2004). Keratin precursors first appear as small dots, elongate into rodlets, and are then integrated into the existing IFs (Gu and Coulombe, 2007; Windoffer et al., 2004). The entire process occurs in the context of a continuous centripetal flow, and is partially dependent on F-actin and on phosporylation (Gu and Coulombe, 2007; Windoffer et al., 2004). As has been shown at least in the case of early-stage mouse embryos, type 2 keratins are translated ahead of their type 1 assembly partners and are temporarily stored unpolymerized in small aggregates (Lu et al., 2005). On the contrary, the type 3 IF proteins vimentin and peripherin are co-translationally assembled (Chang et al., 2006; Isaacs et al., 1989), move in a saltatoric and bidirectional fashion (Ho et al., 1998; Yoon et al., 1998), and their organization is markedly sensitive to MT disruption (Helfand et al., 2004).

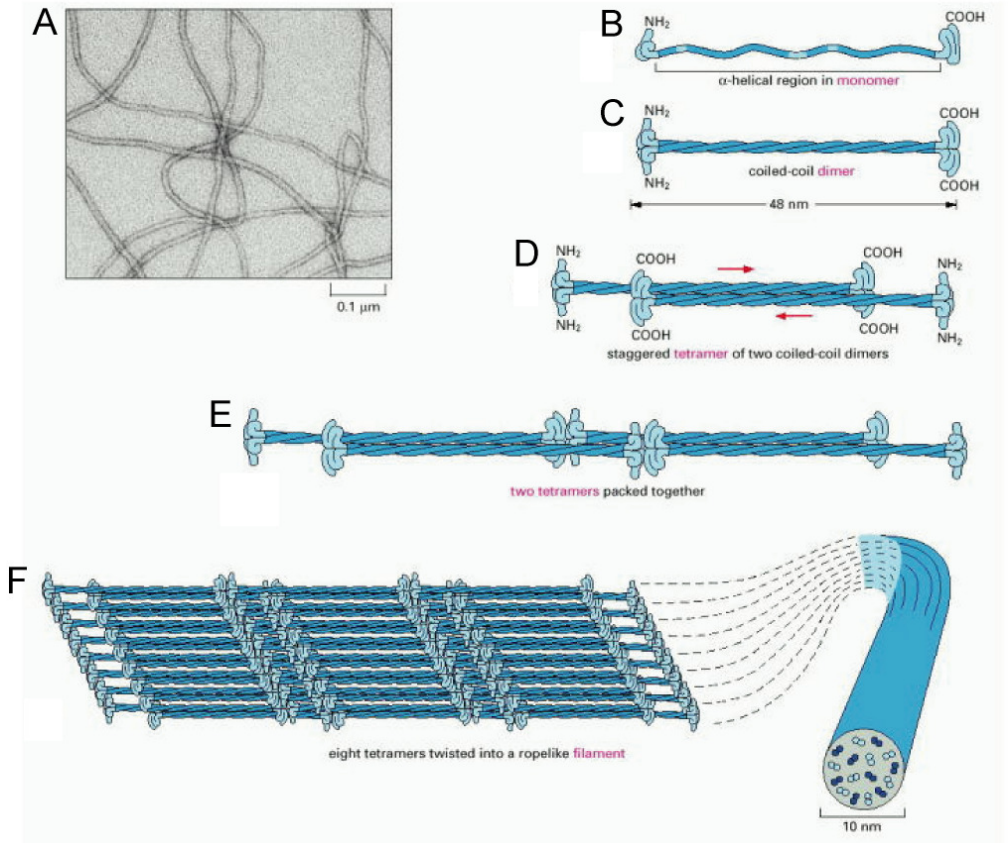

Figure 4. A model of intermediate filament assembly. (A) Electron micrograph of in vitro assembled IFs. The monomer shown in (B) pairs with an identical monomer to form a dimer (C), in which the central rod domains are aligned in parallel and in register to form a coiled coil. (D) Two dimers then line up side by side to form an antiparallel tetramer of four polypeptide chains. The tetramer is the soluble subunit of intermediate filaments. (E) Within each tetramer, the two dimers are offset with respect to one another, thereby allowing it to associate with another tetramer. (F) In the final 10-nm rope-like filament, IF tetramers are packed together in a helical array, which has 16 dimers in cross-section. Half of these dimers are pointing in each direction. (Modified from (Alberts et al., 2002)).

IFs and disease

It is known today that over 40 genetically determined diseases are caused by a mutation in an IF-encoding gene (Fuchs and Cleveland, 1998; Irvine and McLean, 1999; Kim and Coulombe, 2007; Omary et al., 2004). The best understood and most studied of these disorders is epidermolysis bullosa simplex (EBS), which is caused by (mostly dominant) mutations in keratin 5 (K5) or keratin 14 (K14) (Pekny and Lane, 2007). In this severe skin disease the basal keratinocyte cell layer of the epidermis is highly vulnerable to rupture when

the skin is exposed to physical trauma, leading to intra epidermal fluid accumulation and blister formation (Bonifas et al., 1991; Coulombe et al., 1991; Herrmann et al., 2007; Lane et al., 1992; Pekny and Lane, 2007). Mutations in lamin A cause a complex set of at least 13 human diseases (Capell and Collins, 2006) including muscular dystrophies (Bonne et al., 1999) and premature ageing. Mutations in desmin cause muscular dystrophies and cardiomyopathy (Goldfarb et al., 2004) and mutations in GFAP generate a devastating neuronal disease termed Alexander disease, a fatal disorder of the central nervous system that is characterized by severe disturbances of brain and skull development (Herrmann et al., 2007; Li et al., 2002a). Disruption of the function of plakin proteins often results in phenotypes that overlap with genetic deficiencies in IF proteins, as is the case with EBS-caused by plectin mutations (Andrä et al., 1997; McLean et al., 1996).

Mechanical stress and keratin IFs

Mutations in keratin genes have pathological consequences in numerous epithelial tissues (Pekny and Lane, 2007). The consequences for tissue integrity caused by these mutations are similar. The epithelial cells fracture specifically within the tissue compartment expressing the mutant keratin as a major structural protein (Pekny and Lane, 2007; Uitto et al., 2007). In these cells, keratin filament bundles often appear compacted and are abnormally distributed in the cell, and in case of the most severe mutations, keratin aggregates are formed (Pekny and Lane, 2007). The strength and stiffness of keratin IF suspensions in vitro is notedly weakened by disease-causing mutations (Gu and Coulombe, 2007). In vivo, mice null for K5 or K14, or transgenic mice expressing mutant K14 at substoichiometric levels, display a severe epithelial blistering phenotype (Coulombe et al., 1991; Lloyd et al., 1995; Peters et al., 2001). In vitro, mechanically stretching keratinocytes that were isolated from patients with severe mutations in K14 caused a substantial disruption of the keratin network in comparison to wild-type cells (Russell et al., 2004).

Optimizing structural support during wound repair and cell migration

The organization of cytoplasmic IFs changes rapidly and considerably when cells begin to migrate after acute injury in several tissues, ranging from skin to the central nervous system (Lariviere and Julien, 2004; Omary et al., 2002; Pekny and Lane, 2007). Concomitant

changes in the regulation of IF proteins and/or transcription of IF genes occur in cells located proximal to the wound margin (Coulombe and Wong, 2004; Wong and Coulombe, 2003). After skin injury, wound-proximal keratinocytes become larger and polarized and reorganize their keratin network (Coulombe and Wong, 2004; Odland and Ross, 1968; Paladini et al., 1996). These cytoskeletal changes occur concomitant with upregulation of K6, K16 and K17 (Mansbridge and Knapp, 1987; Paladini et al., 1996; Wong et al., 2000). Accumulation of K6/16 IFs is believed to provide the mechanical resilience needed by the wound edge keratinocytes (Wong and Coulombe, 2003). However, K6/16 upregulation seems to happen at the cost of partially reducing the migratory potential of keratinocytes (Wong and Coulombe, 2003). In contrast, K17 acts by regulating protein synthesis and cell size via Akt and mTOR signaling (Kim et al., 2006). During activation of astrocytes in stress and pathology (generally referred to as "reactive gliosis"), upregulation of GFAP and vimentin IFs contributes to the ability of reactive astrocytes to counteract the stress of neurotrauma (Pekny and Lane, 2007). Direct influence of IFs on the cellular viscoelastic properties was demonstrated by studies with pancreatic tumor cells, which upon stimulation with spingosylphosphorylcoline, reorganize their keratin IF network from a cytoplasmic- to a pronuclear-enriched localization, leading to "softening" of the cytoplasm and enhanced cell migration (Beil et al., 2003). A similar mechanism was found in extravagating lymphocytes, which retract and condense their vimentin IF network into a dense perinuclear aggregate (Brown et al., 2001).

The plakin protein family of cytoskeletal linker proteins

Plakins constitute a group of exceptionally large multi-domain proteins that have evolved to link cytoskeletal elements together and to connect them to junctional complexes (Leung et al., 2001). Owing to their capacity to link two or more cytoskeletal networks these proteins are also called cytolinkers or cytoskeletal linkers (Wiche, 1998).

Seven plakin family members have been identified to date (Leung et al., 2002): desmoplakin, bullous pemphigoid antigen 1 (BPAG1), plectin, envoplakin, periplakin, epiplakin and ACF7, also referred to as microtubule actin crosslinking factor 1 (MACF1). Plakin family members are built from combinations of specific modules (Fig. 5): a calponin-type actin-binding domain (ABD); a plakin domain harboring several spectrin repeats interrupted by a SH3 domain; a heptad-repeat-containing coiled-coil rod domain (CC-rod); a plakin-repeat domain (PRD) generally thought to have intermediate filament (IF)-binding

properties, a function that in some cases requires an associated linker (L) region; a spectrin repeat-containing rod domain (SR-rod); two EF-hand calcium-binding motifs; a Gas2-homology region called the GAR domain; and a domain containing GSR (Gly-Ser-Arg) repeats (Leung et al., 2002; Sonnenberg and Liem, 2007). The PRD comprises varying numbers of repeating unit subdomains (each of 176 residues), which are termed A, B or C, depending on their degree of sequence similarity to each other (Leung et al., 2002).

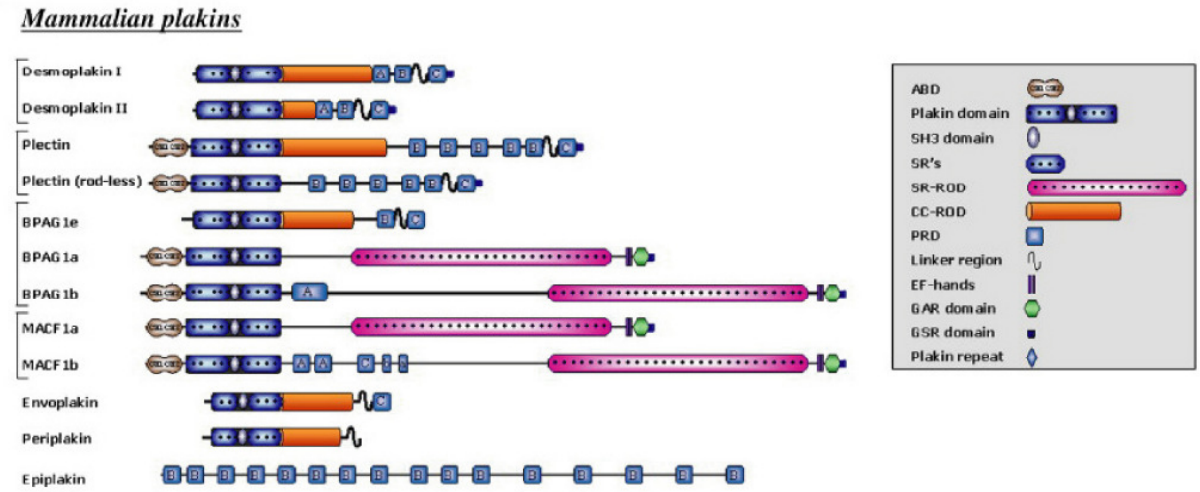

Figure 5. Schematic diagram of the plakin family members and their splice variants. Functional domains that can be found in plakin proteins, comprise calponin-type actin-binding (ABD), plakin, and SH3 domains, spectrin repeats (SRs), spectrin-repeat-containing rod (SR-rod), and coiled-coil rod (CC-rod) domains, plakin-repeat domains (PRD), and IF-binding domain-associated linker region (L), EF-hand calcium-binding motifs, Gas2-related (GAR) and glycine–serine–arginine (GSR) domains. Isoforms that are created by alternative splicing of the ABD exons are not shown; note that in some cases, the resulting 'ABD' does not bind to actin. The PRD comprising plakin repeats and linker (L) subdomains is important for the binding of plakins to intermediate filaments. The GAR domain and the GSR domain together constitute the microtubule-binding domain of BPAG1-a, BPAG1-b and MACF1. Epiplakin is an atypical plakin because the protein entirely comprises 16 highly homologous B repeats and lacks other domains (Spazierer et al., 2003) (Modified from (Sonnenberg and Liem, 2007)).

The L subdomain, which is important for IF binding, usually resides between the B and C repeats of the plakin repeat domain (Leung et al., 2002). As has been shown for some plakins, the GAR domain and GSR-containing domain can associate directly with microtubules (MTs) and thus defines a novel MT-binding domain (MTBD) (Leung et al.,

2002; Sonnenberg and Liem, 2007). Most plakins are expressed in tissues that must withstand mechanical stress, such as epithelia and skeletal -and heart muscle. There they play a crucial role in maintaining tissue integrity by crosslinking the different cytoskeletal filaments and anchoring them to membrane complexes (Leung et al., 2002). Hence, both autoimmune and genetic diseases that affect plakins can lead to disorders involving tissue fragility and skin blistering (Gallicano et al., 2001; Leung et al., 2002; Pfendner et al., 2005; Pulkkinen and Uitto, 1999). Plakins are also important in the development and survival of neurons. In flies and mice, mutations in genes encoding plakins can cause defects in axonal outgrowth and sensory motor neuronal degeneration (Guo et al., 1995; Lee et al., 2000; Leung et al., 2002). In addition to their cytoskeletal crosslinking function, certain members of the plakin family act as scaffold proteins that recruit signaling proteins to sites of cytoskeletal activity (Chen et al., 2006; Gregor et al., 2006; Lunter and Wiche, 2002; Osmanagic-Myers and Wiche, 2004).

Plectin - the optimally designed cytoskeletal linker protein

Structure and function of plectin

Plectin was first identified as a major component of IF preparations obtained from rat glioma C6 cells (Pytela and Wiche, 1980) and was subsequently found to be abundantly expressed in a wide variety of mammalian tissues and cells types. In fact, plectin was found to be expressed in almost every mammalian cell type examined (Wiche, 1989), with the exception of certain neurons (Errante et al., 1994). Plectin is prominently expressed along the basal cell surface membranes of stratified epithelia, at Z-lines of striated muscle, dense plaques of smooth muscle, and intercalated discs of cardiac muscle (Wiche, 1998; Wiche et al., 1984). Furthermore, plectin is expressed in cells of tissue layers located at the interface between tissues and fluid-filled cavities, such as the surfaces of kidney glomeruli, liver bile canaliculi, gut villi, bladder urothelium, ependymal layers lining the cavities of brain and spinal cord, and vascular endothelial cells (Errante et al., 1994; Wiche et al., 1983; Yaoita et al., 1996). Depending on the cell type examined, plectin is expressed throughout the cytoplasm colocalizing with IFs, MTs, and actin stress fibers, and accumulates at focal adhesion contacts (Seifert et al., 1992), and at membrane attachment sites of IFs or in peripheral regions at cellular junctions (Foisner et al., 1994; Seifert et al., 1992; Svitkina et al., 1996; Wiche et al., 1983; Wiche et al., 1984). Secondary structure predictions based on

cDNA and deduced amino acid sequences (Fuchs et al., 1999; Wiche et al., 1991) as well as electron microscopy of purified plectin molecules (Foisner and Wiche, 1987; Liu et al., 1996) revealed a multidomain structure consistent with the three domain structural model characteristic for most cytoskeletal linker proteins. A 200 nm-long α-helical coiled-coil rod domain is flanked by globular N- and C-terminal domains (Fig. 6), giving the protein a dumbbell-like shape (Foisner and Wiche, 1987; Wiche, 1998).

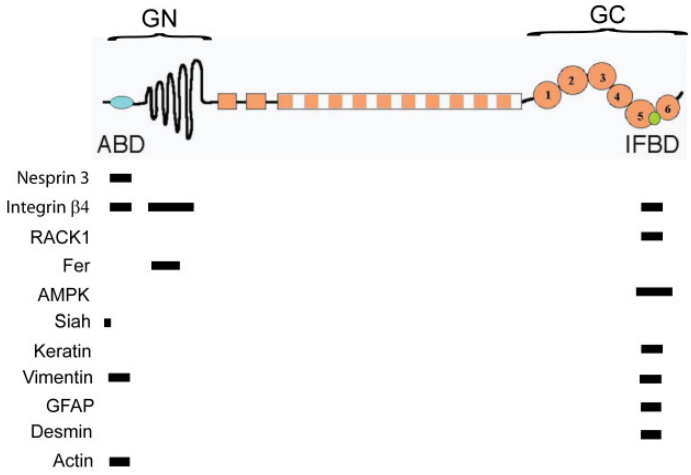

Figure 6. Domain map of plectin. The tripartite structure of plectin molecules comprises a central rod flanked by globular amino-terminal (GN) and carboxy-terminal (GC) domains. The GC domain consists of 6 highly homologous repeat regions. Defined subdomains for binding to actin (ABD) and IFs (IFBD) (vimentin/desmin/GFAP/cytokeratins) are indicated. Defined binding sites for known plectin binding partners are indicated with black bars. (Modified from (Wiche, 1998)).

The N-terminal domain of plectin contains a highly conserved ABD, consisting of a pair of calponin-homology (CH) subdomains (Goldsmith et al., 1997), which are found in many plakin protein family members (Elliott et al., 1997; Fuchs et al., 1999). Overlapping with the ABD is the major binding site for integrin β_4 (Geerts et al., 1999; Rezniczek et al., 1998). Moreover, a binding site for vimentin residing within the CH1 subdomain of the ABD has been recently revealed (Sevcik et al., 2004). Additionally, the ABD serves also as a binding site for the outer nuclear membrane protein Nesprin 3 (Wilhelmsen et al., 2005). A binding site for the nonreceptor tyrosine kinase Fer has been identified in the N-terminal region of plectin downstream of the ABD (Lunter and Wiche, 2002).

The 200 nm-long α-helical coiled-coil rod domain is most likely involved in forming parallel dimers. The long rod domain appears to be ideally suited for plectin to function as a

molecular spacer between different cytoskeletal filament networks and to connect binding partners over relatively long distances (Foisner and Wiche, 1987; Weitzer and Wiche, 1987).

The C-terminal domain consists of six highly homologous repeats and a short tail region. All six repeats contain a core region comprising multiple copies of a tandemly repeated 19 amino acid motif (Wiche et al., 1991). The IF-binding site of plectin has been mapped to a stretch of about 50 amino acid residues between repeats 5 and 6 (Nikolic et al., 1996). Vimentin, cytokeratins, desmin (Nikolic et al., 1996; Reipert et al., 1999), and GFAP (Tian et al., 2006) were found to bind to this site. Other interaction partners at this site are the signaling proteins RACK1 (Osmanagic-Myers and Wiche, 2004) and AMPK (Gregor et al., 2006). Located not far from the IF-binding site is a unique site (threonine 4542) in plectin´s repeat 6, which is phosphorylated by CDK1 during the M-phase of the cell cycle (Foisner et al., 1996; Malecz et al., 1996). Furthermore, a second binding site for integrin β4 has been mapped within this domain (Rezniczek et al., 1998).

Several other interaction partners of plectin have been identified, but so far their binding sites on the plectin molecule are unknown. This diverse group of proteins includes several other types of IF subunit proteins, including neurofilament proteins 210/160/70, as well as microtubule-associated proteins 1 and 2 (MAP1, MAP2), the desmosomal protein desmoplakin, and the membrane skeleton proteins fodrin/α-spectrin (Wiche, 1998). Plectin's manifold molecular interactions and strategic cellular localization clearly confirmed the concept that plectin stabilizes cells mechanically by acting as a versatile linker and scaffolding protein of the cytoskeleton in different cell types (Wiche, 1998). (Fig. 7).

The molecular characterization of the human plectin gene revealed a coding sequence containing >40 exons and spanning over 32 kb of the human genome. The gene was mapped to the telomeric region of the long arm of chromosome 8 (q24) (Liu et al., 1996; McLean et al., 1996). In humans, eight different first coding exons (1, 1a, 1b, 1c) have been identified (Zhang et al., 2004). These first exons show high sequence homology to the first coding exons reported for the rat plectin gene (Elliott et al., 1997). Investigation of the murine plectin gene also revealed a remarkable complexity of the N-terminal region. In total, 16 alternatively spliced exons were identified, 11 (1-1j) of them directly splicing into exon 2, which is the first exon encoding the highly conserved ABD (Fuchs et al., 1999). Three of the exons are non-coding and splice into exon 1c, and two additional exons (2α and 3α) are optionally spliced within the exons 2-8 encoding the ABD (Fuchs et al., 1999).

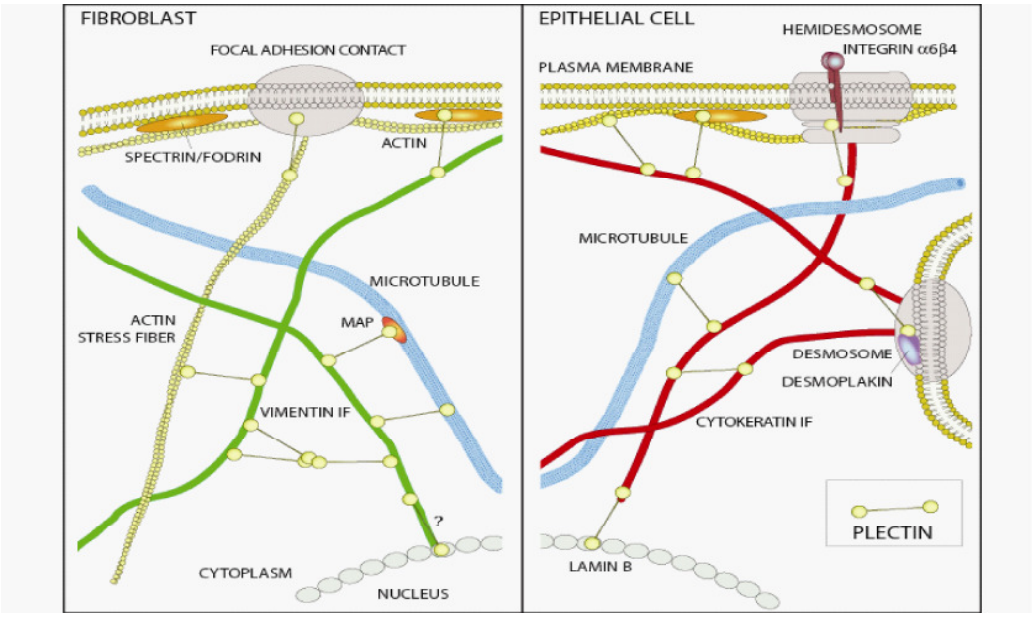

Figure 7. Model outlining plectin's role in cytoarchitecture organization and stabilization in fibroblasts (left panel) and epithelial cells (right panel). Plectin molecules are depicted as linkers between IFs (vimentin, cytokeratins) and various cytoskeletal structures, including other filament networks (MTs, actin stress fibers, peripheral actin filaments), the subplasma membrane protein skeleton (spectrin/fodrin), specialized transmembrane complexes (focal adhesion contacts, hemidesmosomes, desmosomes), and the nuclear lamina. Constituent proteins of plectin associated structures that have been shown to specifically bind to plectin on the molecular level are indicated (modified from (Wiche, 1998)).

In addition, plectin splice variants lacking exon 31 which encodes for the entire rod domain of the molecule, were identified in a variety of tissues, including skin, brain and muscle (Elliott et al., 1997). Importantly, rodless plectin protein was found to be expressed in cultured keratinocytes (Koster et al., 2004).

Plectin and disease

Based on plectin's prominence at plasma membrane-located junctional complexes, in particular HDs of basal keratinocytes, an involvement of plectin in bullous skin diseases has long been anticipated (Wiche, 1998; Wiche et al., 1984). It took over a decade, however, until a connection between defects in plectin expression and human disease was first demonstrated. In 1996, it was reported for the first time that patients suffering from epidermolysis bullosa simplex (EBS)-combined with late onset of muscular dystrophy (MD), an autosomal

recessive skin blistering disease, lack expression of plectin due to a homozygous mutation within the plectin gene (Chavanas et al., 1996; Gache et al., 1996; McLean et al., 1996; Pulkkinen et al., 1996; Smith et al., 1996). By the end of year 2005, 29 different mutations in the plectin gene leading to EBS-MD had been mapped, with 20 of them residing in the exon encoding the rod domain (Pfendner et al., 2005). These mutations are, in general, nonsense mutations or out-of-frame insertions or deletions (Pfendner et al., 2005) (Fig. 8). Thus, they result in premature termination codons, predicting truncated polypeptides and downregulation of the corresponding mRNA through nonsense mediated mRNA decay (Baker and Condon, 2004).

More recently, plectin mutations have been found to be also the reason for another variant of EBS, EBS-PA (pyloric atresia), which manifests with severe neonatal blistering associated with gastric abnormalities, primarily pyloric or duodenal atresia (Pfendner and Uitto, 2005). Extreme skin fragility at birth together with gastric abnormalities frequently leads to early postnatal demise of the affected children. Until now, eight mutations within the plectin gene leading to this new lethal variant of EBS have been mapped (Pfendner et al., 2005) (Fig. 8).

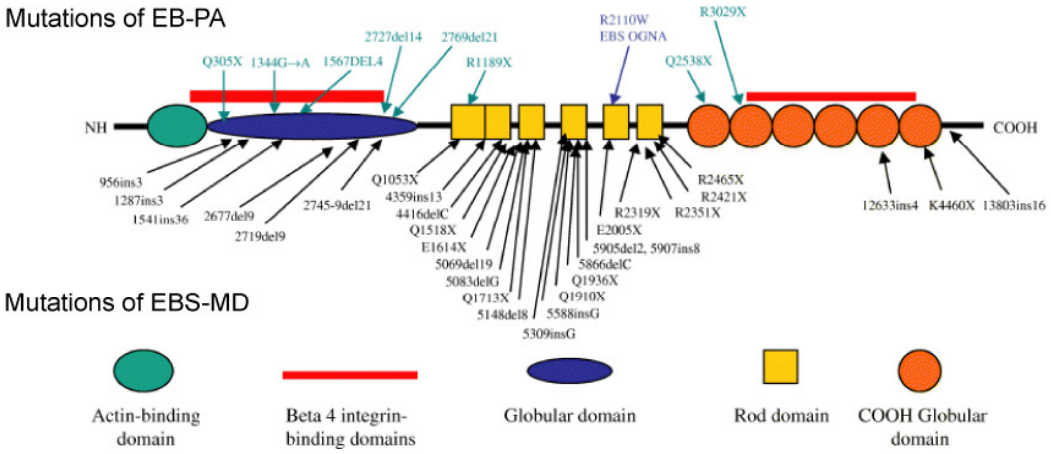

Figure 8. Plectin mutations in EBS-MD and EB-PA. Schematic representation of the modular structure of plectin corresponding to the domains shown at the bottom of the figure. Arrows indicate published mutations as well as unpublished ones identified by the DebRA Molecular Diagnostics Laboratory (Philadelphia, USA). Those identified in families with EBS-MD are shown below the schematic structure of plectin. The positions of mutations in patients with EBS-PA are shown above. Note the specific R2110W mutation associated with EBS of the Ogna type (blue). (Adapted from (Pfendner et al., 2005)).

Plectin mutations in EB-PA were shown to reside outside of exon 31, and will thus not be compensated by rodless plectin (Pfendner et al., 2005). Some EB-PA associated plectin mutations located in the N-terminus of the protein might even lead to complete plectin deficiency (Charlesworth et al., 2003).

Both EBS-MD and EBS-PA caused by plectin mutations are inherited in an autosomal recessive fashion. In addition, an autosomal dominant form, designated as EBS-Ogna, has been shown to result from a mutation in the plectin gene (Koss-Harnes et al., 1997). The EBS-Ogna phenotype results from a single site-specific missense mutation in exon 31, at the end of the coiled-coil rod domain of plectin (Koss-Harnes et al., 1997). Patients suffering from EBS-Ogna show abnormalities in plectin expression in basal keratinocytes and defective HDs at the ultrastructural level in the skin. However, they do not develop any muscular pathology and there is no evidence of PA (Koss-Harnes et al., 2001; Koss-Harnes et al., 1997).

Plectin deficiency in mice

To define plectin's role in tissue development and integrity and also to investigate its relation to EBS-MD, plectin-deficient mice were generated (Andrä et al., 1997). Homozygous plectin-deficient mice die two to three days after birth exhibiting severe skin blistering, especially at the fore- and hindlimbs (Andrä et al., 1997). In addition, these mice revealed abnormalities reminiscent of minicore myopathies in skeletal muscle and disintegration of intercalated discs in the heart (Andrä et al., 1997). The early death of plectin knockout mice previously has not been fully resolved. It was believed that the animals die due to loss of body fluid as a consequence of skin blistering, combined with malfunction of the heart and/or vasculature (Andrä et al., 1997).

The establishment of plectin (-/-) cell cultures from plectin-null mice has yielded new insights into plectin's functions (reviewed in Wiche, 1998). Plectin (-/-) keratinocytes formed fewer hemidesmosome-like clusters in culture (Andrä et al., 2003) correlating with the reduced HD number in plectin-null mice (Andrä et al., 1997). Cultivated plectin (-/-) dermal fibroblasts displayed a dramatic increase in the number of actin stress fibers and focal adhesion contacts (Andrä et al., 1998). This phenomenon was noticeable within a short period (2 hours) after seeding the cells. Moreover, in contrast to control cells, actin stress fibers were insensitive to extracellular stimuli activating Rho, Rac, and Cdc42 GTPase signaling cascades

which control actin stress fiber (Rho), lamellipodia (Rac), and filopodia (Cdc42) formation (Andrä et al., 1998; Wiche, 1998). In addition, plectin-deficient fibroblasts showed a diminished migratory activity in an in vitro wound healing assay (Andrä et al., 1998; Wiche, 1998). These observations strongly support the idea that plectin not only provides cells with mechanical strength, but also plays an essential role as regulator of cellular processes linked to actin filament dynamics (Wiche, 1998).

Molecular cell biology of the skin

Histology of the epidermis

The skin is composed of two distinct tissue layers. The dermis (forming the bulk of skin) is made up of ECM molecules, such as collagen, elastin, glycosaminoglycans, as well as fibroblasts that form and construct the ECM (Menon, 2002). The dermis is a highly vascular tissue, and also includes the philosebaceous units, sweat glands, dermal adipose cells, mast cell, and infiltrating leucocytes (Kühnel, 2002). The overlying avascular epidermis is composed of a multilayer of cells known as keratinocytes, so called because they synthesize intermediate filament proteins called keratins (Menon, 2002). About 95% of the epidermal layer is built up of keratinocytes, and the rest are melanocytes, Langerhans cells, and Merkel cells (mechanoreceptors) (Menon, 2002). The stratified epidermis is built up of four distinct layers (Menon, 2002): the stratum basale (SB), stratum spinosum (SS), stratum granulosum (SG), and stratum corneum (SC).

Epidermal homeostasis

The epidermis provides a physical and permeability barrier, which is essential for mammalian survival as an adaptation to terrestrial life (Candi et al., 2005). This barrier against the environment – which keeps harmful microorganisms out in order to protect against infection and retains vital body fluids in order to prevent dehydration – is provided, and continuously regenerated, by terminally differentiating keratinocytes (Fuchs and Raghavan, 2002). This process is known as cornification and is highly organized in space and

time (Candi et al., 2005). Epidermal differentiation begins with the migration of keratinocytes from the mitotically active basal layer (stratum basale) into the spinous layer (stratum spinosum), continues with movement of the cells through the granular layer (stratum granulosum), where the cornified envelope is formed, and ends with the formation of the cornified layer (also known as the stratum corneum), which represents the uppermost layer of the skin (Candi et al., 2005; Kalinin et al., 2002; Michel et al., 1988). Keratinocyte proliferation, differentiation and apoptosis occur sequentially, and each process is characterized by the expression of a specific set of proteins (Fig. 9) (Candi et al., 2005). In normal epidermis, the proliferation rate is precisely balanced by desquamation of the cornified layer at the skin surface (Candi et al., 2005). This epidermal homeostasis constantly rejuvenates the epidermis (Candi et al., 2005).

Keratins K5 and K14 are the major structural proteins in basal keratinocytes. The K5/K14 network, in cooperation with MTs and MFs, forms the cytoskeleton of the keratinocyte cell (Candi et al., 2005) (Fig. 3). Triggered by yet poorly understood mechanisms, certain basal keratinocytes migrate from the basal cell layer into the spinous layers, loose their mitotic activity, and begin to synthesize a new set of structural proteins and enzymes that are characteristic of cornification (Candi et al., 2005).

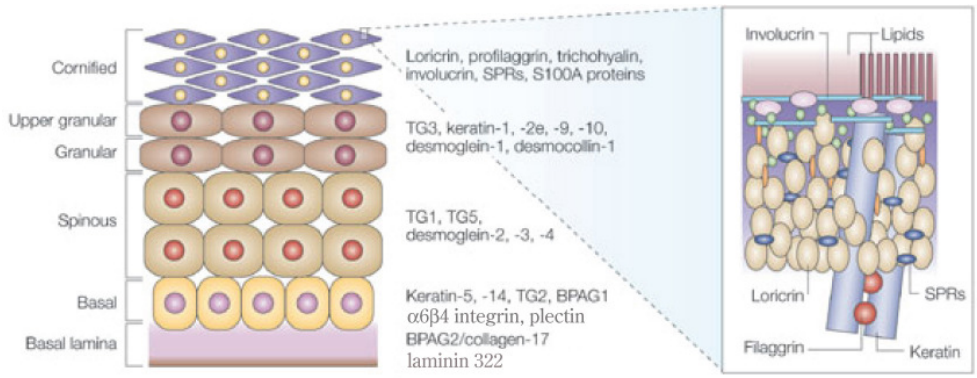

Figure 9. Terminal differentiation in the epidermis. Shown are the proteins that are expressed in particular locations in the epidermis during skin differentiation. Cornification occurs in the supra-basal layers, to form a cornified envelope (see insert). At the molecular level, the cornified envelope is formed by proteins that are highly crosslinked by transglutaminases, with specific lipids on the outside, to guarantee specific physical properties. BPAG, bullous pemphigoid antigen; SPR, small proline-rich proteins; TG, transglutaminase. (Modified from (Candi et al., 2005)).

Keratins K1 and K10 are among the first proteins to be expressed during cornification and replace the pre-existing K5 and K14 IF network (Candi et al., 2005). At a more advanced stage of differentiation, the cells acquire keratohyalin granules, which contain profilaggrin - the precursor of the keratin filament bundling protein filaggrin (Candi et al., 2005). Filaggrin aggregates and aligns the keratin filaments into tight bundles, which promotes the collapse of the cell into a flattened shape - a characteristic of the corneocytes in the cornified layer (Candi et al., 2005).

Keratin filament bundles and filaggrin together form a scaffold for the subsequent maturation and reinforcement steps of cornified-envelope assembly (Candi et al., 2005). Concomitantly, a number of other structural proteins, including involucrin, loricrin, trichohyalin and the class of small proline-rich proteins, are synthesized and subsequently become crosslinked by several transglutaminase enzymes to reinforce the cornified envelope beneath the plasma membrane (Candi et al., 2005; Steinert and Marekov, 1995). Besides the cornified envelope proteins, a complex mixture of lipids are synthesized and secreted into the intercellular spaces of the cornified envelope, some of which become covalently attached to cornified envelope proteins, and most of which form intracellular lamellae that help complete the barrier (Candi et al., 2005).

Desmosomes

Desmosomes are specialized intercellular junctions that mediate strong cell-cell adhesion in epithelial tissues, cardiac muscle and lymph nodes (Green and Gaudry, 2000). They are highly symmetrical plasma membrane multiprotein complexes that are associated with IFs (Kottke et al., 2006). The core region of the desmosome, including the intercellular space, is a region of tight cell-cell interaction (Kottke et al., 2006; Kowalczyk et al., 1999; Kremer et al., 2005; Ku and Omary, 2000; Kühnel, 2002; Kulesz-Martin et al., 1983) (Fig. 10). Intercellular adhesion is mediated by the transmembrane proteins desmoglein and desmocollin, two members of the cadherin protein family (Garrod et al., 2002). The cytoplasmic plaque couples these adhesive interactions to the IF network (Kottke et al., 2006) (Fig. 10). Located within the desmosomal cytoplasmic plaque are plakoglobin and plakophilin, both members of the armadillo protein family (Hatzfeld, 2007; Hatzfeld et al., 2000), and desmoplakin, a member of the plakin family (Yin and Green, 2004) which provides anchorage to IFs (Fig. 10). Plakoglobin interacts with desmoplakin and thereby links

the cadherin tails to the IF network (Yin and Green, 2004). Additionally, plakophilins bind tightly to desmoplakin and probably play a role in the clustering of desmosomal components into densly packed structures (Kottke et al., 2006; Kowalczyk et al., 1999). Plectin was also localized to desmosomes (Eger et al., 1997; Skalli et al., 1994) but appears to play only an auxiliary role. During terminal differentiation of keratinocytes, desmosomes are reinforced by association of envoplakin (Ruhrberg et al., 1996), periplakin (DiColandrea et al., 2000) and corneodesmosin (Montezin et al., 1997), which later become crosslinked to the desmosomal complex by transglutaminase activity in order to form the corneodesmosomes of cornified layer (Steinert and Marekov, 1995). Autosomal dominant and negative mutations have been identified in several components of desmosomes, including desmoglein (Hunt et al., 2001), plakoglobin (McKoy et al., 2000), plakophilin (McGrath et al., 1997) and desmoplakin (Lai Cheong et al., 2005). Clinically, some of these mutations result in skin blistering with loss of desmosome adhesion in the epidermis (McGrath et al., 1997; Whittock et al., 2002). However, several inherited desmosome disorders have other features, such as alopecia, woolly hair or keratoderma (McKoy et al., 2000; Norgett et al., 2000).

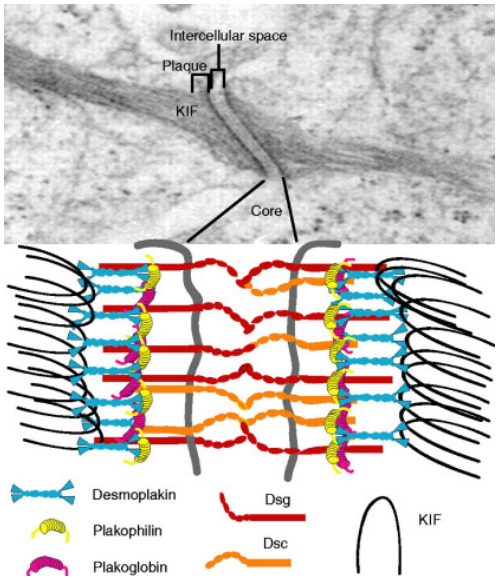

Figure 10. Ultrastructure and molecular model of a desmosome. Shown on top is an electron micrograph of a desmosome, showing the typical organization with the core region filling the intracellular space, and the plaque region with attached keratin intermediate filaments (KIFs). Depicted below is the relative organization of major desmosomal proteins. Dsg, Desmoglein. Dsc, Desmocollin. (Adapted from (Kottke et al., 2006)).

Hemidesmosomes

HDs are highly specialized membrane-located multiprotein adhesion complexes that promote epithelial stromal attachment in stratified and complex epithelia (Litjens et al.,

2006). In skin, the hemidesmosomal protein complex provides stable adhesion of the epidermis to the underlying dermis and ensures resistance to mechanical stress when applied to the skin (Litjens et al., 2006). Skin HDs contain three transmembrane proteins, the integrin α6β4 heterodimer and the type XVII collagen BP180 (BPAG2), two plakin family members, plectin and BP230 (BPAG1), and the tetraspanin CD151 (Borradori and Sonnenberg, 1999; Jones et al., 1998) (Fig. 11). Integrin α6β4 connects the basal keratinocytes to a major component of the basement membrane, laminin-5 [now referred to as laminin-322 (Aumailley et al., 2005)], whereas the cytoplasmic proteins plectin and BP230 connect HDs to keratin filaments (Litjens et al., 2006) (Fig. 11).

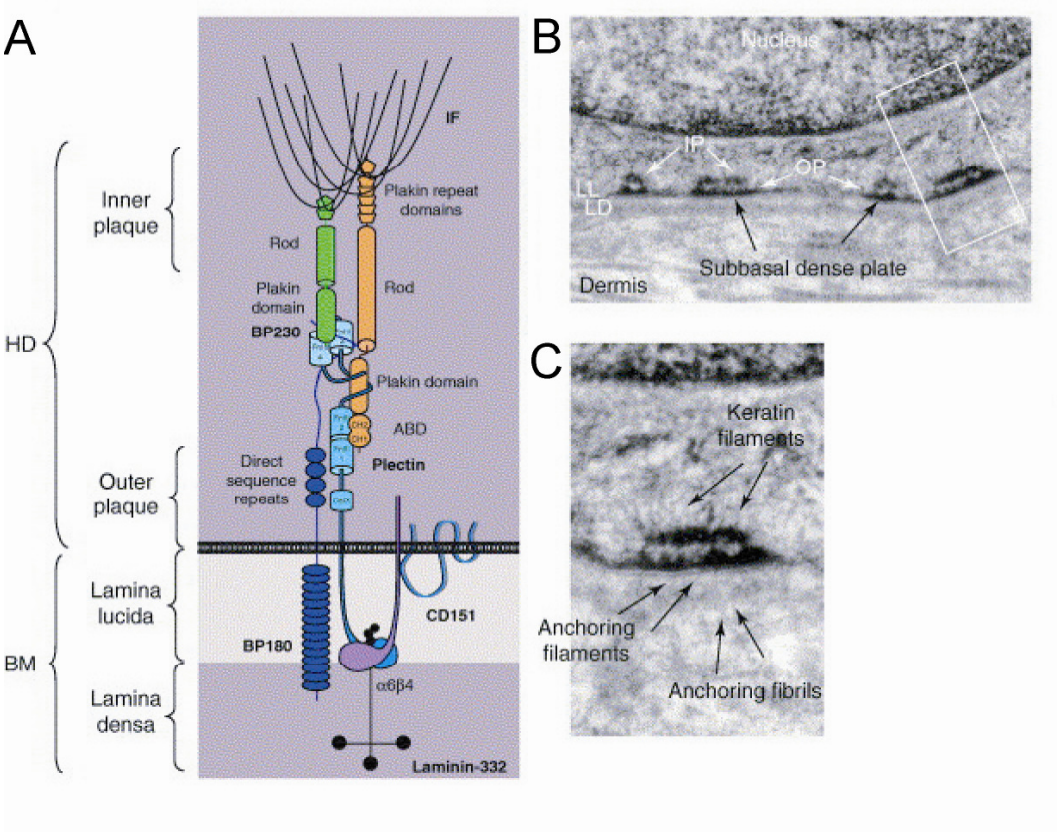

Figure 11. Components and structure of HDs. (A) A schematic drawing of the HD, showing its six components [integrin α6β4 heterodimer (violet/light blue), CD151 (blue), BP180 (dark blue), BP230 (green) and plectin (orange)] together with the integrin ligand laminin-332 and intracellular intermediate filament partners K5 and K14 (IF). (B) An electron micrograph of several HDs at the basal surface of basal keratinocytes in the epidermis. (C) An enlargement of the indicated area in the panel B. Abbreviations: BM, basement membrane; CH, calponin homology domain; HD, hemidesmosome; IP, inner plaque; LD, lamina densa; LL, lamina lucida; OP, outer plaque (Modified from (Litjens et al., 2006)).

Stable attachment of basal keratinocytes to the basement membrane through HDs is of fundamental importance for the maintainance of skin integrity (Litjens et al., 2006). Inherited or acquired diseases in which either of the hemidesmosomal components are affected lead to a variety of skin blistering disorders (Litjens et al., 2006; Pfendner et al., 2005; Pulkkinen and Uitto, 1999; Zillikens, 1999). In cultured keratinocytes, HD formation is driven both from within the cell through an interaction of the cytoplasmic domain of integrin β4 with plectin and from outside the cell through binding of integrin α6β4 to laminin-322 (Geuijen and Sonnenberg, 2002; Goldfinger et al., 1999; Sadowski et al., 2005).

Skin wound healing

Skin wound healing represents a complex, highly dynamic and well-ordered biological process (Martin, 1997). Tissue injury initially causes disruption of vascular vessels and subsequent extravasation. A temporary fibrin clot is then formed to reestablish tissue homeostasis and epidermal barrier function, and to provide a transient adhesive substrate for platelets that secrete growth factors, cytokines and ECM (Santoro and Gaudino, 2005). These mediators of the inflammation response recruit macrophages and neutrophils that subsequently secrete a battery of specific factors to the site of injury, orchestrating the following phase of tissue reepithelization (Eming et al., 2007; Santoro and Gaudino, 2005). Reepithelization is defined as the resurfacing of a wound with new epithelium and consists of both migration and proliferation of keratinocytes at the periphery of the wound (Santoro and Gaudino, 2005).

During reepithelization, migrating keratinocytes proximal to the wound margin undergo many subcellular modifications including (i) disassembly of HDs, (ii) retraction of keratin IFs, (iii) dissolution of most desmosomes, and (iv) formation of lamellipodia and focal contacts (Santoro and Gaudino, 2005). As epidermal migration moves on, keratinocytes at the wound margin begin to strongly proliferate behind the actively migrating cells (Santoro and Gaudino, 2005). The resulting dense hyperproliferative epithelium then serves to feed the migrating keratinocyte sheets at the wound margins (Santoro and Gaudino, 2005; Werner and Grose, 2003).

Molecular events regulating keratinocyte migration

In intact skin, keratinocytes are assembled in a quiescent epidermal tissue, tied up by cell-cell and cell-matrix junctions (Santoro and Gaudino, 2005). Injury to the skin causes the transition of quiescent keratinocytes adherent to laminin-322 into migrating cells on the newly formed provisional matrix containing fibrin, fibronectin, collagen I and III, and vitronectin (Litjens et al., 2006; O'Toole, 2001). Concomitantly, various growth factors and cytokines are secreted to orchestrate healing of the wound (Eming et al., 2007). Consequently, stable adhesion of keratinocytes to the basement membrane by integrin α6β4 is lost, as HDs are disassembled, and integrin α6β4 is redistributed from HDs to lamellipodia (Litjens et al., 2006; Lotz et al., 2000; Santoro et al., 2003). This mobilization is mediated by PKC-mediated serine/threonine phosphorylation of integrin β4 (Alt et al., 2004; Rabinovitz et al., 2004; Santoro et al., 2003; Wilhelmsen et al., 2007). In response to reepithelization, the expression of integrin α2β1 and integrin α3β1, which are normally mostly restricted to the lateral membranes of basal keratinocytes, becomes extended throughout the entire epidermis and their concentration at the basal membrane increases (Santoro and Gaudino, 2005; Werner and Grose, 2003). Moreover, the expression of the fibronectin-binding integrins α5β1 and αvβ1, and the vitronectin-binding integrins αvβ5 and αvβ6 is also upregulated (Hakkinen et al., 2000; Santoro and Gaudino, 2005). Initially, keratinocytes attach to collagen I in the wound bed through focal adhesions and intergin α2β1, which activates the GTPase RhoA (Nguyen et al., 2000a; Nguyen et al., 2001; Nguyen et al., 2000b). After binding to newly deposited laminin-322 by integrins α6β4 and α3β1, keratinocytes then switch to the T lymphoma invasion and metastasis (TIAM1)-Rac1 signalling pathway to promote lamellipodia formation and directional migration (Choma et al., 2007; Choma et al., 2004; Frank and Carter, 2004; Hamelers et al., 2005; Litjens et al., 2006). Additionally, a plethora of other signaling proteins/cascades such as PKCδ, c-Src, PI3K and the mitogen-activated protein kinase (MAPK) cascades are also involved in mediating keratinocyte migration (Fitsialos et al., 2007; Li et al., 2004; Li et al., 2002b; Pankow et al., 2006; Yamada et al., 2000), and together control gene expression and cytoskeleton remodeling.

The contribution of α6β4 integrin to the development of squamous cell carcinoma

Skin cancer can be divided into two broad categories, melanoma and nonmelanoma skin cancer (NMSC). The two most common forms of NMSC are basal cell carcinoma (BCC) and squamous cell carcinoma (SCC) (Chakrabarty and Geisse, 2004), both originating from epidermal keratinocytes. Expression of integrin α6β4 is noticeably increased in the highly metastatic SCC, but not in the relatively non-metastatic BCC (Rossen et al., 1994). Laminin-322 and integrin α6β4 have both been shown to cooperate with Ras and inhibitor of κBα (IκBα) to induce primary human epidermal keratinocytes to form SCCs in immune-deficient mice (Dajee et al., 2003). In this tumor model, antibodies directed against laminin-322 and integrin α6β4 inhibited tumor formation, and laminin-322- or integrin β4-null keratinocytes isolated from patients with epidermolysis bullosa failed to form tumors upon transduction with Ras and IκBα. In a related study, targeted overexpression of integrin α6β4 in the suprabasal layers of the epidermis of transgenic mice significantly increased the frequency of papillomas, carcinomas and metastases induced by chemical carcinogenesis (Owens et al., 2003). One important mechanism by which integrin α6β4 functions to promote formation of SCC is by cooperating with the epidermal growth-factor receptor (EGFR) (Mariotti et al., 2001) and other receptor tyrosine kinases such as RON (Santoro et al., 2003) and MET (Trusolino et al., 2001). The tumor promoting function of α6β4 is correlated with release of the integrin from its mechanical, adhesive role at HDs to HD-independent, and to some extend, ligand-independent, signaling functions (Janes and Watt, 2006; Mariotti et al., 2001; Owens et al., 2003; Rabinovitz et al., 1999; Santoro et al., 2003; Trusolino et al., 2001).

Generation of conditional knockout mice by Cre-mediated recombination

Strategies for conditional gene targeting have been developed in mice based on the Cre/*loxP* recombination system (Gu et al., 1994; Misra and Duncan, 2002; Sauer and Henderson, 1989). Cre (cyclization recombination) is a site-specific DNA recombinase of the

Int family (Argos et al., 1986), that was identified in the bacteriophage P1 (Sternberg et al., 1986). Cre recognizes a 34 bp-long sequence called *loxP* (locus of X-over of P1) and efficiently catalyzes reciprocal conservative DNA recombination between pairs of *loxP* sites (Hoess et al., 1990), leading to excision of the stretch of DNA between them as a covalently closed circle which will ultimately be degraded. *LoxP* sites are sufficiently large, so that these sequences are not expected to naturally occur in the mammalian genome (Sauer, 1996). Furthermore, no accessory host factor or a certain DNA topology is required for efficient Cre-mediated recombination (Grindley et al., 2006). These key features make the Cre/*loxP* system ideally suitable for genomic manipulation in eukaryotic cells.

The strategy for generating a spatially or temporally controlled conditional mutation is to modify the target gene by homologous recombination in ES cells so that it is flanked by *loxP* sites (Sauer, 1998). Mice with such a modified gene are then crossed with mice expressing Cre in the desired target tissue (Sauer, 1996). Subsequent Cre-mediated DNA excision results in tissue-specific gene ablation. Recombinational eradication of a certain gene of interest can thus be targeted to a particular tissue, by simply controlling Cre expression (Sauer, 1998).

A particularly powerful feature of the conditional gene inactivation strategy using Cre is that the same *loxP*-tagged mouse can be used for gene ablation in a large number of different tissues, or at different developmental times, by simply mating it with a corresponding Cre transgenic that displays the desired tissue or temporal specificity of Cre expression (Muller and Keck, 2002). Thus, the same genetically modified animal can be used to answer a variety of different questions relating to the expression and function of the target gene in different tisues (Muller and Keck, 2002).

Further development of the system has yielded the exciting possibility of spatial and temporal control of the recombination event (Leone et al., 2003). This was achieved by fusing the mutated ligand-binding domain of either the progesterone receptor (Kellendonk et al., 1999) or the estrogen receptor to the Cre recombinase (Feil et al., 1996; Metzger et al., 1995; Schwenk et al., 1998). In the latter case, the mutation in the estrogen receptor prevents binding to its natural ligand β estradiol, but allows binding of the synthetic ligands tamoxifen and 4-hydroxy-tamoxifen (OHT) and subsequent activation of the recombinase. In the absence of the ligand, the fusion protein Cre-ER is restricted to the cytoplasm by the bound heatshock protein HSP90 and is thus inhibited from entering the nucleus. Upon administration of OHT (or tamoxifen, which is converted to OHT in the liver), it binds to the

ER domain, causing HSP90 to dissociate from the complex and allowing Cre-ER to translocatw into the nucleus, where it mediates recombination between the *loxP* sites. The inducible Cre-ER system has been refined to optimize its performance and was successfully used in cultured keratinocytes and in developing and adult mice (Brocard et al., 1997; Danielian et al., 1998; Feil et al., 1997; Indra et al., 1999; McLean et al., 2004; Metzger and Chambon, 2001; Stratis et al., 2006; Vasioukhin et al., 1999; Vooijs et al., 2001).

AIM OF THESIS

Plectin is an extremely versatile cytoskeletal linker, serving essential functions in maintaining the integrity of skin, muscle, and heart cytoarchitecture (Andrä et al., 1997). Plectin-deficient mice die 1-3 days after birth exhibiting skin blistering caused by disruption of basal keratinocytes, as well as myopathies in skeletal muscle and disintegration of intercalated disks in the heart (Andrä et al., 1997). The early lethality of plectin-null mice precluded the analysis of possible plectin functions at later stages of postnatal development and maturation of mice. To circumvent this problem, mice with floxed plectin alleles, rendering the plectin locus susceptible to conditional elimination by Cre recombinase, have been generated in our lab (Ackerl et al., 2007). Such mice should provide an answer to the still unsolved question whether the early death of plectin-null mice is indeed due to skin blistering and fluid loss, or possibly due to malfunctions of the heart and the vascular endothelial system.

In the first part of my thesis, I was going to characterize the phenotype of a mouse line showing a complete knockout of plectin restricted to keratin 5-expressing epithelia. However, since mice with plectin-deficiency in the skin might also die within a few days after birth and therefore will not allow for the analysis of plectin function in skin at later stages in lifetime, additionally an inducible mouse model, where plectin expression can be knocked out in the epidermis at the adult stage of the animal had to be generated. The analysis of these mice should provide deeper insights into the pathology of plectin-linked EBS.

The important question of whether plectin affects IF network cytoarchitecture and its dynamics had previously not been addressed, except for a study showing that a recombinant fragment containing plectin's C-terminal IF-binding site inhibits IF formation in vitro in a dose-dependent manner (Steinbock et al., 2000). Therefore, in the second part of this thesis the aim was to investigate the role of plectin in the organization of keratin network cytoarchitecture and migration of cultured keratinocytes.

In the third part of my thesis, a number of questions related to the interaction of plectin with MTs on mechanistic and functional levels should be addressed: Is plectin-MT binding Isoform-specific? Does plectin bind directly or indirectly to MTs? Does the absence of plectin, especially of isoform 1c, affect the rearrangement of MTs during stratification of keratinocytes?

Finally, to learn more about the mechanisms leading to impaired migration of plectin-deficient fibroblasts (Andrä et al., 1998), in the fourth part of this thesis, the correlation between RACK1/PKCδ signaling and cell migration should be investigated in plectin-deficient and wild-type fibroblast cell lines.

RESULTS

This section will be organized as outlined in Aim of Thesis. The first chapter will deal with the phenotypic characterization of mouse lines with a conditional knockout of plectin in stratified epithelia. The second chapter will define plectin`s role in regulating keratin filament network cytoarchitecture and migration of keratinocytes and in chapter three, some light will be shed on the molecular nature of the association of plectin isoform 1c with MTs. Finally, chapter four will give some insight into mechanisms slowing down migration of plectin-deficient fibroblasts.

PART I - The conditional knockout of plectin in stratified epithelia

It has previously been shown that plectin gene inactivation in the mouse germ line results in postnatal death, with pups showing severe skin blistering as well as muscular dystrophy (Andrä et al., 1997). To assess whether blistering of the epidermis, or of other stratified epithelia, was causing the animals death, a gene-targeting approach was used to create mice with a constitutive knockout of plectin in stratified epithelia, but not in other types of tissues.

Generation of mice with a conditional deletion of plectin in stratified epithelia

All the mouse lines used in this thesis were generated by R. Ackerl and some of the data discussed in part 1 of this thesis have been generated in close collaboration with R. Ackerl. Therefore, I will restrict the presentation of data to those that were genuinely generated from my part, while the rest will be just discussed. A detailed description of the conditional knockout strategy can be found in (Ackerl et al., 2007).

Inactivation of the plectin gene in mouse skin leads to severe skin fragility

To inactivate plectin in the skin, *Plec*$^{flox/flox}$ mice carrying two floxed plectin alleles (see supplementary Fig. S1 in manuscript copy 1 included as Appendix) were crossed with transgenic mice expressing the Cre-recombinase under the control of the K5 promoter (Tarutani et al., 1997). *Plec*$^{\Delta/\Delta}$:K5-Cre mice thus generated will be referred to as K5-Cre KO. They were born at the expected mendelian ratios and died 1-3 days after birth. They showed severe skin detachment, especially at fore- and hindlimbs (Fig. 12A,B), and in some cases around the mouth and nasal cavities; rarely, aplasia cutis of the forelimbs was also noted (not shown).

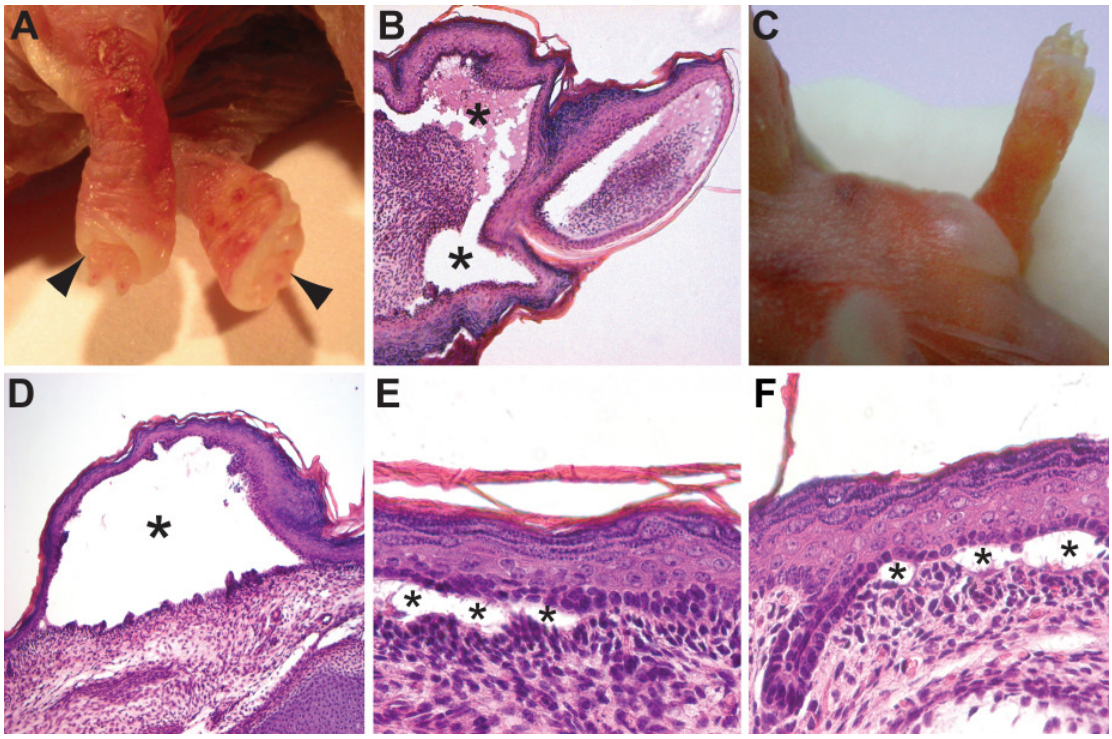

Figure 12. Phenotypic analysis of K5-Cre KO mice. (A) 2-days-old K5-Cre KO pup showing severe skin detachment on its forelimbs (arrows). (B) H/E staining of K5-Cre KO paw section, showing detachment of toe epidermis (asterisks) together with nail bed and nail. (C) 2-days-old K5-Cre KO pup displaying a huge fluid filled blister in the hind armpit. (D-F) H/E stainings of K5-Cre KO skin, showing epidermal detachment (asterisks) at the level of the basal keratinocyte layer.

The extent of phenotypic alterations exhibited before death varied among knockout mice. Most common was skin detachment at forepaws (Fig. 12A,B), but also large blisters

reaching the size of up to one square centimetre were found at the upper extremities and in the armpits (Fig. 12C). Sometimes blisters were torn open. A histological tissue examination revealed blister formation between the dermis and the superficial epidermal layers (Fig. 12D). Furthermore, macroscopically non-visible microblisters were revealed in K5-Cre KO skin (Fig. 12E,F). *Plec*$^{flox/flox}$ mice lacking the K5-Cre transgene, *Plec*$^{+/flox}$ mice (carrying one floxed and one wild-type allele), and *Plec*$^{+/+}$:K5-Cre mice (carrying two wild-type alleles and the K5-Cre transgene) did not show any pathological skin phenotype. Thus, *Plec*$^{flox/flox}$ mice lacking the K5-Cre transgene were used - and will be referred to - as (wild-type) controls. By the type of skin disorder, reduced bodyweight (see below), and postnatal death, K5-Cre KO mice were indistinguishable from plectin-null (*Plec*$^{-/-}$) mice (Andrä et al., 1997).

To detect small localized breaches in skin barrier I performed dye penetration assays with 1-day old littermates. In contrast to control mice (Fig. 13A), K5-Cre KO pubs showed numerous dark spots, especially on their heads and forelegs (Fig. 13B,C), indicating localized loss of barrier function. Measurements of transepidermal water loss (TEWL), to detect increased fluid loss through lesions, revealed a ~3.5-fold increased TEWL value compared to intact skin (Fig. 14). However, no differences in TEWL values were observed between intact skin of K5-Cre KO and control pubs demonstrating the absence of intrinsic barrier defects in K5-Cre KO mice. A histological examination of stained spots revealed microlesions at various stages of wound healing (Fig. 13D,E). Most lesions had a histological appearance as shown in Fig. 13D, with a thick, acanthotic and weakly differentiated new epidermis having formed under a crust that was still covered with the old (dead) epidermis. In some lesions, a thin, multilayered sheet of keratinocytes could be seen under the crust, indicating ongoing reepithelialization (Fig. 13E). To test, whether such lesions could be induced by trauma, I applied mild mechanical stress in the form of consecutive tape strippings with D-squame disks, (a procedure normally used to sequentially remove stratum corneum layers), to the back skin of newborn K5-Cre KO and control mice, followed by dye penetration assays. Indeed, I found small blue-stained spots in 10-times stripped K5-Cre KO (Fig. 13G), but not in control skin (Fig. 13F). Histological examination of stripped K5-Cre KO skin areas showed that stripping had induced basal keratinocyte cytolysis (Fig. 13H). Moreover, a few tape strippings were often enough to induce the formation of a large blister (Fig. 13I). When stronger adhesive tape (Tesa 3M) was used, one stripping was sufficient to remove the entire epidermis of the stripped area (not shown). Together, these data demonstrated an extreme fragility of K5-Cre KO epidermis.

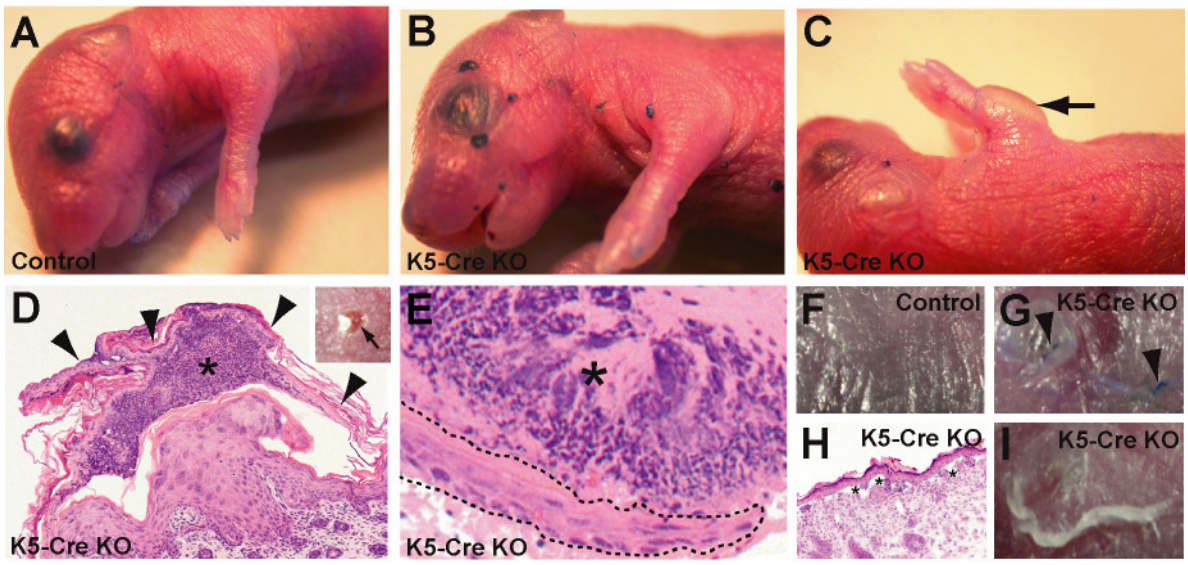

Figure 13. Skin barrier analysis. (A-C) Toluidine blue dye penetration assay. Note localized breaches in skin barrier of K5-Cre KO pups allowing penetration of dye. Toluidine blue does not penetrate intact fluid filled blisters (arrow in C). (D, E) Representative H/E stainings of toluidine blue stained spots, revealing microlesions. In (D), note newly formed acanthotic epidermis under a crust (asterisk) that is covered by pieces of the old (dead) epidermis (arrowheads). The insert in (D) shows a photograph of a microlesion (arrow). The lesion in (E) is covered by a crust (asterisk) and is in the process of reepithelialization (dashed line). (F-I) Induction of microlesions by mild trauma. Flank skins of newborn mice were tape-stripped 10 times and subsequently stained with toluidine blue (F, G). Note blue stained microlesions (arrowheads) in stripped skin of K5-Cre KO (G). Tape stripping caused epidermal detachment (H, asterisks) and blister formation (I) in K5-Cre KO skin.

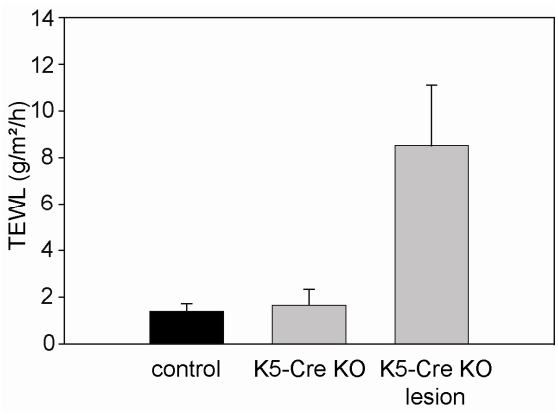

Figure 14. Increased TEWL over skin lesions of K5-Cre KO mice. TEWL was measured on unaffected back skins of 1-day old K5-Cre KO and control mice. A total number of 6 K5-Cre KO and control littermates were measured. Mean values ± 2 x SEM are shown. In addition, TEWL was measured over 6 lesions from 3 K5-Cre KO mice. Lesions were identified by examination of pubs under a binocular dissection microscope. Note increased TEWL over lesions in K5-Cre KO skin.

Highly efficient reduction of plectin levels by K5-controlled Cre expression.

To examine to which extent plectin expression was reduced in the epidermis of conditional knockout compared to control animals, immunoblotting of tissue homogenates was performed. Using an antiserum raised against a recombinant rat plectin protein fragment corresponding to exons 9-12 (Andrä et al., 2003; Andrä et al., 1997) (from now on referred to as anti-pan-plectin antiserum) and thus recognizing all plectin isoforms, only a very weak, in fact barely detectable, signal was obtained for K5-Cre KO epidermis compared with the strong signal for control tissue (see Fig. 2A in manuscript copy 1 included as Appendix). This remaining signal was likely to originate from non-keratinocyte cells present in the epidermis, such as dendritic (Langerhans) cells and pigment cells (melanocytes), which are known to express a set of plectin isoforms different from that of keratinocytes (Abrahamsberg et al., 2005; and unpublished data). In fact, when an antiserum specific to plectin 1a, the major plectin isoform found in keratinocytes (Andrä et al., 2003), was used instead of the anti-pan-plectin antiserum, not even a weak signal was anymore detectable in epidermal tissue extracts (data not shown). As expected, in tissue extracts from the dermis of K5-Cre KO animals, reduction of plectin expression was much less dramatic (see Fig. 2A in manuscript copy 1 included as Appendix). Since neither the anti-plectin 1a nor the anti-pan-plectin antiserum (both recognizing epitopes in plectin domains preceding the rod), detected proteins in K5-Cre KO tissue homogenates, that were of lower molecular weight than full length plectin, the expression of rodless-plectin in K5-Cre KO epidermis could be ruled out (data not shown).

To examine the plectin gene locus of K5-Cre KO animals in Cre-affected (epidermal) tissue compared to putatively unaffected (dermal) tissue, DNAs isolated from epidermal and dermal K5-Cre KO tissues were subjected to Southern blot analysis, along with corresponding samples from control ($Plec^{flox/flox}$) animals. In K5-Cre KO epidermis, the only signal detected (9 kb) corresponded to the $Plec^{\Delta}$ allele, indicating a recombination efficiency of 100% (see Fig. 2B in manuscript copy 1 included as Appendix). In K5-Cre KO dermis, on the other hand, the 15 kb wild-type signal was predominant, with an additional (lesser) signal seen at 9 kb (see Fig. 2B in manuscript copy 1 included as Appendix). Considering that enzymatic detachment of the epidermis leaves some hair follicles embedded in the dermis (Vasioukhin et al., 1999), it is likely that the recombination signal observed in K5-Cre KO dermis stemmed from a contamination with keratinocytes. The absence of the 9 kb mutated gene signal in both controls (epidermis and dermis) indicated that aberrant (non-Cre-mediated) recombination between the *loxP* sites did not occur.

Additionally, immunofluorescence microscopy was used to assess the absence of plectin from the epidermis of knockout mice. While a pronounced staining of the dermo-epidermal borderline, along with a weaker staining of the cytoplasm and membranes of all epidermal keratinocytes, was detected in normal mouse skin using an antiserum raised against plectin`s rod domain (Andrä et al., 1997) (see Fig. 2C,a in manuscript copy 1 included as Appendix) in the corresponding K5-Cre KO tissue, staining above background was observed for only a few insular cells (see Fig. 2C,b in manuscript copy 1 included as Appendix). These plectin-positive cells most likely represented melanocytes (especially those between and underneath basal keratinocytes and around hair follicles) and dendritic cells (in the suprabasal keratinocyte layers) which do not express K5 (Mahrle et al., 1989), and consequently no Cre recombinase. Plectin was also absent from the oral epithelia of K5-Cre KO animals (Fig. 15B), whereas in the oral cavity of wild-type mice it was strongly expressed along the basal membranes of palate and tongue epithelia (Fig. 15A), both of which express K5 at high levels (Fig. 15E,F). Plectin expression was also strongly reduced in oesophagus epithelium (Fig. 15D), where K5 is expressed at high levels (Fig. 15G,H) (Byrne and Fuchs, 1993), but not in the pseudostratified epithelium of the trachea (Fig. 15J), where K5 expression is restricted to a small subset of airway epithelial cells (Fig. 15M,N) (Schoch et al., 2004). As expected, plectin expression in heart (Fig. 15K,L,O,P) and skeletal muscle (data not shown) of K5-Cre KO mice was not affected.

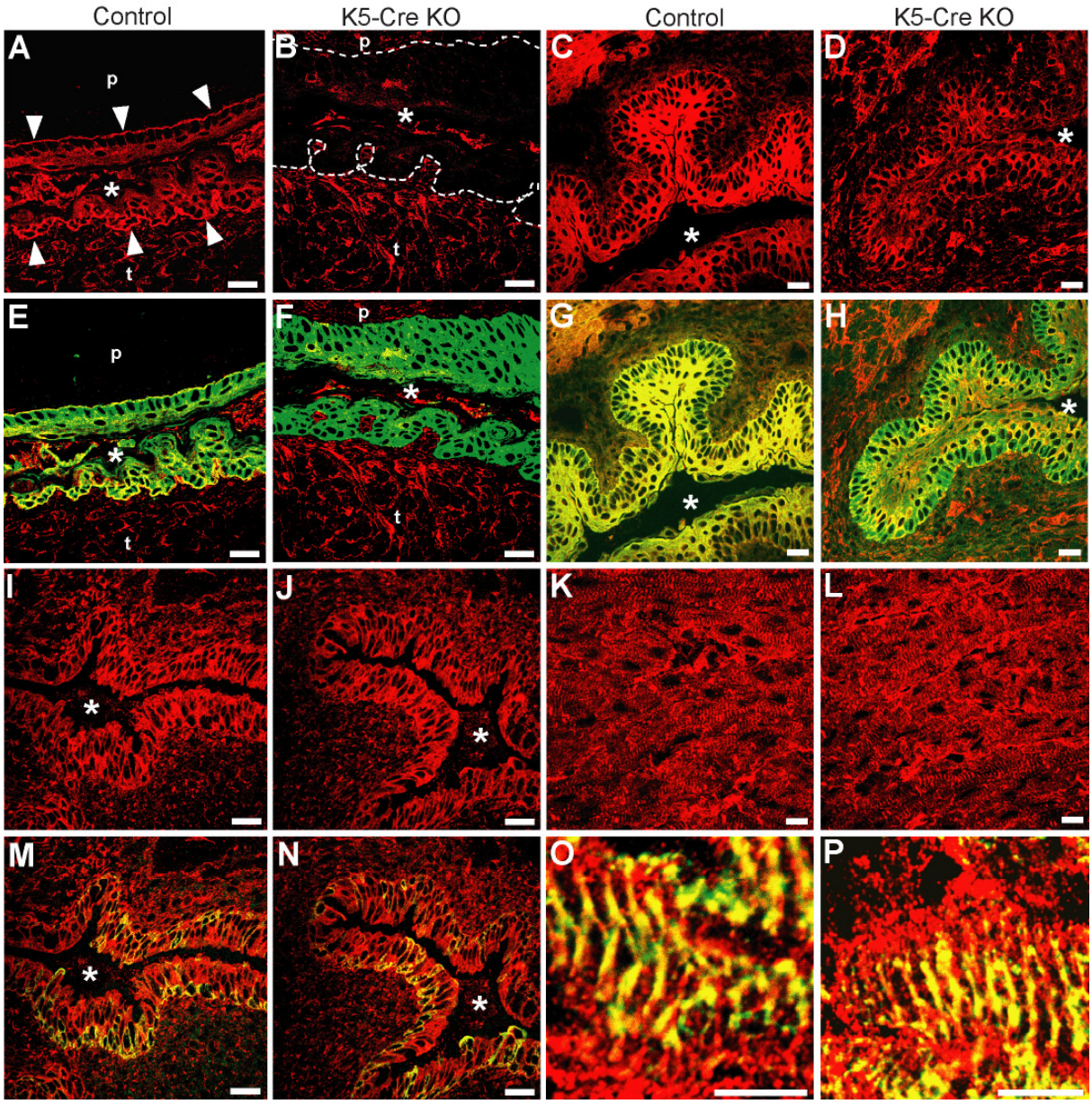

Figure 15. High efficiency of Cre-mediated plectin deletion in stratified internal epithelia. (A-P) Immunofluorescence microscopy of frozen tongue/palate (A, B, E, F), oesophagus (C, D, G, H), trachea (I, J, M, N) and heart (K, L, O, P) tissue sections of newborn control and K5-Cre KO specimens using anti-pan-plectin antiserum (A-P), anti K5,6,18 antibodies (E-H, M, N) and anti-desmin antiserum (O, P). In the oral cavity, the plectin signal is most prominent along the basal membranes of palate and tongue epithelia (arrowheads in A). Also note strongly reduced plectin-specific label in K5-Cre KO oesophagus (D), while in K5-Cre KO heart muscle, plectin expression was not reduced (L). p, palate; t, tongue. Plectin expression is also not reduced in the trachea of K5-Cre KO mice (J). The dashed line in (B) outlines the basement membrane. Asterisks indicate lumens of oral cavity, oesophagus and trachea. Bars, 20 µm.

Unaltered epidermal stratification and differentiation in K5-Cre KO mice

To investigate whether plectin deficiency had any influence on skin development and differentiation I undertook a detailed immunohistological analysis of skin sections from 1-day-old K5-Cre KO and control mice. First, I assessed the expression of two major hemidesmosomal proteins, integrin β4 and BPAG1, the former binding directly to plectin (Rezniczek et al., 1998). As expected, the integrin β4 signal was found confined to the basal membrane of basal keratinocytes and the outer root sheath of hair follicles (Fig. 16A,B). Similar to plectin-null mice (Andrä et al., 1997), the integrin β4 signal was slightly weaker in the K5-Cre KO epidermis compared to controls (Fig. 16B). This observation was confirmed by immunoblotting data showing reduced integrin β4 levels in detergent resistant, keratin-containing cell fractions from trunk skin of K5-Cre KO mice (Fig. 17B). In addition, in the absence of plectin the localization of integrin β4 seemed to be less polarized, since the protein was also found at lateral cell borders of basal keratinocytes (Fig. 16B). In blistered areas, the integrin β4 signal was located at blister floors, indicating disruption of basal keratinocytes at the level of the inner hemidesmosomal plaque (insert in Fig. 16B). BPAG1 staining at the basal surface membrane of K5-Cre KO keratinocytes was well preserved, although it appeared more patchy than in the control samples (Fig. 16C,D). Similar to integrin β4, in blistered areas, the BPAG1 signal was located at the blister floor (insert in Fig. 16D). K5, the cytoskeletal binding partner of hemidesmosomal plectin, was faithfully located in the basal keratinocyte cell layer as well as in transit amplifying cells (arrow in Fig. 16E), with similar fluorescence intensities in control and K5-Cre KO specimens (Fig. 16E,F). In blisters, K5 was localized in blister roofs (insert in Fig. 16F). Regarding K6, which is normally expressed in hair follicle keratinocytes and in some basal and suprabasal keratinocytes in ridged skin (Swensson et al., 1998), expression was found in the companion layer of epidermal hair follicles without any difference between K5-Cre KO and control animals (Fig. 16G,H). However, consistent with its known upregulation under pathological and hyperproliferative conditions (Coulombe et al., 2004) K6 was found strongly upregulated in areas of K5-Cre KO fore- and hindleg tissue, where the epidermis had become detached from the dermis (Fig. 16I). Similar observations were previously reported for other mouse models of skin blistering diseases (Dowling et al., 1996; Swensson et al., 1998) Peters et al., 2001; (Raymond et al., 2005). In addition, our observation was confirmed by immunoblotting data revealing increased expression levels of K6 in knockout compared to wild-type skin (Fig. 17B).

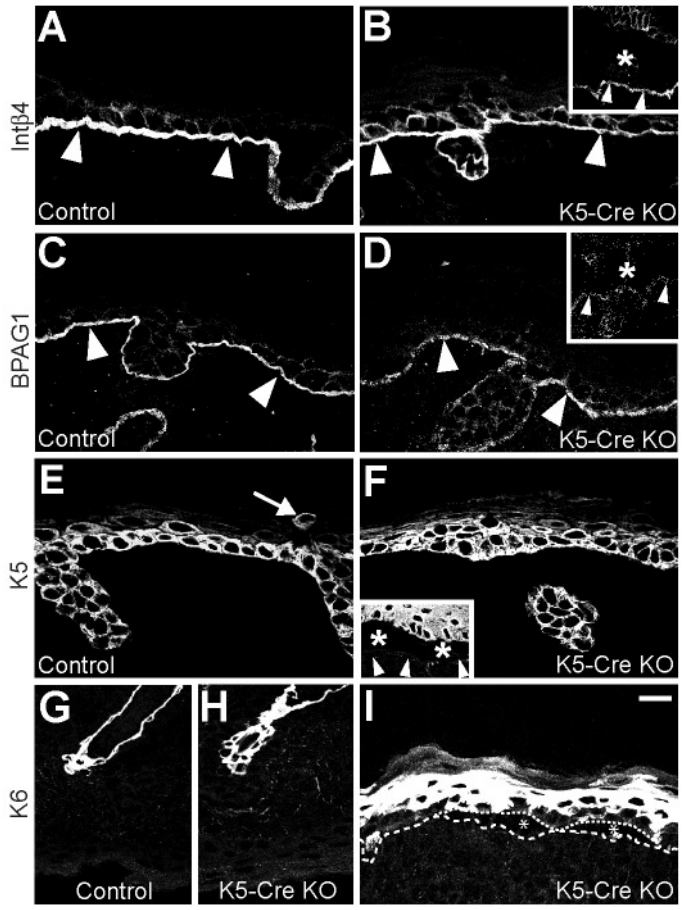

Figure 16. Expression of hemidesmosomal proteins in K5-Cre KO epidermis. Immunolocalization of integrin β4 (Intβ4; A, B), BPAG1 (C, D), K5 (E, F), and K6 (G-I) was examined in skin sections from 1-day-old control and K5-Cre KO mice. (A, B) In control epidermis, the integrin β4 signal was confined to the basal membrane (arrowheads) of basal keratinocytes and the outer root sheath of hair follicles, while in K5-Cre KO epidermis, it was slightly reduced and less polarized. In blistered areas (insert in B, asterisk), integrin β4 was located at blister floors. (C, D). Note more discontinuous BPAG1 staining along basal keratinocyte membranes (arrowheads) in K5-Cre KO compared to control epidermis. Insert in D shows BPAG1 localization at the floor (arrowheads) of blisters (asterisk). (E, F) The K5 signal was restricted to basal keratinocytes and rare transit amplifying cells (arrow), without noticable differences between control and K5-Cre KO epidermis. In blistered areas (insert in F, asterisks), K5 was located at blister roofs (arrowheads denote the blister floor). (G-I) In control skin, K6 was exclusively expressed in hair follicles (G), while in leg skins of K5-Cre KO mice, in addition to hair follicles (H), patches of suprabasal keratinocytes above microblisters were K6-positive (I). Dashed line in I indicates dermo-epidermal border. Dotted line, microblister separating the epidermis from the underlying dermis. Asterisks, blister. Bar, 20 µm.

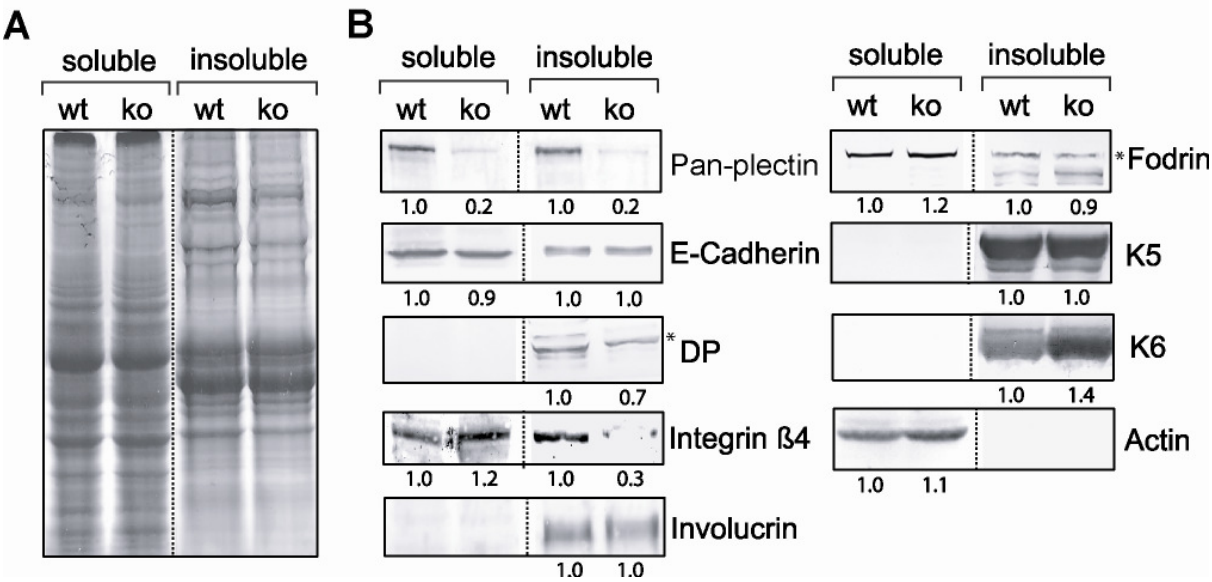

Figure 17. Relative expression levels of cytoskeletal and cell-cell adhesion proteins in detergent-soluble and insoluble fractions from 1-day-old K5-Cre KO versus control skin. Proteins were extracted from skin as described in materials and methods and equal amounts of proteins were analyzed by SDS-PAGE and immunoblotting using antibodies indicated. (A) Coomassie staining. (B) Immunoblotting. Numbers underneath lanes represent the protein ratios relative to an arbitrary level of 1.0 determined by the control samples. One of two experiments is shown. Asterisks, bands used for quantification.

Apart from HDs, actin-linked adherens junctions (AJs) and desmosomes have central functions in establishing the epithelial sheet and its polarity (Jamora and Fuchs, 2002). However, AJ formation appeared to be normal in K5-Cre KO epidermis as visualized using antibody (E-cadherin) and phalloidin labeling (actin) (see supplementary Fig. S4A-D in manuscript copy 1 included as Appendix), whereas desmoplakin staining revealed a slight reduction of desmosome structures in suprabasal epidermal cell layers of K5-Cre KO epidermis (see supplementary Fig. S4E-F in manuscript copy 1 included as Appendix). Similar trends were observed by immunoblotting (Fig. 17B). However, when macroscopically intact K5-Cre KO backskin was subjected to electron microscopy (performed by S. Reipert), neither desmosomal structures nor anchored keratin filaments showed any striking abnormalities (Fig. 18).

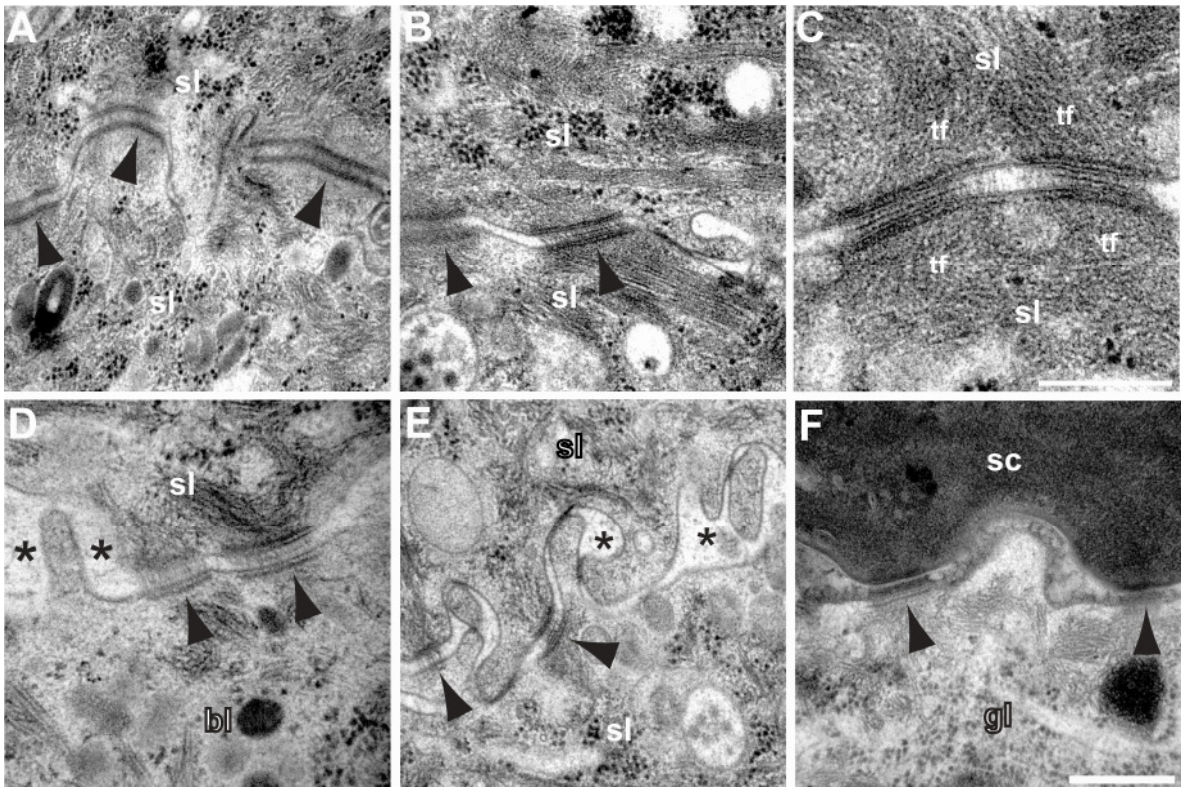

Figure 18. Ultrastructural analysis of desmosomes in control (A) and macroscopically intact K5-Cre KO backskin (B-F). Desmosomes of K5-Cre KO epidermis display a normal morphology (B) with regularly attached tonofilaments (C) in all epidermal layers (D-F). In some areas of K5-Cre KO epidermis, desmosome size and numbers appeared to be slightly reduced (E) compared to control epidermis (A) and intercellular spaces between cells of the basal and spinous layers were larger (D, E). Acantholysis was not oberserved. Arrowheads point to desmosomal structures. Asterisks indicate increased intercellular gaps in some areas of K5-Cre KO epidermis. sc, stratum corneum. gl, granular layer. sl, spinous layer. bl, basal layer. tf, tonofilaments. Bars, 400 nm.

Finally, the differentiation capacity of knockout epidermis was examined by tracing K10 and involucrin as early and late differentiation markers. However, neither for K10 nor involucrin were differences in staining patterns of control and K5-Cre KO keratinocytes detectable (see supplementary Fig. S5A-D in manuscript copy 1 included as Appendix). I also did not observe alterations in the distribution of involucrin to soluble and insoluble cell fractions (Fig. 17B). These data indicated that in K5-Cre KO mice epidermal stratification and differentiation proceeded normally.

Plectin-deficiency does not affect proliferation and survival of keratinocytes

To investigate whether plectin deficiency affects epidermal proliferation, leg skin sections from 1-day-old K5-Cre Ko and control mice were immunostained using antibodies to Ki-67, a nuclear protein expressed exclusively during the S, G2, and M phase of the cell cycle (Schluter et al., 1993). Ki-67-positive cells were found in basal and immediate suprabasal keratinocytes of both control and K5-Cre KO epidermis (Fig. 19A,B). A statistical analysis carried out in nonlesional areas of interfollicular epidermis showed that similar numbers of stained cells were present per linear milimeter of basal membrane, namely 58 ± 13.1 and 61 ± 14.3 for wild-type and knockout, respectively (Fig. 19C).

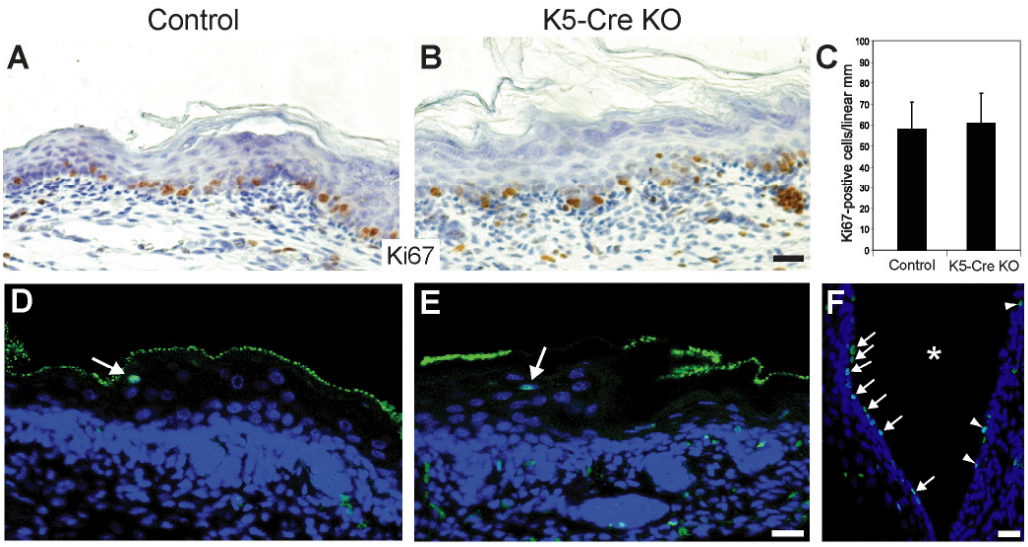

Figure 19. Analysis of epidermal proliferation and keratinocyte survival. (A-B) Sections from the leg skin of 1-day-old control and K5-Cre KO mice were subjected to immunoperoxidase staining using antibodies to Ki-67 and counterstained with hematoxylin. (C) Statistical analysis of Ki-67-positive keratinocytes counted per linear millimeter of interfollicular epidermis basement membrane. Mean values ± standard deviations of three littermate pairs are shown. Note that the numbers of Ki-67-positive cells were similar in control and K5-Cre KO epidermis. (D-F) Control and K5-Cre KO skin sections were subjected to TUNEL assays to detect the presence of apoptotic cells. Nuclei were stained with Hoechst. Arrows, apoptotic cells in the suprabasal layers of the epidermis. No signs of accelerated cell death of basal keratinocytes were visible in interfollicular K5-Cre KO epidermis. The staining along the surface of the stratum corneum is unspecific. In (F), note the occasional presence of apoptotic cells in blister roofs (arrows) and blister floors (arrowheads) of K5-Cre KO skin. Bars, 20 µm.

This result indicated that plectin deficiency did not affect proliferation of keratinocytes in vivo. We also examined the effects of plectin deficiency on apoptosis by TUNEL labeling of the skin of newborn mice. Neither K5-Cre KO basal keratinocytes, nor control cells showed signs of apoptotic cell death (Fig. 19D,E). Similar to another mouse model for EB (Raymond et al., 2005), apoptotic cells were found in the suprabasal cell layers of intrafollicular epidermis, but no differences in their numbers were observed between K5-Cre KO and control mice. Occasionally, singular TUNEL-positive cells lining the exposed epidermal surface of blister roofs were found in K5-Cre KO mice (Fig. 19F), indicating the occurrence of some apoptotic events after epidermal detachment.

Inactivation of the plectin gene in stratified mouse epithelia leads to early postnatal death, caused by severe blistering of the oral epithelium

K5-Cre KO animals were smaller than control animals obviously due to a reduced gain in body weight during their short life span (Fig. 20A). Conditional knockout mice that were nursed at least once after their birth regularly exhibited blisters in their oral cavities (Fig. 20B,C). A detailed analysis of serial sections covering the entire oral cavities of these mice revealed on average 3-4 blisters on their palates (Fig. 20B) and rarely, blister formation on their tongues was observed (Fig. 20C). In contrast, no signs of epithelial detachment were detected in proximal oesophagus of K5-Cre KO mice (Fig. 20D-G). Oral blistering most probably impaired the food intake of K5-Cre KO mice, so that death due to malnutrition ensued, as has been suspected in the case of plectin-null mice (Andrä et al., 1997). Newly born K5-Cre KO pubs were able to suckle milk initially, as indicated by the milk patch shining through the skin of pups (data not shown) and a milk-filled gut (Fig. 20I), similar to control pups (Fig. 20H). However, after initial food intake, subsequent intake seemed to be impaired due to formed blisters, since the stomachs of still-living 2-days-old K5-Cre KO pubs were always empty (Fig. 20I, insert). The presence of milk in the stomach and the intestine of K5-Cre KO pubs (Fig. 20K) after food intake showed that, like in control pups (Fig. 20J), the transport of coagulated milk was not obstructed. Therefore, it could be ruled out that the mutant mice suffered from pyloric atresia, characterized by congenital obstruction of the gastric outlet.

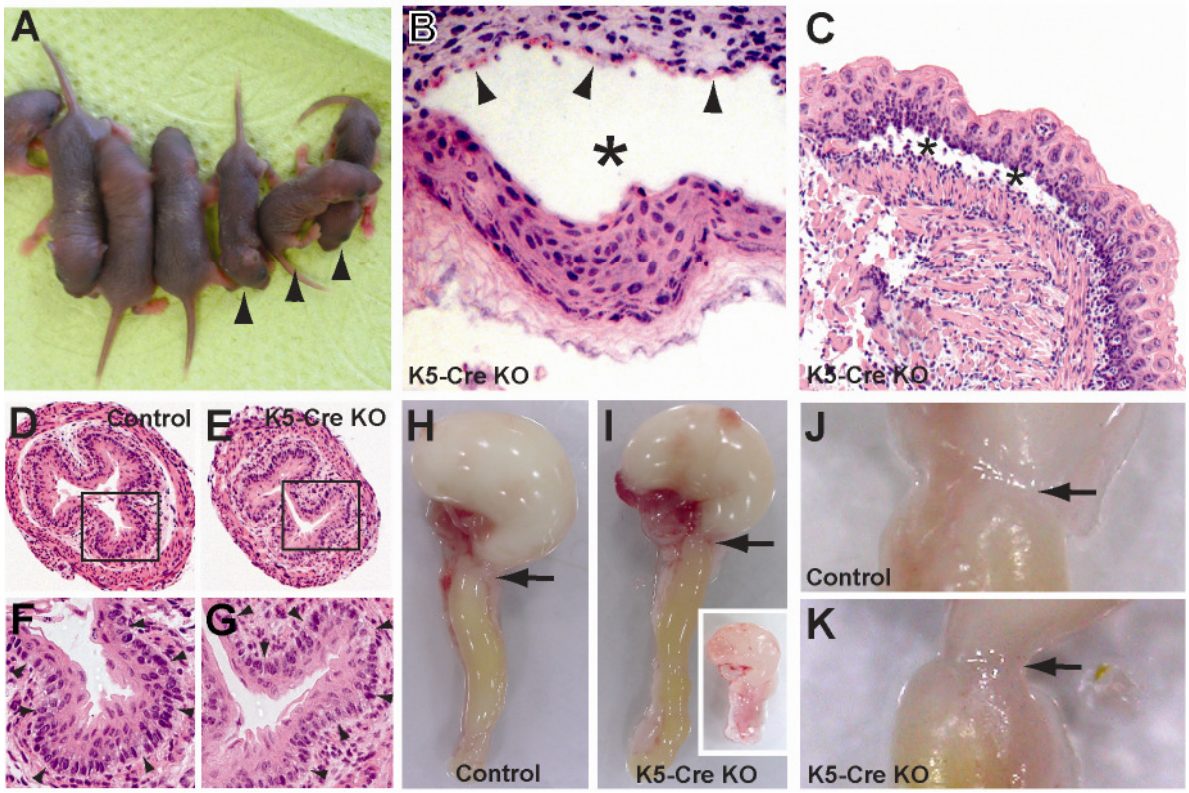

Figure 20. Phenotypic analysis of stratified internal epithelia of K5-Cre KO mice. (A) Size comparison of 2-days-old control and K5-Cre KO pubs (arrowheads). (B) Huge blister (asterisk) detected in the upper palate of a 2-days-old K5-Cre KO pup. Parts of the epithelial tissue (arrowheads) are still attached to the connective tissue, indicating disruption of basal oral keratinocytes. (C) Blister formed at the surface of the tongue. (D-G) H/E stainings of cross-sections of proximal oesophagus from K5-Cre KO (E, G) and control mice (D, F). F and G show magnifications of the boxed areas in D and E. No detachment of the epithelium was observed. Arrowheads in (F, G) denote basement membrane. (H, I) Comparison of stomachs and upper intestines of newborn control and K5-Cre KO pups. (J, K) Magnifications of pyloric regions. Note the translocation of the milk from the stomach to the gut, showing that the K5-Cre KO pup has not been affected by pyloric atresia. The insert in (I) shows the empty stomach of a 2-days-old KO pub. Arrows point to the pyloric regions.

Inducible knockout of plectin in adult mouse skin leads to increased epidermal fragility

Since K5-Cre KO mice, similar to plectin-null mice, died within a few days after birth, they were not suitable as an animal model for studying consequences of plectin loss at later stages in lifetime. To overcome these limitations, conditional gene targeting was employed, using the Cre/*loxP* recombination system with an inducible chimeric Cre-ER^T recombinase that can be activated by tamoxifen or 4-hydroxy-tamoxifen (OHT), but not by endogenous estradiol (Feil et al., 1996). To achieve temporally controlled somatic plectin ablation in the epidermis, I crossed mice with one *floxed* and one null allele ($Plec^{flox/-}$) with transgenic mice expressing the chimeric Cre-ER^T recombinase under the control of the bovine K5 promoter (Indra et al., 1999). Resulting mice with a $Plec^{flox/-}$:K5-Cre-ER^T genotype were injected intraperitoneally with 1 mg OHT per day for five consecutive days and were subjected to phenotypic analyses two weeks after the last injections. Southern blotting analysis showed that the floxed plectin allele was converted to the Δ allele to an extent of ~35% under these conditions (Fig. 21A).

Immunofluorescence microscopy of frozen tissue sections, using anti-pan-plectin antiserum, revealed that plectin deletion in skin was in fact mosaic. In leg as well as in tail and ear skin, large patches of epidermis expressing plectin were interspersed with small patches lacking plectin expression (Fig. 21B-D). Histological analysis of sections from tail and shaved back skin revealed normal organization of the epidermis and the absence of microblisters (Fig. 21E). However, small blisters could be induced by repeated tape strippings using D-squame disks (Fig. 21F,G), indicating that localized (mosaic) plectin deficiency made the epidermis of adult mice more susceptible to mechanical stress, although the rest of plectin-expressing cells were sufficient to prevent epidermal detachment.

Overall, the data obtained with the inducible mouse model demonstrated that even localized plectin deficiency in the epidermis renders keratinocytes more prone to mechanical stress-inflicted damage.

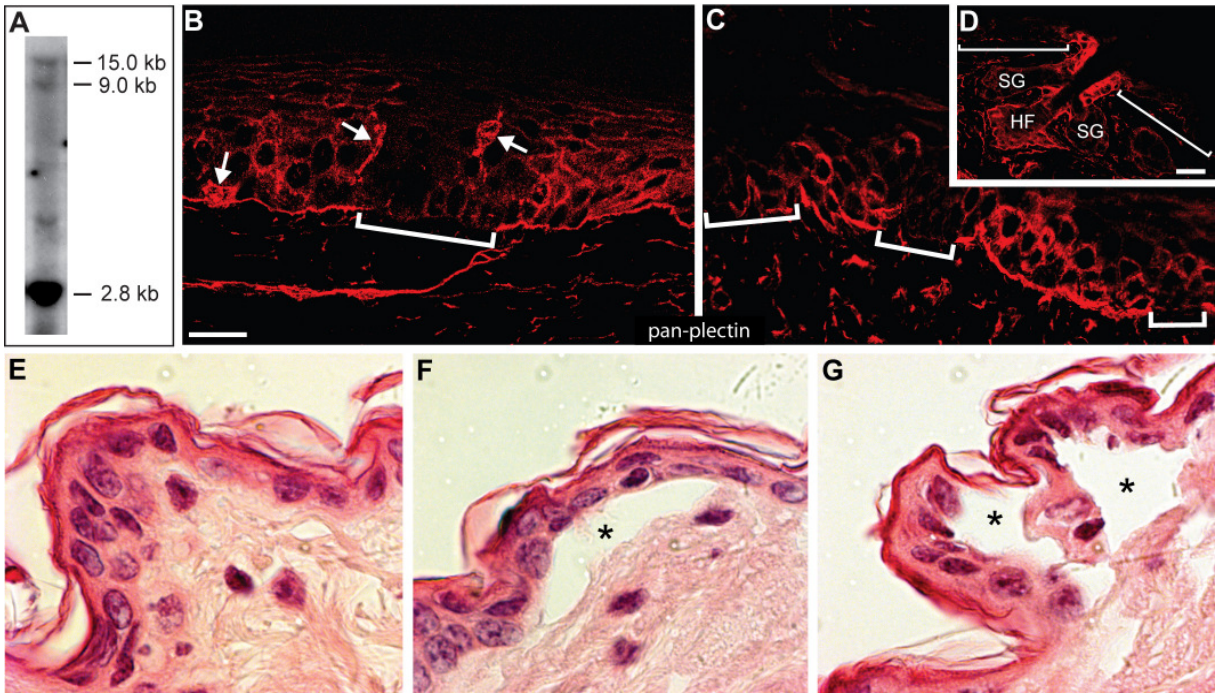

Figure 21. Inducible knockout of plectin in mice and examination of epidermal integrity. (A) Southern blot analysis (autoradiography) of DNA isolated from the epidermis of a *PLEC*$^{flox/-}$:K5-Cre-ER^{T} mouse after treatment with OHT. DNA was digested with *Nco*I as described in (see supplementary Fig. 2 in manuscript copy 1 included as Appendix), and hybridized with the Nco probe shown in (see supplementary Fig. S1A in manuscript copy 1 included as Appendix). The 2.8 kb signal stems from the plectin-null allele. Note partial Cre-mediated recombination after OHT treatment. (B-D) Immunofluorescence microscopy of frozen leg (B), ear (C) and tail (D) skin sections of OHT-treated *PLEC*$^{flox/-}$:K5-Cre-ER^{T} mouse specimens using anti-pan-plectin antiserum. Note patches of plectin-deficient keratinocytes in intrafollicular epidermis (brackets). Arrows in (B) depict non-keratinocyte plectin-positive cells, most likely melanocytes and Langerhans cells. HF, hairfollicle. SG, sebaceous gland. (E-G) H/E stainings of tail skin (E, F) and shaved back skin (G) specimens from OHT-treated *PLEC*$^{flox/-}$:K5-Cre-ER^{T} mice, showing normal skin morphology and absence of microblisters in unstressed skin (E) and formation of microblisters (asterisks) after repeated (10 x) tape strippings with D-squame disks (F, G). Bars, 20 µm.

PART II – Plectin as a regulator of keratinocyte cytoarchitecture and migration.

Molecular characterization of an immortalized mouse keratinocyte cell line

In general the isolation of keratinocytes from the epidermis of newborn or one-day old plectin null or K5-Cre KO mice gave a very low yield of viable cells (data not shown). Since one step in the isolation procedure of keratinocytes involves mechanical separation of the epidermis from the dermis (Caldelari et al., 2000; Hager et al., 1999), it is likely, that plectin-deficient keratinocytes in the basal epidermal layer were ruptured due to their extreme fragility (see Fig. 13H,I). Since the basal epidermal layer comprises stem cells and transit amplifying cells, cytolysis of these cells results in a culture with only few proliferating cells.

For that reason, I used for my experiments two immortalized keratinocyte cell lines that had previously been generated in our lab by A. Jörgl (Andrä et al., 2003). These cell lines were derived from plectin (+/+), p53 (-/-) and plectin (-/-), p53 (-/-) mice and from now on will be referred to as plectin (+/+) and plectin (-/-) keratinocytes, respectively. Plectin (-/-) keratinocytes originated from plectin-null mice (line 29) carrying a disruption in plectin`s rod-encoding exon 31, which completely prevents expression of the protein (Andrä et al., 2003; Andrä et al., 1997). Inactivation or loss of p53 facilitates keratinocyte immortalization (Boukamp et al., 1988; Raymond et al., 2005; Raymond et al., 2007; Sedman et al., 1992), but does not cause cell transformation (Sedman et al., 1992), in contrast to, i.e., expression of human papilloma virus E6 and E7 proteins (Sedman et al., 1992), or infection with SV40 virus (Steinberg and Defendi, 1983).

Freshly isolated (primary) keratinocytes in culture express a specific set of keratins, namely K5 and K14, K6 and K16, and K17 (Boukamp et al., 1988; Lloyd et al., 1995; Troy and Turksen, 1999). Comparison of the keratin expression profile in high-salt resistant cell fractions of primary mouse keratinocytes and plectin (+/+) keratinocytes revealed identical patterns (Fig. 22A). Moreover, similar expression levels of the basal keratinocyte-specific keratins K5 and K14 could be detected in primary compared to plectin (+/+) and plectin (-/-) keratinocytes (Fig. 22B). In addition to K5 and K14, plectin (+/+) and plectin (-/-) keratinocytes expressed K6 and K16 at similar levels (Fig. 22C).

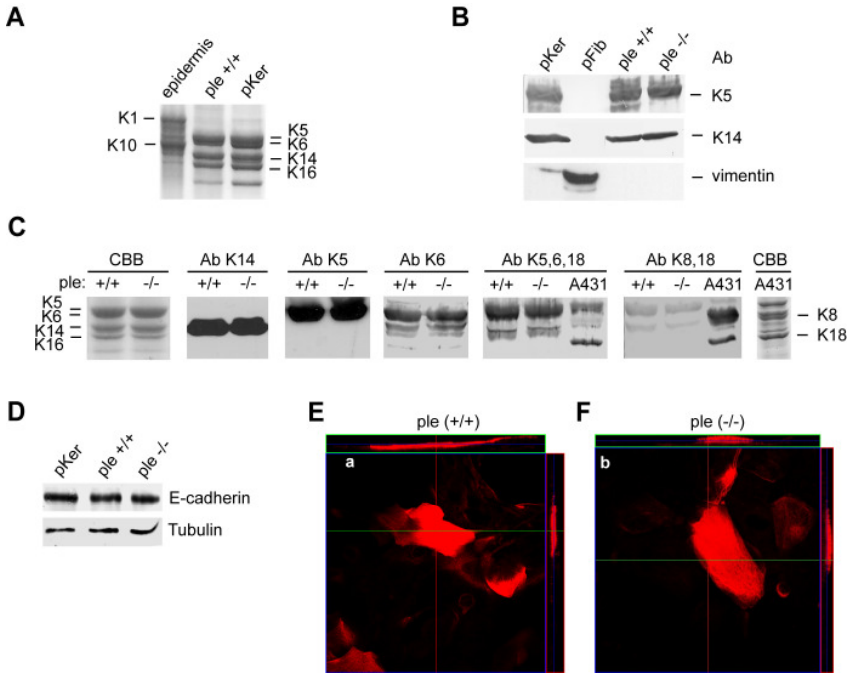

Figure 22. Expression levels of keratins in wild-type and plectin-deficient cells monitored by immunoblotting. Total cell lysates or high-salt extract (HSE) cell fractions prepared from primary keratinocytes (pKer), primary fibroblasts (pFib) and immortalized (p53-deficient) plectin (+/+) (ple +/+) and plectin (-/-) (ple -/-) keratinocytes were subjected to SDS-PAGE, and protein bands were either directly visualized with Coomassie brilliant blue (CBB) or subjected to immunoblotting using the antibodies (Ab) indicated. (A) Keratin expression patterns (CBB-staining) assessed in HSE fractions from whole epidermis, immortalized plectin (+/+) keratinocytes, and primary keratinocytes (pKer). Note that pKer and plectin (+/+) cells show similar expression patterns and that K1 and K10, which are typical for differentiated keratinocytes, are hardly expressed in plectin (+/+) cells. (B) Immunoblotting of cell lysates revealing comparable expression levels of K5 and K14 in primary keratinocytes (pKer), plectin (+/+), and plectin (-/-) cells. Note that immortalized keratinocytes do not express vimentin, whereas the faint signal observed with primary cell cultures stems from contaminating melanocytes. (C) Comparative immunoblotting analysis of different keratins present in cell lysates and HSE fractions (CBB only) of immortalized keratinocytes. The relative positions of keratinocyte and A431 cell keratins are indicated on the flanking CBB-stained PA gels. Note that plectin (+/+) and (-/-) keratinocytes express comparable levels of K14 (Ab K14), K5 (Ab K5), and K6 (Ab K6). Anti-pan-keratin antibodies, recognizing keratins 5, 6, and 18 (Ab K5, K6, and K18), are immunoreactive with corresponding antigens in plectin (+/+) and (-/-) cells and in A431 cells. Keratins 8 and 18 (Ab K8 and K18) are expressed in A431 cells, but not in immortalized keratinocytes. Note weak cross-reactivities of Ab K5, K6, K18 and Ab K6 with K14, and of Ab K8 and K18 with K5 and K14. (D) E-Cadherin expression levels. Tubulin, loading control. (E, F) Projection images generated from Z-stacks through K10 stainings of stratified epithelial sheets.

Neither cell line expressed K8 and K18 (refer to Fig. 22C), and the type 3 IF protein vimentin (Fig. 22B), which become expressed during malignant transformation of keratinocytes (Cano et al., 1996; Davies et al., 2005; Pei et al., 1992; Taki et al., 2003) and moreover were found to be expressed in many commonly used keratinocyte cell lines (Geerts et al., 1999). One hallmark of malignant transformation of keratinocytes is the downregulation of cell-cell junction-associated proteins such as E-cadherin (Faraldo et al., 1997; Taki et al., 2003; Wilding et al., 1996), concomitant with the disassembly of cell-cell contacts (Cano et al., 1996) and resistance against calcium-induced differentiation (Kulesz-Martin et al., 1983; Raymond et al., 2007; Wilding et al., 1996). Howver, E-cadherin was expressed at similar levels in plectin (+/+) and plectin (-/-) keratinocytes (Fig. 22D) and cell-cell contact formation was not compromised (see Figs. 43 and 44). Upon calcium-induced differentiation (Hennings et al., 1980; O'Keefe et al., 1987), both, plectin (+/+) and plectin (-/-) keratinocyte cultures stratified and expression of the suprabasal keratinocyte-specific keratin K10 was upregulated in differentiating suprabasal keratinocytes (Fig. 22E;F). In summary, both keratinocyte cell lines displayed all biological features typical for cultured keratinocytes, including stratification and differentiation, and did not show signs of ongoing malignant transformation. Nevertheless, throughout this project I used low passage cultures (passages 4-10) of the keratinocyte cell lines in order to exclude cellular alterations that might occur after spontaneous acquirement of other mutations.

Plectin links keratin filaments alternatively to integrin α6β4 or actin filaments

Physical proximity and mutual dependence of keratin and actin filaments in keratinocytes has long been known (Green et al., 1987). The original observation was supported by pharmacological studies using actin-depolymerizing drugs to destroy the F-actin network in keratinocytes (Kitajima et al., 1986) and in keratin-transfected SW-13 cells (Woll et al., 2005). Complete destruction of actin filaments leads to a concentration of keratin filaments in dense bundles around the nucleus (Woll et al., 2005), along with the formation of networks of star-like knots or foci colocalizing with actin aggregates (Kitajima et al., 1986), demonstrating a tight interaction of keratin and actin filaments.

Plectin, with its N- and C-terminally located actin and IF-binding domains, is believed to play an essential part in the integration of the keratin and actin networks in keratinocytes.

In fact, codistribution of plectin and MFs has been noted in cultured keratinocytes (Geerts et al., 1999), in addition to plectin`s predominant association with hemidesmsome-like structures (Andrä et al., 2003; Geerts et al., 1999). To obtain more insight into plectin`s role in the crosslinking of keratin and actin filaments and in the organization of the keratin network, I determined the subcellular distribution of plectin, as well as of actin and of keratin filaments in plectin (+/+) keratinocytes, and analyzed their distribution patterns after pharmacological destruction of the actin filaments.

Both, plectin (+/+) and plectin (-/-) keratinocytes, adhered on collagen I matrices within 1 hour after seeding and thereafter started to spread. Spreading was characterized by flattening of cells, followed by extension of lamellipodia. In plectin (+/+) keratinocytes that had attached to the collagen I matrix and were beginning to spread, the actin cytoskeleton was most frequently found to be composed of numerous concentrically arranged bundles of MFs that were intersected by a series of radial spoke-like MF bundles that extended radially from the cell center to the cell periphery (Fig. 23B).

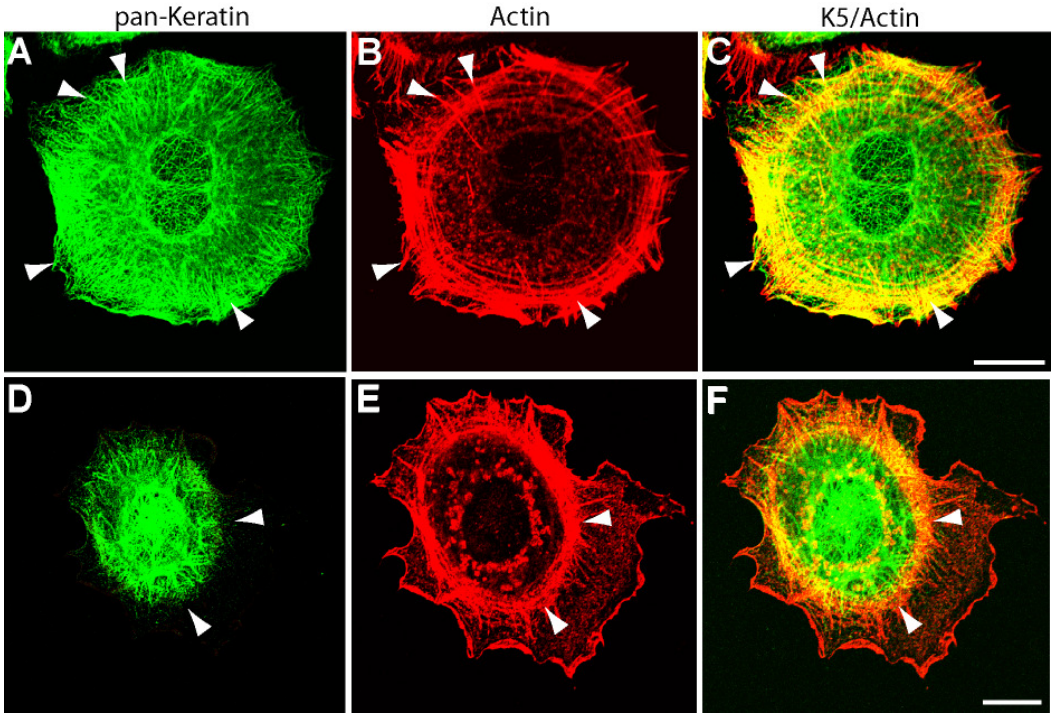

Figure 23. Cytoarchitecture of keratin and actin filament networks in adherent vs. spreading mouse keratinocytes. Cells were immunolabeled using antiserum to actin (B, C, E, F) and anti-pan-keratin mAbs (A, C, D, F). Arrowheads in A-C depict codistribution of keratin filaments with radial actin bundles in a spread cell. Arrowheads in D-E point to a concentric ring of MFs forming a boundary for keratin filament extension. Bars, 10 µm.

Such an organization of actin filaments is typical of subconfluent keratinocyte cultures (Green et al., 1987; Vasioukhin et al., 2000). Keratin filaments extended from the nucleus, where they were forming a cage-like envelope, to the cell periphery (Fig. 23A), where they were colocalizing with MFs (Fig. 23C, arrowheads). As keratinocytes spread and started to migrate, they formed multiple lamellipodia along the outside of the concentrically arranged MF bundles (Fig. 23E). Interestingly, keratin filaments were restricted to the boundaries defined by the outermost of the concentric MF bundles (Fig. 23D,F).

Freshly spreading keratinocytes formed a peripheral ring-shaped zone densely packed with plectin structures (Fig. 24A) which codistributed with MFs (Fig. 24C) and clusters of integrin α6β4 (insert in Fig. 24C).

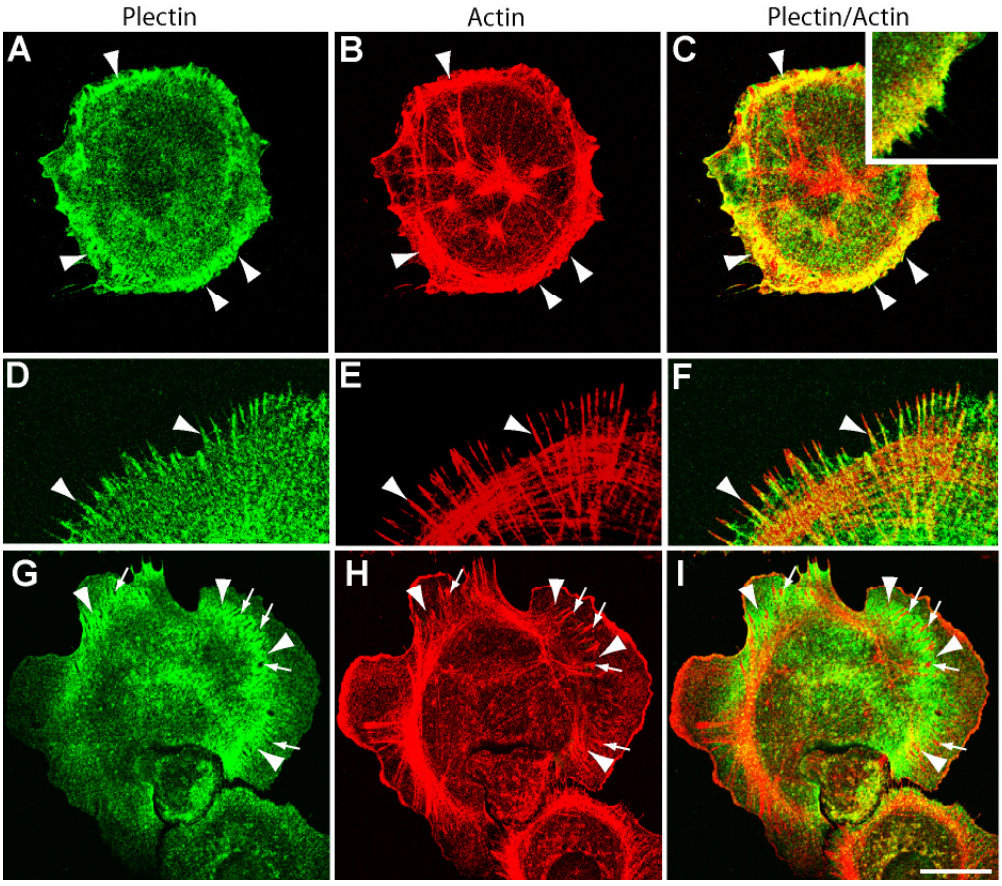

Figure 24. Distribution of plectin in adherent versus spreading mouse keratinocytes. Cells were immunolabelled using antiserum to plectin (A, C, D, F, G, I) and mAbs to actin (B, C, E, F, H, I). Arrowheads in A-C, codistribution of plectin with cortical actin bundles in a freshly spreading cell. Arrowheads in D-F, codistribution of plectin with radial actin bundles. (G-I) At early timepoints of spreading, plectin and actin segregate into stable anchoring contacts (SACs) and stress fibers/focal adhesion contacts (small arrows), respectively. Bar, 10 μm.

Moreover, in some cells, colocalization of actin with discontinuous plectin-positive structures could be observed along radial MF bundles (Fig. 24F). As keratinocytes started to form lamellipodia, plectin/integrin α6β4 clusters enlarged and clearly segregated from MFs (Fig. 24I, arrowheads), however, they were still found in close proximity to focal adhesions, that were identified as the origins of stress fibers (Fig. 24I, arrows). These clusters of plectin and integrin α6β4 proteins have been previously called stable anchoring contacts (SACs) and correspond to HDs of basal keratinocytes found in the epidermis in situ (Carter et al., 1990).

Ultimately, SACs became reorganized into a peripheral ring-shaped structure, with keratin filaments extending to the inner circumference of this ring (Fig. 25A, arrows), as if SACs acted inhibitory on filament extension. At early timepoints of spreading (e.g. shortly after the 1 hour adhesion period) plectin-positive dots could be seen along the tips of keratin filaments extending to the cell periphery (insert in Fig. 25C), indicating that keratin filaments were possibly captured by plectin molecules at maturing SACs.

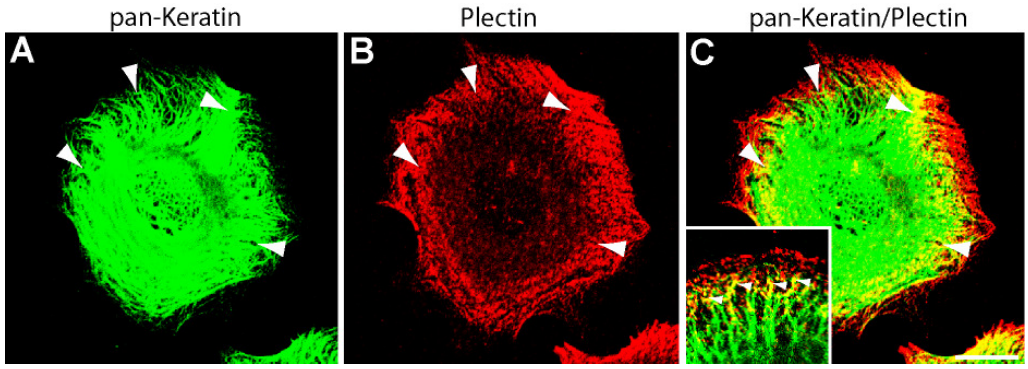

Figure 25. Relative distribution of plectin and keratin filament networks in freshly spreading mouse keratinocytes. Cells were immunolabeled using antiserum to plectin (B, C) and anti-pan-keratin mAbs (A, C). Arrowheads depict peripheral endings of keratin filaments. The insert in C shows plectin distribution along the tips of peripheral keratin filaments in a cell which has just started to spread. Bar, 10 µm.

Treatment with cytochalasin D during the spreading period resulted in destruction of the MF network and the formation of actin aggregates by depolymerization of MFs (Fig. 26B). As a consequence, keratin filaments showed a dramatic reorganization into a network of connecting star-like knots or foci (Fig. 26A) that coincided with the actin aggregates (Fig. 26C).

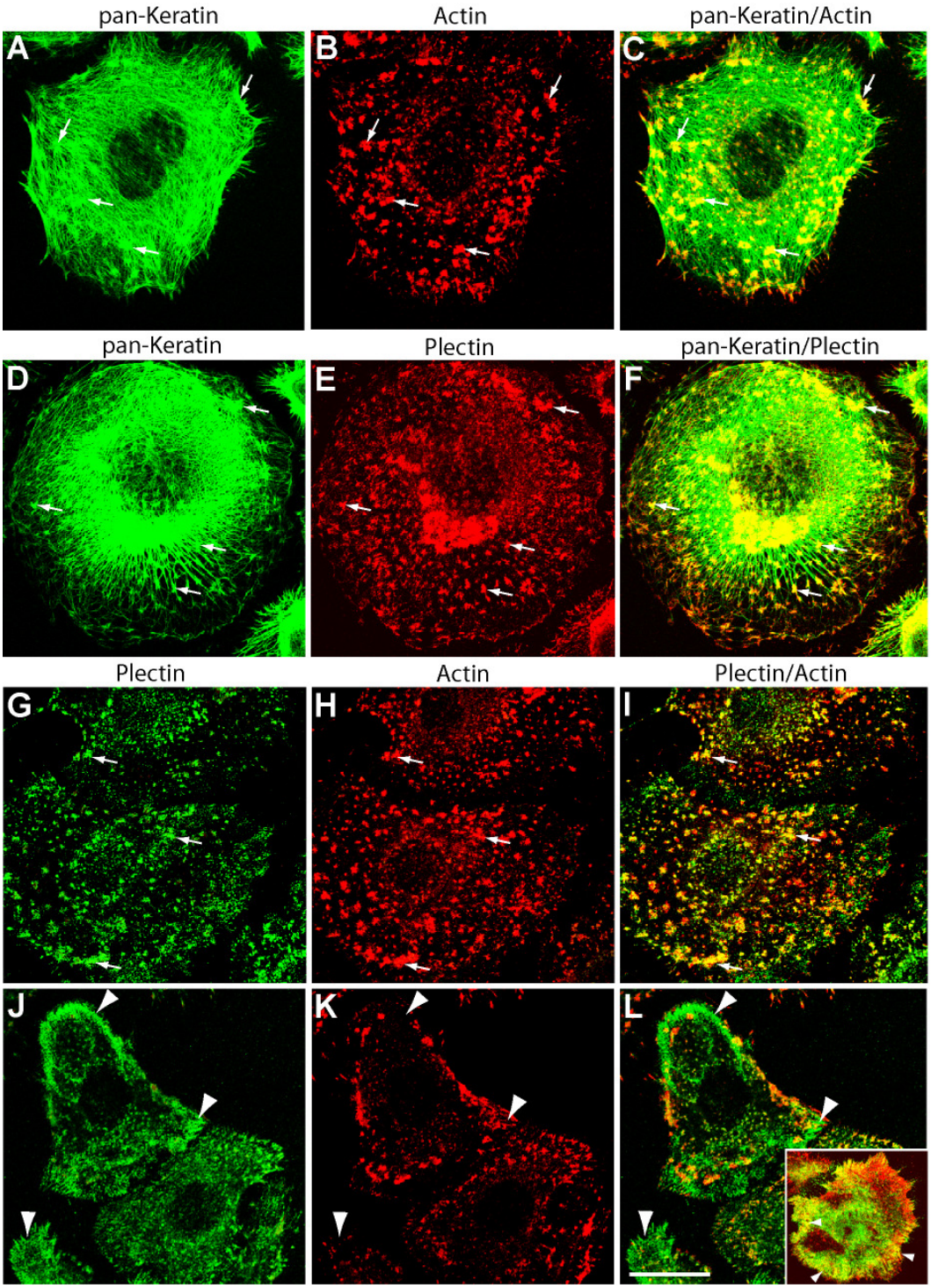

Figure 26. Distribution of plectin, actin, and keratin filament networks after cytochalasin D treatment. Cells were immunolabelled using antiserum to actin (B, C, H, I, K, L), antiserum to plectin (E-G, I, J, L, insert in L), anti-pan-keratin mAbs (A, C, D, F) and mAbs to integrin α6 (insert in L). Arrows in A-I depict actin-containing patches coinciding with keratin filament foci (C) and plectin (I). Arrowheads in J-K point at cytochalasin-D resistant plectin localizing in SACs. The insert in L shows cytochalasin D-resistant colocalization of plectin with integrin α6. Bar, 10 µm.

No changes in the organization of the MT network could be observed under these conditions (data not shown). As expected, plectin was also found to codistribute together with keratin (Fig. 26F) and actin (Fig. 26I) in the star-like foci. However, in many cells, plectin remained also partially associated with integrin α6 in SACs at the cellular periphery (Fig. 26L). Thus, when plectin is associated with SACs, it cannot redistribute together with actin. These data are in excellent agreement with Geerts et al. (1999), who showed that plectin binds actin and integrin β4 in a mutually exclusive manner, and confirm plectin as a crosslinker of keratin filaments to either integrin α6β4 or MFs. Moreover, these data show that the stability of SACs is not dependent on MFs.

Plectin-deficient keratinocytes display enhanced spreading along with reduced integrin ß4 clustering

During routine subculture of our immortalized keratinocyte cell lines, I regularly observed an increased number of lamellipodia in freshly passaged cultures of plectin (-/-) keratinocytes (data not shown), indicative of enhanced spreading and cell migration. To quantify cell spreading, freshly seeded cultures of plectin (+/+) and plectin (-/-) keratinocytes were fixed after 1 and 3 hours, respectively, stained with phalloidin to visualize F-actin (Fig. 27A-D), and their cell circumferences were measured. Both, plectin (+/+) and plectin (-/-) keratinocytes, adhered on collagen I matrices within 1 hour after seeding and displayed a similar subcortical organization of MFs (Fig. 27A,B). After 3 hours of adhesion to collagen I, keratinocytes started to spread (Fig. 27C,D). Plectin (-/-) keratinocytes that had adhered to collagen I matrices for 3 hours showed higher cell circumference values, demonstrating increased lamellipodia formation (Fig. 27D,I). Vinculin staining patterns were similar between spreading plectin (+/+) and plectin (-/-) keratinocytes (Fig. 27E-H), indictaing normal assembly and turnover of focal adhesions contacts.

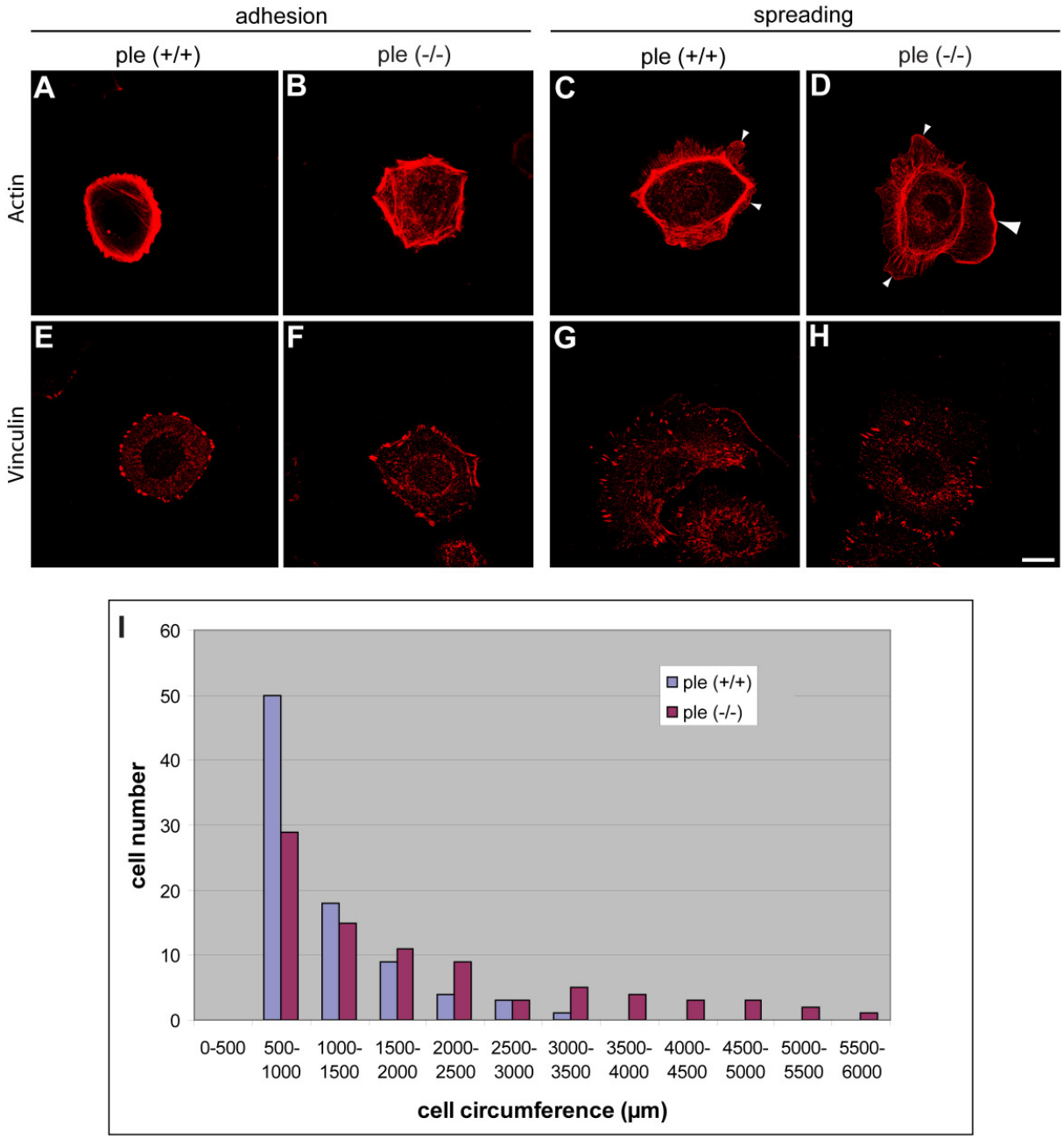

Figure 27. Distribution of actin filament networks and focal adhesion contacts in adhering versus spreading wild-type and plectin-deficient keratinocytes. Freshly adhered (1 hour after seeding), or spreading (3 hours after seeding) wild-type [ple (+/+)] and knockout [ple (-/-)] cells were immunolabeled using antiserum to actin (A-D) or mAbs to vinculin (E-H). Small arrowheads in (C, D) depict small lamellipodia found in both cell types; in addition plectin (-/-) keratinocytes formed large lamellipodia (large arrowhead in D). (I) Quantitative analysis of keratinocyte spreading. Histogram shows the distribution of measured cell circumference of 50 wild-type (ple +/+) and plectin-deficient (ple -/-) keratinocytes, each, after 3 hour of adhesion. Bar, 10 µm.

Faster migration of plectin (-/-) keratinocytes

As plectin-deficient keratinocytes showed enhanced spreading (Fig. 27I), it was of interest to analyze their migratory behavior. Migration was analyzed of single keratinocyte cells and of keratinocytes in epithelial monolayers. A so called "scratch wound closure assay" was used to analyze the migration of keratinocytes that were growing in a confluent epithelial cell monolayer into an artificially introduced "wound". Average migration distances measured for plectin (-/-) cells in this assay were almost twice as long as those of plectin (+/+) cells (Fig. 28A-C).

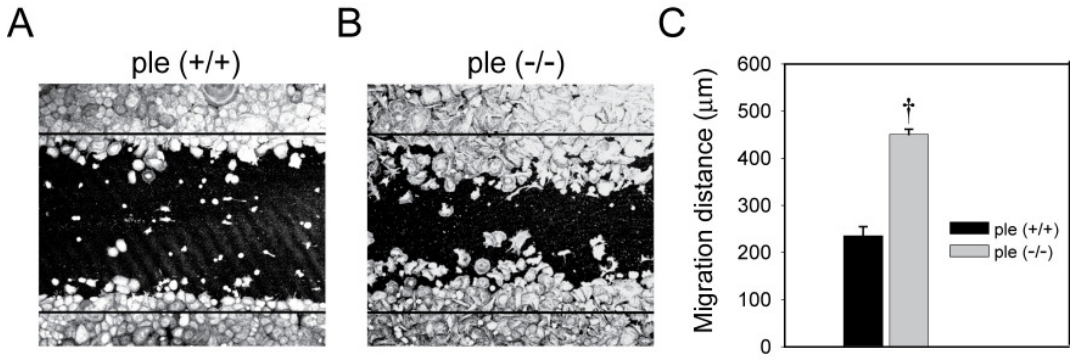

Figure 28. Faster migration of plectin (-/-) keratinocytes in scratch wound closure assays. (A, B) Cells were stained using mAbs to actin (false gray color). The lines drawn in the images represent reference lines marking the width of the scratch when it was made. (C) Average values of migration distances from 10 different optical fields (10x objective) from three independent experiments are shown (mean ± the SEM). †, $P < 0.001$.

In addition, migration of single cells in sub-confluent wild-type and plectin (-/-) keratinocyte cultures was measured by time-lapse video microscopy (measurements were done together with G. Burgstaller). Migration measurements were started after initial adhesion and spreading. In accordance with migration distances measured in "scratch wound closure assays" (Fig. 28C), plectin (-/-) keratinocytes displayed a migration velocity (1.58 µm/min) approximately two times as high as that of plectin (+/+) cells (0.82 µm/min), when observed 3-6 hours after plating (data not shown). By analysis of the migrated distances and the processive index, which describes the directionality of migration (see materials and methods), cells could be clustered into three groups according to their migratory behavior (Fig. 29).

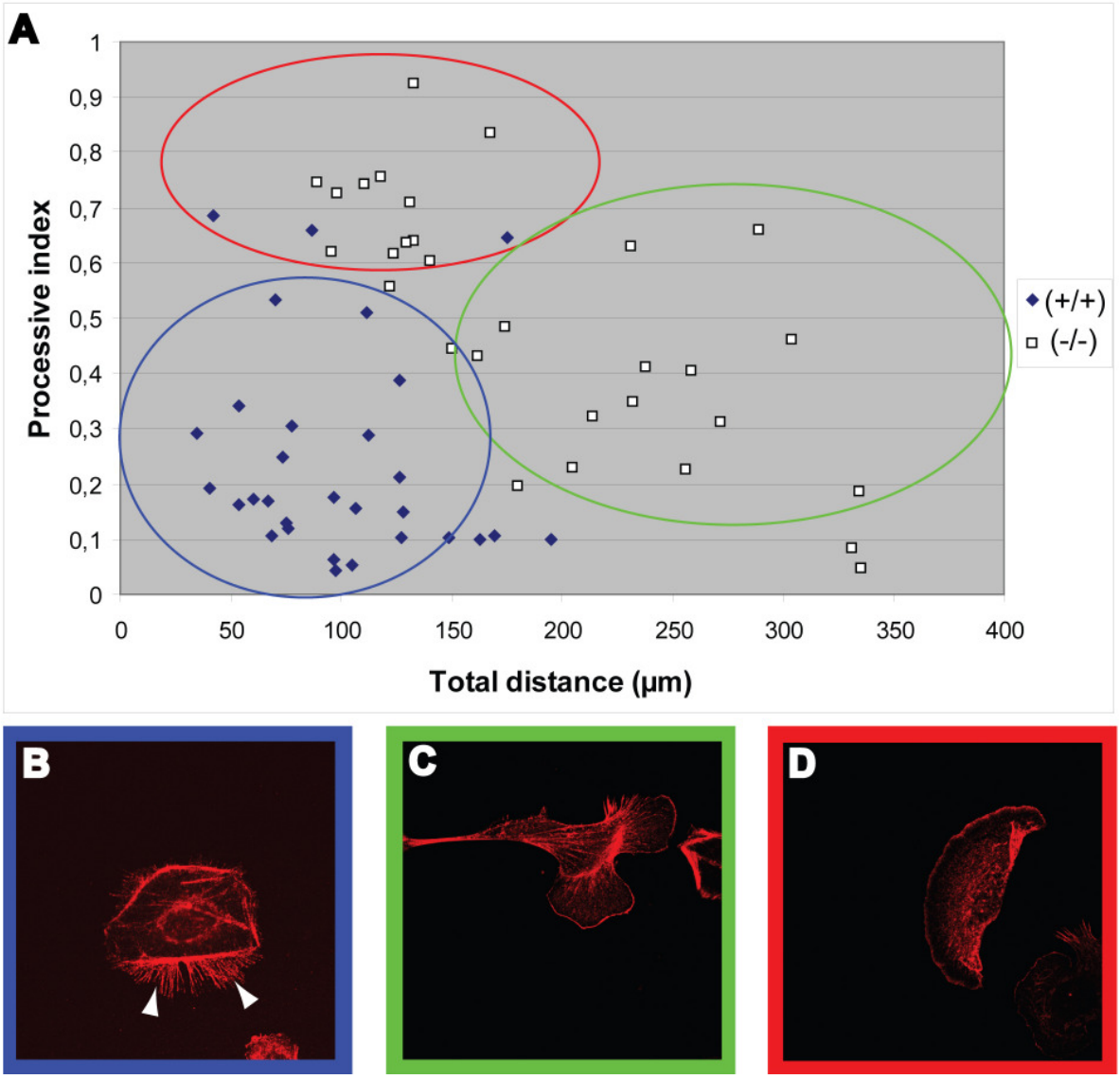

Figure 29. Faster migration of single plectin (-/-) keratinocytes. (A) Processive indexes of 30 wildtype (+/+) and plectin-deficient (-/-) cells are shown as a function of the total migrated distance. Three clusters defined by distinct migratory behavior are indicated by colour coded circles. (B-D) Representative images of the shapes of cells belonging to one of the clusters defined in (A). Cells were stained using mAbs to actin. The association with a cluster is indicated by colour coded image borders.

The first group consisted of cells that had migrated only over short distances and displayed a relatively low processive index, meaning that cells migrated with little directional persistence (Fig. 29A,B). Cells belonging to this group showed a flattened, spread morphology and frequently displayed retraction fibers (Fig. 29B, arrows). Only plectin (+/+) keratinocytes belonged to the first group. The second group comprised cells with relatively

long migration distances and low processive indexes (Fig. 29A). These cells were usually characterized by an aberrantly spread morphology with multiple, randomly oriented protrusions (Fig. 29C). Interestingly, almost only plectin (-/-) keratinocytes could be found within the second group (Fig. 29A). The third and final group included cells with a low to medium migration distance and a high processive index, indicative of a processive, polarized migration (Frank and Carter, 2004). Accordingly, such cells possessed a large, thin lamellipodium extending at the leading edge that encompassed half the perimeter of the cell (Fig. 29D). Again, mostly plectin (-/-) keratinocytes were found in this group (Fig. 29A). In summary, plectin (-/-) keratinocytes displayed an enhanced migratory ability and showed two distinct modes of migration: one was fast, but little polarized, -and the other was slower, but highly polarized.

Plectin organizes the keratin network in migrating keratinocytes

Within one hour after adhesion, clusters of integrin α6 formed along the basal surfaces of plectin (+/+) and plectin (-/-) keratinocytes (Fig. 30A,B), but their numbers appeared to be reduced in plectin-deficient cells (Fig. 30B).

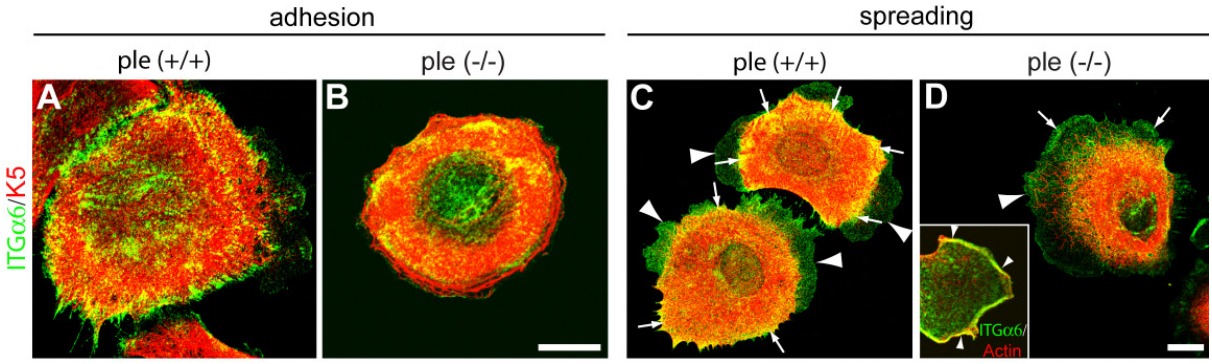

Figure 30. Relative distribution of keratin filament networks and SACs in spreading wild-type and plectin-deficient keratinocytes. Keratinocytes at early (A, B), or late timepoints (C, D) during spreading, were double immunolabeled using antiserum to K5 (A-D), antiserum to actin (insert in D) and mAbs to integrin α6 (ITGα6, A-D). Arrowheads in C and D point to lamellipodial edges. Arrows in C and D depict localization of integrin α6 at peripheral endings of keratin filaments in wild-type cells (C) or at lamellipodial edges in plectin-deficient cells (D). The insert in D shows integrin α6 assoctiation with actin at a lamellipodial edge. Bar, 10 µm.

Both, plectin (+/+) and plectin (-/-) keratinocytes exhibited dense cytoplasmic networks of keratin filaments shortly after adhesion (Fig. 30A,B). During spreading of plectin (+/+) keratinocytes, integrin α6β4 clusters became reorganized into SACs at the cellular periphery, with keratin filaments extending to the inner circumference of this ring (Fig. 30C, arrows). In strong contrast, plectin (-/-) keratinocytes displayed reduced assembly of SACs and integrin α6 was instead located at lamellipodial edges (Fig. 30D, arrows), were it frequently co-localized with F-actin (Fig. 30D, insert).

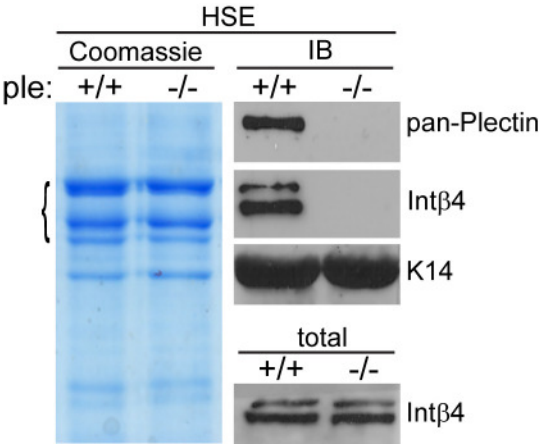

Figure 31. Association of integrin ß4 with the keratin filament network. High-salt extracts (HSE) and total cell lysates (total) from plectin (+/+) and (-/-) keratinocytes were subjected to immunoblotting (IB) using anti-pan-plectin, -integrin ß4 (Intß4) and –keratin 14 (K14) antibodies as indicated, or stained with Coomassie. HSE sample loadings were normalized to equal amounts of keratin. Total cell lysates were normalized to equal protein content. Bracket, positions of keratins.

To address this issue biochemically, I prepared cytokeratin-enriched cell fractions from plectin (+/+) and plectin (-/-) keratinocytes, and compared their integrin β4 content using antibodies to integrin ß4. Cell fractions were highly enriched in K5 (unpublished data) and K14 (Fig. 31) and, in the case of wild-type cells, contained considerable amounts of plectin. Integrin β4 was, however, completely absent from cytokeratin fractions of plectin (-/-) cells. The absence of integrin β4 from the cytokeratin fraction of plectin (-/-) keratinocytes correlated well with the reduced number of SACs found in these cells during spreading (this study) and after overnight culture (Andrä et al., 2003).

Compared to wild-type cells, where the keratin network seemed to be more densely packed around the cell center and keratin filaments appeared to be anchored to SACs (Fig. 30C and Fig. 25I), keratin filaments of plectin (-/-) cells extended further to the cell periphery, often reaching far into lamellipodia (Fig. 30D). This phenotype was noticed independently of whether anti-pan-keratin (recognizing K5, K6 and K18), or anti-K5 antibodies alone were used (data not shown). Regarding expression levels of different keratins, no differences were observed between plectin (+/+) and plectin (-/-) keratinocytes,

as revealed by immunoblotting analysis (Fig. 22A-C). The keratin phenotype became even more pronounced in subconfluent over-night cell cultures (~60% confluence). Plectin (-/-) cells exhibited a significantly enlarged mesh size of keratin networks at their periphery compared to wild-type cells (Fig. 32, compare A with C, and their corresponding magnifications). A quantitative analysis of subconfluent cell populations revealed that more than 70% of plectin (-/-), but only less than 8% of plectin (+/+) keratinocytes displayed such a phenotype. Similar phenotypic alterations of the keratin network were observed in primary keratinocyte cultures obtained from K5-Cre KO mice (Fig. 32E-L) and plectin null mice (see Fig. 1A-F in manuscript copy 2 included as Appendix).

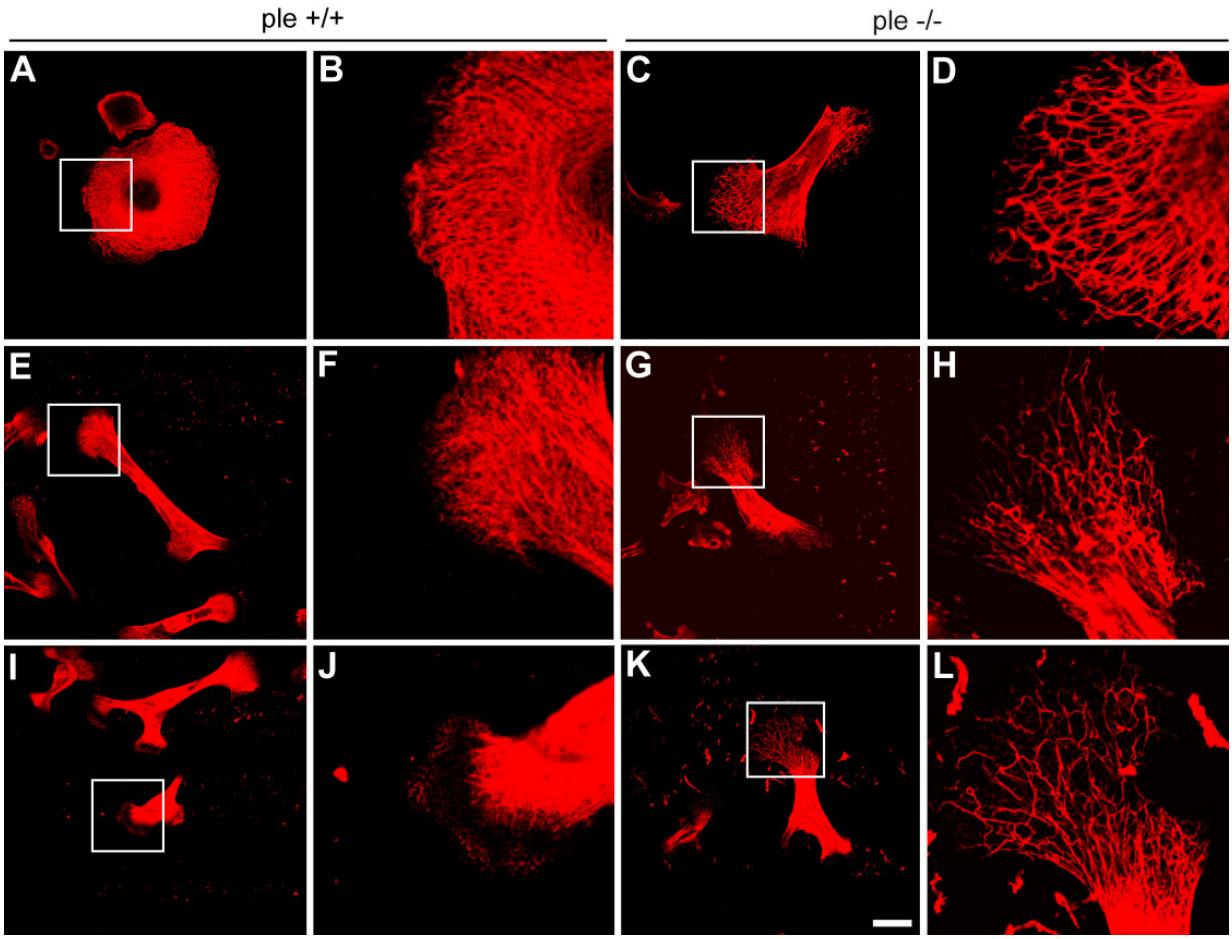

Figure 32. Cytoarchitecture of keratin filament networks in wild-type and plectin-deficient mouse keratinocytes. Immortalized (A-D), and primary (E-L) keratinocytes that were isolated from K5-Cre KO (G, H, K, L) and control (E, F, I, J) mice, were immunolabeled using anti-pan-keratin mAbs. Boxed areas in A, C, E, G, I and K are shown as 4x-magnified images in (B, D, F, H, J, and L), respectively. Bar in K (representative of A, C, E, G, I, and K, respectively), 10 µm.

As described in (Osmanagic-Myers et al., 2006), transmission electron microscopy revealed a prominent lateral bundling of keratin filaments in peripheral regions of immortalized plectin (-/-) cells, resulting in larger spaces between individual and bundled filaments (see Fig. 2A,b in manuscript copy 2 included as Appendix). In some regions, filaments showed a complete lateral collapse, appearing as one massive filamentous bundle (see Fig. 2A,b, arrow, in manuscript copy 2 included as Appendix). Bundling to such an extent was never observed in plectin (+/+) cells, where corresponding areas were dominated by numerous fine, and apparently short filamentous structures, with orthogonal cross-bridges filling the space between the filament bundles (see Fig. 2A,a and c in manuscript copy 2 included as Appendix).

To demonstrate, that the observed changes in keratin network organization where directly connected to plectin deficiency, the phenotypic rescue potential of plectin was examined by transient transfection of plectin (-/-) keratinocytes with an expression plasmid encoding full length mouse plectin isoform 1a, the major isoform normally expressed in this type of cells (Andrä et al., 2003). Similar to endogenous plectin of corresponding wild-type cells (see Fig. 25B), reexpressed plectin 1a showed a punctated distribution pattern (Fig. 33B). However, when expressed at a higher level, plectin 1a was more prominently distributed along keratin filaments than was the endogenous plectin. A quantitative analysis revealed that 90% of plectin (-/-) cells expressing plectin 1a at significantly high levels displayed keratin networks with mesh sizes as small as those of plectin (+/+) cells (Fig. 33F). This strong rescue potential of plectin 1a clearly demonstrated a direct link between the absence of plectin and the observed alterations of the keratin network cytoarchitecture.

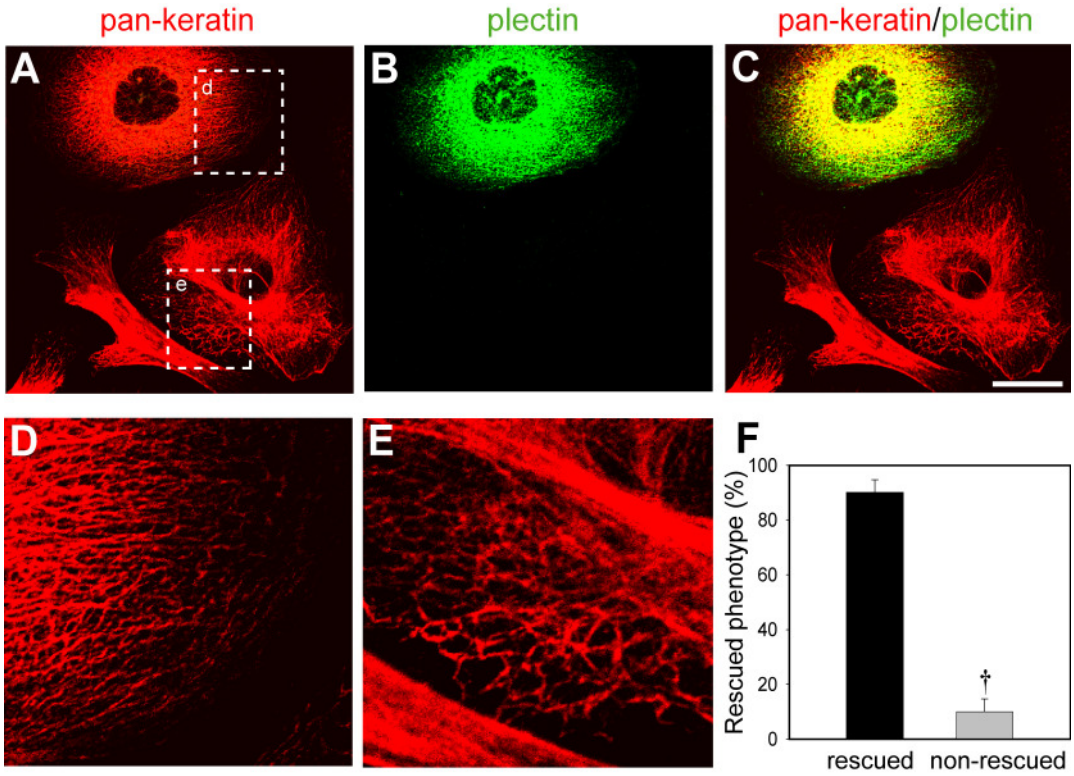

Figure 33. Plectin reduces the mesh size of IF networks. Plectin (-/-) keratinocytes transfected with full-length plectin (isoform 1a) were fixed and immunolabeled for pan-keratin (A, C-E) and plectin (B,C). Boxed areas in A are shown as 4x-magnified images in D and E. Note that there are more delicate filamentous network in cells upon forced expression of plectin (D). (F) Rescue efficiency was determined by analysis of >100 plectin (-/-) cells transiently expressing plectin (three independent experiments). Keratinocytes with average filament–filament distances of below or above 1.5 nm were considered as rescued and nonrescued, respectively. Mean values ± the SEM are shown. †, $P < 0.001$. Bar, 10 µm.

To assess the relationship between the increased mesh size of the keratin network of plectin (-/-) keratinocytes and keratin solubility, I analyzed NP-40-solubilized, Empigen-BB-solubilized and detergent-resistant cell fractions (Liao and Omary, 1996) that were sequentially separated from subconfluent plectin (+/+) and plectin (-/-) cultures (Fig. 34) for their keratin content. Interestingly, K5 and K14, but not K6 and K16, were slightly reduced in the Empigen-BB-soluble fraction, and significantly reduced in the detergent-resistant fraction. Since SACs are enriched in the detergent-resistant fraction (Skalli et al., 1994), these data confirmed the decreased association of K5 filaments with SACs at the cellular periphery that was observed by immunofluorescence microscopy, demonstrating that plectin specifically modulates the K5/14 network.

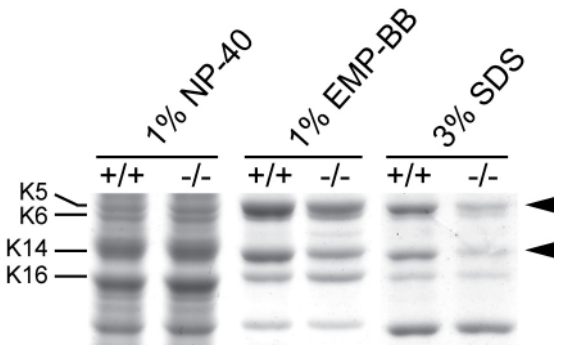

Figure 34. Distribution of keratins in NP-40, Empigen BB-solubilized, and detergent-resistant fractions. Equal numbers of plectin (+/+) and plectin (-/-) cells were solubilized in 1% NP-40 followed by centrifugation to obtain the NP-40 fraction. The residual pellets were solubilized in 1% Empigen BB followed by centrifugation to obtain the EMP-BB fraction. The post-EMP-BB pellet was then solubilized in SDS lysis buffer (SDS-fraction). Equivalent portions of each fraction were subjected to SDS-PAGE, followed by Coomassie staining. The positions of K5 and K14 are indicated by arrowheads.

To establish a direct link between the keratin phenotype and keratinocyte migration, I looked at the distribution of plectin and the organization of keratin network in migrating cells at the wound edge of scratched monolayers of plectin (+/+) and plectin (-/-) cells (Figs. 35 and 36). In migrating wound edge keratinocytes, plectin`s localization changed from SAC-associated to keratin filament-associated (compare Fig. 35C with Fig. 36C). Interestingly, the mesh size of the keratin network in plectin (-/-) keratinocytes along the wound edge was much larger compared to that of cells at a distance from the wound (compare Fig. 35F with Fig. 36F), and in these regions the differences to the keratin network of plectin (+/+) cells became most apparent (Fig. 36 compare A,G with D,J). This was consistent with the finding that an increased keratin network mesh-size characteristic of plectin (-/-) keratinocytes was particularly evident in spreading and subconfluent cell cultures (see Figs. 30 and 32). Together these data highlighted the importance of plectin in organizing keratin cytoarchitecture during cell migration.

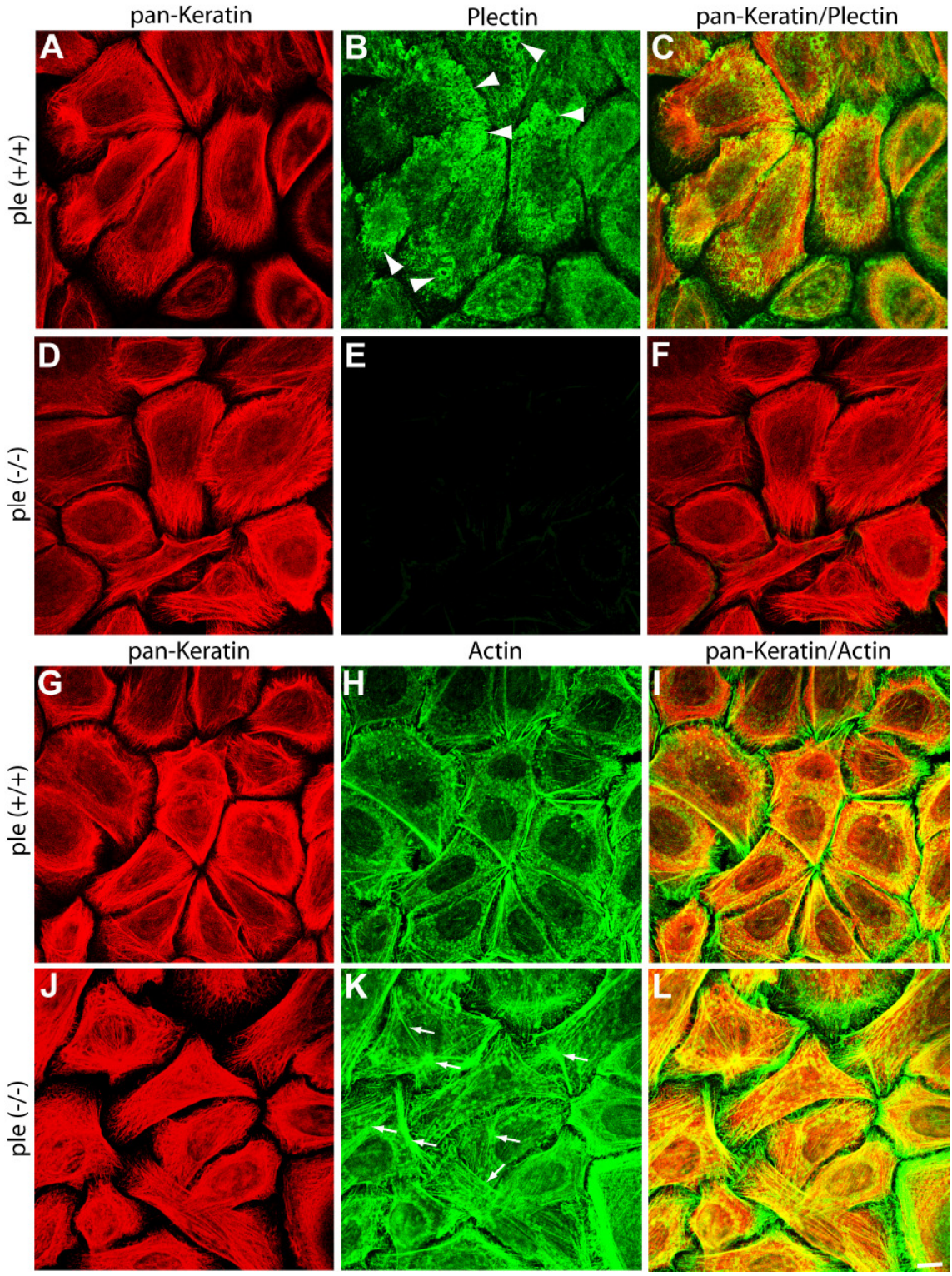

Figure 35. Relative distribution of keratin and actin filament networks in wild-type and plectin-deficient keratinocyte monolayers. Cells were immunolabeled using antiserum to plectin (B, C, E, F), antiserum to actin (H, I, K, L) and anti-pan-keratin mAbs (A, C, D, F, G, I, J, L). Arrowheads in B depict plectin localization at SACs at the basal surface of wild-type keratinocytes. Arrows in K point at prominent actin filament bundles that formed in plectin-deficient keratinocytes. Bar, 10 µm.

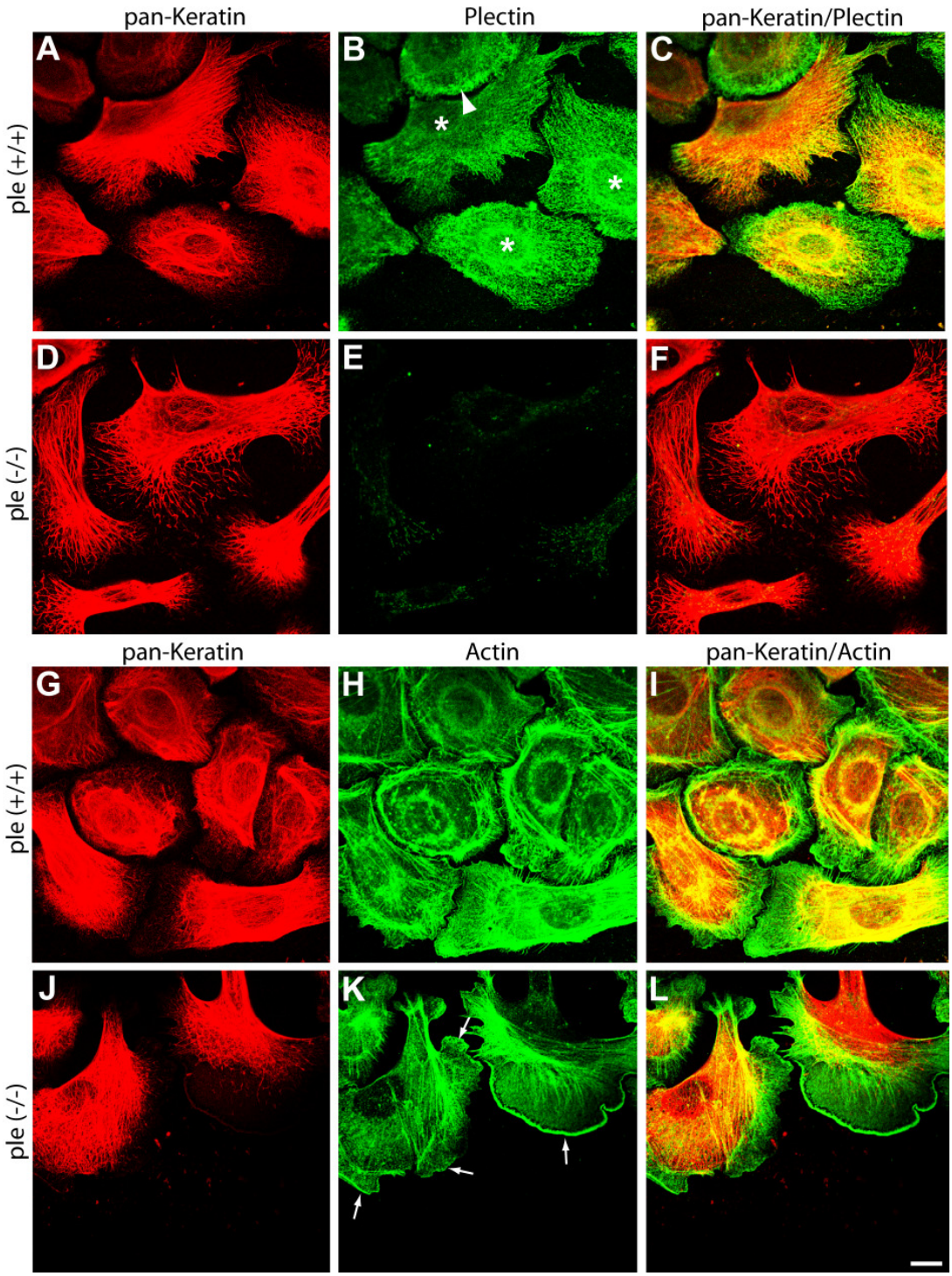

Figure 36. Relative distribution of keratin and actin filament networks in wild-type and plectin-deficient keratinocytes migrating at wound edges. Cells were immunolabeled using antiserum to plectin (B, C, E, F), antiserum to actin (H, I, K, L) and anti-pan-keratin mAbs (A, C, D, F, G, I, J, L). Arrowhead in B depicts plectin localization at SACs at the basal surface of a cell that is resting within the monolyer. Asterisks mark cells that are migrating into the wound and display association of plectin with keratin filaments. Arrows in K point at large lamellipodia that formed in migrating plectin-deficient keratinocytes. Bar, 10 µm.

Faster keratinocyte migration is driven by increased activation of Src/Erk and PKCδ signaling

Keratinocyte migration is driven by two sorts of signals: ECM components and growth factors (Li et al., 2004). Certain ECM components, such as collagens I and IV, fibronectin and precursor laminin 322 are able to initiate migration in the absence of growth factors (Frank and Carter, 2004; Li et al., 2004). On the contrary, the role of growth factors is to augment ECM-initiated motiliy and provide directionality (Li et al., 2004). The Erk1/2 MAPK cascade is the major signaling pathway involved in mediating the initiation signal and the growth factor augmentation signal of the ECM, whereas the p38 cascade specifically mediates only growth factor signals (Li et al., 2004). The Erk1/2 pathway controls the majority of genes expressed early after scratch wounding, whereas p38 mostly participates in the stimulation of immediate and late genes (Fitsialos et al., 2007). In addition, important roles in keratinocyte migration have been attributed to PKCδ (Li et al., 2002b), PI3K (Pankow et al., 2006), Rac1 (Choma et al., 2004; Tscharntke et al., 2007) and c-Src (Yamada et al., 2000).

Since we had observed enhanced migration of plectin (-/-) keratinocytes, I assessed whether Erk1/2 activities were upregulated in these cells. Indeed, I found Erk1/2 activites to be upregulated ~2-fold in plectin (-/-) keratinocytes compared to wild-type cells (Fig. 37A) [using immunoblotting with antibodies recognizing the active (phosphorylated) forms of the kinases]. In contrast, no alterations in the phosphorylation levels of p38 and JNK1/2 could be found (Fig. 37B). Pharmacological inhibition of MEK1, the upstream kinase of Erk1/2, with PD98059 reduced the migration distances of plectin (-/-) keratinocytes by almost a factor of two (Fig. 37C), bringing their level close to that of untreated wild-type cells. Wild-type cells showed a similar drug response. The observed decrease in migration of drug-treated cells directly correlated with the inhibition of Erk1/2 activities, as demonstrated by analysis of Erk1/2 phosphorylation (Fig. 37D).

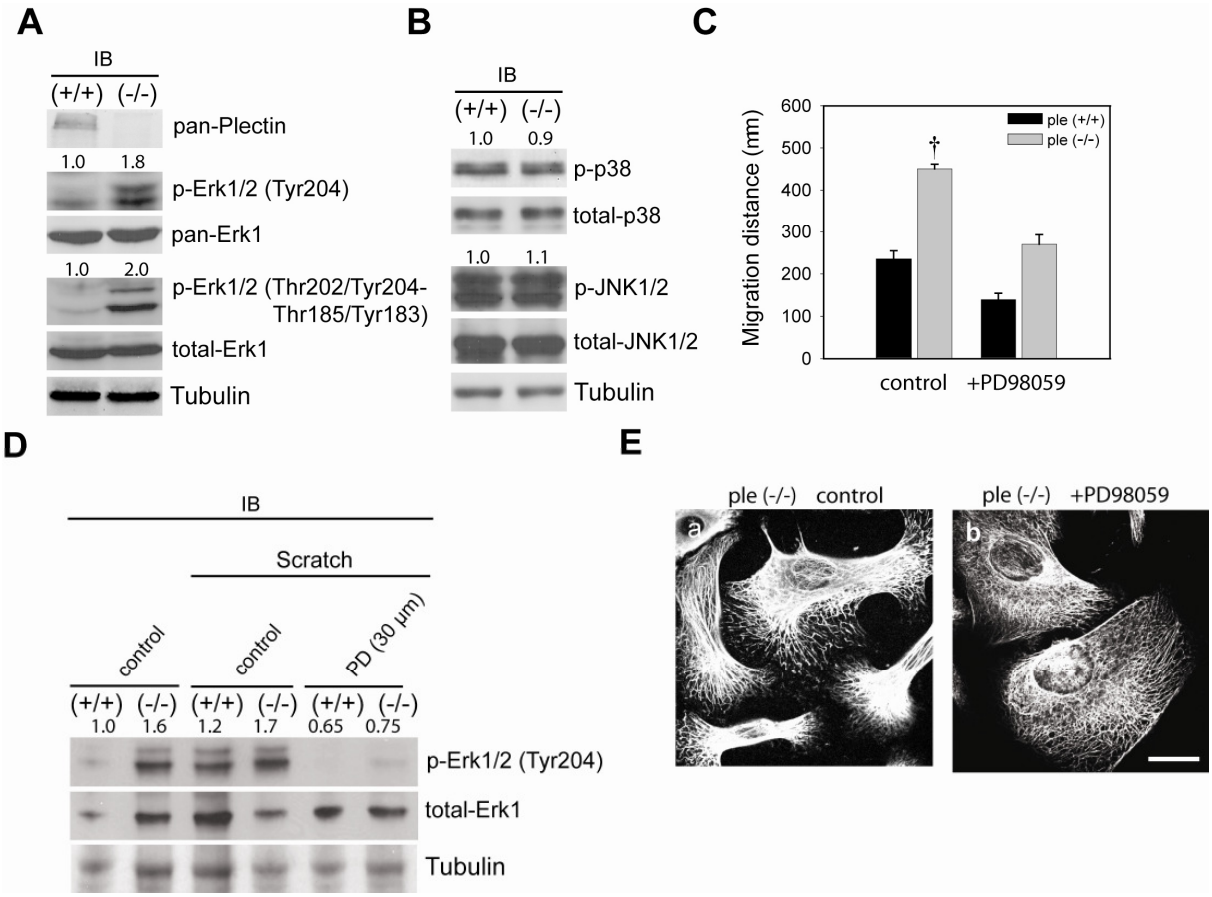

Figure 37. Increased Erk1/2 activites in plectin (-/-) keratinocytes. (A) Total cell lysates of migrating cells (prepared 6 hours after adhesion) were subjected to immunoblotting using antibodies to total (unphosphorylated/phosphorylated) Erk1, (Thr202/Tyr204- and Thr185/Tyr183-phosphorylated) p–Erk1/2, or (Tyr204-phosphorylated) p–Erk1/2. Tubulin was used as a loading control. (B) Total cell lysates of migrating cells (prepared 6 hours after adhesion) were subjected to immunoblotting using antibodies to total (unphosphorylated/phosphorylated) p38 and JNK1/2, (Thr180/Tyr182-phosphorylated) p–p38, or (Thr183/Tyr185-phosphorylated) p–JNK1/2. Tubulin was used as a loading control. (C) Average values of migration distances from 10 different optical fields (10x objective) from three independent experiments are shown (mean ± SEM). †, $P < 0.001$. (D) Total cell lysates from controls, scratched cells (scratch) and PD98059-treated (PD) scratched cells were subjected to immunoblotting using antibodies to total (unphosphorylated/phosphorylated) Erk1, or (Tyr204 phosphorylated) p–Erk1/2. Tubulin was used as a loading control. (E) Representative images of keratinocytes at the wound edge, stained with anti-pan-keratin mAbs. PD98059 had no effect on the keratin filament cytoarchitecture (b). Numbers above lanes in (A, B, D) represent the protein ratios relative to an arbitrary level of 1.0 determined by the first sample in each lane. One representative experiment of three is shown in each case. Bar, 10 µm.

Importantly, although MEK1 inhibition decreased the migration rate of plectin (-/-) keratinocytes, it had no effect on their aberrant keratin network organization (Fig. 37E), clearly placing plectin in the MAP kinase cascade upstream of Erk1/2. These data established a causal relationship between plectin deficiency and accelerated migration of keratinocytes, showing hyperactivation of Erk1/2 to be a consequence of plectin deficiency.

PKCδ and src-family kinases (SFKs), such as c-Src, yes and fyn, have been suggested as major players in signaling pathways responsible for migration of keratinocytes (Li et al., 2002b; Yamada et al., 2000), and both have been shown to be upstream activators of Erk1/2 (Gagnoux-Palacios et al., 2003; Miranti et al., 1999). For that reason, I next investigated activation of these kinases in membrane fractions of plectin (+/+) and (-/-) keratinocytes. As shown in Fig. 38A, membrane fractions of plectin (-/-) keratinocytes showed increased reactivity to anti-phospho PKCδ and anti-phospho Src Y418 (which monitors phosphorylation of tyrosine in the activation loop of SFKs) antibodies, compared to wild-type cell fractions. While total SFK levels (detected with antibodies recognizing Src, Fyn and Yes) in membrane fractions from both cell types were comparable, those of PKCδ were lower in the membrane fraction of plectin (-/-) compared to plectin (+/+) cells. In accordance with previous data (Osmanagic-Myers and Wiche, 2004), the reduced PKCδ protein levels were most likely a consequence of an increased degradation of the enzyme due to elevated enzymatic activity (Osmanagic-Myers and Wiche, 2004).

To assess whether upregulation of SFKs was related to enhanced Erk1/2-dependent migration of plectin (-/-) keratinocytes, cells were treated with the SFK inhibitor PP2, a suppressor of cell motility and Erk activation (Matsubayashi et al., 2004), prior to scratch wound -or spreading assays. As expected, this treatment led to a dose-dependent decrease in phosphorylation (activities) of Erk1/2 during spreading (Fig. 38B) and migration (Fig. 38C).

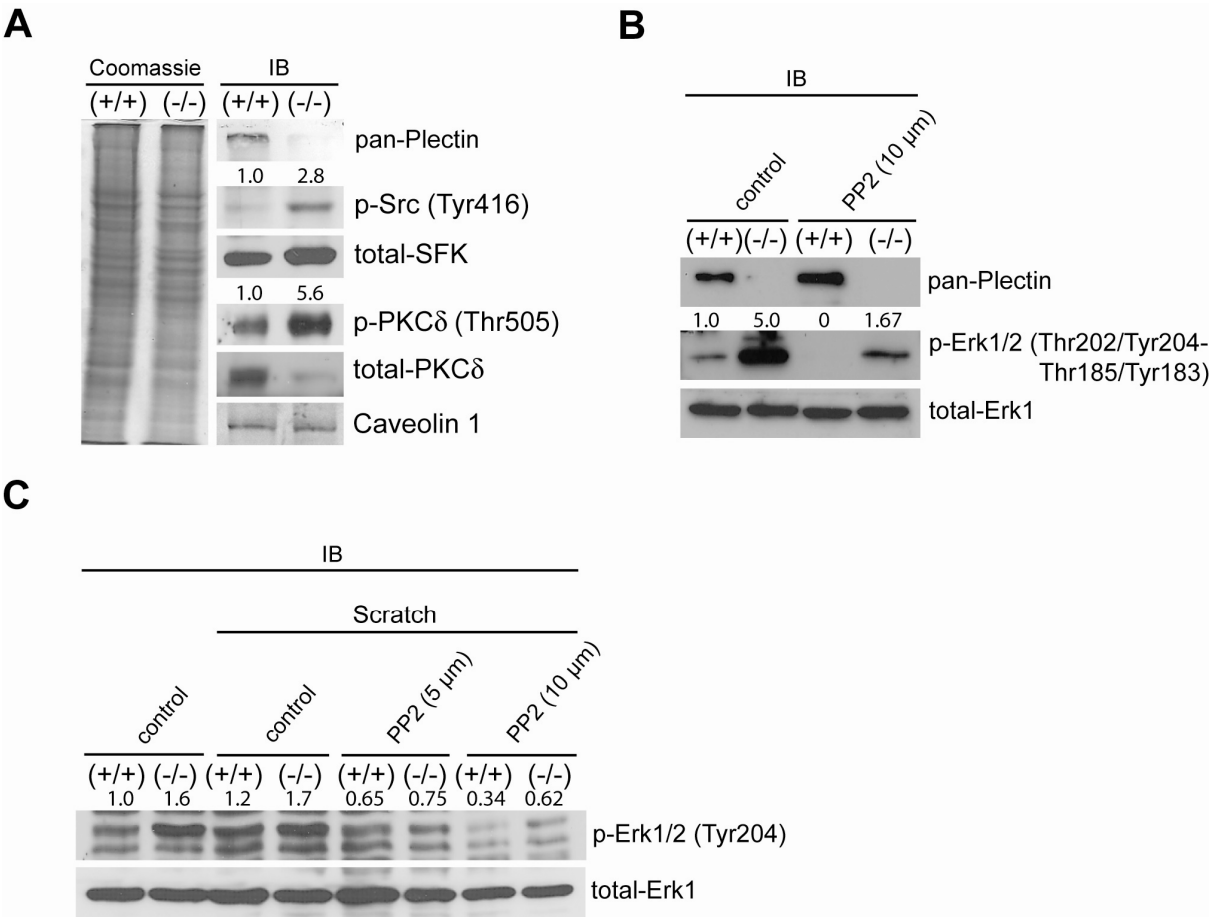

Figure 38. Upregulation of SFKs and PKCδ in plectin (-/-) keratinocytes. (A) Membrane subfractions of keratinocytes, normalized for equal protein contents, were immunoblotted using antibodies recognizing total (unphosphorylated/phosphorylated) Src, Fyn and Yes (total-SFK), total (unphosphorylated/phosphorylated) PKCδ, (Tyr416-phosphorylated) p–SFKs (p-SRc), and (Thr505-phosphorylated) p–PKCδ. Caveolin1 was used as a loading control. (B) Total cell lysates from migrating control cells (prepared 6 hours after adhesion) and from cells incubated with PP2 were subjected to immunoblotting using antibodies to total (unphosphorylated/phosphorylated) Erk1 or (Thr202/Tyr204- and Thr185/Tyr183-phosphorylated) p–Erk1/2. (C) Total cell lysates from control cells and cells incubated with PP2, as indicated, were subjected to immunoblotting using antibodies to total (unphosphorylated/phosphorylated) Erk1 or (Tyr204-phosphorylated) p–Erk1/2. Numbers above lanes in (A-C) represent the protein ratios relative to an arbitrary level of 1.0 determined by the first sample in each lane. One representative experiment of three is shown.

The effect of SFK-inhibition on the spreading behavior of plectin (-/-) keratinocytes was monitored by actin and cortactin immunofluorescence (Fig. 39A-D). Cortactin is a Src substrate which plays an important role in keratinocyte migration (Ceccarelli et al., 2007). Src

phosphorylation of cortactin leads to its translocation to the membrane (Ceccarelli et al., 2007), where cortactin is required for the regulation of actin polymerization (Tehrani et al., 2007). In line with these findings, lamellipodial edges of spreading plectin (-/-) keratinocytes demonstrated bright cortactin immunofluorescence (Fig. 39B), when compared to plectin (+/+) cells (Fig. 39A). PP2 treatment of spreading plectin (-/-) keratinocytes reduced cell circumference to numbers typical of untreated, spreading plectin (+/+) keratinocytes (Fig. 39E) concomitant with a decrease in peripheral cortactin accumulation (Fig. 39D).

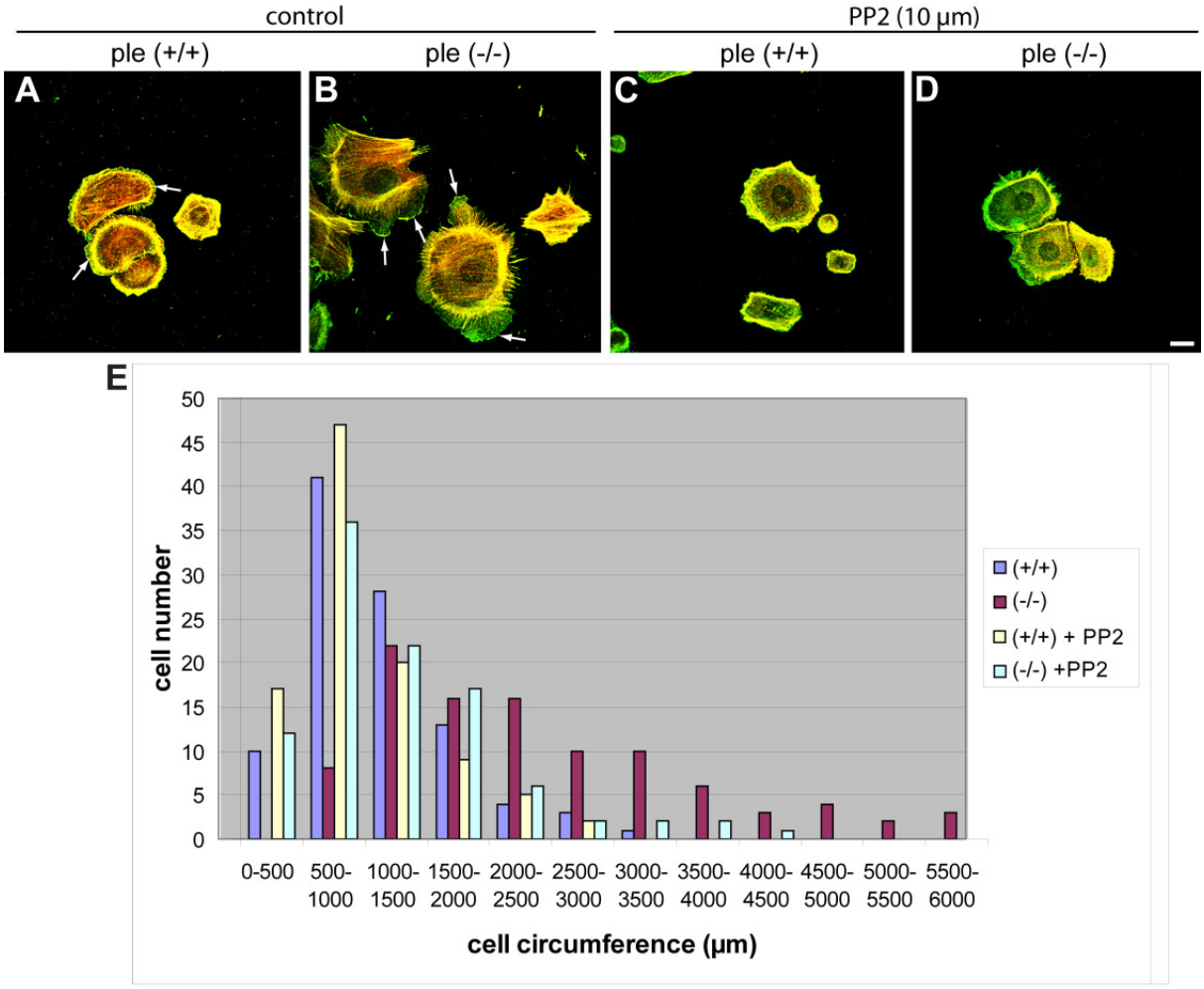

Figure 39. Inhibition of cell spreading by SFK-inhibition. (A-D) Relative distribution of cortactin and actin filaments in spreading control cells and cell treated with PP2. Cells were double immunolabeled using antiserum to actin and mAbs to cortactin. Arrows in A and B indicate cortactin localization at lamellipodial edges in untreated cells. (E) Quantitative analysis of keratinocyte spreading in the absence and presence of PP2. Histogram shows the distribution of cell circumferences of 100 cells per culture condition. Bar, 10 µm.

Ligation of integrin α6β4 by laminin 322 has previously been shown to be directly connected to migration in many different cell systems, including keratinocytes (Hintermann et al., 2001; Kippenberger et al., 2004; Sehgal et al., 2006). To address, whether ligation of integrin α6β4 is responsible for the faster migration of plectin (-/-) keratinocytes, cell migration was determined in a scratch wound closure assay in the presence or absence of GoH3 antibodies, which are known to block the adhesion of integrin α6β4 to laminin 322. As can be seen in Fig. 40, migration distances covered by plectin (-/-) keratinocytes were significantly reduced in the presence of GoH3 (Fig. 40G).

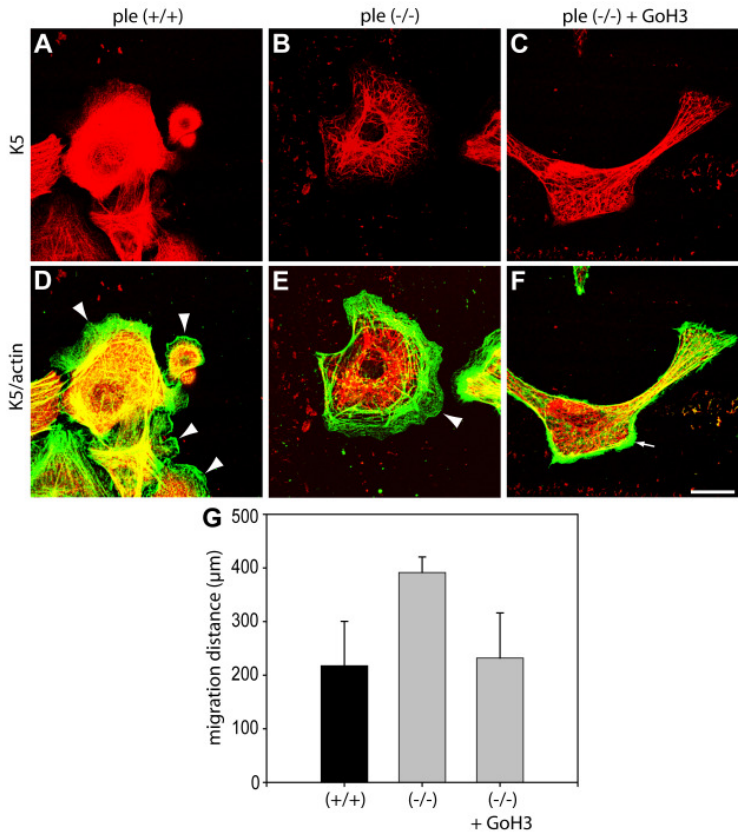

Figure 40. Reduction of faster migration of plectin (-/-) keratinocytes by blocking integrin α6β4 binding to laminin 322. Monolayers of plectin (+/+) and plectin (-/-) cells and of plectin (-/-) cells treated with mAb GoH3 (10µg/ml), were subjected to scratch wound closure assays. (A-F) Cells migrating into scratch wounds were double immunolabeled using antiserum to actin and anti-pan-keratin mAbs. (A-C), anti-keratin stainings; (D-F) merged anti-actin and anti-keratin stainings. Arrows in (D) and (E) point to lamellipodial edges, whereas the arrow in (F) points to cortical actin bundles that appear as a consequence of GoH3 treatment. (G) Average values of migration distances from 10 different optical fields (10x objective) from three independent experiments (mean ± SEM). Note shorter migration distances of plectin (-/-) keratinocytes after treatment with mAb GoH3. Bar, 10 µm.

Moreover, GoH3 treatment directly affected the organization of the actin network, as migrating GoH3-treated plectin (-/-) keratinocytes displayed no lamellipodia, but a thick cortical actin belt (Fig. 40C). Keratin network organization was however not altered by GoH3-treatment, as plectin (-/-) cells at the wound edge still had keratin networks with increased mesh sizes (Fig. 40F). These data leave no doubt that integrin β4 is in control of migration in plectin (-/-) keratinocytes.

Recently it was shown, that integrin α6β4 regulates laminin 322 organization by a pathway involving Rac1, slingshot phosphatase (SHH) and cofilin (Kligys et al., 2007). Increased phosphorylation and thereby inactivation of cofilin in keratinocytes leads to enhanced spreading (Honma et al., 2006) and an increase in the number of lamellipodia, similar to the phenotype observed in a subpopulation of migrating plectin (-/-) keratinocytes (see Fig. 30). Therefore I analyzed the phosphorylation of cofilin in spreading cultures of plectin (-/-) and wild-type keratinocytes (Fig. 42). Immunoblotting analysis revealed a strong increase of phosphorylated (inactive) cofilin in plectin (-/-) keratinocytes compared to wild-type cells. Thus, increased cofilin inactivation might indeed be the reason for the unpolarized migration of some plectin (-/-) keratinocytes.

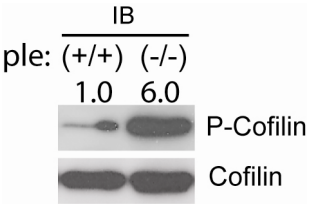

Figure 41. Upregulation of cofilin phosphorylation in plectin (-/-) keratinocytes. Total cell lysates from migrating cells (prepared 6 hours after adhesion) were subjected to immunoblotting using antibodies to total (unphosphorylated/phosphorylated) Cofilin or (Ser3-phosphorylated) p-Cofilin. Numbers above lanes represent the protein ratios relative to an arbitrary level of 1.0 determined by the first sample in each lane. One of two experiments is shown.

Absence of plectin reduces desmoplakin expression levels, but does not influence desmosome formation and function

Plectin was previously identified as a component of desmosomes of polarized monolayers of simple epithelial cells (Eger et al., 1997), of the epidermis (Skalli et al., 1994; Wiche et al., 1983) and of differentiated keratinocytes in culture (Skalli et al., 1994). Since

electron microscopic analysis had revealed subtle changes in sizes and numbers of desmosomes of plectin-deficient epidermis (see Fig. 18), I decided to investigate plectin`s possible role in desmosome function in more detail using cultured primary and immortalized keratinocytes.

Within several hours of switching the calcium concentration from 0.05 mM to more than 1.2 mM, keratinocytes form adhesion zippers, which are precursor structures of adherens junctions, followed by the formation of nascent desmosomes (Green et al., 1987; Vaezi et al., 2002). Subsequently, actin-myosin-based tension, by moving the apical surfaces of cells relative to their bases, drives the expansion of zones of cellular overlap, thereby generating new sites for nascent cellular junctions and catalyzing maturation of adherens junctions and desmosomes (Vaezi et al., 2002). By 24 hours, a stratified epithelial sheet consisting of two to three cell layers, with an organization of intercellular junctions similar to that of the epidermis in vivo, forms in some parts of the keratinocyte monolayer (Vaezi et al., 2002).

After 3 hours of incubation with 1.8 mM calcium, primary plectin-deficient keratinocytes (ple -/-) that were derived from K5-Cre KO mice (Ackerl et al., 2007) had formed adhesive zippers and nascent desmomes of normal appearance (Fig. 42B,F), that were indiscernible from intercellular junction precursors of control cultures (Fig. 42A,E). By 48 hours, single cells and cell clusters that had stratified were found on the surfaces of monolayers of ple (-/-) and control keratinocytes (Fig. 22E;F and Fig. 42C,D). Formation of mature desmosomes and adherens junction, visible as thick cortical belts of desmoplakin and E-Cadherin, respectively, could be readily observed at this timepoint in clusters of stratified plectin-deficient and control cells (Fig. 42 compare C with D and G with H). Similar results were observed with epithelial sheets generated from plectin (+/+) and plectin (-/-) keratinocytes (Fig. 43A,B). Together, these data strongly speak against a role of plectin in the formation of desmosomes and the establishment of a polarized stratified epithelium. However, these results are consistent with the absence of altered stratification/differentiation in the epidermis of K5-Cre KO mice (see above).

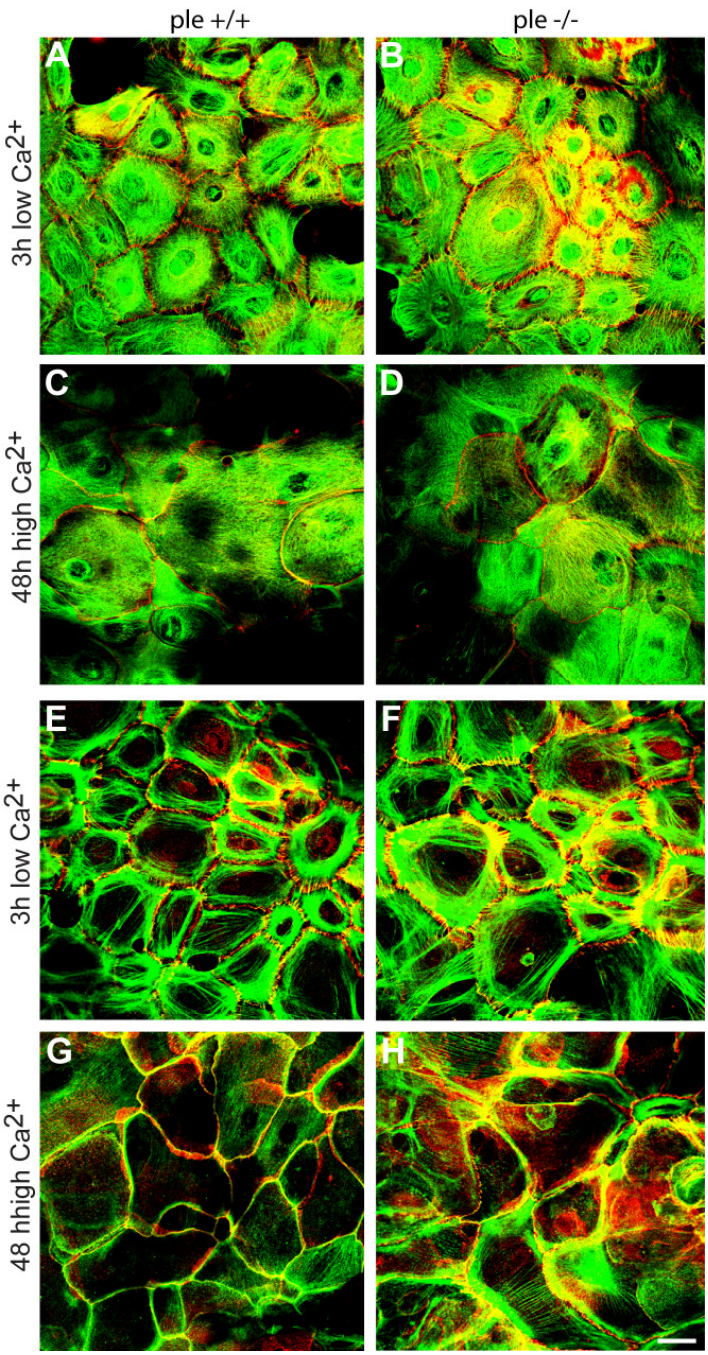

Figure 42. Cell-cell contact formation and stratification of primary wild-type and plectin-deficient keratinocytes. Primary keratinocytes were isolated from skins of K5-Cre KO (ple -/-) and control mice (ple +/+) and after reaching confluence, were cultured in the presence of 1.8 mM Ca^{2+} for three- (A, B, E, F) or 48 hours (C, D, G, H) to induce cell-cell junction formation and stratification, respectively. Cells were immunolabeled using antiserum to K5 (A-488-conjugated secondary Abs, green) and mAbs to desmoplakin (Texas Red-conjugated secondary Abs, red) (A-D), or antiserum to actin (A-488-conjugated secondary Abs, green) and mAbs to E-cadherin (Texas Red-conjugated secondary Abs, red) (E-H). Note, (i) regular formation of nascent desmosomes (A, B) and adhesion zippers (E, F), and (ii) normal stratification along with formation of mature desmosomes (C, D) and adherens junctions (G, H) in epithelial sheets of control and plectin-deficient keratinocytes. Bar, 10 µm.

Interestingly, stratified epithelial sheets of immortalized and primary plectin (-/-) keratinocytes expressed slightly less desmoplakin protein than their wild-type counterparts (Fig. 43C,D). Moreover, the relative amounts of desmoplakin in the detergent-resistant fraction of stratified plectin (-/-) keratinocytes were reduced (Fig. 44B), which correlates with a reduced incorporation of desmoplakin into desmosomes (Yin et al., 2005). Plectin-deficiency did only affect desmoplakin expression, since E-cadherin expression levels were similar in stratified plectin (+/+) and plectin (-/-) epithelial sheets (Fig. 43C,D and Fig. 44B).

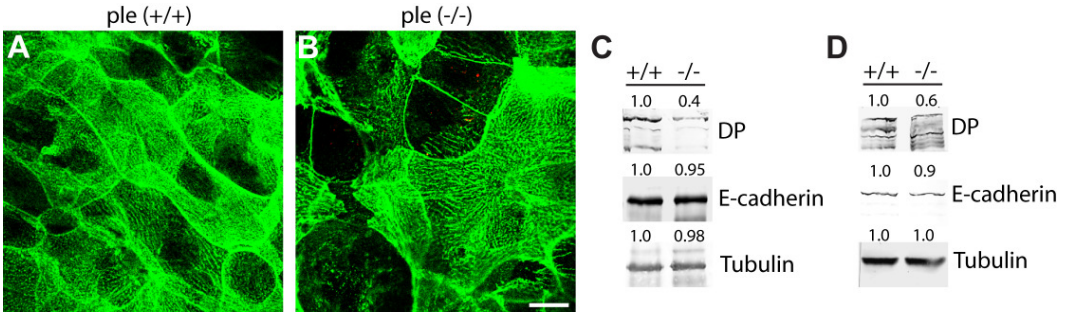

Figure 43. Cell-cell contact formation and stratification of immortalized wild-type and plectin-deficient keratinocytes. (A, B) After reaching confluence, cells were cultured in the presence of 1.8 mM Ca^{2+} for 48 hours to induce cell-cell junction formation and stratification. Cells were immunolabeled using mAbs to desmoplakin. Note regular formation of desmosomes in epithelial sheets of plectin (+/+) and plectin (-/-) keratinocytes. (C, D) Total cell lysates of stratified epithelial sheets generated from immortalized (C) or primary (D) keratinocytes were subjected to immunoblotting using antibodies to desmoplakin, or E-cadherin. Tubulin was used as a loading control. Numbers above lanes represent the protein ratios relative to an arbitrary level of 1.0 determined by the first sample in each lane. One of two experiments is shown. Bar, 10 µm.

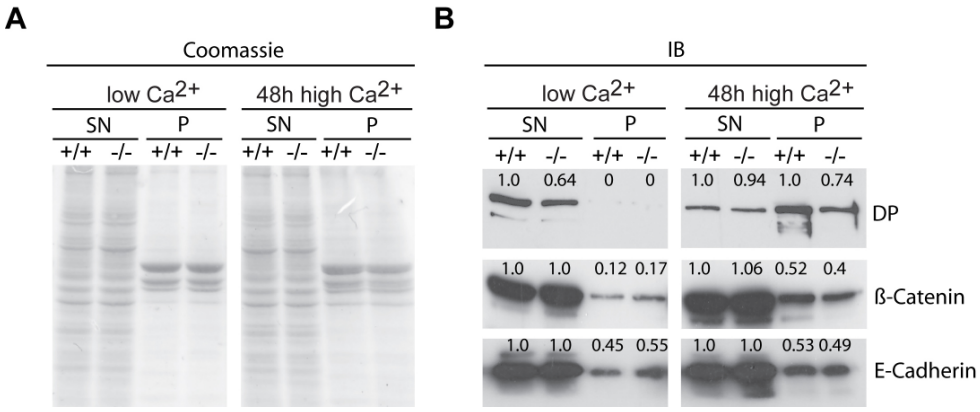

Figure 44. Association of desmoplakin with desmosomal complexes. Relative expression levels of desmoplakin, β–catenin and E-cadherin in detergent-soluble (SN) and insoluble (P) fractions obtained from unstratified monolayers (low Ca^{2+}) and stratified epithelial sheets (48 hours high Ca^{2+}) of wild-type (+/+) and plectin-deficient (-/-) keratinocytes. Proteins were extracted from cells as described in materials and methods and equal amounts of proteins were analyzed by SDS-PAGE and immunoblotting using antibodies indicated. (A) Coomassie staining. (B) Immunoblotting using antibodies indicated. Numbers above lanes represent the protein ratios relative to an arbitrary level of 1.0 determined by the first sample in each lane. One representative experiment of three is shown.

To test whether the reduced desmosome-associated desmoplakin levels observed in stratified plectin (-/-) epithelial sheets had consequences on the stress-resistance of the keratin-desmosome network, stratified epithelial sheets were subjected to oscillating mechanical stretch at a frequency of 1 Hz (i.e. one cycle of stretch and relaxation per second) and a 12% stretch (i.e. a 12% increase in diameter across the silicone membrane). Continuous stretching of plectin (+/+) and plectin (-/-) keratinocyte sheets over a 24 hour period did not affect cell integrity, nor did it cause changes in the organisation of the keratin network and desmosomes, but led to a re-orientation of keratinocytes within the sheet along the stretch-axis (Fig. 45C,D). However, signs of cell rupture along cell-cell interfaces or rupture of keratin filaments, such as were described previously for EBS keratinocytes (Russell et al., 2004), were not observed in plectin (-/-) keratinocytes. From these results one may conclude that plectin-deficiency and the resulting downregulation of desmoplakin have no effect on the stress resistance of the keratin-desmosome network of cultured keratinocytes. However, it can not excluded, that the keratin-desmosome network would react differently if higher frequencies are applied (Russell et al., 2004).

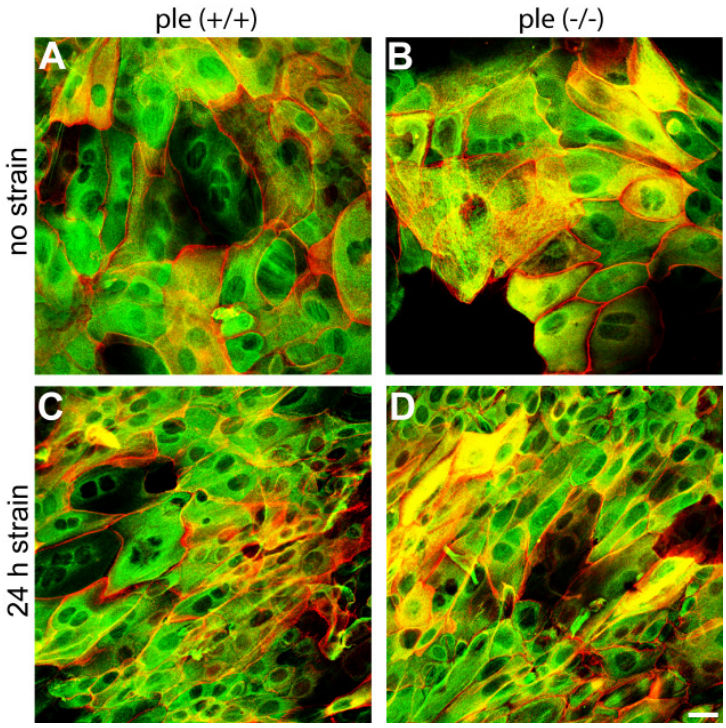

Figure 45. Effect of cyclic strain stress on stratified plectin (-/-) keratinocyte sheets. Confluent monolayers were allowed to stratify for 48 hours and were subsequently subjected to mechanical stress using an oscillating stretch with frequency of 1 Hz and amplitude of 12% for 24 hours (C, D) or left un-stressed (A, B). Cells were double immunolabeled using antiserum to K5 and mAbs to desmoplakin. Note, elongated cell shape and alignment of cells along the stretch axis in wild-type and plectin-deficient epithelial sheets after stretching, but intact keratin filament network and desmosomal cell-cell contacts in plectin-deficient epithelial sheets. Bar, 10 µm.

To directly analyze cell-cell adhesion, I next used a so called "dispase-based cell dissociation assay", which is directly related to desmosomal adhesion, because it involves splitting of the desmosomal material by application of shear stress (Kimura et al., 2007; Yin et al., 2005). The degree of dissociation was quantified by counting the number of fragments released from stratified keratinocyte sheets during the assay. As shown in Fig. 46, there was no statistically significant difference between the number of fragments released from plectin (+/+) and plectin (-/-) sheets, indicating similar adhesive strength in both cell types.

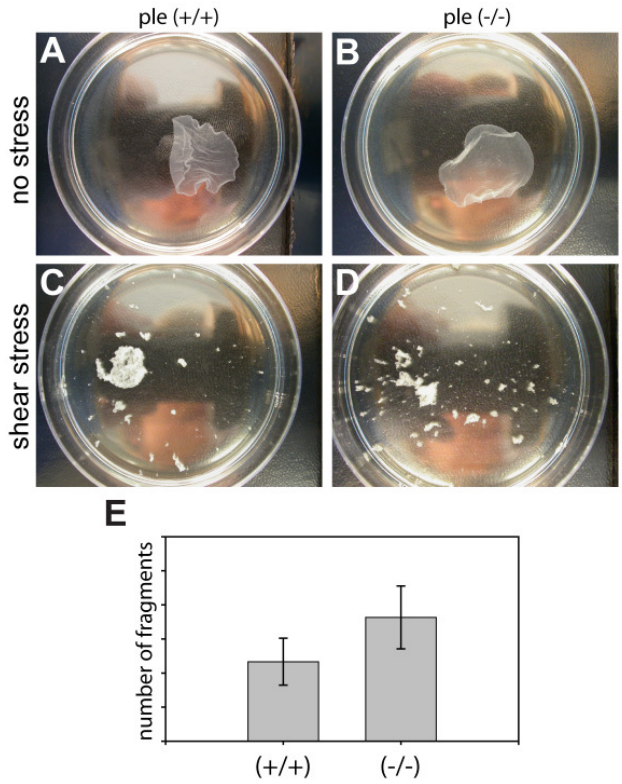

Figure 46. Effect of shear stress on stratified plectin (-/-) keratinocyte sheets. (A-D) Stratified epithelial sheets after their detachment from culture dishes with dispase (A, B), or after subsequent 50 rotations in falcon tubes in 4 ml of PBS containing 1.8 mM Ca^{2+} (B, C). (E) Quantification of the degree of dissociation of epithelial sheets by counting fragments of the sheet after rotation. Mean values ± SEM from three experiments are shown.

Summarized, my experiments with cultured keratinocytes did not reveal a role of plectin in the reinforcement of desmosomes; however, they showed that steady state expression levels of desmoplakin are partially regulated by plectin.

Part III – Biochemical characterization of plectin isoform 1c as a microtubule binding protein

In a study on plectin isoform expression on the mRNA level in epithelial tissues, a dominance of transcripts containing exon 1a or exon 1c has been observed (Fuchs et al., 1999). This was onfirmed by quantitative RNase protection assays of RNA isolated from primary human keratinocytes, where it was revealed that the predominant plectin isoforms expressed contained exon 1a (71% of all transcripts detected), exon 1c (22%), exon 1 (4%), and exon 1b (1%) (Andrä et al., 2003). As the role of plectin 1a as a stabilizer for HDs has been established (Andrä et al., 2003), this part of the thesis was focused on the second major epithelial isoform, plectin 1c.

Plectin 1c is expressed in stratified mouse epithelia

In skin, plectin 1c is expressed in all living cell layers of the epidermis (Andrä et al., 2003). To find out, whether this isoform was also expressed in other stratified epithelia, oesophageal and palate tissues were subjected to immunofluorescence microscopy using anti-plectin 1c antibodies (Fig. 47).

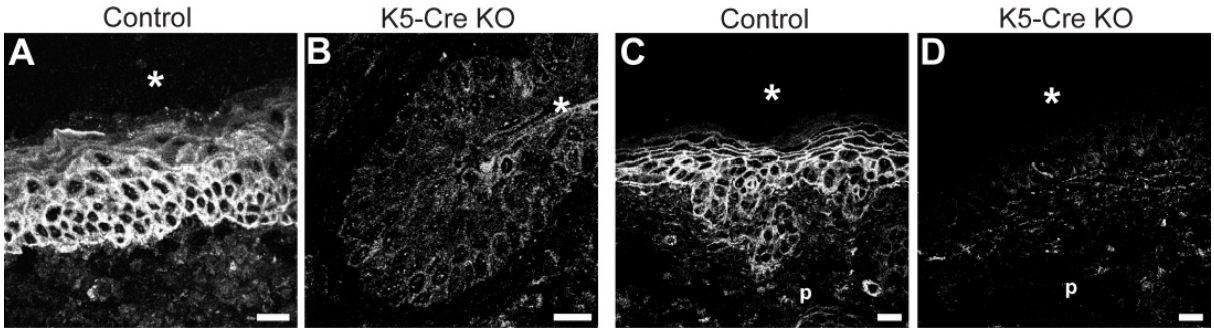

Figure 47. Expression and localization of plectin 1c in stratified internal mouse epithelia. Immunofluorescence microscopy of frozen oesophagus (A, B) and palate (C, D) tissue sections of newborn control and K5-Cre KO specimens using anti-plectin 1c antibodies. In the epithelia of the oesophagus (A) and the palate (C), the plectin 1c signal is most prominent along cell borders and the basal membranes. Also note absence of plectin 1c-specific label in K5-Cre KO oesophagus (B) and palate (D). Asterisks indicate lumens of oesophagus and oral cavity. Bars, 20 µm.

Indeed, antibodies to plectin 1c strongly labelled the periphery of keratinocytes in these epithelia similar to the staining pattern obtained in epidermis (Andrä et al., 2003). Thus, plectin 1c is specifically expressed in basal and suprabasal keratinocytes of stratified epithelia.

Plectin 1c expression remains stable during differentiation of keratinocytes in-vitro.

Expression levels of plectin 1a and plectin 1c during the process of epithelial sheet formation were examined using immunoblotting. Total cells lysates were prepared from immortalized plectin (+/+) keratinocyte at different time points after increasing the concentration of calcium to 1.8 mM. After 24 hours of stratification, involucrin expression began slightly to increase (Fig. 48A), indicative of keratinocytes undergoing terminal differentiation (Watt et al., 1984), and was strongly upregulated at day 5 of differentiation. In two days-old epithelial sheets, reduced immunodetection of plectin 1a was observed and expression levels decreased further with progressing terminal differentiation.

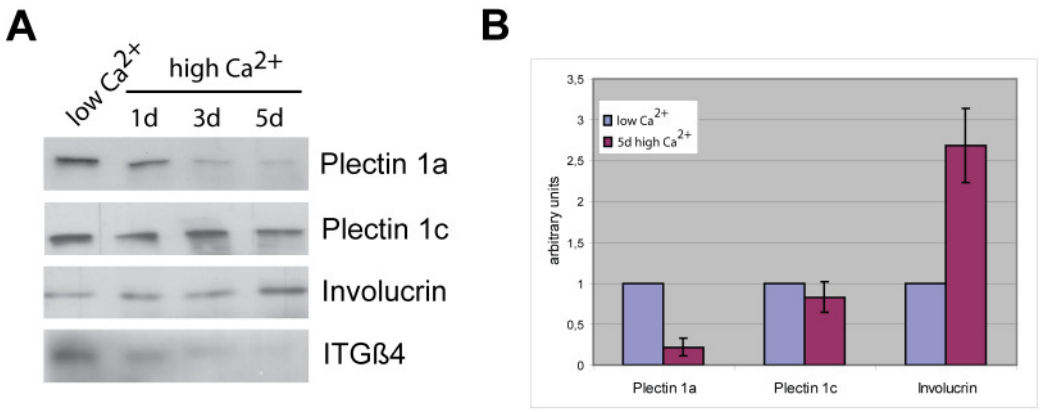

Figure 48. Regulation of plectin 1a and 1c expression levels during terminal differentiation of keratinocytes. (A) Immunoblotting analysis of plectin 1a, plectin 1c, integrin β_4, and involucrin expression levels during Ca^{2+}-induced terminal differentiation of plectin (+/+) keratinocytes. Note, the hemidesmosomal components integrin β_4 and plectin 1a were downregulated during terminal differentiation of keratinocyte monolayers, whereas plectin 1c expression remained stable. The upregulated involucrin expression is indicative of keratinocyte differentiation. (B) Comparison of relative expression levels of plectin 1a, plectin 1c, integrin β_4, and involucrin at days null and five of differentiation, respectively. Mean values ± SEM from three experiments are shown.

Since differentiation of keratinocytes in vitro was shown to be associated with downregulation of hemidesmosomal integrins (Tennenbaum et al., 1996), the expression of integrin β_4 was also analyzed. Integrin β_4 expression started to decrease after 24 hours, and no immunoreactivity could be detected after five days of stratification. In contrast to plectin 1a, plectin 1c was more or less stably expressed during the time course of epithelial sheet formation, and plectin 1c immunoreactivity was still detectable even after five days of differentiation (Fig. 48A). For a comparison of plectin 1a and plectin 1c expression levels at days null and five of differentiation, immunoblots were subjected to densitometric analysis (Fig. 48B).

Plectin 1c associates with MTs in vivo

It was previously reported by our group that plectin 1c, contrary to isoforms lacking the 1c-specific sequence, such as plectin 1a or plectin 1, colocalized with MTs in keratinocytes (Andrä et al., 2003), suggesting that this sequence might contain a MT-binding site. To study plectin 1c-MT interaction in more detail, I decided to use immortalized mouse keratinocytes which express plectin 1c at relatively high levels (Andrä et al., 2003). Since plectin 1c is most prominently expressed in brain (Fuchs et al., 1999), additionally I used the cell lines N2a and PC12, both of which are of neuronal origin and express plectin 1c (Walko, 2002). Immunofluorescence microscopy using isoform-specific antibodies revealed a clear colocalization of plectin 1c with MTs in N2a cells (Fig. 49A-C). Codistribution of plectin 1c with MTs was most prominent at the cellular periphery (Fig. 49C) with a similar distribution pattern as observed in plectin (+/+) keratinocytes (Andrä et al., 2003). Plectin 1c-positive structures resembled “speckles” arranged in a discontinuous pattern alongside single MTs (Fig. 49C, arrowheads), and were often found near intersections of MTs (Fig. 49C, arrows). Similar structures have previously been found to contain non-neuronal MAPs or MT-bound MAP fragments (Faire et al., 1999). Correlating with the density of MTs, the staining intensity of plectin 1c was generally higher near the nucleus compared to peripheral regions of the cell (Fig. 49A,B). However, high plectin 1c staining intensities were also often noticed in MT-rich domains at the cellular periphery (Fig. 49D-F). Using an antiserum recognizing all isoforms of plectin (anti-pan-plectin), a similar staining was observed (Fig. 49G-I). Pan-plectin staining was most intensive in perinuclear areas and appeared more dotlike at the cellular periphery, with plectin-positive dots coaligning with MTs (Fig. 49I, arrowheads).

When neurite outgrowth was induced in these cells, plectin 1c redistributed with MTs into neurites and growth cones (Fig. 49J, K).

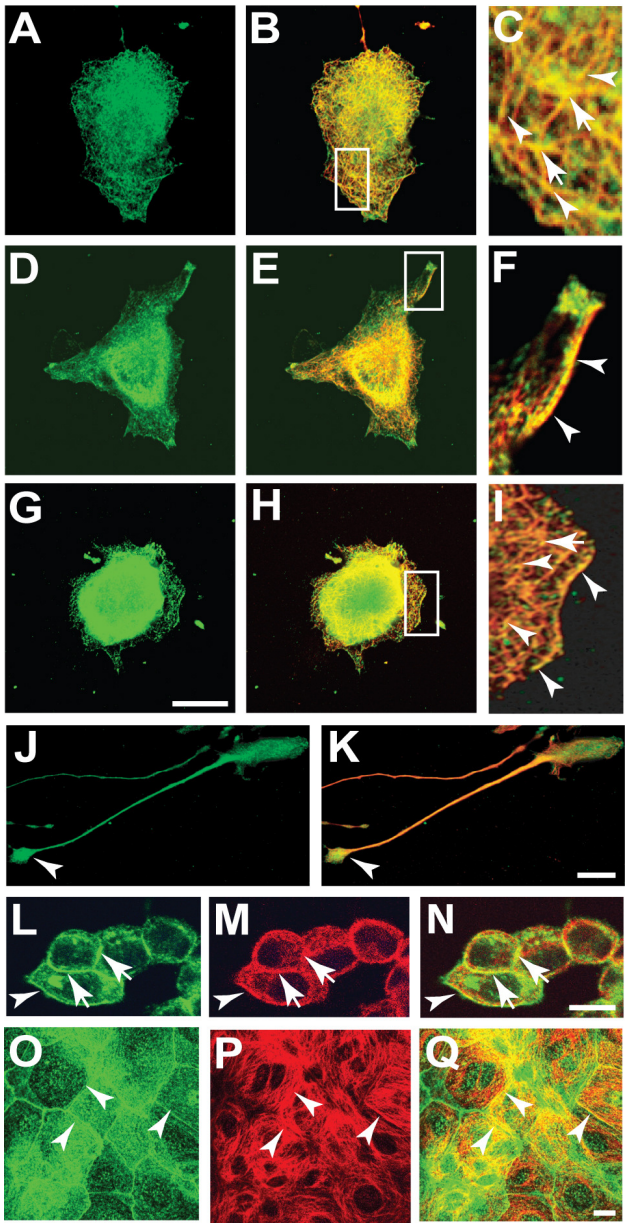

Figure 49. Isoform 1c-specific association of plectin with MTs and the plasma membrane in neuronal cells and keratinocytes. N2a cells (A-K), PC-12 cells (L-N) and stratified plectin (+/+) epithelial sheets (O-Q) were processed for immunofluorescence microscopy using anti-plectin 1c (A, B, D, E, J-L, N, O, Q), anti-pan-plectin (G, H), and anti-tubulin (B, E, H, K, M, N, P, Q)-specific primary antibodies. (A-C) Note extensive colocalization of plectin 1c with N2a MTs, often in a discontinuous pattern (C, arrowheads) and at MT intersections (C, arrows). (D-F) Localization of plectin 1c at MT-rich cortical domains (arrows in F) in N2a cells. (G-I) Anti-pan-plectin antibodies decorate the peripheral MT network in N2a cells (I, arrowheads) and MT intersections (I, arrow). Note, that pan-plectin staining shows a pattern similar to plectin 1c (compare C with I). (J, K) Plectin 1c redistributes to neurites and growth cones (arrowhead) of differentiating N2a cells. (L-N) Localization of plectin 1c and tubulin at cell-cell contact areas (arrows) and at the cellular membrane (arrowheads) in PC-12 cells. (O-Q) Redistribution of plectin 1c to the cellular periphery upon keratinocyte stratification. Note cortical bundles of MTs in stratifying keratinocytes (arrowheads in P). Bars, 10 µm.

Upon stratification of keratinocytes, plectin 1c redistributed to the cellular periphery, were it was frequently found in close association with cortical bundles of MTs (Fig. 49Q), which form in suprabasal keratinocytes during stratification (Lechler and Fuchs, 2007). Anti-plectin 1c antibodies did not label cell-cell borders in plectin-deficient keratinocytes, demonstrating that the peripheral staining of stratified plectin (+/+) keratinocyte sheets was

not an antibody artifact (data not shown). A similar codistribution of plectin 1c with cortical MTs was also observed in clusters of adrenal PC-12 pheochromocytoma cells (Fig. 49L-N).

In stratified keratinocyte sheets, plectin 1c partially codistributed with desmoplakin at areas of cell-cell contact (Fig. 50A-C), but subcellular fractionation of stratifying keratinocytes showed only a mild enrichment (~ 1.5 times after 24 hours) of plectin 1c in the detergent/high-salt insoluble fraction in contrast to desmoplakin and γ-catenin, which became highly insoluble after 24 hours of stratification [referr to Fig. 30 in (Ackerl, 2005)], indicating that plectin 1c was not an integral component of desmosomes.

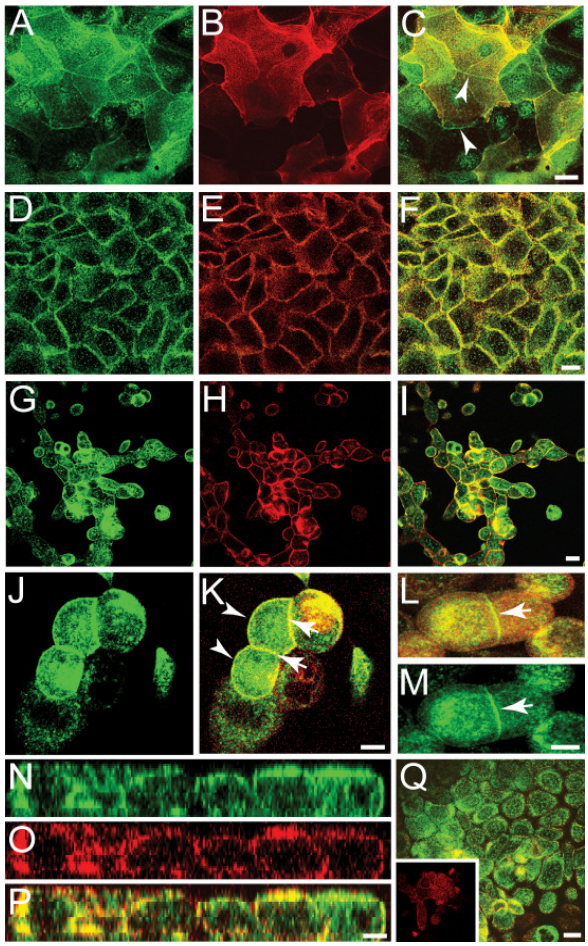

Figure 50. Plectin 1c associates with the submembrane cytoskeleton of stratified keratinocytes. (A-F) Keratinocytes were allowed to stratify and form epithelial sheets for 48 hours in high calcium medium. (G-Q) Ca^{2+}-switch assays. Epithelial sheets were incubated in keratinocyte growth medium with 0.05 mM Ca^{2+} for 24 hours. Cells were processed for immunofluorescence microscopy using anti-plectin 1c (A, C, D, F, G, I, J-M, N, P, Q), anti-desmoplakin (B, C, Q, insert in Q), anti-fodrin (E, F, H, I, K, O, P), and anti-K10 (L) -specific primary antibodies. (A-C) Partial codistribution of plectin 1c (A) and desmoplakin (B) in stratified plectin (+/+) keratinocyte cultures. Note absent colocalization of plectin 1c and desmoplakin in some areas of stratification (C, arrowheads). (D-F) Colocalization of plectin 1c (D) and fodrin (F) at cell-cell borders of stratified plectin (+/+) keratinocyte epithelia sheets. (G-Q) Upon Ca^{2+}-switch, basal keratinocytes loose their cell-cell contacts (Q), whereas clusters of suprabasal keratinocytes retain desmosomes (insert in Q). Plectin 1c and fodrin colocalize in these suprabasal clusters of keratinocytes (I). Close-up view of a suprabasal cell cluster shows codistribution of plectin 1c with fodrin at cell-cell contact areas (K-M, arrows) and at the plasma membrane (K, arrowheads). Suprabasal cell cluster consist of differentiated keratinocytes, which express K10 (L). Side view of a suprabasal keratinocyte cluster generated from a Z-stack through a plectin 1c/fodrin co-staining shows codistribution of plectin 1c and fodrin at lateral cell-cell contact areas and at lateral and apical plasma membranes (P). Bars, 10 µm.

Previous data have demonstrated an association of plectin with the submembrane cytoskeleton of simple epithelial cells via fodrin (Hermann and Wiche, 1987; Eger et al. 1997). In accordance, I observed extensive colocalization of plectin 1c with fodrin in stratified keratinocyte sheets (Fig. 50D-F). When stratified keratinocyte sheets were subjected to a low Ca^{2+} switch (South et al., 2003), cell-cell contacts disassembled, but clusters of suprabasal, K10-expressing (Fig. 50L), keratinocytes retained calcium-independent desmosomes (insert in Fig. 50Q). Plectin 1c clearly colocalized with fodrin at areas of cell-cell contact (arrows in Fig. 51K) and at the plasma membrane (Fig. 50N-P and arrowheads in Fig. 50K) of this suprabasal cell clusters, indicating a strong association of plectin 1c with the submembrane cytoskeleton upon cell-cell contact-maturation.

Plectin 1c binds to MTs in vitro

To demonstrate association of plectin 1c with MTs in vitro, I performed MT cosedimentation assays. First, MTs, isolated from either mouse or hog brain homogenates by repeated cycles of temperature-dependent polymerization and depolymerization, were subjected to immunoblotting using anti-plectin 1c antibodies. Immunoreactive bands comigrating with HMW MAPs were clearly detected in both cases (Fig. 51A). These bands were also recognized by antibodies directed to epitopes encoded by exons 9-12 (N-term) or to the C-terminal repeat domain 5 of plectin (C-term) (Fig. 51B). This, and previous experiments showing comigration of plectin with HMW MAPs in brain tissue homogenates (Hermann and Wiche, 1987) confirmed the association of full length versions of plectin 1c with MTs isolated by in vitro assembly. Antibodies specific to plectin 1a showed no reaction with these or any other bands contained in brain samples (Fig. 51C), consistent with published mRNA expression data (Fuchs et al., 1999).

MT cosedimentation of plectin 1c was assessed also in a similar way using high speed-supernatant (hs-SN) fractions from N2a cells (Fig. 51D). In this case MT polymerization was induced by taxol. When various fractions obtained during the isolation procedure were subjected to immunoblotting using antibodies specific to plectin 1c and the presence of tubulin was visualized by Coomassie staining, an enrichment of both tubulin and plectin 1c in the taxol-stabilized MT fraction was clearly observable (Fig. 51D, lane 6); in controls without taxol neither plectin 1c nor tubulin were detectable in this fraction (Fig. 51D, lane 9).

To exclude the possibility of unspecific trapping of plectin 1c during taxol-polymerization of endogenous tubulin, in another experiment, hs-SNs from N2a cells were incubated with exogenous (pre-assembled) brain MTs, followed by centrifugation (Fig. 51E). Similar to MAP1b heavy chain, tested in parallel as a control, again, a considerable portion of plectin 1c was found to cosediment with MTs (Fig. 51E, lane 3). These data clearly showed that a major fraction of full length plectin 1c present in neuronal cells specifically bound to MT polymers.

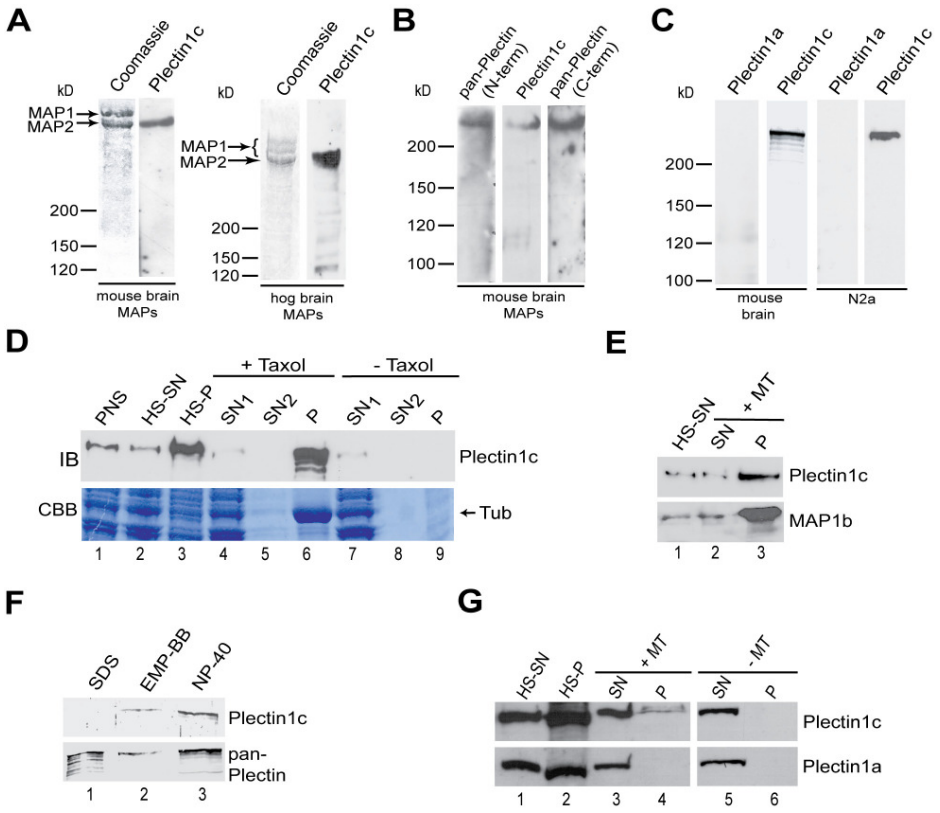

Figure 51. Cosedimentation of plectin 1c with MTs. (A) Cosedimentation of plectin 1c with twice-cycled tubulin from adult mouse and hog brain. Positions of molecular mass markers and of MAP1 and MAP2 are indicated. Presence of plectin 1c in MT pellets was analyzed by immunoblotting. (B) Immunoblotting analysis of mouse brain MT pellets using antibodies to plectin`s N and C termini and plectin 1c. Positions of molecular mass markers are indicated. (C) Immunoblotting analysis of mouse brain homogenates and N2a cell lysates using antibodies to plectin 1a and plectin 1c. Positions of molecular mass markers are indicated. (D) Cosedimentation of plectin 1c with taxol-stabilized endogenous MTs from N2a cells. N2a postnuclear supernatant (PNS, lane 1) was subjected to centrifugation to obtain high-speed supernatant (hs-SN, lane 2) and pellet (hs-P, lane 3) fractions. hs-SN aliquots were incubated with (+), or without (-) taxol. Formed MTs were sedimented by centrifugation, leaving a SN_1, and the MT-pellet was subjected to two cycles of resuspension and

centrifugation to obtain a final pellet (P) and SN (SN_2) fractions. All fractions were analyzed by SDS-PAGE, followed by coomassie-staining (CBB) or immunoblotting (IB) using anti-plectin 1c antibodies. Note high amounts of plectin 1c cosedimenting with MTs (compare lanes 6, 9). The position of tubulin (Tub) on the gel is indicated. (E) A plectin 1c-containing hs-SN was incubated with exogenous taxol-polymerized tubulin (+ MT), and MTs sedimented by centrifugation. Fractions were analyzed with anti-plectin 1c and anti-MAP-1b heavy chain antibodies, revealing partial cosedimentation of plectin 1c and MAP-1b heavy chain with pre-formed MTs. (F) Distribution of plectin 1c and pan-plectin (detected with N-term antibodies) in subcellular fractions of keratinocytes obtained by sequential extraction with NP-40, Empigen-BB and SDS. Note absence of plectin 1c from the SDS-soluble fraction. (G) Plectin (+/+) keratinocyte supernatant freed of nuclei was subjected to centrifugation to obtain high-speed supernatant (hs-SN, lane 1) and pellet (hs-P, lane 2) fractions. hs-SN aliquots were incubated with (+MT) or without (-MT) taxol-stabilized MTs. Centrifugation yielded pellet (P) and supernatant (SN) fractions. Aliquots from each fraction were analyzed by SDS-PAGE, followed by immunoblotting using anti-plectin 1c and plectin 1a antibodies. Note that endogenous plectin 1c, but not plectin 1a from keratinocytes partially cosediments with pre-assembled MTs.

To investigate the ability of plectin 1c to associate with keratin filaments in-vivo, I followed a sequential detergent extraction protocol (Liao and Omary, 1996), which uses first NP-40 and then Empigen-BB to solubilize large amounts of keratin. Indeed, 22% and 46% of keratin 5/14 were solubilized by NP-40 and Empigen-BB, respectively, whereas 32% of keratins remained unsoluble and could only be solubilized with SDS (see Fig. 34). Immunoblotting analysis using anti-plectin 1c and anti-pan-plectin antibodies revealed that plectin 1c was not present in the SDS-soluble pool (Fig. 51F), whereas a strong signal was obtained using pan-plectin (N-term) antibodies. These data indicate a differential association of plectin 1c with keratin-based cytoskeletal structures in comparison to other plectin isoforms present in keratinocytes.

Next, I carried out cosedimentation assays with soluble cell extracts from plectin (+/+) keratinocytes using pre-assembled brain MTs as an affinity matrix (Fig. 51G). The two major keratinocyte isoforms of plectin, plectin 1a and plectin 1c (Andrä et al., 2003), were present in high-speed cell supernatants in comparable amounts (Fig. 51G, lane 1). However, only plectin 1c showed partial cosedimentation with pre-assembled MTs, while plectin 1a remained unbound (Fig. 51G, lane 4). No plectin was sedimented in the absence of MTs (Fig. 51G, lanes 5,6). These results showed that association of plectin with MTs in keratinocytes was isoform-specific, with plectin 1c exhibiting MAP-like behavior.

The plectin C terminus does not associate with keratinocyte MTs in-vivo

A fragment of the C-terminal tail domain of plectin harboring 4 GSR repeats has previously been reported to decorate and bundle MTs upon transfection into COS7 cells (Sun et al. 2001). To verify the ability of the plectin tail to bind to MTs, a plasmid encoding an EGFP-fusion protein containing a tail fragment of plectin (Fig. 52A), similar to the one used by Sun et al. (2001), was transfected into plectin-deficient keratinocytes (Fig. 52B-D). Albeit this fragment was expressed in cells at the correct size (Fig. 52E), no decoration or bundling of MTs using immunofluorescence microscopy could be observed. Instead, we found this fragment to be diffusely distributed in the cytoplasm and/or associated with cytoplasmic aggregates (Fig. 52C, D), inconsistent with a role of plectin`s tail in MT-binding.

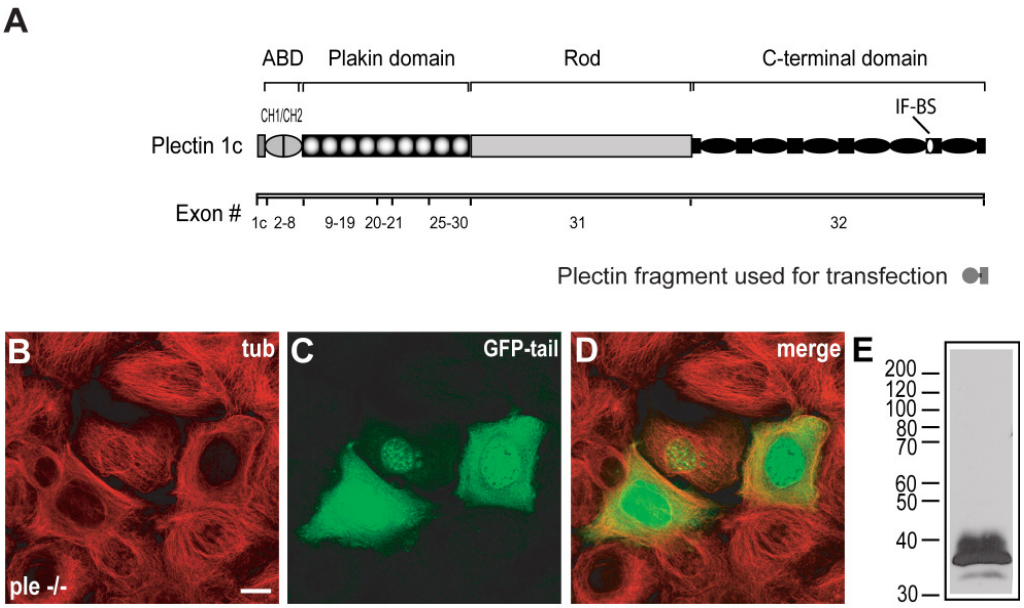

Figure 52. Plectin`s tail fragment does not colocalize with MTs upon transient transfection of plectin (-/-) cells. (A) Schematic representation of plectin subdomains, exon allocations and the tail fragment of plectin used for transfection. Segments to which functions have been assigned are indicated. ABD, actin-binding domain consisting of CH1/CH2 regions; IF-BS, intermediate filament binding site. (B-D) Transfected plectin (-/-) keratinocytes were stained with anti-tubulin antibodies to visualize MTs. Localization of the tail-fragment was visualized by GFP fluorescence. Note diffuse cytoplasmic and nuclear distribution of plectin`s tail, but no decoration of MTs. (E) Immunoblot analysis of a total cell lysate of transfected (-/-) cells using anti-GFP antibodies. Note expression of GFP-tail fragment of the expected size (35.5 kD). The observed band-shift is likely due to phosphorylation of GSR-repeats within the tail sequence. Bar, 10 µm

SH3-like domain in plectin`s plakin domain binds to MAPs in vitro

Earlier experiments had shown that plectin purified from glioma C6 cells bound to high-Mr MAPs from hog brain (Hermann and Wiche, 1987). To investigate which interaction sites were involved in plectin's binding to high-Mr MAPs (Herrmann and Wiche, 1987) various fragments of plectin 1c were expressed as fusion proteins with N- or C-terminal GST tags (Fig. 53A) and used for blot overlay assays. In studies on ACF7/MACF (Yang et al., 1999) the M1 domain which represents a segment of the N-terminal plakin domain, and thus is common to all known plakin protein family members, has recently been identified as a putative MT-binding site.

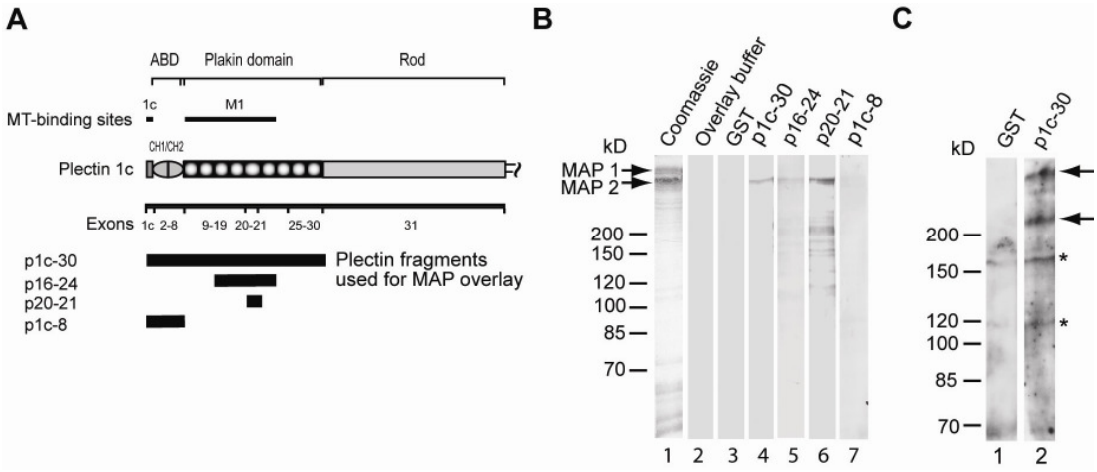

Figure 53. Binding of plectin`s SH3-like domain to MAPs. (A) Schematic representation of plectin subdomains, exon allocations and fragments of plectin used for cosedimentation and overlay assays. Note that the C terminus of plectin is not shown. ABD, plakin and rod domains are indicated. Putative MT-binding sites are indicated. (B, C) MAPs prepared from hog brain (B, arrows) and plectin (+/+) keratinocytes (C) were separated by SDS-PAGE (B, Coomassie), transferred to nitrocellulose membrane and overlaid with 8 μg/ml of indicated GST-tagged plectin fragments, or GST alone, or overlay buffer as negative control. Bound proteins were visualized using antibodies to GST. Note specific binding of plectin fragments p1c-30, p16-24 and p20-21 to hog brain MAPs (B), and of p1c-30 to two HMW keratinocyte MAPs (C, arrows). Protein bands showing unspecific binding are marked by asterisks in (C). Positions of molecular mass markers are indicated.

When fragments of plectin containing the entire N terminus, including the ABD and plakin domain (p1c-30) or parts of it (p16-24 and p20-21; see Fig. 53A, C) were purified (Fig. 53C)

and overlaid onto nitrocellulose-blotted MAPs prepared from hog brain (Fig. 53D), all of them showed binding to a neuronal high-M_r MAP (Fig. 53D, lanes 4-6), whereas p1c-8 and the GST tag alone showed no binding (lanes 3 and 7). Similarly, p1c-30 showed specific binding to two high-M_r MAPs isolated from plectin (+/+) keratinocyte homogenates (Fig. 53E, arrows). These data led me to conclude that plectin 1c can interact with MTs via two independent N-terminal binding sites, one representing an isoform-specific tubulin targeting site, the other an additional MAP interaction site.

Interestingly the minimal sequence of the plectin plakin domain (p20-21) that bound to MAP2 encompassed exons 20-21. Protein sequence alignment of the sequence encoded by plectin exons 20-21 and a putative SH3 domain residing within BPAG1`s plakin domain (Jefferson et al., 2006) revealed the presence of an SH3-like domain also within the plakin domain of plectin (Fig. 54)

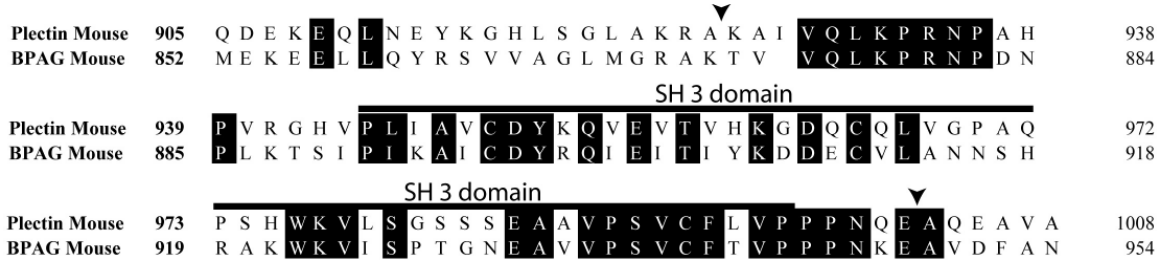

Figure 54. Localization of a putative SH3 domain in sequences of plectin encoded by exons 20-21. Protein sequence alignment of the putative SH3 domains of BPAG1 (Jefferson et al., 2006) and of plectin. The position of the SH3 domain is indicated with a black line. The amino acid sequence of plectin fragment p20-21 is marked with arrowheads. Background in black indicates identical amino acids, that in light grey similar amino acids.

Absence of plectin leads to increased density and stability of MTs during Ca^{2+}-induced stratification of keratinocytes.

MTs are dynamic polymers that change their distribution during the cell cycle and differentiation of cells. To study possible effects of plectin deficiency on MT organization in vivo in cells undergoing stratification, plectin (+/+) keratinocytes and their plectin-deficient counterparts were subjected to Ca^{2+}-induced stratification. Stratification of keratinocyte monolayers in vitro is accompanied by a dynamic rearrangement of MTs (Lewis et al., 1987). Immunfluorescence microscopy of plectin (+/+) and plectin (-/-) keratinocytes grown in

normal (low Ca^{2+}) medium, revealed typical MT networks radiating from the nucleus towards the cellular periphery in both cell types, with a slight tendency to a higher density of MTs observed in plectin (-/-) cells (Fig. 55A,B). When the concentration of Ca^{2+} in the culture medium was raised, formation of desmoplakin and E-cadherin-positive cell-cell contacts occurred in both cell types (see Figs. 43 and 44). MTs in plectin (+/+) keratinocytes did not undergo significant changes during the initial stages of stratification, except that in some cells, they were found to accumulate in peripheral bundles oriented in parallel to cell-cell contact sites (Fig. 55C, arrowheads). Contrary to this, in plectin-deficient keratinocytes a strongly increased tubulin signal and dense arrays of MTs extending throughout the whole cell were observed (Fig. 55D).

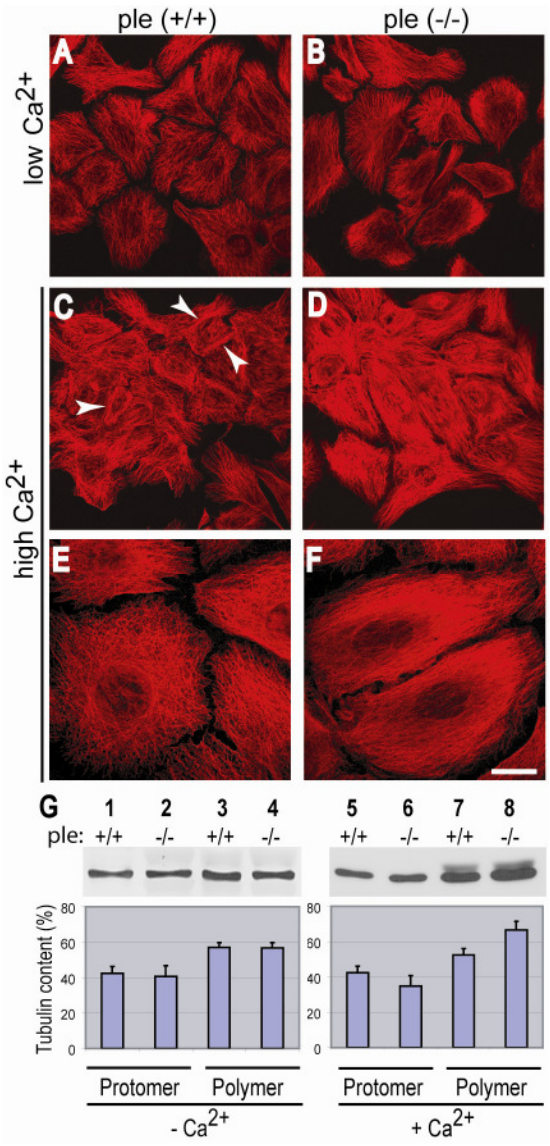

Figure 55. Increased MT formation and MT density in plectin-null keratinocytes. (A-F) Immunofluorescence microscopy of control (+/+) and plectin-deficient (-/-) keratinocytes. Cells were processed for immunofluorescence microscopy after cultivation in 0.05 mM Ca^{2+} medium (low Ca^{2+}) (A, B), or after exposure to 1.8 mM Ca^{2+} (high Ca^{2+}) for 3h (C-F). MTs were visualized using anti-tubulin antibodies. Note denser arrays of MTs in plectin (-/-) keratinocytes after Ca^{2+}-induced stratification (D, F), compared to control cells (C, E). Bars, 10 µm. (G) Fractions containing protomeric and polymeric tubulin pools were prepared from cells cultured in low Ca^{2+} (- Ca^{2+}) or high Ca^{2+} for 3 hours (+ Ca^{2+}) and subjected to immunoblotting using anti-tubulin antibodies. Note increased amount of tubulin in the polymer-fraction in plectin (-/-) cells after Ca^{2+}-induced stratification. Fractionation experiments were repeated at least three times and quantification was done by densitometric scanning of immunoblots. Blots from one representative experiment of three and mean values ± SEM from three experiments are shown.

As revealed at higher magnification (Fig. 55F), these densely packed MTs appeared to be laterally aligned, whereas in most plectin (+/+) keratinocytes MTs were still distributed in a network-like, more orthogonal pattern (Fig. 55E). Using a protocol to obtain subcellular fractions containing protomeric and polymeric tubulin, I observed that stratifying (-/-) keratinocytes contained increased amounts of polymeric tubulin compared to (+/+) cells (Fig. 55G, lanes 7 and 8 and quantitation below). This indicated that the increase in fluorescence intensity observed during stratification was due to increased MT formation.

These observations were further supported by electron microscopy of embedded thin sections from stratifying plectin (+/+) and (-/-) keratinocytes. In this way, networks of densely bundled MTs were revealed in plectin (-/-) cells, but not in wild-type cells (S. Reipert and K. Andrä, unpublished data). These data left no doubt that the absence of plectin led to a dense packing or bundling of cytoplasmic MTs.

Immunoblotting analysis of cell lysates of plectin (+/+) monolayers, prepared at different timepoints of Ca^{2+}-induced differentiation, using antibodies to tyrosinated, detyrosinated, and acetylated tubulin revealed a slight increase in the amount of detyrosinated tubulin-containing, and thus stable, MTs (Fig. 56A), during terminal differentiation, whereas the content of acetylated tubulin did not change and levels of tyrosinated tubulin were downregulated. Tubulin detyrosination, which happens as a consequence of increased MT stability, increased only very late in terminal differentiation. To address the question, whether the bundled MT arrays observed in plectin (-/-) keratinocytes consisted of stable MTs, I performed immunoblotting on lysates of undifferentiated and stratifying plectin (-/-) and wild-type keratinocytes using antibodies to acetylated tubulin. Interestingly, undifferentiated monolayers of plectin (-/-) cells already contained a significantly increased amount of acetylated tubulin in comparison to their wild-type counterparts (Fig. 56B). This elevated levels of acetylated tubulin in plectin (-/-) keratinocytes became even higher during stratification (Figs. 56B and C), whereas in wild-type cells, the levels of acetylated tubulin remained generally low. These data confirmed the presence of more stable (less dynamic) MT arrays in plectin (-/-) keratinocytes. In fact, MTs of stratifying plectin (-/-) keratinocytes showed a strong resistance against nocodazole or colchicine-induced depolymerization (K. Andrä, unpublished data).

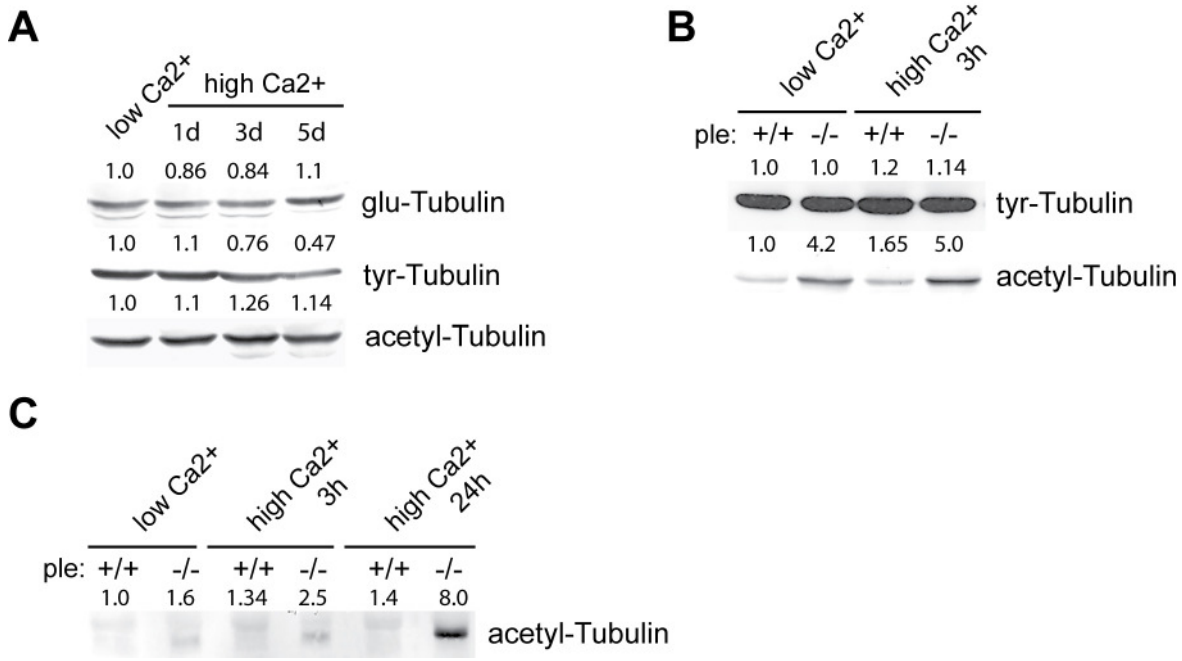

Figure 56. Increased acetylated tubulin content in plectin (-/-) keratinocytes. (A) Immunoblotting analysis of post-translational tubulin modifications in differentiating keratinocytes using antibodies to detyrosinated (glu-), tyosinated (tyr-), or acetylated (acetyl-) tubulin. Note a slight increase in levels of detyrosinated tubulin and a strong decrease in levels of tyrosinated tubulin. (B, C) Immunoblotting analysis of post-translational tubulin modifications in plectin (+/+) versus plectin (-/-) keratinocytes grown in low Ca^{2+} or in high Ca^{2+} for 3 (B, C) or 24 (C) hours. Numbers above lanes represent the protein ratios relative to an arbitrary level of 1.0 determined by the first sample in each lane. One of two experiments is shown.

Part IV – Analysis of the migration defect of a plectin-deficient fibroblast cell line

In contrast to plectin-deficient keratinocytes, plectin-deficient primary fibroblasts were shown to migrate slower than their wild-type counter parts (Andrä et al., 1998). Participating in a project to analyze the molecular mechanisms causing the slower migration of wild-type and plectin-deficient plectin-deficient fibroblasts, I compared the migratory behavior of

immortalized fibroblast cell lines. These cell lines were derived from plectin (+/+)/p53 (-/-) and plectin (-/-)/p53 (-/-) mice and will be referred to as plectin (+/+) and plectin (-/-) fibroblasts, respectively. Similar to plectin (-/-) keratinocytes, plectin (-/-) fibroblasts were isolated from plectin-null mice (line 29) carrying a disruption in plectin`s rod-encoding exon 31, which leads to a null phenotype (Andrä et al., 1997).

Slower PDGF-dependent migration of plectin-deficient fibroblasts

In a scratch wound closure assay, plectin (-/-) fibroblasts turned out to migrate more slowly into the denuded monolayer area in response to PDGF-BB (biologically active dimeric PDGF composed of two B subunits) stimulation than plectin (+/+) fibroblasts (Fig. 57), similar to the migration behavior that was originally described for primary plectin-deficient fibroblasts (Andrä et al., 1998). The reduced migratory ability of plectin (-/-) fibroblasts was later confirmed by time lapse video microscopy (Gregor et al., manuscript in preparation).

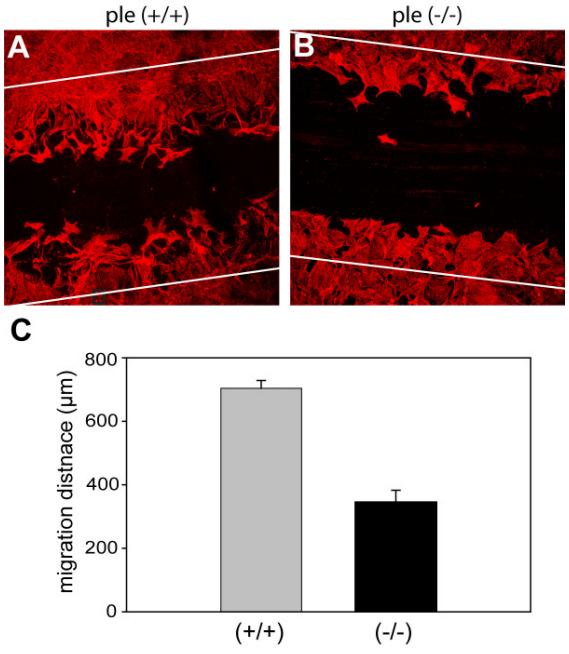

Figure 57. Slower PDGF-dependent migration of plectin (-/-) fibroblasts. (A, B) Plectin (+/+) and plectin (-/-) fibroblasts were grown in parallel until reaching confluence (~48 h) and serum-starved o/n. Subsequently, a scratch wound was introduced into the monolayer and cells were further incubated for 12 h in medium supplemented with PDGF-BB. Cells were fixed and stained using mAbs to actin. The lines drawn in the images represent reference lines marking the width of the scratch when it was made. (C) Average values of migration distances from 10 different optical fields (10x objective) from three independent experiments are shown (mean ± the SEM).

The migration phenotype manifested itself only, when cells were stimulated with serum or PDGF-BB, but not when growth factors were absent from the medium, indicating a defect in the chemotactic response of plectin (-/-) fibroblasts (Gregor et al., manuscript in preparation).

Increased peripheral RACK1 accumulation and PKCδ activity in migrating plectin (-/-) fibroblasts

It has previously been shown that in fibroblasts, plectin serves as a regulator of PKC signaling, through sequestration of the PKC-scaffolding protein "receptor for activated C kinase 1" (RACK1) (Osmanagic-Myers and Wiche, 2004). In plectin (-/-) fibroblasts, the cytoskeleton-associated fraction of RACK1 was found to be reduced, and the protein was found predominantly at sites to which it normally translocated upon growth factor-induced PKC activation. Concomitantly, dislocation of PKCδ and elevated enzymatic activity were observed in these cells (Osmanagic-Myers and Wiche, 2004). Importantly, PDGF-BB-stimulated membrane translocation and clustering of PKCδ at the leading edge was shown to drive migration of fibroblasts (Fan et al., 2006). Therefore, I analyzed activation of PKCδ in fibroblasts migrating into a scratch wound. PKCδ was found to be reproducibly hyperactivated in three plectin (-/-) fibroblast cell lines (isolated from individual plectin knockout pubs) when compared to two independent plectin (+/+) fibroblast cell lines (Fig. 58A). (These cell lines were prepared and kindly provided by L. Winter, our laboratory).

Since PKCδ hyperactivation in plectin (-/-) fibroblasts happens concomitantly with accumulation of RACK1 at the cellular periphery (Osmanagic-Myers and Wiche, 2004), I next looked at the localization of RACK1 in cells migrating at wound margins (Fig. 58B-I). As expected, numerous plectin (-/-) fibroblasts that were migrating into the scratched area displayed increased peripheral accumulation of RACK1 (Fig. 58C, arrows), in contrast to plectin (+/+) cells, which rarely showed peripheral RACK1 accumulation (Fig. 58B, arrow). Higher resolution images demonstrated extensive localization of RACK1 in membrane ruffles and at lamellipodial edges of plectin (-/-) cells (Fig. 58G-I). Thus, peripheral RACK1 accumulation and increased PKCδ activation, as they were originally observed in subconfluent plectin (-/-) cell cultures, are definitely related to the reduced migratory ability of plectin-deficient fibroblasts.

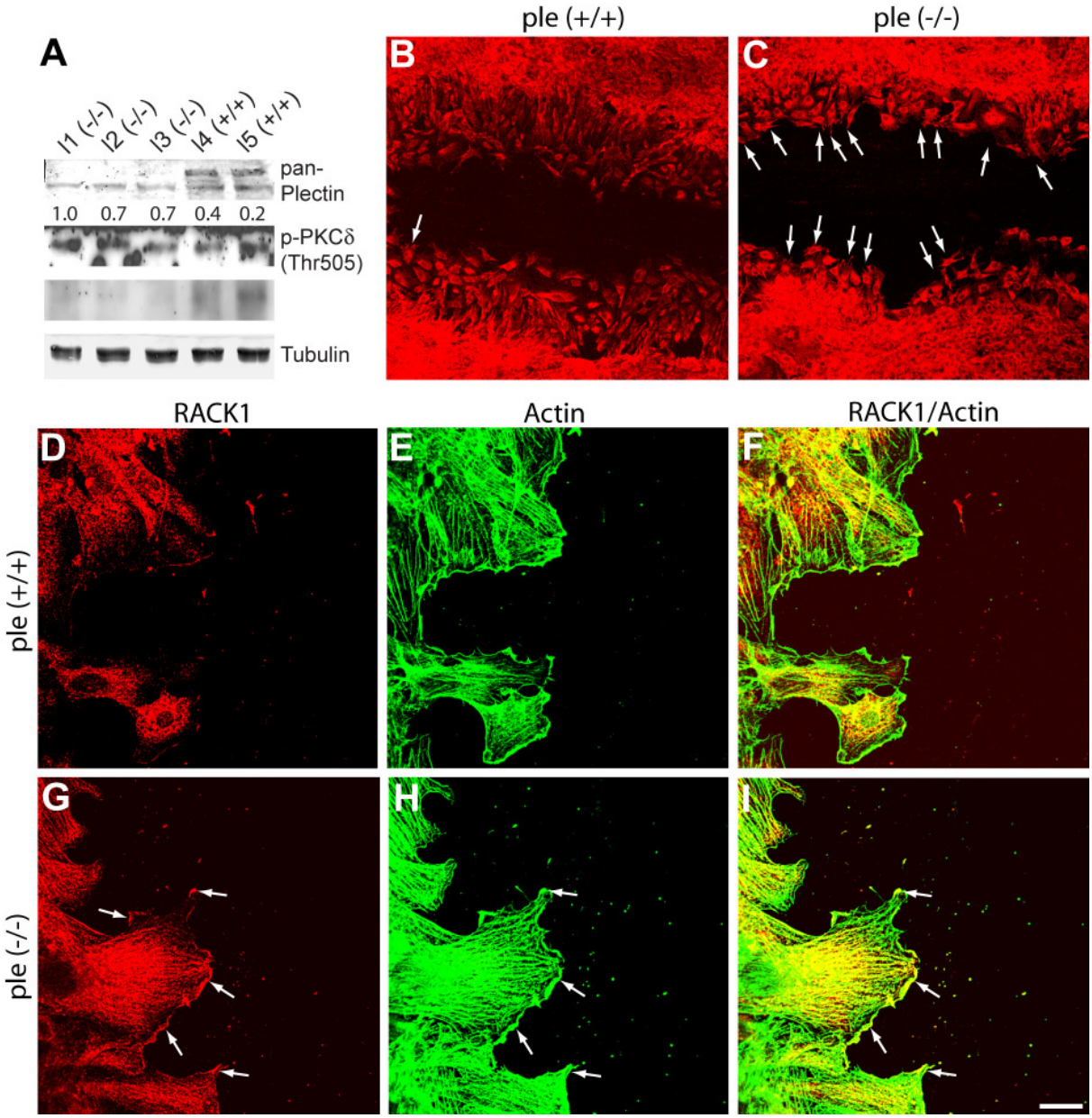

Figure 58. Slower PDGF-dependent migration of plectin (-/-) fibroblasts correlates with altered activation of Rack/PKCδ complex. (A) Total cell lysates from 3 different scratched plectin (+/+) cell lines (designated l4 and l5) and 3 plectin (-/-) cell lines (designated l1, l2 and l3) were subjected to immunoblotting using antibodies to pan-plectin (N-term), (Thr505-phosphorylated) p-PKC, and total (unphosphorylated/phosphorylated) PKCδ. Tubulin was used as a loading control. (B, C) Representative images of scratch wounds. Plectin (+/+) (line l5) and plectin (-/-) (line l1) cells were immunolabeled with antibodies to RACK1. Arrows point to cells displaying peripheral RACK1 accumulation. (D-I) Representative images of fibroblasts at the wound edge stimulated with PDGF. Cells were double immunolabeled for RACK1 (D, F, G, I) and actin (E, F, H, I). Note increased accumulation of RACK1 at lamellipodial edges of plectin (-/-) in comparison to plectin (+/+) cells (arrows in G-I). Bar, 10 µm.

Increased focal adhesion contact numbers and decreased focal adhesion kinase/paxillin phosphorylation levels in migrating plectin (-/-) fibroblasts

Other hallmarks of the cytoskeletal phenotype of primary plectin-deficient fibroblasts are increased formation of stress fibers and enlargement and increase in numbers of focal adhesion contacts (FACs) (Andrä et al., 1998). As expected, plectin (-/-) fibroblasts migrating at the wound margin displayed both these phenotypes (Fig. 59B). Immunoblotting analysis with anti-pan-phospho-tyrosine antibodies revealed reduced tyrosine-phosphorylation of proteins corresponding to focal adhesion kinase (FAK) and paxillin (Burridge et al., 1992) in lysates of scratched plectin (-/-), compared to wild-type fibroblast monolayers (Fig. 59C). Reduced phosphorylation of these proteins is correlative with reduced FAC turnover (Tilghman et al., 2005; Zaidel-Bar et al., 2007), suggesting that the increased number and size of FACs in migrating plectin (-/-) fibroblasts can be attributed to their reduced turnover.

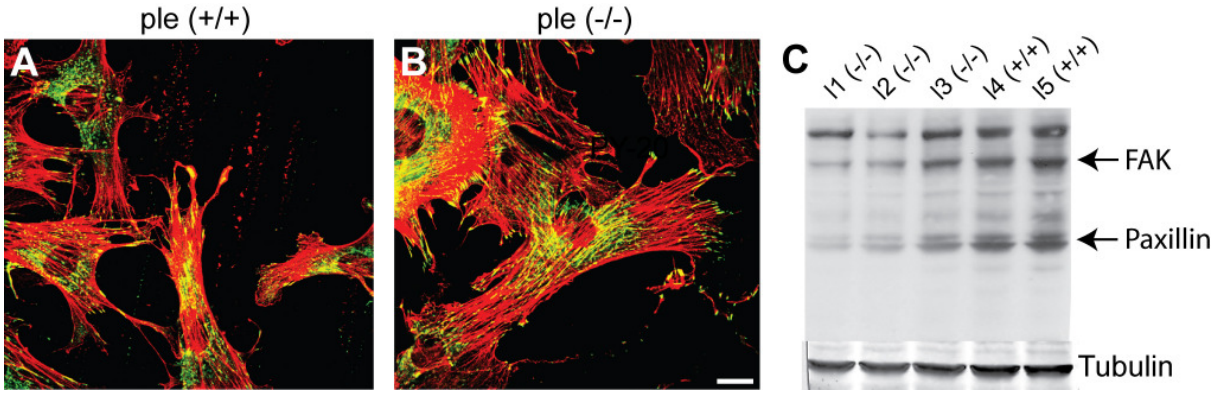

Figure 59. Increased stress fibers and focal adhesion contacts content in plectin (-/-) fibroblasts. (A, B) Cells were fixed and immunolabeled for actin (red) and vinculin (green). Note increased numbers of stress fibers and vinculin-positive focal adhesion contacts in plectin (-/-) cells migrating at wound edges. (C) Total cell lysates from different scratched plectin (+/+) (lines l4 and l5) and plectin (-/-) cell lines (lines l1, l2 and l3) were subjected to immunoblotting using antibodies to pan-phospho-tyrosine. Tubulin was used as a loading control. The positions of phosphorylated FAK and paxillin are indicated. Bar, 10 µm.

DISCUSSION

Conditional targeting of plectin in prenatal and adult mouse stratified epithelia causes keratinocyte fragility and lesional barrier defects

Similar to plectin-null mice, K5-Cre KO mice with a specific deletion of plectin in stratified epithelia died within 1-3 days postnatally exhibiting severe skin fragility, focal skin barrier defects and growth retardation. Focal skin barrier defects appeared to arise as a consequence of localized keratinocyte cytolysis and thus did not imply a direct role of plectin inbarrier formation. Similar skin lesions with increased TEWL have previously been reported for desmocollin 1-null mice (Chidgey et al., 2001) where they were related to localized acantholysis. Small Toluidine-Blue-stained lesions were also found in the skin of K5 knockout mice, where they were attributed to cytolysis of basal keratinocytes (Peters et al., 2001). The early onset of blister formation and the severity of tissue fragility clearly showed that plectin is more important than BPAG1 in linking keratin filaments to HDs, as BPAG1 knockout mice grow to adulthood and display only mild blistering (Guo et al., 1995). The association of the α6β4 integrin with plectin via the β4 subunit and their clustering is crucial for the formation of SACs (Koster et al., 2003). In cultured keratinocytes, subsequent interaction of BP180 with plectin ultimately leads to incorporation of BPAG1 into SACs and the maturation/stabilization of these complexes (Koster et al., 2003). In accordance with these data, I found that BPAG1 expression was downregulated in vivo in K5-Cre KO epidermis, and that hemidesmosomal localization of BPAG1 was compromized. Apart from the formation of blisters and lesions due to epidermal detachment, the epidermis of K5-Cre KO displayed a normal stratified organization and correct expression patterns of differentiation markers, and proliferation and survival of keratinocytes were unaffected. The occasional presence of apoptotic cells in the lumenproximal keratinocyte layer of blister roofs indicated that, although cytolysis due to keratinocyte disruption above the HDs predominated, some still intact keratinocytes underwent programmed cell death. However, massive apoptosis of basal keratinocytes, as it was observed upon epidermal detachment in integrin β4-deficient mice (DiPersio et al., 2000; Dowling et al., 1996), was not evident. The skin phenotype of K5-Cre KO mice resembled that of children suffering from EB-PA (OMIM accession no. 226730), who are born with an extremely fragile skin (Charlesworth et al., 2003; Pfendner

and Uitto, 2005). As most of these patients harbored premature termination codon or nonsense mutations in exons encoding N-terminal parts of the protein, a rapid decay of the prematurely terminated short RNA transcripts formed is very likely, leading to a complete absence of the protein (Charlesworth et al., 2003). EB-PA mutations being located upstream of exon 31 (the exon encoding plectin's rod domain; (Liu et al., 1996) could therefore not be compensated for by rodless plectin isoforms, explaining the more severe phenotype of patients with plectin-associated EB-PA, compared with patients suffering from EB-MD. Thus, mice with a specific deletion of plectin in stratified epithelia, such as our K5-Cre KO mice, can be considered as an ideal model for the stratified epithelia phenotypes of patients with severe forms of plectin-associated EB-PA. Before dying, K5-Cre KO mice became progressively weaker, ceased to grow and apparently became unable to suckle, as their stomachs remained empty. Inspection of the oral cavities of newborn K5-Cre KO mice after at least one nursing showed the presence of multiple blisters on their palates and in some cases also on their tongues. Therefore, we reason that the mechanical stress applied to the oral epithelia by sucking and swallowing was the cause of the oral blister formation. As a consequence, the pups' desire for food was probably reduced due to pain and possibly obstruction of the oral cavity by especially large blisters or cellular debris. A similar runting due to prevention of feeding by erosive mucosal blistering was described for mice lacking desmoglein 3 (Koch et al., 1997). In these mice, lesions were initially caused by sucking and became even worse when growing mice began eating solid food. The finding that K5-Cre KO mice did not show epithelial detachment in the esophagus was not surprising, as the liquid diet of neonatal mice exerts only low mechanical stress on such organs. Mucosal involvement is common in various forms of EB and cases of mucosal blistering associated with EB-MD (OMIM accession no. 226670) have been described (Kunz et al., 2000; Schara et al., 2004). The mouth and throat problems of patients suffering from EB have been reported to often cause a serious disruption of nutrient intake, similar to what we observed with K5-Cre KO mice. Because of oral blistering these children barely grow, as there is a higher need for nutrients because the body loses proteins along with the wound exudate and also has to sustain normal metabolism (information available at the DebRA website: www.debra-international.org). Pyloric atresia manifests with gastric abnormalities, primarily pyloric and duodenal atresia. However, in K5-Cre KO mice, the movement of coagulated milk from the pylorus into the intestine was not obstructed and consequently, the stomachs were not distended, ruling out that conditional knockout animals were suffering from pyloric atresia.

Moreover, the absence of gastric pathologies in K5-Cre KO mice proved the targeting of the plectin gene to be exclusive for stratified epithelia, without affecting simple epithelia.

Even though the epidermis of OHT-treated *PLEC*$^{flox/-}$:K5-Cre-ER^{T} mice showed only a mosaic pattern of plectin deletion, its susceptibility towards mechanical stress-induced damage was found to be clearly increased. Evidently, the patchwise deletion of plectin rendered the epidermis more prone to trauma, as revealed by increased TEWL (Ackerl et al., 2007) and lesion formation. The observed more readily removable cells of the deeper epidermal cell layers by tape stripping may also be related to the lesion formation, although reduced cohesion of keratinocytes in the outer epidermal layers due to weakened desmosomal connections cannot be ruled out at the present stage. Although we used quite high concentrations of OHT to activate Cre recombinase, plectin deletion was achieved only in patches of adult mouse epidermis. Inducible deletion of floxed genes in adult mice via Cre-ER^{T} recombinase is not always 100% effective and appears to be especially difficult to achieve when cytoskeleton-associated proteins with a long half-life are targeted (Lopez-Rovira et al., 2005). The very low turn-over rate of plectin in polarized epithelia (Eger et al., 1997) might explain the relatively weak deletion of plectin expression 14 days after Cre activation, since Cre is activated within 24 hours of the final OHT treatment (Indra et al., 1999). It might be advantageous for future studies to use K14-Cre-ER^{T2} mice, in which induction efficiency is more potent than in K5-Cre-ER$_{T}$ mice (Indra et al., 1999), and to combine this approach with topical application of OHT, which is less toxic than intraperitoneal injection (Vasioukhin et al., 1999) and can be done over longer periods (Benitah et al., 2005). Once more efficient deletion of plectin in adult stratified epithelia has been achieved, it will be interesting to re-evaluate skin barrier function, and moreover, investigate other yet unaddressed skin related topics, such as wound healing and hair growth. Interestingly, it was shown that keratin mutations contribute to EBS in a mouse model by inducing local inflammation that mediates a stress response with possible involvement of matrix metalloproteinases (Lu et al., 2007). It would thus be interesting to investigate by using the mouse models presented in this study, whether similar mechanisms might be involved in the pathologies of EBS-MD and EB-PA. In summary, the generation of conditional stratified epithelia-specific plectin knockout mice has improved our understanding of the phenotypic manifestations of plectin deficiency in multilayered epithelia. Most importantly, the generation of mice carrying floxed plectin alleles makes it now possible to analyze the function of plectin in various other tissues known to be affected by EB-MD, such as skeletal muscle and brain. In addition, by refining the inducible knockout

of plectin in skin, deeper insights into plectin functions in the adult organism might be gained, and a test system for the development of therapeutic approaches for skin blistering in EB-MD/EB-PA might be obtained.

Plectin organizes IF networks and mediates formation of SACs in cultured keratinocytes

This study provides evidence that plectin plays a crucial role in the appropriate organization of IF networks in keratinocytes. As discussed in (Osmanagic-Myers et al., 2006), in plectin's absence, these networks are less delicate, their mesh size is increased, and individual filaments appear bundled and more straight. Plectin appears to control the properties of other IF systems as well, as alterations of IF networks resembling those described here for keratinocytes were also observed in plectin-deficient fibroblasts (Martin Gregor, unpublished data). Furthermore, a recent study suggests that plectin regulates both the organization and solubility of GFAP in astrocytes (Tian et al., 2006).

Interestingly, the keratin phenotype in plectin-deficient keratinocytes becomes most apparent in cells that are migrating. Upon initiation of migration, plectin relocates from SACs at the basal surface to the periphery of cells, where it associates with the tips of keratin filaments. Thus it appears that plectin plays an important role in organizing keratin network cytoarchitecture during keratinocyte migration. In fact, plectin mRNA expression was found to be quickly upregulated upon wounding of human skin (Cole et al., 2001). The importance of keratins as negative regulators of epithelial migration has been previously studied in keratinocytes and simple epithelial cells. Gene targeting of both K6a and K6b increases keratinocyte outgrowth in skin explant assays (Wong and Coulombe, 2003) and K8-ablated HeLa and Panc-1 cells migrate faster than control cells (Long et al., 2006). Likewise, epidermolysis bullosa simplex cell lines carrying K14 mutations display fast migration in vitro (Morley et al., 2003). Importantly, perinuclear reorganization of intact K8/18 filaments in Panc-1 cancer cells upon treatment with sphingosylphosphorylcholine has been shown to increase cellular elasticity and to stimulate migration (Beil et al., 2003). Shortly after we published our paper, two reports showed that depletion of periplakin or plectin in MCF-7 cells, contrary to keratinocytes, leads to slower migration rates, caused by defects in the re-organization of K8/18 filaments at the wound edge (Boczonadi et al., 2007; Long et al., 2006;

Nievers et al., 2000). Likewise, plectin deficiency in hepatocellular carcinoma cells leads to altered organization of their K8/K18 network (Cheng et al., 2007). Thus, plectin appears to have opposite effects on cell migration in different epithelial cell types (i.e. keratinocytes versus simple epithelial cells). Taken together, it appears that the three-dimensional organization of the keratin network is crucial for adjusting epithelial cell migration, and that cytoskeletal linker proteins of the plakin family act as key regulators in this process.

Based on ultrastructural analysis, we suggested (Osmanagic-Myers and Wiche, 2004) that the mechanism behind the observed phenotype is a reduction of orthogonal cross-linkages between individual keratin IFs and of keratin filaments with F-actin in the absence of plectin. In cross-linking individual filaments at high angles, plectin's interaction with IFs would resemble that of filamin with microfilaments. Such a mode of action would be consistent with earlier studies showing plectin to be predominantly localized at crossover and branching points of IFs (Foisner et al., 1988). Similar to filamin, plectin was shown to exist in dimeric and tetrameric states. Tetrameric structures are assumed to be formed by antiparallel alignment of two parallel plectin dimers (Wiche, 1998). Thus, exposed C-terminal IF-binding sites on both ends of such structure have the ability to cross-link two filaments. Even individual parallel dimers may have a cross-linking capacity, as an additional N-terminal vimentin-binding site resides in the N-terminal actin-binding domain of plectin (Sevcik et al., 2004). Oligomers of plectin tetramers, which are generated by the head-to-head fusion of dumbbell-shaped plectin molecules (Foisner and Wiche, 1987), have been shown to form at IF branching points (Foisner et al., 1988). Cross-linking functions of plectin have also been clearly demonstrated by (Svitkina et al., 1996), who used immunogold electron microscopy to show that plectin is organized in millipede-like structures around the core of individual IFs, with plectin sidearms frequently making Y contacts with each other. Conceivably, such Y-shaped structures may emerge from head-to-head fusion of plectin molecules, allowing cross-linking at high angles. Moreover, these authors reported that plectin was not localized regularly all along IFs, but was more concentrated at their distal ends, which is consistent with my finding that defects in IF organization were most prominent in the peripheral regions of plectin (–/–) cells.

In line with plectin`s well defined role in the assembly and stabilization of hemidesmosomal complexes (Andrä et al., 1997; Koster et al., 2004; McMillan et al., 1998; Nievers et al., 2000; Schaapveld et al., 1998), I found the numbers of SACs, the in vitro equivalent of HDs in the epidermis, to be reduced in cultured plectin-deficient keratinocytes. Concomitantly, integrin β4 was only partially associated with SACs and instead co-

distributed with F-actin at lamellipodial edges. Thus, plectin-mediated clustering of Integrin β4 and subsequent stabilization of the bond of integrin 4 and laminin 322 in the ECM by anchoring of integrin β4 to the keratin network appears to be an important initial step in the formation of SACs (see Fig. 60). As SACs are being formed, strong binding of plectin to integrin α6β4 via its ABD and plakin domain (Koster et al., 2004; Litjens et al., 2003; Litjens et al., 2005; Rezniczek et al., 1998) prevents plectin association with F-actin, thereby generating microdomains that exclude microfilaments (Fig. 60). Destruction of actin filaments does not impair SAC assembly (Tsuruta et al., 2003), but increases the recovery of fluorescent integrin β4 after photobleaching (Tsuruta et al., 2003), indicating that F-actin might act as a "brake" to integrin β4 dynamics by limiting lateral diffusion of integrin β4 molecules. After SACs have been established, the anchorage of keratin filaments to the stable complex of laminin 322, integrin β4 and plectin then provides stress resistance for the keratin nework. In support of this view, keratin filaments of plectin (-/-) keratinocytes show a dramatic retraction from the cellular periphery upon hypoosmotic shock-induced cell swelling (Osmanagic-Myers et al., 2006). Importantly, during the time this thesis was written, Raymond et al. (2007) produced phenotypes similar to the ones observed in plectin (-/-) keratinocytes, including altered keratin network cytoarchitecture and integrin β4 distribution, by siRNA-mediated downregulation of plectin in a pre-cancerous keratinocyte cell line, thus confirming our data.

Mobilization of integrin α6β4 from HDs and subsequent re-localization in lamellipodia and filopodia accompanied by activation of integrin β4`s signalling potential is a major mechanism driving migration of keratinocytes (Geuijen and Sonnenberg, 2002; Santoro et al., 2003). Moreover, it contributes to carcinoma progression (Herold-Mende et al., 2001; Owens et al., 2003; Rabinovitz and Mercurio, 1997; Rabinovitz et al., 1999; Witkowski et al., 2000). Consistent with findings that a lack of integrin ß4 association with hemidesmosomes drives keratinocyte migration, a mutation in integrin ß4 that prevents plectin–integrin ß4 interaction leads to accelerated migration of keratinocytes (Geuijen and Sonnenberg, 2002; Herold-Mende et al., 2001). Fully in line with this, my studies demonstrate that in the absence of plectin keratinocytes show a completely abolished association of integrin α6ß4 with keratins, and consequently have an elevated migration potential. Importantly, the migration of plectin-deficient cells was significantly reduced when plectin was reexpressed (Osmanagic-Myers et al., 2006).

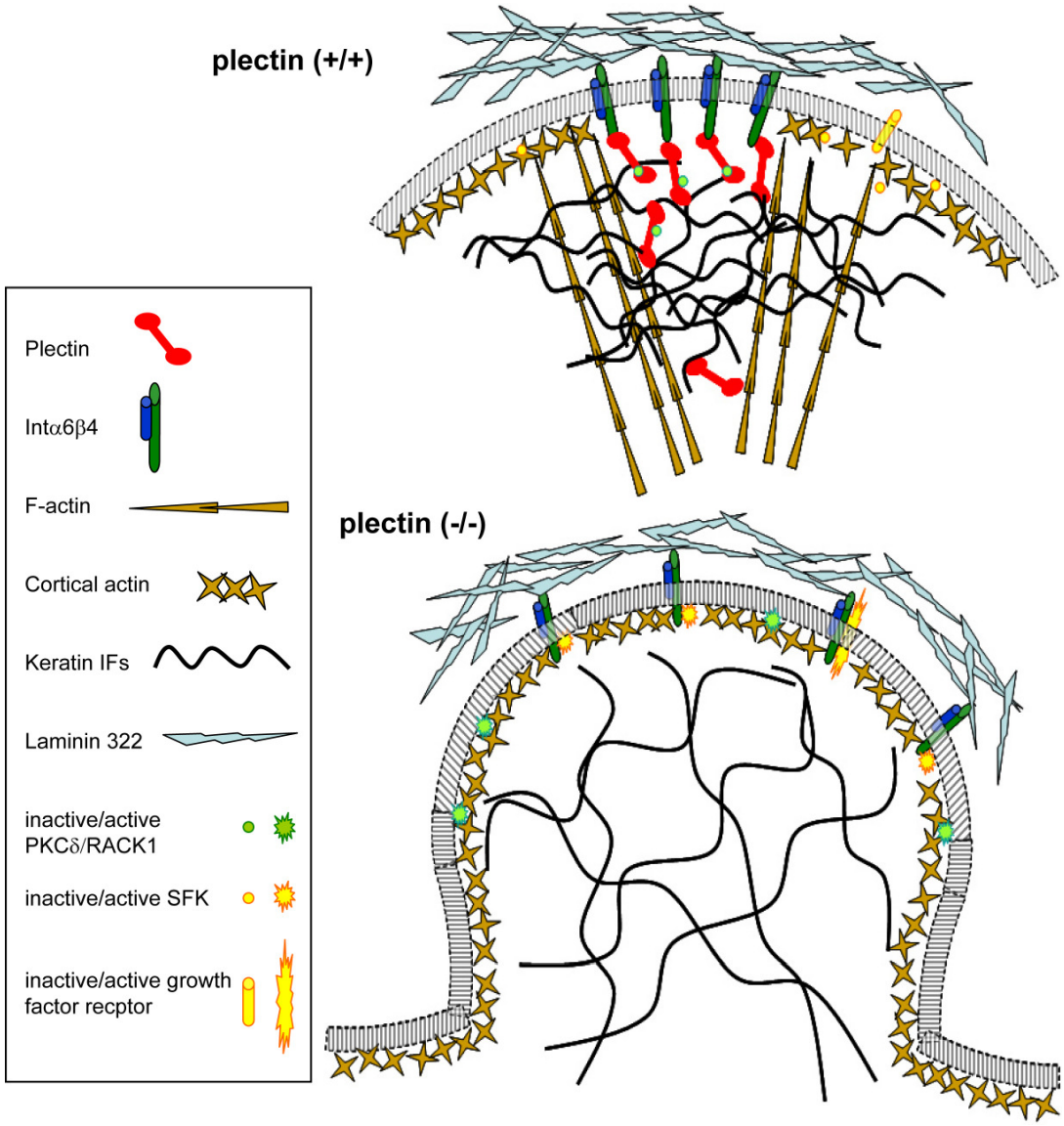

Figure 60. Model summarizing plectin`s role in organizing keratin filament cytoarchitecture and SAC formation. In plectin (+/+) keratinocytes, binding of integrin α6β4 to laminin 322 in the ECM, and connection of integrin α6β4 to the keratin filament cytoskeleton via plectin leads to the formation of SACs. SACs are keratin IF-anchored membrane-based multiprotein complexes which exclude actin filaments. Outside of SACs, plectin orthogonally crosslinks keratin filaments and connects them to F-actin. The scheme also depicts plectin as a cytoskeletal sequestering platform for RACK1/PKCδ. When plectin is absent [plectin (-/-)], integrin α6β4 re-distributes to lamellipodial edges where it associates with cortical actin. Clustering of integrin α6β4 in this "signaling-competent" compartment likely leads to binding and activation of SFKs and initiation of downstream signaling casccades, including the MAPK cascade. Absence of its scaffolding partner could also lead to accumulation of RACK1 (and possibly other plectin-binding regulatory proteins) at the cell periphery. As a consequence (direct or indirect), membrane-associated PKCδ activities become activated.

The plectin-MAP kinase link and its consequences for keratinocyte migration

The studies presented in my thesis show that the increased migration potential of plectin (-/-) compared with plectin (+/+) keratinocytes is directly linked to increased activation of a signaling cascade involving SFKs, MEK1/2 and Erk1/2. Erk has been implicated in the migration of numerous cell types (Huang et al., 2004), and it has been shown to be the sole kinase responsible for ECM-initiated migration of keratinocytes (Li et al., 2004). On the other hand, enhancement and directionality of growth factor signaling is mediated by both Erk and p38 kinases, whereas JNKs were reported to be uninvolved in keratinocyte motility (Li et al., 2004). By pharmacological inhibition of Erk's upstream kinases MEK1/2, the aberrant high migratory potential of plectin (–/–) keratinocytes could be restored to normal levels, but the abnormal keratin network organization of these cells could not be rescued. Therefore, it is safe to conclude that hyperactivation of Erk1/2 is a result of keratin network alterations and/or altered integrin β4 localization caused by plectin deficiency, rather than the opposite. In support of this, keratinocytes from EBS patients, with mutations in keratins leading to spontaneous formation of keratin aggregates, migrate significantly faster in comparison to control cells (Morley et al., 2003). Although Erk activities were not investigated in this study, elevated basal levels of the stress-activated kinase SAPK/JNK found in these cells (D'Alessandro et al., 2002) were implicated in their faster migration. This raises the intriguing question of whether distinct alterations in keratin network organization, such as aggregation in keratin-related EBS versus bundling in EBS caused by plectin deficiency, may lead to the up-regulation of distinct signaling pathways, such as SAPK/JNK versus MAPK.

The signaling pathway leading from plectin-related keratin network alterations to hyperactivation of the MAPK cascade still remains elusive. The analysis conducted so far shows that the activities of SFKs and PKCδ, key proteins known to be involved in the regulation of keratinocyte migration, are up-regulated in the membrane fraction of plectin-deficient cells, and that PP2-inhibition of SFKs indeed down-regulates Erk1/2 activities. Moreover, inhibition of PKCδ activity in keratinocytes by rottlerin also decreases Erk1/2 phosphorylation (Martin Gregor, unpublished data). Thus, membrane-associated SFKs and PKCδ are likely candidates for mediating of signals from plectin to Erk1/2. Both, SFKs and PKC can signal to the MAPK cascade. PKC can activate RAF-1 trough a mechanism involving RAF kinase inhibitory protein (RKIP) (Corbit et al., 2003), and c-Src was shown to

relieve RAF-1 autoinhibition (Tran and Frost, 2003). It remains to be answered, however, whether signals from SFKs and PKCδ plectin (-/-) keratinocytes converge in the MAPK cascade, or if both signaling proteins are part of the same signaling cascade. A signaling pathway involving c-Src activity upstream of PKC which transduces mechnical pressure signals has been described in keratinocytes (Hofmann et al., 2004). However, if the same signaling cascade is at play in plectin (-/-) keratinocytes remains to be established.

For the transduction of signals from the IF network to the membrane, the following mechanism might apply. Similar to a model proposed for PKCδ regulation through plectin-sequestration of RACK1 on vimentin IFs of fibroblasts (Osmanagic-Myers and Wiche, 2004), I propose that in keratinocytes PKCδ is sequestered on keratin IF-associated plectin molecules in a wild-type scenario, but is unbound to keratin IFs and has free access to the membrane because of its missing anchor in plectin-deficient cells. Upon pro-migratory signals, the complex of plectin, RACK1, and PKCδ dissociates from keratin filaments, PKCδ becomes activated and translocates to the cellular membrane, where it phosphorylates its targets, among them integrin β4 (Alt et al., 2001; Rabinovitz et al., 1999; Rabinovitz et al., 2004; Wilhelmsen et al., 2007). Release of integrin β4 from SACs by PKCδ phosphorylation and re-location to signaling competent domains (see below) then drives migration (Mariotti et al., 2001). In plectin (-/-) keratinocytes, RACK1 and PKCδ constitutively accumulate at the cellular periphery where they normally only relocate after pro-migratory signals. This leads to uncontrolled PKCδ activation (Fig. 60). Faster migration of plectin (+/+) keratinocytes overexpressing RACK1 (Osmanagic-Myers et al., 2006), is consistent with such a model.

Laminin-binding of integrin α6β4 was shown to trigger dimerization of integrin β4, followed by binding and activation of tyrosine phosphatase SHP-2 and the activation of SFKs. SFK-mediated phosphorylation of the cytoplasmic tail of integrin β4 then leads to recruitment of Shc, and activation of Ras and PI3K (Mainiero et al., 1997; Mainiero et al., 1995; Merdek et al., 2007). For these signaling events to occur, integrin β4 must be released from SACs and be palmitoylated, causing its association with lipid rafts (Gagnoux-Palacios et al., 2003). Based on these data, I propose as a hypothesis that in plectin (-/-) keratinocytes, where integrin β4 is released from its mechanical, adhesive role at SACs, more integrin becomes incorporated into signaling competent lipid rafts, leading to increased SFK activation and downstream Erk1/2 signaling (Fig. 60). There is no doubt about a major involvement of integrin β4 in the enhanced migratory potential of plectin (-/-) keratinocytes, since blocking laminin-binding by use of an inhibitory antibody lead to reduced migration

rates and moreover, caused changes in the MF network. Such a link between integrin β4 and actin organization has been discovered also in colon carcinoma cells (Rabinovitz and Mercurio, 1997).

Cortactin, an immediate downstream effector of c-Src, which is directly involved in actin assembly (Tehrani et al., 2007) at the lamellipodial edge, and is required for keratinocyte migration (Ceccarelli et al., 2007), showed strong accumulation at lamellipodial edges of plectin (-/-) keratinocytes, which was completely inhibited by PP2-treatment. Therefore, elevated SFK activities in plectin (-/-) keratinocytes are directly linked to enhanced migration via cortactin activation.

Fiftyfive % of migrating plectin (-/-) keratinocytes displayed a morphology with multiple, randomly oriented protrusions and migrated in a fast, but highly unpolarzied manner. The nature of the switch between slow directional and fast, but non-directional migration of plectin (-/-) keratinocytes remains elusive at the moment, but could involve activation/deactivation of cofilin. Integrin β4 was recently shown to activate cofilin via a pathway involving Rac1 and slingshot family (SSH) phosphatases (Kligys et al., 2007). Inactivation of cofilin by overexpression of dominant negative Rac1 or phosphatase dead SSH proteins in keratinocytes leads to formation of multiple lamellipodia and loss of cell polarity (Kligys et al., 2007; Sehgal et al., 2006). Kligys and collegues proposed a model, where integrin β4 activates cofilin in migrating keratinocytes allowing for local actin depolymerization at the leading edge of the cell, increasing integrin β4 dynamics and a concomitant modelling of laminin 322 matrix to generate a trail over which the cells migrate (Kligys et al., 2007). How exactly the high levels of inactivated cofilin in plectin (-/-) keratinocytes are brought about, is unclear at the moment, but changes in Rac1 activities due to plectin deficiency-caused alterations of integrin β4 localization could be involved.

In conclusion, I believe the results reported here have important implications for our understanding of the complexity involved in IF network regulation and formation and its influence on cell migration. In addition, they provide a better view on the actual severity and extent of EBS caused by plectin deficiency, as well as the basic molecular mechanism underlying this disease.

Plectin 1c – a novel microtubule binding protein

It is shown in this thesis that only one of several plectin isoforms expressed in neuronal N2A cells and epidermal keratinocytes, namely plectin 1c, specifically associates with MTs. Involving two distinct molecular domains of plectin, binding occurs to MTs without MAPS, and additionally to high-M_r MAPs. The association with MTs apparently dominates other potential interactions of this isoform, such as those with actin and cytokeratins. Direct binding to MTs appeared to occurr via plectin 1c-specific sequences, since plectin 1a did not cosediment with MTs. It is interesting to note that a segment in the sequence encoded by exon 1c shares high homology with the sequence repeats in the MT binding region of MAP 2 and Tau, where they are present in multiple copies (Dehmelt and Halpain, 2005). One can speculate that by proper localization of the 66 amino acids of the 1c sequence close to the core of the ABD of plectin a proper MT binding domain with a large positively charged interaction surface for tubulin could be formed.

Furthermore, a MAP-binding site in the plectin molecule could be narrowed down to an amino acid sequence within the plakin domain corresponding to exons 20 and 21 of its gene. Structural analysis of the plakin domain of plectin has recently revealed a molecular architecture that is defined by two pairs of spectrin repeats interrupted by a putative SH3 domain (Sonnenberg et al., 2007). Moreover, sequence alignments with other plakin family members have shown that the combination of spectrin repeats and a SH3 domain is a general feature of the entire plakin family (Jefferson et al., 2007; Jefferson et al., 2006). Interestingly the minimal sequence of plectin`s plakin domain (encoded by exons 20-21) that bound to MAP2 encompasses the putative SH3 domain (see Fig. 54). Several specific ligands of the SH3 domain of spectrin have been identified (Chow et al., 1999; Nedrelow et al., 2003). SH3 domains commonly recognize proline-rich sequences (Li, 2005), such as the ones present in multiple copies in members of the MAP2/tau family. We therefore strongly favor a model, where plectin binds to the PXXP motifs of MAP2/tau family members via its SH3 domain. The present results are in agreement with earlier reports showing specific binding of purified plectin from glioma C6 cells to MAP2 and MAP1 subtypes from brain (Herrmann and Wiche, 1987) and strong association of a BPAG1n-3 fragment, corresponding to the highly conserved M1 domain, with MTs (Yang et al., 1999). Based on the strong conservationd of the SH3-like domain among all plakin family members, it is likely that reported MT-binding of the ACF7 M1 domain (Karakesisoglou et al., 2000) is mediated by MAPs.

Upon transient transfection of plectins's C-terminal tail fragment into keratinocytes and COS7 cells, we could not observe an association with MTs. This does not confirm a recent study where a C-terminal tail fragment of plectin expressed in COS7 cells was claimed to decorate and bundle MTs (Sun et al., 2001). This obvious discrepancy might stem from the use of different protein tags (GFP vs. FLAG) or different cell systems (keratinocytes vs. COS7 cells), which might differentially affect putative MT-binding activity of the tail fragment.

The dual mode of binding to MTs described here for plectin 1c has recently also been characterized for another plakin family member, ACF7, which in addition to direct MT-binding via the M1 (Karakesisoglou et al., 2000) and/or the GAS2/GAR2 domain (Sun et al., 2001) can associate with EB1 (Slep et al., 2005), and therefore bind to MTs also indirectly. Moreover, desmoplakin was recently shown to regulate microtubule organization in stratifying keratinocytes by localizing the centrosomal microtubule-anchoring protein ninein to desmosomes (Lechler and Fuchs, 2007).

The involvement of MAPs in MT interaction of plectin suggests that this particular function of the protein has to be seen in a specific cellular context, as morphogenesis, status of cells, and specific cellular responses depend on a precise regulation of the MT network mediated by a balance of stabilizing (structural) MAPs and destabilizing factors. Plectin 1c and maybe other plectin isoforms, may play a key role in modulating this balance, however, in a strictly cell type-specific manner. This could explain why, for example, the MT network in plectin-deficient fibroblasts from mouse appears normal at least morphologically (Andrä et al., 1998), distinguishing it from differentiating keratinocytes.

The functional aspects of the interactions of cytolinkers, such as BPAG1n and ACF7/MACF, with MTs up to now have mainly been characterized as stabilization of MT networks (Kodama et al., 2003; Lee and Kolodziej, 2002; Lee S, 2002; Sun et al., 2001; Yang et al., 1999). Thus, it came as a surprise to find that the absence of plectin in keratinocytes undergoing Ca^{2+}-induced stratification resulted in densely packed and disorientated MT arrays. Moreover, MTs in plectin-deficient keratinocytes show increased stability towards MT-depolymerizing drugs. This phenotype can be rescued by forced expression of plectin 1c (Kerstin Andrä-Marobela, unpublished data), demonstrating that indeed plectin isoform 1c modulates MT dynamics in keratinocytes.

Regarding the molecular mechanisms operating in plectin 1c-mediated regulation of the MT system, the following scenarios may apply (Fig. 61). Plectin 1c is targeted to MTs via its ABD including exon 1c-specific sequences, and subsequently binds to MT-bound MAPs

of the MAP2/Tau family via the SH3 domain, acting as an antagonist of their MT-stabilizing role. This modulates the stability and dynamics of MTs during cellular rearrangements, such as Ca^{2+}-induced stratification of keratinocytes. E-MAP115 (ensconsin), for example, is a MAP that redistributes during Ca^{2+}-induced stratification of keratinocytes to the periphery of cells and bundles and stabilizes MTs in this process (Fabre-Jonca et al., 1999). A lacking antagonist to such MAPs might i) results in an impaired redistribution during stratification and ii) lead to higher density and stabilization of MTs. Such a modulator of MAP activities has recently been identified for the broadly expressed, non-neuronal MAP2/tau family member MAP4 (Kremer et al., 2005). The authors showed that depletion of the septin 2:6:7 trimer, a complex of GTP-binding proteins which was originally identified in budding yeast as a scaffold protein localized at the bud neck during cytokinesis, leads to increased stabilization of MTs by allowing more cytoplasmic MAP4 protein, which is normally sequestered by septins, to bind to MTs. Moreover, pathological overexpression of MAP4, occurring in pressure overload cardiac hypertrophy (Sato et al., 1997), was shown to induce a persistent stabilization of MTs that accounts for the contractile dysfunction of affected cardiocytes. One can envisage a mechanism for the regulation of MAP activities by plectin similar to the one described for septins and MAP4.

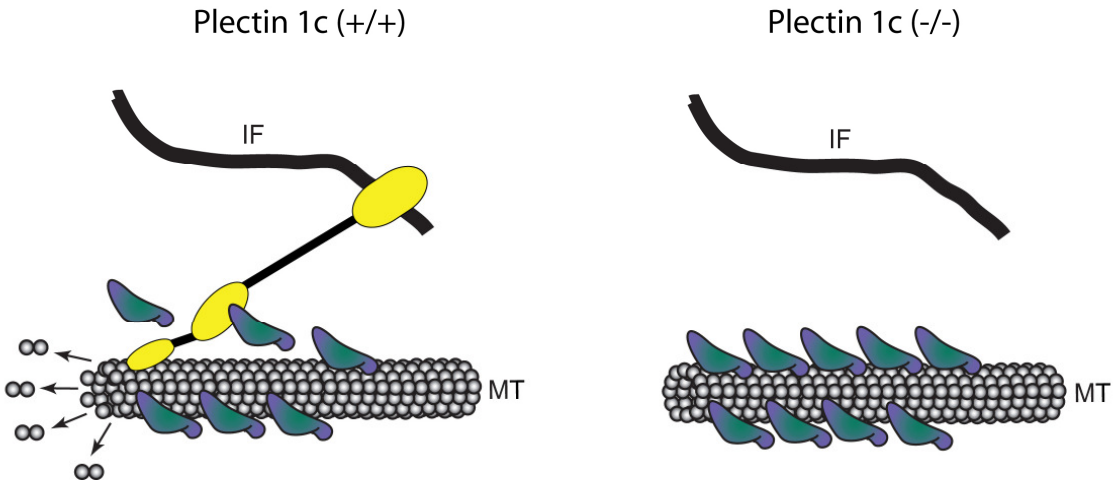

Figure 61. Model depicting plectins`s role in the regulation of MT dynamics. Plectin 1c-MT binding occurs via the plectin 1c-ABD. The SH3 domain binds to MAPs. Interference with MAP function(s) regulates the dynamics of MTs in wild-type cells [plectin 1c (+/+)]. When plectin 1c is absent [plectin 1c (-/-)], MAPs are hyperactive and MTs become hyperstabilized.

Only a few MAPs, such as E-MAP115 (Fabre-Jonca et al., 1999), have sofar been identified in keratinocytes. My findings that a recombinant N-terminal fragment of plectin 1c bound to a ~220 kD band (the approximate size of MAP4) in blot overlay assays of MAPs isolated from keratinocytes, would speak in favor of MAP4 being plectin`s binding partner in keratinocytes. However, the MAP binding partner(s) of plectin in keratinocytes must still be established.

Previous data have defined ACF7 and desmoplakin as regulators of MT-stability and cortical MT networks in keratinocytes (Kodama et al., 2003; Lechler and Fuchs, 2007). With plectin 1c, a third member of the spectraplakin family, to be likely involved in the regulation of keratinocyte MT networks, has now been identified.

Plectin`s function in desmosomes

Plectin has been identified as a desmosomal protein in stratified as well as simple epithelia (Eger et al., 1997; Skalli et al., 1994; Wiche et al., 1983). However, the desmosomal function of plectin remained elusive. So far, only one study has described the presence of "hypoplastic" desmosomes in the epidermis of a patient suffering from EBS-MD (Bauer et al., 2001). My studies in mice and cultured keratinocytes showed that plectin is not required for the formation and stability of desmosomes. Instead, I found that plectin-deficiency leads to reduced expression levels of desmoplakin. However, desmoplakin reduction was only moderate and did not affect desmosome formation and stress resistance of desmosomes, possibly as a consequence of compensation by other upregulated desmosomal plakins, such as envoplakin and periplakin. The mechanism behind the reduction of desmoplakin expression levels in plectin-deficient keratinocytes could possibly be the formation of a complex of desmoplakin and plectin, which stabilizes desmoplakin during transport to cell-cell contact areas. In fact, IF-associated particles containing desmoplakin have been observed in close proximity to microfilaments near cell borders and microfilament-associated adherens junctions at cell contact sites, upon induction of cell-cell contact (Godsel et al., 2005). Plectin might assist in the formation of such particles along IFs and keep desmoplakin in a soluble, transport-ready complex, similar to heterodimers of envoplakin and periplakin (DiColandrea et al., 2000; Karashima and Watt, 2002). Direct binding of plectin and desmoplakin has been

reported (Eger et al., 1997), and recently, plectin was shown to exist also in a complex together with periplakin, thereby preventing its aggregation (Boczonadi et al., 2007).

Differential regulation of cell migration by plectin in keratinocytes and fibroblasts

In contrast to the faster migration of plectin-deficient keratinocytes, plectin-deficient fibroblasts migrate slower than their wild-type counterparts (Andrä et al., 1998). I found that their slower migration correlated with increased activation of PKCδ and enhanced accumulation of RACK1 at lamellipodial edges of migrating cells. Release of RACK1 from the cytoskeleton and subsequent hyperactivation of PKCδ could lead to inactivation of c-Src (Chang et al., 2001; Chang et al., 1998; Chang et al., 2002), thereby inhibiting chemotactic migration (Shah and Vincent, 2005). Reduced phosphorylation of FAK and paxillin, as well as increased stress fiber formation in plectin-deficient fibroblasts, such as were observed in fibroblasts with inactive c-Src (Shah and Vincent, 2005), would be in line with such a model. In fact, our most recent data show that c-Src activity is indeed decreased in plectin-deficient fibroblasts (Gregor et al., manuscript in preparation). Interestingly, whereas overexpression of RACK1 in keratinocytes enhances their migration (Osmanagic-Myers et al., 2006), it slows down migration of fibroblasts (Gregor et al., manuscript in preparation). Thus, although the same molecular mechanism seems to be at play in keratinocytes and fibroblasts (i.e. loss of cytoskeleton-association of RACK1 in the absence of plectin-scaffolding), hyperactivation of RACK1/PKCδ apparently has cell-type-specific outcomes. In keratinocytes RACK1/PKCδ most likely act on integrin α6β4, causing it to dissociate from HDs (Rabinovitz et al., 1999; Wilhelmsen et al., 2007) and to activate migration-related signaling cascades (Gagnoux-Palacios et al., 2003; Mainiero et al., 1997). While in fibroblasts, RACK1/PKCδ activation leads to downregulation of c-Src activity, which directly affects migration by reducing focal adhesion contact turnover (Schlaepfer et al., 1997; Schober et al., 2007).

MATERIALS AND METHODS

Commonly used buffers

1x TE (Tris-EDTA)
- Tris/HCl ..... 10 mM
- EDTA ..... 1 mM
- pH 8.0

10x PBS (phosphate buffered saline)
- NaCl ..... 81.8 g
- KCl ..... 2.01 g
- KH_2PO_4 ..... 2.04 g
- K_2HPO_4 ..... 11.32 g
- pH 7.4; ddH_2O to 1000 ml

1x TBS (Tris buffered saline)
- Tris-HCl ..... 20 mM
- NaCl ..... 150 mM
- pH 7.5

1x PBS-T
- PBS containing 0.1% Tween-20

1x SSC (sodium chloride/sodium citrate)
- NaCl ..... 150 mM
- Na-citrat ..... 15 mM
- pH 7.0

1x TAE (Tris-acetate-EDTA)
- Tris-acetate ..... 400 mM
- EDTA ..... 20 mM
- pH 8.2

1x TBE (Tris-borate-EDTA)
- Tris-HCl ..... 90 mM
- Boric acid ..... 90 mM

EDTA...2 mM

Antibodies, antisera and enzyme conjugates

Antibody name/ clone name	Antibody type	Antigen/ Epitope	Dilution	Vendor/ Reference
# 9	serum, rabbit	plectin (exon 9-12)	1:3000 (WB)	Andrä et al., 2003
# 21	serum, rabbit	plectin (rod-domain)	1:200 (IF-C) 1:200 (IF-T)	Andrä et al., 2003
# 46	serum, rabbit	plectin (rod-domain)	1:400 (IF, C) 1:100 (IF, T)	Andrä et al., 2003
# 61	serum, rabbit	GST-coupled peptide encoded by plectin 1c	1:200 (IF-C) 1:200 (IF-T) 1:1000 (WB)	Andrä et al., 2003
β-Catenin (LP 14)	monoclonal, mouse	C-terminal end of human β-catenin	1:500 (WB)	BD Transduction Laboratories, Lexington, KY, USA
γ-Catenin (LP 15)	monoclonal, mouse	C-terminal end of human γ-catenin	1:2000 (WB)	BD Transduction Laboratories, Lexington, KY, USA
Acetylated Tubulin (6-11B-1)	monoclonal, mouse	acetylated tubulin from outer arm of sea urchin sperm axoneme	1:1500 (WB)	Sigma-Aldrich, Austria
Actin (AC-40)	monoclonal, mouse	C-terminal end of actin	1:100 (IF-C) 1:200 (WB)	Sigma-Aldrich, Austria
Actin	serum, rabbit	C-terminal actin fragment	1:80 (IF-C)	Sigma-Aldrich, Austria
BPAG1 (Mab-5E)	monoclonal, mouse	n.d.	1:100 (IF-T)	Hashimoto et al., 1993
Caveolin 1	polyclonal, rabbit	fragment of central portion of human caveolin 1	1:10000 (WB)	BD Transduction Laboratories, Lexington, KY, USA
Cofilin	polyclonal, rabbit	synthetic phospho-peptide corresponding to residues surrounding Ser3 of human cofilin	1:1000 (WB)	Cell Signaling Technology, Danvers, MA, USA

Antibody name/ clone name	Antibody type	Antigen/ Epitope	Dilution	Vendor/ Reference
p-Cofilin	polyclonal, rabbit	synthetic phospho-peptide corresponding to residues surrounding Ser3 of human cofilin	1:1000 (WB)	Cell Signaling Technology, Danvers, MA, USA
Cortactin (4F11)	monoclonal, mouse	affinity-purified tyrosine phosphoproteins from chick embryo fibroblasts	1:100 (IF-C)	Upstate Biotechnology, Lake Placid, NY, USA
Desmin	serum, rabbit	purified chicken gizzard desmin	1:20 (IF-T)	Sigma-Aldrich, Austria
Desmoplakin I, II (DP-2.15, DP-2.17, DP-2.20)	monoclonal, mouse	bovine desmoplakin I, II	1:50 (IF-C) undil. (IF-T) 1:100 (WB)	Progen, Heidelberg, Germany
E-Cadherin (LP 36)	monoclonal, mouse	C-terminal end of human E-cadherin	1:200 (IF-C) 1:100 (IF-T) 1:2000 (WB)	BD Transduction Laboratories, Lexington, KY, USA
Erk2 (D-2)	monoclonal, mouse	C-terminal End of human Erk2	1:800 (WB)	Santa Cruz Biotechnology, Santa Cruz, CA, USA
p-Erk1/2 (E-4)	monoclonal, mouse	phospho-peptide containing Tyr204	1:800 (WB)	Santa Cruz Biotechnology, Santa Cruz, CA, USA
p-Erk1/2	polyclonal, rabbit	phospho-peptides for Erk1, containing Thr202/Tyr204 and Erk2, containing Thr185/Tyr187	1:10000 (WB)	Sigma-Aldrich, Austria
Fodrin (D8B7)	monoclonal, mouse	n.d.	1:500 (WB)	Signet Laboratories, Dedham, MA, USA
GFP	serum, rabbit	purified *A.victoria* GFP	1:700 (IF-C) 1:2000 (WB)	Molecular Probes, Eugene, OR, USA
GST (GST-2)	monoclonal, mouse	purified recombinant GST	1:1000 (WB)	Sigma-Aldrich, Austria

Antibody name/ clone name	Antibody type	Antigen/ Epitope	Dilution	Vendor/ Reference
Glu-Tubulin (Super-Glu)	polyclonal, rabbit	C-terminal peptide of non-tyrosinated α-tubulin	1: 500 (WB)	Gundersen et al., 1984
Integrin α_6 (GoH3)	monoclonal, rat	n.d.	1:100 (IF-C)	BD Bioscience
Integrin β_4 (H-101)	polyclonal, rabbit	N-terminal domain of human integrin β_4	1:200 (WB)	Santa Cruz Biotechnology, Santa Cruz, CA, USA
Integrin β_4 (356-11A)	monoclonal, rat	C-terminal domain of human integrin β_4	1:100 (IF-T)	Kennel et al., 1989
Integrin β_4	serum, rabbit	C-terminal domain of human integrin β_4	1:200 (WB)	Mainiero et al., 1997
Involucrin (PRB-140C)	serum, rabbit	peptide of mouse involucrin	1:1000 (WB)	Covance, Princeton, NJ, USA
Keratin 5 (PR-B160-P)	serum, rabbit	C-terminal end of mouse keratin 5	1:1500 (IF-C) 1:800 (IF-T) 1:2000 (WB)	Covance, Princeton, NJ, USA
Keratin 6 (PR-B169-P)	serum, rabbit	C-terminal end of mouse keratin 6	1:1000 (IF-C) 1:500 (IF-T) 1:2500 (WB)	Covance, Princeton, NJ, USA
Keratins 5, 6, 18 (LP 34)	monoclonal, mouse	human stratum corneum keratin preparation	1:100 (IF-C) 1:100 (IF-T) 1:1000 (WB)	Dako-Cytomation, Glostrup, Denmark
Keratin 8 (Ks 8.07)	monoclonal, mouse	human keratin 8	1: 100 (WB)	Progen, Heidelberg, Germany
Keratin 14 (LL001)	monoclonal, mouse	n.d.	1: 100 (WB)	Morley et al., 1995
Keratin 18 (Ks 18.04)	monoclonal, mouse	human keratin 18	1: 100 (WB)	Progen, Heidelberg, Germany
Ki-67 (TEC-3)	monoclonal, mouse	n.d.	1:50 (IHC)	Dako-Cytomation, Glostrup, Denmark
MAP1b (AA6)	monoclonal, mouse	purified rat brain MAPs	1:500 (WB)	Sigma-Aldrich, Austria
PKCδ (clone 14)	monoclonal, mouse	cysteine-rich repeat fragment of human PKCδ	1:500 (WB)	BD Transduction Laboratories, Lexington, KY, USA

Antibody name/ clone name	Antibody type	Antigen/ Epitope	Dilution	Vendor/ Reference
p-PKCδ	polyclonal, rabbit	synthetic phospho-peptide of human PKCδ containig Thr505	1:500 (WB)	Cell Signaling Technology, Danvers, MA, USA
Plectin 1a	serum, rabbit	synthetic peptide corresponding to a 12-amino acid residue-long sequence of human exon 1a	1:1000 (WB)	(Rezniczek et al., 1998)
RACK1 (Clone 20)	monoclonal, mouse	C-terminal fragment of rat Rack1	1:100 (IF-C) 1:2500 (WB)	BD Transduction Laboratories, Lexington, KY, USA
c-Src (SRC-2)	polyclonal, rabbit	peptide mapping C-terminus of Fyn p59 of human origin	1:200 (WB)	Santa Cruz Biotechnology, Santa Cruz, CA, USA
c-Src Tyr416	polyclonal, rabbit	synthetic phospho-peptide containing tyrosine 418	1:1000 (WB)	Biozol Diagnostica, Eching, Germany
α-Tubulin (B-5-1-2)	monoclonal, mouse	*Strongylocentros purpuratus* sperm axoneme filaments	1:1000 (IF-C) 1:500 (WB)	Sigma-Aldrich, Austria
Phospho Tyrosine (PY-20)	monoclonal, mouse	n.d.	1:1000 (WB)	BD Transduction Laboratories, Lexington, KY, USA
Tyr-Tubulin (TUB-1A2)	monoclonal, mouse	C-terminal peptide of tyrosinated α-tubulin	1:800 (WB)	Sigma-Aldrich, Austria
Vimentin	polyclonal, goat	n.d.	1:400 (IF) 1:500 (WB)	P. Traub
Vinculin (VIN-11-5)	monoclonal, mouse	purified chicken gizzard smooth muscle vinculin	1:200 (IF-C)	Sigma-Aldrich, Austria

Table 2. Primary antibodies used in immunofluorescence microscopy (IF) studies and immunoblotting (WB) analyses. IF-C, immunofluorescence microscopy of methanol-fixed cells; IF-T, immunofluorescence microscopy of cryo-fixated tissues; IHC, immunohistochemistry of paraformaldehyde-fixed tissues

Enzyme conjugate	Dilution used	Source
Goat-anti-mouse-IgG-Texas Red	1:200 (IF-C)	Jackson Immuno-Research Laboratories Europe
Goat-anti-mouse-IgG-Alexa FluorTM 488	1:800 (IF-C)	Molecular Probes, Eugene, OR, USA
Donkey-anti-mouse-IgG-Cy5	1:400 (IF-C)	Jackson Immuno-Research Laboratories Europe
Goat-anti-mouse-IgG-AP	1:5000 (WB)	Jackson Immuno-Research Laboratories Europe
Goat-anti-mouse-IgG-HRPO	1:10000 (WB)	Jackson Immuno-Research Laboratories Europe
Donkey-anti-IgM (µ-chain)-Texas Red	1:200 (IF-C)	Jackson Immuno-Research Laboratories Europe
Donkey-anti-rabbit-Texas Red	1:200 (IF-C)	Jackson Immuno-Research Laboratories Europe
Goat-anti-rabbit-Texas Red	1:200 (IF-C)	Jackson Immuno-Research Laboratories Europe
Goat-anti-rabbit-Alexa FluorTM 488	1:800 (IF-C)	Molecular Probes, Eugene, OR, USA
Goat-anti-rabbit-Cy5	1:400 (IF-C)	Jackson Immuno-Research Laboratories Europe
Goat-anti-rabbit-AP	1:5000 (WB)	Jackson Immuno-Research Laboratories Europe
Goat-anti-rabbit-HRPO	1:10000 (WB)	Jackson Immuno-Research Laboratories Europe
Goat-anti-rat-IgG-Cy2	1:150 (IF-C)	Jackson Immuno-Research Laboratories Europe
Donkey-anti-goat-Alexa FluorTM 488	1:3000	Molecular Probes, Eugene, OR, USA

Table 3. Secondary antibodies used in immunofluorescence microscopy studies and immunoblotting analyses (WB). AP, alkaline phosphatase; HRPO, horseradish peroxidase; IF-C, immunofluorescence microscopy of methanol-fixed cells; IF-T, immunofluorescence microscopy of cryo-fixated tissues.

DNA and RNA

Synthetic oligonucleotides

Primer	Primer sequence 5´-3´	Primer specification
mPleEx26L	CTTCAAGCTCTTGGAGAGTGGCAGG	
mPleIn25-26U	GTATTTGGATTCAGAGGCACAGTAG	
mPle32/L7714	GCAGCCGCTGGTTTTCCTCCGCCAG	
Cre sense	CCAATTTACTGACCGTACACC	5 nt 3´ of the ATG
Cre antisense	TAATCGCCATCTTCCAGCAGG	1010 nt 3´ of the ATG

Table 4. Primers used for PCR on genomic DNA. The 5´-end of the oligonucleotide was used to determine exact primer specification.

Preparation of plasmid DNA

Small scale preparation of plasmid DNA from bacteria was carried out according to the method of Holmes and Quigley (Holmes and Quigley, 1981). Large scale preparation of plasmid DNA was performed using JetStar columns according the manufacturer´s protocol (Genomed).

Phenol-purification and precipitation of DNA from aqueous solutions

For extraction with phenol-chloroform (PC 1:1) the same volume of PC-solution (phenol was equilibrated in 0.5 M Tris-HCl, pH 8.0) was added to the DNA solution, mixed by vortexing for 15 seconds and centrifuged at 14000 rpm for 1 minute (Eppendorf centrifuge). The aqueous phase was transferred to a new tube and extracted with chloroform twice.

For precipitation of DNA 1/10 volume of 3 M NaOAc, pH 5.2 and 2.5 volumes EtOH were added. After incubation at -20°C for 30 minutes, the DNA was pelleted (14000 rpm, 20 minutes, Eppendorf centrifuge, RT), washed with 70% EtOH, air dried and dissolved in dH_2O or 1x TE. Alternatively DNA can be precipitated by adding 0.7 volumes isopropanol and incubation at RT for 5 minutes.

Determination of DNA-concentration

The concentration of double stranded DNA was measured spectrophotometrically at 260 nm. An extinction of 1 OD corresponds to a DNA concentration of 50 µg/ml.

Separation of DNA by agarose gel electrophoresis

50x TAE

Tris	242 g
Acetic acid	57 ml
$Na_2EDTA \cdot 2H_2O$	4 g
ddH_2O to	1000 ml

10x DNA sample buffer

Urea	4 M
Saccharose	50% (w/v)
EDTA	1 mM
EDTA	1 mM
Bromphenol-blue	0.1% (w/v)

Agarose was suspended in 1x TAE and dissolved by boiling in a microwave oven. The solution was cooled down and ethidiumbromide (0.01 mg/ml) was added prior to pouring the gel. Before electrophoresis, the gel was overlaid with 1x TAE and the DNA samples were mixed with 1/10 10x DNA sample buffer. Gels were run at 80-120 Volts.

Preparation of electrocompetent bacteria and transformation

5 ml of a fresh over-night culture of bacteria (XL-1, XL-2, BL21) were used for inoculation of 1000 ml LB-medium (Luria-Bertani-Medium 10 g Bacto-Trypton, 5 g Bacto-Yeast extract, 10 g NaCl per 1000 ml; pH 7.5). Bacterial cells were grown at 37°C until an OD_{600} of 0.5 was attained. The bacterial cultures were placed on ice for 15 minutes and pelleted for 20 minutes at 3500 rpm (GSA rotor, 4°C). The supernatant was poured off, the pellet resuspended in 1000 ml ice-cold, autoclaved dH_2O and centrifuged again. The supernatant was discarded, the pellet again dissolved in 500 ml dH_2O, and the bacterial cells

pelleted. The pellet was dissolved in 40 ml 10% glycerol (sterilized by filtration) and centrifuged for 10 minutes in an SS34-rotor at 4100 rpm (4°C). The resulting bacterial pellet was resuspended in 4 ml 10% glycerol and aliquoted into Eppendorf tubes. The electro-competent, bacterial cells were either used immediately or frozen in liquid nitrogen and stored at -80°C.

For transformation an aliquot was thawed on ice and DNA was added to the competent bacteria. The mixture was transferred to a cuvette (Biorad) and a pulse (2.5 kV, 25 µF, 200 W; Biorad) was applied. 1 ml of pre-warmed LB-medium was added and bacteria were incubated at 37°C for 30 minutes. Thereafter they were plated onto LB-agar plates containing the appropriate antibiotics.

Polymerase chain reaction

For genotyping of transgenic mice polymerase chain (PCR) reactions were carried out in a total volume of 25 µl containing 5 µl 5x PCR buffer (Promega, Mannheim, Germany), 0.5 µl of each primer (10 pmol/µl), 0.25 µl Go-TAQ-polymerase (Promega, Mannheim, Germany), 0.5 µl dNTPs (10 mM each) and 1 µl of template DNA. The Perkin Elmer Gene Amp® PCR System 2400/9700 was used. 1/3 of the PCR reaction products were analyzed on a 0.8-1.0% agarose gel. Table 4 shows the PCR program used for genotyping of different mouse-lines.

Duration	Temperature	Step
300 sec.	94°C	initial denaturation
30 sec.	94°C	denaturation
30 sec.	62°C	annealing 35 cycles
120 sec.	72°C	extension
7 min.	72°C	final extension
∞	04°C	storage

Table 5. PCR program used for genotyping of different transgenic mouse-lines. The extension time varies, depending on the length of the template (1 kb per minute).

Isolation of genomic DNA from mouse tails

For isolation of genomic DNA from mouse tails, a piece (0.5 cm) of tail was cut and incubated in 750 µl of lysis buffer (50 mM Tris-HCl, pH 8.0; 100 mM EDTA; 100 mM NaCl; 1% SDS, 0.5 mg/ml Proteinase K) at 55°C overnight on an Eppendorf thermomixer with gentle agitation. 300 µl 5 M NaCl were added, mixed vigorously and centrifuged at 14000 rpm in an Eppendorf centrifuge at RT for 10 minutes. 700 µl of the supernatant was transferred to a fresh tube and the genomic DNA was precipitated by adding 500 µl isopropanol and subsequent centrifugation (14000 rpm, 10 minutes at RT). The pellet was washed with 70% EtOH, again centrifuged, and resuspended in 200 µl dH_2O by incubation at 37°C for several hours.

Southern blot analysis

10 µg of genomic DNA were digested with 30-40 U of restriction enzyme in a total volume of 300 µl of the respective enzyme buffer. Genomic DNA fragments were precipitated with NaOAc/EtOH abs. and redissolved in 40 µl 1x TE. Thereafter the digested DNA was separated by agarose gel electrophoresis (0.8% agarosegel). The DNA was depurinated by soaking the gel once for 15 minutes in 500 ml of 0.25 M HCl, then denatured twice for 15 minutes in 500 ml of 0.5 M NaOH; 1.5 M NaCl. Semi-dry alkaline blotting was used to transfer DNA fragments to a nylon membrane (PALL Biodyne®B, pore size 0.45 µm, the membrane was rinsed with dH_2O prior to the assembly of the blot). The next day the blot was disassembled and the membrane neutralized for 1 minute in 0.2 M Tris/HCl pH 7.5, 1x SSC. Then the DNA was fixed to the membrane by baking the membrane for 30 minutes at 80°C, followed by crosslinking using a UV Stratalinker 2400 (Stratagene; 120 mJ/cm^2). For hybridization, probes were radioactively labeled (α-^{32}P dCTP) using the Prime-it II random labeling kit (Stratagene). Labeled probes were purified with ProbeQuant™ G-50 Micro columns (Amersham Pharmacia Biotech). The activity of the labeled probe was measured by Cerenkov-counting (Liquid Scintillation Analyzer, Packard). The membrane was pre-hybridized for 2-3 hours in Church buffer (0.5 M NaP_i, pH 7.2; 7% SDS; 1 mM EDTA) at 65°C. For hybridization, the labeled probe was denatured at 95°C for 5 minutes, then immediately cooled on ice for 3 minutes and added to the membrane. Hybridization was carried out at 65°C overnight. The following day, the membrane was once washed at RT and

three times for 20 minutes at 65°C with Church wash buffer (12 mM NaP_i, pH 7.2; 1% SDS). The membrane was exposed to an X-ray sensitive film (Fuji medical X-ray film HR-E30) at -80°C using an intensifying screen.

Isolation of RNA

Total RNA was isolated from cultured mouse keratinocytes using TRIzol Reagent (Life Technologies).

Determination of RNA-concentration

The concentration of RNA was measured spectrophotometrically at 260 nm. An extinction of 1 corresponds to a RNA concentration of 40 µg/ml.

Proteins

Expression of recombinant proteins in bacteria

cDNA expression plasmids encoding GST fusions of plectin fragments corresponding to exons 1c-8 (p1c-8, pGR337) (Rezniczek et al., 2003); 1c-30 (p1c-30, pGR324); 16-24 (p16-24, pGR329); 20-21 (p20-21, pGR331) were generated by PCR using mouse cDNAs and primers based on published sequences (Fuchs et al., 1998; Rezniczek et al., 2003; Andrä et al., 2003; GenBank accession nos X59601, Z54367 and NM_011117) containing ends with suitable restriction sites. For protein expression in bacteria, final cDNA constructs were cloned into the expression vector pGEX4-T (Pharmacia) digested with EcoRI. GST fusion proteins were expressed in BL21 $(DE3)_{RIL}$ *E. coli.*

Purification of GST-tagged proteins

Bacterially expressed GST fusion proteins were purified on gluthathione-Sepharose 4B beads as described in the manufacturer's instructions (Amersham Biosciences).

Determination of protein concentration (Bradford Method)

Coomassie solution

Coomassie G-250	100 mg
95% Ethanol	50 ml
85% Phosphoric acid	100 ml
ddH_2O to 1000 ml	

Standard protein solution

BSA	0.5 mg/ml

Protein concentrations were measured according the method of Bradford (Bradford, 1976). 5-20 µl of protein solution were diluted to 100 µl with 150 mM NaCl. 1 ml of Bradford solution (100 mg Coomassie G-250, 50 ml 95% ethanol and 100 ml 85% phosphoric acid were filled up to 1000 ml with dH_2O, filtrated and stored at 4°C) was added to each sample. The solution was mixed and incubated for 5 minutes at RT. The absorbance was measured at 595 nm using a Spectrophotometer.

SDS-polyacrylamide gel electrophoresis (PAGE)

Running buffer

Tris	25 mM
Glycine	250 mM
SDS	0.1%

30% acrylamide mix (29:1)

Acrylamide	29 g
Bis-acrylamide	1 g
ddH_20 to 100 ml	

	Separating gel		Stacking gel	
	5%	10%	3%	5%
ddH_2O	5.6 ml	4 ml	3 ml	2.7 ml
30% Acrylamide mix	1.65 ml	3.3 ml	0.4 ml	0.67 ml
1.5 M Tris-HCl (pH 8.8)	2.5 ml	2.5 ml	-	-
1.5 M Tris-HCl (pH 6.8)	-	-	0.5 ml	0.5 ml
10% SDS	100 µl	100 µl	40 µl	40 µl
10% Ammonium persulfate	100 µl	100 µl	40 µl	40 µl
TEMED	4 µl	4 µl	6 µl	6 µl

Table 6. Separating and stacking gel solutions (10 ml and 4 ml, respectively).

SDS-PAGE was performed according to Laemmli (Laemmli, 1970). The Mini-Protean Electrophoresesystem (Biorad) was used. The separating gel was poured, overlaid with isopropanol and left to polymerize. The isopropanol was removed and the stacking gel was poured on top of the separation gel. A comb was introduced to allow sample application after polymerization. The protein samples were mixed with 5x SDS-PAGE sample buffer (0.4 M Tris-HCl pH 6.8, 10% SDS, 50% glycerol, 0.5 M Dithiothreitol, 0.1% bromphenolblue) and heated to 95°C for 5 minutes. Running conditions were 20 mA per minigel in a 1x running buffer.

Comassie staining and drying of gels

Comassie stock

Coomassie G-250.....1 g

Methanol ..... 200 ml

H_20 ..... 200 ml

Staining solution

Coomassie stock	30%
Acetic acid	10%
Methanol	30%
H_20	30%

Destaining solution

Acetic acid	10%
Methanol	30%
H_20	60%

After electrophoresis, the gel was briefly rinsed with dH_2O, then incubated in staining solution for at least 20 minutes on a shaker at RT, and thereafter destained by several changes of destaining solution.

Wet-blotting of proteins onto nitrocellulose membranes

Transfer buffer (10x)

Tris	0.48 M
Glycine	0.4 M
SDS	0.01%

Proteins were separated by SDS-PAGE as described above. The polyacrylamide gel was laid onto a nitrocellulose membrane (Schleicher & Schuell), sandwiched between two 3MM Whatman filter papers and fixed in appropriate blotting frames. The transfer was performed in a BioRad Mini Protean II wet-blotting chamber containing transfer buffer at constant voltage (25 V/16 hours at 4°C).

Reversible staining of proteins (Ponceau-S)

Ponceau S staining solution

Ponceau S	0.5 g
Acetic acid	1 ml

ddH_20 to 100 ml

To control the efficiency of the transfer the membrane were reversibly stained with Ponceau-S solution. Excess staining was removed by washing with dH_2O. Blots were destained by washing with PBS.

Western blot analysis

Blocking solution

PBS-T containing either 5% non-fat dry milk or 3% BSA

After transfer and Ponceau S staining, the membrane was blocked for 1 hour at RT in blocking solution. The membrane was briefly washed with PBS-T and incubated in the appropriate primary antibody dilution (in blocking solution) for 1 hour at RT (or alternatively o/n at 4°C). Thereafter the membrane was washed three times with PBS-T for ten minutes and then incubated with the secondary antibody dilution (in PBS-T) for 1-2 hours. The washing step was repeated and the bound secondary antibodies were visualized either using the ECL-detection system (Super Signal West PicoSystem, Pierce) or by incubating the membrane in AP (alkaline phosphatase) buffer (100 mM Tris-HCl pH 9.6, 100 mM NaCl, 5 mM $MgCl_{2)}$ with 66 µl NBT (nitroblue terazolium chloride; 50 mg/ml in 70% DMF) and 33 µl BCIP (5-bromo-4-chloro-3-indolyl phosphate; 50 mg/ml in 100% DMF) added per 10 ml AP-buffer. The AP-reaction was stopped by washing the membrane in PBS.

Quantification of protein bands on immunoblots

After immunoblotting using peroxidase-coupled secondary antibodies, protein bands were visualized by exposure to a X-ray film. Several exposures for different time periods were performed. The bands were then scanned and quantified using ImageQuant 5.1 software (Molecular dynamics). Normalization calculations were done in Microsoft Excel 2002. Values obtained were plotted against corresponding exposure times to establish the range of signal linearity. For quantitative comparisons only band intensities falling into these linear ranges were used.

Preparation of cell and tissue extracts

Preparation of tissue extracts

Tissue lysis buffer

HEPES	50 mM
$MgCl_2$	5 mM
EGTA	1 mM
NaCl	100 mM
Triton X-100	0.5%
DTT	0.1 mM
DNase I	0.5 mg/ml
RNAse A	0.2 mg/ml
Na_3VO_4	1 mM

pH 7.0

+ Protease inhibitor tablet (Roche, Vienna, Austria)

+ Serine/Threonine-phosphatase inibitor cocktail I (Sigma)

Mouse tissues were collected, immediately shock frozen and pulverized in liquid nitrogen. Lysis buffer (1 µl/mg of tissue) was added and tissues were homogenized using a Polytron PT 3000 Kinematica homogenizer (Kinematica AG, Switzerland) at 12000 rpm, 4°C. Samples were incubated at RT for 5 minutes and 1 volume of 2x SDS- sample buffer was added. Insoluble material was removed by centrifugation (Eppendorf centrifuge; 14000 rpm, 2 minutes at RT). Samples were heated to 95°C for 5 minutes before subjection to SDS-PAGE.

Preparation of soluble/insoluble fractions from mouse tissues

Extraction buffer 1

Triton X-100 ..... 1%
NP-40 ..... 0.5%
Tris/HCl ..... 20 mM
NaCl ..... 150 mM
EDTA ..... 1 mM
DTT ..... 0.2 mM
Na_3VO_4 ..... 2 mM
pH 7.5
+ Protease inhibitor tablet (Roche, Vienna, Austria)
+ Serine/Threonine-phosphatase inibitor cocktail I (Sigma-Aldrich)

Extraction buffer 2

Triton X-100 ..... 1%
NP-40 ..... 0.5%
Tris/HCl ..... 20 mM
NaCl ..... 150 mM
EDTA ..... 1 mM
DTT ..... 50 mM
Urea ..... 9 M
Na_3VO_4 ..... 2 mM
pH 7.5
+ Protease inhibitor tablet (Roche, Vienna, Austria)
+ Serine/Threonine-phosphatase inibitor cocktail I (Sigma-Aldrich)

Mouse tissues were collected, immediately shock frozen and pulverized in liquid nitrogen. Extraction buffer 1 was added (1 µl/mg of tissue), and tissues were homogenized using a Polytron PT 3000 Kinematica homogenizer (Kinematica AG, Switzerland) at 12000 rpm, 4°C. Tissue homogenates were then incubated for 30 minutes on an orbital shaker at 4°C. Thereafter, soluble and insoluble protein fractions were separated by centrifugation at 13000 rpm for 20 minutes, 4°C. The supernatant (soluble fraction) was transferred to a new tube and 5x SDS sample buffer was added immediately. The pellet was rinsed once with two volumes of PBS. An identical volume of extraction buffer 2 (as was used for the initial extraction) was added and the resuspended pellet was incubated for 2 hours at RT with

shaking. Insoluble material was pelleted by centrifugation at 13000 rpm for 10 minutes at 4°C and the supernatant (insoluble fraction) was removed and supplemented with 5x SDS-sample buffer. Both fractions were stored at -80°C, or immediately subjected to SDS-PAGE.

Total cell lysates

2x SDS-sample buffer (Laemmli)

Tris-HCl	160 mM
DTT	200 mM
SDS	4%
Bromphenol blue	0.1%
Glycerol	20%
Na_3VO_4	4 mM

pH 6.8

+ Serine/Threonine-phosphatase inibitor cocktail I (Sigma-Aldrich)

5x SDS-sample buffer (Laemmli)

Tris-HCl	400 mM
DTT	500 mM
SDS	10%
Bromphenol blue	0.25%
Glycerol	50%
Na_3VO_4	10 mM

pH 6.8

+ Serine/Threonine-phosphatase inibitor cocktail I (Sigma-Aldrich)

Cells were washed once with 1x PBS and then scraped off with a cell scraper into 2x SDS-PAGE sample buffer. DNA was sheared by pressing the samples through a 27 gauge needle and samples were heated to 95°C for 5 minutes before usage for SDS-PAGE

Cell fractionation (high salt method)

Triton X-100 Buffer

Tris-HC ..... 10 mM
Triton X-100 ..... 1%
EDTA ..... 5 mM
NaCl ..... 140 mM
DTT ..... 5 mM
Na_3VO_4 ..... 2 mM
pH 7.6
+ Protease-inhibitor tablet (Roche, Vienna, Austria)

High-salt buffer

Tris-HCl ..... 10 mM
Triton X-100 ..... 0.5%
KCl ..... 1.5 M
NaCl ..... 140 mM
EDTA ..... 5 mM
DTT ..... 5 mM
Na_3VO_4 ..... 2 mM
pH 7.6
+ Protease inhibitor tablet (Roche, Vienna, Austria)
+ Serine/Threonine-phosphatase inibitor cocktail I (Sigma-Aldrich)

Washing buffer

Tris-HCl ..... 10 mM
pH 7.6
+ Protease inhibitor tablet (Roche, Vienna, Austria)

Cells were washed twice with 1x PBS, one volume of Triton X-100 buffer was added and plates were incubated with agitation for 2 minutes on ice. The supernatant (soluble fraction) was collected, SDS-sample buffer was added immediately and the samples were heated to 95°C for 5 minutes. Two volumes of high-salt buffer were added to the cell residues still adherent to the plate and those incubated further for 30 minutes at 4°C with agitation. Insoluble cytoskeletal residues were scraped off with a cell scraper, resuspended in the buffer

and homogenized by pressing through a 27 gauge needle. The high-salt buffer resistant pellet obtained after centrifugation (2500 rpm for 30 minutes at 4°C), which was greatly enriched in IFs, was washed with washing buffer and pelleted again (8000 rpm for 5 minutes at 4°C). The pellet (insoluble fraction) was dissolved in 8M urea at 4°C for 30 minutes, SDS-sample buffer was added and the samples stored at - 80°C until usage.

Cell fractionation (digitonin-based method)

Digitonin buffer

Digitonin (Sigma-Aldrich)..... 0.01%
Piperazine-N,N'-bis(ethanesulfonic acid (PIPES).... 10mM
Succrose ..... 300 mM
NaCl ..... 100 mM
$MgCl_2$ ..... 3 mM
EDTA ..... 5 mM
DTT ..... 0.2 mM
Na_3VO_4 ..... 1 mM
pH 6.8
+ Protease inhibitor tablet (Roche, Vienna, Austria)
+ Serine/Threonine-phosphatase inibitor cocktail I (Sigma-Aldrich)

Buffer 2

Triton X-100 ..... 0.5%
Piperazine-N,N'-bis(ethanesulfonic acid), PIPES 10mM
Succrose ..... 300 mM
NaCl ..... 100 mM
$MgCl_2$ ..... 3 mM
EDTA ..... 3 mM
DTT ..... 0.2 mM
Na_3VO_4 ..... 2 mM
pH 7.4
+ Protease inhibitor tablet (Roche, Vienna, Austria)
+ Serine/Threonine-phosphatase inibitor cocktail I (Sigma-Aldrich)

Cells were scraped into 1x PBS, collected by centrifugation at 1000 rpm (at 4°C), gently resuspended in 300 µl of ice-cold digitonin buffer and incubated with end-over-end agitation for 10 minutes at 4°C. After centrifugation at 16000 rpm for 1 minute (4°C), the cytosolic supernatant fraction was collected and the pellet resuspended in buffer 2. After 20 minutes of end-over-end rotation (4°C), the suspension was centrifuged at 16000 rpm for 1 minute (4°C) to obtain membrane (supernatant), and cytoskeleton (pellet) fractions. Aliquots of fractions were dissolved in 5x SDS-sample buffer.

Cell fractionation (sequential detergent extraction)

NP-40 buffer

NP-40 ..... 1%
EDTA ..... 10 mM
DTT ..... 0.2 mM
Na_3VO_4 ..... 2 mM
PBS 1x
pH 7.5
+ Protease inhibitor tablet (Roche, Vienna, Austria)
+ Serine/Threonine-phosphatase inibitor cocktail I (Sigma-Aldrich)

EMP-BB buffer

Empigen BB 1%
EDTA ..... 10 mM
DTT ..... 0.2 mM
Na_3VO_4 ..... 2 mM
PBS 1x
pH 7.5
+ Protease inhibitor tablet (Roche, Vienna, Austria)
+ Serine/Threonine-phosphatase inibitor cocktail I (Sigma-Aldrich)

Cells were washed twice with 1x PBS and then lysed in the dish with NP-40 buffer. The lysate was collected, subjected to centrifugation (16000 rpm, 30 minutes, 4°C), and the supernatant (NP-40 fraction) was collected. The residual cytoskeletal pellet was solubilized

with EMP-BB-buffer (30 minutes, 4°C), followed by centrifugation (16000 rpm, 15 minutes, 4°C) and collecting the EMP-BB fraction. The residual detergent-resistant cytoskeletons were then solubilized with 5x SDS sample buffer. Fractions were stored at -80°C. Fractions were adjusted for equal protein concentration using the BCA-kit (Pierce Biotechnology, Rockford, IL, USA) and the adjustments controlled by coomassie staining of samples separated by SDS-PAGE.

Cell fractionation (two-detergents-based method)

Extraction buffer 1

Triton X-100 ..... 1%
NP-40 ..... 0.5%
Tris/HCl ..... 20 mM
NaCl ..... 150 mM
EDTA ..... 1 mM
DTT ..... 0.2 mM
Na_3VO_4 ..... 2 mM
pH 7.5
+ Protease inhibitor tablet (Roche, Vienna, Austria)
+ Serine/Threonine-phosphatase inibitor cocktail I (Sigma-Aldrich)

Extraction buffer 2

Triton X-100 ..... 1%
NP-40 ..... 0.5%
Tris/HCl ..... 20 mM
NaCl ..... 150 mM
EDTA ..... 1 mM
DTT ..... 50 mM
Urea ..... 9 M
Na_3VO_4 ..... 2 mM
pH 7.5
+ Protease inhibitor tablet (Roche, Vienna, Austria)
+ Serine/Threonine-phosphatase inibitor cocktail I (Sigma-Aldrich)

Cells were washed once with ice cooled 1x PBS. One volume of cold detergent lysis buffer was added, and cells were scraped off with a cell scraper into the buffer. The cell suspension was sonicated once (50% cycles, 80% power; on ice) and incubated for 30 minutes on an orbital shaker at 4°C. Thereafter, soluble and insoluble protein fractions were separated by centrifugation at 13000 rpm for 20 minutes (at 4°C). The supernatant was transferred to a new tube and 5x SDS sample buffer was added immediately. The pellet was rinsed once with two volumes of 1x PBS, one volume of extraction buffer 2 was added and the resuspended pellet was incubated for 2 hours at RT with shaking. Thereafter, the pellet fraction was supplemented with 5x SDS-sample buffer. Both fractions were stored at -80°C, or immediately subjected to SDS-PAGE.

Preparation of fractions containing protomeric and polymeric tubulin

Tubulin protomer and polymer fractions were prepared as described (Gundersen et al. 1987). Cells growing on 10 cm dishes were rapidly rinsed twice in microtubule-stabilizing buffer (MSB) [85 mM Pipes, pH 6.9, 1 mM EG'I'A, 1 mM $MgCl_2$, 2 M glycerol, and protease inhibitor cocktail (Roche, Vienna, Austria)] and then extracted with 1.6 ml of MSB containing 0.5 % Triton X-100. After 3 minutes, the Triton extract (monomer fraction) was gently removed to a graduated tube, the volume was noted and 1/5 volume of 5x SDS buffer was added. This sample was then boiled for 5 minutes. The cytoskeletons remaining on the dish were carefully rinsed once with MSB and then solubilized with 1.6 ml MSB plus 0.4 ml 5× SDS buffer. After 5 minutes, this extract (polymer fraction) was removed from the plate and boiled 5 minutes. Samples were stored at -80°C until analyzed by immunoblotting. Samples were adjusted for equal protein concentration using the BCA-kit (Pierce Biotechnology, Rockford, IL, USA) and the adjustments controlled by coomassie staining of samples separated by SDS-PAGE.

Preparation of high-speed supernatants from cultured cells

Confluent monolayers of keratinocytes or N2a cells were harvested in icecold PBS, collected by centrifugation at 1000 rpm for 5 minutes at 4°C, and washed in 140 mM NaCl, 8 mM Na_2PO_4, 1.5 mM KH_2PO_4, 3 mM KCl, 0.5 mM $MgCl_2$, 5.5 mM glucose, 1 mM EGTA, supplemented with protease inhibitor cocktail (Roche, Vienna, Austria). Cells were then

homogenized in 100 mM MES, pH 7.0, 0.5 mM $MgCl_2$, 1 mM EGTA, 1mM GTP, 520 mM sucrose, 50 mM DTT, protease inhibitor cocktail (Roche, Vienna, Austria), using a syringe with 22G needle or a dounce homogenizer (ratio of unbroken cells : free nuclei ~20:80). After removal of cells and nuclei by centrifugation the supernatant was retrieved, drawn 10 times through a 27G needle, and subjected to ultracentrifugation (Beckmann Tabletop TL-100) at 45000 rpm for 90 minutes at 2°C to obtain a high-speed supernatant (hs-SN).

Purification of MAPs from tissues and cultured cells

MAPs from hog brain were prepared and purified according to (Karr et al., 1979). MAPs from adult mouse brain were prepared as described (Shelanski et al., 1973). Hog brain MAP isolations were performed by I. Fischer. For isolation of MAPs from cultured N2a cells, taxol (Paclitaxel, Calbiochem) was added (to 20 µM) to hs-SNs (see above) which were then incubated at 37°C for 15 minutes, and centrifuged at 14000 rpm for 30 minutes at 4°C. The sedimented material was resuspended and centrifuged 2x in 100 mM MES pH 7.0, 1 mM EGTA, 0.5 mM $MgCl_2$, 1 mM GTP, 20 µM taxol, and protease inhibitor cocktail, prior to SDS 5%-PAGE.

Affinity isolation of MAPs using preformed microtubules

MTs were generated from hog brain tubulin (99.9% pure, Cytoskeleton Inc.) according to (Vallee, 1986). Briefly, 5 mg/ml of tubulin was incubated with 200 µm taxol and 1 mM GTP for 30 minutes at 37°C to induce formation of MTs. 650 µg/ml of preformed MTs were added to hs-SNs (see above), and incubated for 1hour at RT. MTs and bound proteins were sedimented and treated as described above.

Protein overlay assay

For overlay assays, hog brain and keratinocyte MAPs were separated by SDS 5%-PAGE and transferred to nitrocellulose membranes. Membranes were then blocked with 3% BSA in PBS-T for two hours at RT and overlayed with 8 µg/ml of purified plectin fragments

dissolved in overlay-buffer (Rezniczek et al., 1998). Bound plectin fragments were detected by immunoblotting using anti-GST antibodies.

Cell culture and immunofluorescence microscopy

Maintenance of cell lines

KGM (keratinocytes growth medium; BioWhittaker CC-3104)

Keratinocyte basal medium	500 ml
Hydrocortisone (CC-4031)	0.5 ml
GA-1000 (CC-4081)	0.5 ml
BPE (CC-4002)	2 ml
hEGF (CC-4015)	0.5 ml
Insulin (CC-4021)	0.5 ml
chelexed FCS	2%
Insulin-Transferrin-Selenium (GibcoBRL)	5 ml
$CaCl_2$ (50 mM)	500 µl

chelexed FCS (Fetal Calf Serum)

To remove Ca2+ from FCS, 5g Chelex were mixed with 100 ml FCS and stirred at 4°C for 1hour. FCS was then sterilized by filtration.

DMEM (Dulbecco's Modified Eagle's Medium)

DMEM	170 ml
FCS	20 ml
Penicillin/streptomycin (P/S)	2 ml
L-Glutamine (100 mM)	2 ml

T/E

Trypsin (filtered)	500 mg/l
EDTA (Na-salt)	0.2%

Sterilized by filtration and stored at -20°C.

Collagen coating of dishes

Collagen I solution (Sigma-Aldrich) was diluted 1:10 in PBS and sterile filtrated. 5 or 3 ml of this dilution were then added per 10 or 6 cm plates, respectively, and incubated for at least 2hours at 37°C or overnight at 4°C. Prior to usage, plates were washed once with 1x PBS.

Frozen cells were quickly thawed in a 37°C water-bath and transferred to a 15 ml tube, containing 10 ml of growth medium and the cells pelleted by centrifugation (Heraeus Megafuge, 1000 rpm, 3 minutes). The cells were resuspended in growth medium and seeded into appropriate cell culture dishes. Cell lines were incubated at 37°C in a humified atmosphere containing 5% CO_2. For splitting of cells, the cell layer was once washed with 1x PBS and then incubated with one volume of T/E (0.05% trypsin, 0.2% EDTA) for 10 minutes (keratinocytes), 3 minutes (N2a cells) or 5 minutes (804G cells, fibroblasts) at 37°C. Three volumes of growth medium were added to inhibit trypsin and the detached cells were transferred to a 15 ml tube. For splitting of PC-12 cells, cells were detached by pipetting, and triturated vigorously by passing the cells through a 12 gauge needle. After centrifugation (Heraeus Megafuge, 1000 rpm, 3 minutes) cells were resuspended in growth medium and split into new culture dishes. 804G cells and fibroblasts were maintained in DMEM, whereas PC-12 cells were cultured in DMEM supplemented with 5 % horse serum. Keratinocytes were maintained in KGM.

For freezing, cells were trypsinized, resuspended in freezing medium (FCS containing 10% DMSO) and aliquoted into cryotubes (Nunc A/S, Roskilde, Denmark). The cryotubes were kept at -80°C for 24 hours and then put into a liquid nitrogen tank for storage.

Differentiation and induction of neurite outgrowth of N2a cells

To obtain a neuronal-like phenotype, the medium was changed to DMEM, supplemented with 1% FCS and db-cAMP (1 mM, Sigma-Aldrich) in which cells were maintained for 48-72 hours.

Keratinocyte differentiation and calcium-switch assay

To induce stratification and subsequent differentiation of cultured keratinocyte monolayers, the $CaCl_2$ level in the medium (KGM) was raised from 0.05 mM to 1.8 mM.

Calcium-switch was performed by culturing keratinocyte monolayers for 24-48 hours in high calcium (1.8 mM) medium followed by exchanging the high calcium medium with low calcium medium (0.05 mM).

Separation of epidermis and dermis from adult mouse skin

Dispase II solution

10 mg Dispase II (Roche, Vienna, Austria) dissolved in 1 ml keratinocyte basal medium

Dispase II (Roche, Vienna, Austria) was used at a concentration of 1.5 U/ml in 1x PBS. Mice were sacrificed and a patch of skin (about 2.5 x 2.5 cm) was freed of hair. This patch was cut out with forceps and scissors and put epidermis-side down on a plastic dish. Connective tissue and fat was mostly removed, before the skin was placed dermis-side down floating on dispase II. After 1.5-2 hours at 37°C skin was put dermis-side down on a plastic dish and epidermis was peeled off with forceps.

Isolation of primary mouse keratinocytes

1-2 days old mice were sacrificed by decapitation and washed twice with 70% ethanol. Using sterile scissors and forceps tails and limbs were amputated and discarded. After making a longitudinal incision from neck to tail, the skin was removed, flattened and put dermis-side down floating on Dispase II solution in a Petri dish. Skins were incubated at 37°C for 30 minutes (knockout skins) or 45 minutes (wild-type skins). Next, skins were placed, epidermis-side down, in a Petri dish and the dermis was gently peeled back with forceps. The epidermal sheets were placed on a glass slide and minced into very small pieces by using sterile razorblades. 3 ml of T/E solution were added and the epidermal pieces gently resuspended using a 5 ml plastic pipette. The suspension was then transferred to a 15 ml tube and incubated for 10 minutes in water bath at 37°C. Subsequently, epidermal cells were released from tissue pieces by pipetting up and down 50 times with a 1 ml pipette and the cell suspension was filtered through a 70 µm cell strainer into a 50 ml tube filled with 40 ml of warm (RT) KGM, and the cells were pelleted by centrifuging at 800 rpm for 8 minutes. The pelleted cells were suspended in KGM (37°C) and plated on collagen IV-coated (Corning

B.V. Life Sciences, Schiphol-Rijk, The Netherlands) or laminin 322-coated (804G cell-derived 3-dimensional matrix) cell culture dishes. The culture dishes were incubated at 37°C, 5% CO_2. After keratinocyte attachment (usually after two hours), cells were washed twice with KGM to remove differentiated and other unattached cells. Medium was changed every second day. For differentiation of primary keratinocytes, the $CaCl_2$ level was raised from 0.05 mM to 1.8 mM and cells were cultured for up to 48 hours.

Preparation of 804G cell-derived 3-dimensional matrix

804G cells were grown on cell culture dishes in DMEM, 10% FCS, 1% P/S, 2 mM L-Glucose to post-confluence. Subsequently, cells were rinsed with 1x PBS and incubated with PBS containing 20 mM NH_4OH for 5 minutes. Cell culture dishes were washed 3 times with ddH_2O to remove cell debris. In case of surviving cells, incubation with 20 mM NH_4OH was repeated. To remove all traces of NH_4OH, cell culture dishes were washed two times more with 1x PBS. Thereafter dishes were used immediately for seeding of primary keratinocytes or frozen at -20°C by using 1x PBS containing 10% DMSO. Frozen plates were thawed at RT and rinsed with 1x PBS and KGM prior to seeding cells.

Cyclic strain stress

Mechanical stress experiments were performed in collaboration with the Trauma Research Laboratories, Department of Trauma Surgery, Vienna General Hospital, Vienna, Austria. For cyclic strain stress experiments, keratinocytes were plated on silicone elastomer-bottomed and collagen IV-coated plates (BioFlex culture plates, Dunn Labortechnik GmbH, Asbach, Germany). After achieving 90 % confluence, stratification was induced with high calcium medium for 24 hours. Stratified keratinocyte sheets were then subjected to mechanical stress with the computer-controlled Cyclic Stress Unite (Flexercell FX-2000) placed in a humidified incubator with 5 % CO2 at 37°C. The Cyclic Strain Unit consisted of a controlled vacuum unit and a base plate to hold the culture plates. Vacuum (15 to 20 kPa) was repeatedly applied to the elastomer-bottomed plates via the base plate. Cyclic deformation was carried out at a frequency of 1 Hz and an amplitude of 12 % for 24 hours. Cells were then prepared for immunofluorescence microscopy.

Dispase-based keratinocyte dissociation assay

This was performed as described previously (Calautti et al., 1995; Kimura et al., 2007). Keratinocytes were seeded in 60 mm diameter dishes to achieve 95% confluence within two days. After reaching confluence, keratinocyte monolayers were allowed to stratify in high calcium medium for 48 hours. Stratified keratinocyte sheets were then washed in PBS containing 1.8 mM $CaCl_2$ and then incubated in dispase II (2.4 U/ml; Roche, Vienna, Austria) for about 45 minutes until the cell sheet had become detached from the dish. The detached cell sheets were washed in PBS containing 1.8 mM $CaCl_2$ and placed in 4 ml PBS containing 1.8 mM $CaCl_2$ in 15 ml conical tubes (BD-Falcon). Tubes were then secured to a tube rotator (Reax2, Heidolph Instruments, Schwabach, Germany) and subjected to 50 rotation cycles before the fragments of cell sheet were counted using a phase-contrast microscope.

Transfection of mammalian cells using FuGENE 6

The FuGENE 6 transfection reagent (Roche, Vienna, Austria) is a non-liposomal formulation that transfects a very wide variety of eukaryotic cells with high efficiency and minimal cytotoxicity. The reagent was stored at -20°C. Before use, FuGENE 6 was warmed to RT and mixed well by inversion or vortexing. Cells were seeded at low densities onto cell culture dishes 3-24 hours prior to transfection. The DNA-FuGENE complex was prepared in polypropylene tubes. For each transfection (6 cm dish), 8 µl FuGENE 6 was diluted into 200 µl serum-free medium, mixed gently (no vortexing) and 5 µg plasmid DNA was added. The solution was mixed gently (no vortexing) and incubated at RT for a minimum of 30 minutes (up to 45 minutes). Then, 300 µl serum-free medium were added and the well-mixed suspension was added drop-wise to the culture dish containing 2.5 ml of normal culture medium. After gentle mixing, the plates were incubated under the appropriate conditions for the cell-line used.

Immunofluorescence microscopy of cells

Mowiol

6 g glycerol and 2.4 g Mowiol (Hoechst) were incubated in 6 ml of dH_2O for 2 hours. 12 ml of 0.2 M Tris-HCl solution, pH 8.5, was added, stirred for 10 minutes, heated to 50°C and spun for 15 minutes. The supernatant was stored at -20°C.

Cells grown on 13 mm diameter glass coverslips or on cell culture dishes were washed with 1x PBS, fixed in 4% paraformaldehyde/PBS (PFA) for 20 minutes at RT and permeabilized in 1x PBS containing 0.2% Triton X-100 for 5 minutes. Alternatively cells were fixed with pre-chilled (-20°C) methanol for 90 seconds and washed with 1x PBS. For blocking of unspecific binding sites, coverslips or dishes were incubated with 3% BSA in PBS for 1 hour at RT. Primary antibody dilutions were prepared in 3% BSA in PBS, and coverslips or dishes were incubated with antibody solution for 1 hour at RT. Thereafter, coverslips or dishes were washed three times for 10 minutes with 1x PBS. Fluorescence-labelled secondary antibodies were diluted in 1x PBS and coverslips or dishes were incubated with the secondary antibodies for 1 hour at RT. Coverslips or dishes were washed as described before, followed by two brief washes with dH_20. Coverslips were mounted by placing them onto a 10 µl drop of mowiol on glass slides. When dishes were used, a 13 mm diameter coverlsip was placed onto a 10 µl drop of mowiol covering the immunolabelled area. The samples were then dried overnight in the dark at RT and examined using a Zeiss fluorescence laser-scanning microscope (LSM) 510 or a Zeiss META microscope. Digital images were processed using LSM, Adobe Photoshop and Adobe Illustrator software.

Immunofluorescence microscopy of cryosections

Tissues were fixed in 4% PFA for 1 hour or overnight at RT, washed three times with 1x PBS and soaked in 2 M sucrose/PBS at 4°C overnight. Thereafter specimens were shock frozen in liquid nitrogen. 2 µm cryosections were obtained by using the Cryostat HM 500 OM at -30°C (sectioning was performed by I. Fischer). Alternatively, unfixed samples were immediately frozen in isopentane (cooled by liquid nitrogen) and sections were obtained as described before. Sections were air-dried for 30 minutes and fixed with ice-cold acetone for 10 minutes. For immunolabeling, specimens were incubated in 2% BSA/PBS for 30 minutes

at RT. Incubation with primary antibodies was followed by three washes with PBS and incubation with secondary antibodies. Again samples were washed three times with PBS, once with dH_2O and embedded in mowiol. Samples were examined using a Zeiss LSM 510 or a Zeiss META microscope.

Live-cell imaging

Live-cell imaging was performed under supervision by G. Burgstaller. Time-lapse video microscopy was implemented on a microscope (Axiovert S100TV; Carl Zeiss MicroImaging, Inc) equipped with phase-contrast and epi-illumination optics. Cells were seeded on collagen I–coated coverslips at a density of 2.8×10^5 cells/cm^2 and kept in KGM during the whole period of observation. Migration was monitored in a closed POCmini cultivation system (Carl Zeiss MicroImaging, Inc) at 37°C and 5% CO_2. Recordings of migrations started 3 hours after plating, and frames were taken with a 10x lens in 1-minute intervals over a period of 90 minutes. Images were obtained using a back-illuminated, cooled charge-coupled device camera (Princeton Research Instruments) driven by a 16-bit controller. The whole video microscopy system was automated by Metamorph 6.3 (Universal Imaging Corporation). The length of trajectories of migrating cells was measured by tracking the central nuclei. Cells that did not spread or remain in the field of view during the whole period of observation were not taken into account for measuring. For statistical evaluation, we used 30 cells per genotype. The processive index, PI, of migration, was defined PI=l/t, where l is the linear distance between the starting point and end endpoint of migration, and t is the total distance traversed by the cell. The ideal PI for linear migration is 1.0

Apoptosis assay

Apoptosis was analyzed on paraformaldehyde-fixed tissue sections using the DeadEnd™ Fluorimetric TUNEL System (Promega, Madison, WI) according to the instructions of the manufacturer. This kit measures the fragmented DNA of apoptotic cells by catalytically incorporating fluorescein-12-dUTP at 3'-OH DNA ends which is then recognized by the enzyme terminal deoxynucleotidyl transferase (TdT), which forms a polymeric tail using the principle of the TUNEL (TdT-mediated dUTP Nick-End Labeling) assay.

Electron Microscopy

High pressure freezing cryoimmobilization of newborn mouse skins and subsequent freeze substitution were performed essentially as described (Reipert et al., 2004). Thin sections were cut with an Ultracut S ultramicrotome (LEICA Microsystems), mounted on copper grids, counterstained with uranyl acetate and lead citrate, and examined at 60 kV in a JEOL JEM-1210 (Jeol Ltd Tokyo, Japan) electron microscope.

Haematoxylin/Eosin-staining of tissue sections

Tissue sections were incubated in Haematoxylin (Papanicolaous solution 1b, Merck) for 5 minutes at RT, then rinsed twice with dH_2O and washed extensively for 5 minutes with H_2O. Thereafter, glass slides were incubated for 10 seconds in 0.5% Eosin-G solution (Merck) and again rinsed twice with dH_2O. Stained sections were dried and embedded using Histofluid (Merck).

Animal husbandry and experiments

Mice were kept under standard housing conditions at the animal facility of the Department of Molecular Cell Biology at the Vienna Biocenter. All experiments involving animals were performed in accordance with Austrian Federal Government laws and regulations.

Preparation of tamoxifen solutions

For intraperitoneal (i.p.) injections 10 mg of tamoxifen (Sigma-Aldrich, free base) were dissolved in ethanol by heating to 55°C to obtain a 10 mg/100 µl tamoxifen suspension. A 10 mg/ml tamoxifen solution was then prepared by addition of sunflower oil (Sigma-Aldrich), followed by brief heating to 55°C and vortexing for 30 minutes at RT.

Application of tamoxifen

Mice were injected i.p. with 1 mg tamoxifen per day for 5 consecutive days.

Tape stripping and TEWL measurements

Test animals were shaved on their backs 48 h prior to tape stripping experiments. Adult mice were anesthetized by intraperitoneal injection of a mixture of 0.22 ml 2% Rompun (Bayer Austria, Vienna, Austria) and 0.66 ml 10% Ketamidor (Richter Pharma, Vienna, Austria) in 1x PBS. Newborn nice were anesthetized by inhalation of Isofluoran (Richter Pharma, Wells, Austria). Test areas were stripped by repeatedly by applying D-Squame tapes (CuDerm Corporation, Dallas, TX, USA) or TESA 3M tape (TESA GmbH, Vienna, Austria), respectively, to disrupt skin barrier. For each stripping, a fresh piece of tape was lightly pressed onto the skin area and pulled of with forceps. To assess epidermal permeability function, transepidermal water loss (TEWL) was measured using an evaporimeter (ServoMed, Stockholm, Sweden). TEWL values were registered in $g/m^2/h$ after equilibration of the probe on the skin (> 60 sec). Environment-related variables at the time of the study were: ambient air temperature 21.3-24.5°C; ambient air humidity 35-42%; atmospheric H_2O pressure 8.8-9.7 mm Hg. Excess air convection was prevented by shielding the measurement zone. TEWL was measured both under baseline conditions, as well as following acute barrier disruption by repeated tape stripping. TEWL of 1-day old mice was measured with a Tewameter TM-300 equipped with a small-diameter (3 mm) probe and measurements were digitally recorded via a MPA5 mulitprobe adapter (Courage and Khazaka, Cologne, Germany).

In-situ skin permeability assay

Newborn mouse pubs were stained as described by (Hardman et al., 1998). Mouse pubs were sacrificed by inhalation of an over-dose (600 µl) of Isofluoran (Richter Pharma, Wells, Austria). They were then dehydrated by incubations (1 minute each) in 25%, 50%, and 75% methanol/PBS followed by 1 minute in 100% methanol. The mouse pubs were then rehydrated with series of methanol solutions (75%, 50%, and 25% methanol/PBS; 1 minute incubations), washed in 1x PBS, and stained for 5 minutes in 0.125% toluidine blue/PBS.

After destaining in 1x PBS, mouse pubs were photographed. Images were processed with Adobe Photoshop software.

REFERENCES

Ackerl, R. (2005). Conditional knockout of plectin and characterization of plectin's role in skin and muscle cells: University of Vienna.

Ackerl, R., Walko, G., Fuchs, P., Fischer, I., Schmuth, M. and Wiche, G. (2007). Conditional targeting of plectin in prenatal and adult mouse stratified epithelia causes keratinocyte fragility and lesional epidermal barrier defects. *J Cell Sci* **120**, 2435-43.

Alberts, B., Johnson, A., Lewis, J., Raff, M., Roberts, K. and Walter, P. (2002). Molecular Biology of the Cell: Garland Science.

Alt, A., Gartsbein, M., Ohba, M., Kuroki, T. and Tennenbaum, T. (2004). Differential regulation of alpha6beta4 integrin by PKC isoforms in murine skin keratinocytes. *Biochem Biophys Res Commun* **314**, 17-23.

Alt, A., Ohba, M., Li, L., Gartsbein, M., Belanger, A., Denning, M. F., Kuroki, T., Yuspa, S. H. and Tennenbaum, T. (2001). Protein kinase Cdelta-mediated phosphorylation of alpha6beta4 is associated with reduced integrin localization to the hemidesmosome and decreased keratinocyte attachment. *Cancer Res* **61**, 4591-8.

Amos, L. A. and Schlieper, D. (2005). Microtubules and maps. *Adv Protein Chem* **71**, 257-98.

Andrä, K., Kornacker, I., Jorgl, A., Zörer, M., Spazierer, D., Fuchs, P., Fischer, I. and Wiche, G. (2003). Plectin-isoform-specific rescue of hemidesmosomal defects in plectin (-/-) keratinocytes. *J Invest Dermatol* **120**, 189-97.

Andrä, K., Lassmann, H., Bittner, R., Shorny, S., Fassler, R., Propst, F. and Wiche, G. (1997). Targeted inactivation of plectin reveals essential function in maintaining the integrity of skin, muscle, and heart cytoarchitecture. *Genes Dev* **11**, 3143-56.

Andrä, K., Nikolic, B., Stocher, M., Drenckhahn, D. and Wiche, G. (1998). Not just scaffolding: plectin regulates actin dynamics in cultured cells. *Genes Dev* **12**, 3442-51.

Argos, P., Landy, A., Abremski, K., Egan, J. B., Haggard-Ljungquist, E., Hoess, R. H., Kahn, M. L., Kalionis, B., Narayana, S. V., Pierson, L. S., 3rd et al. (1986). The integrase family of site-specific recombinases: regional similarities and global diversity. *Embo J* **5**, 433-40.

Aumailley, M., Bruckner-Tuderman, L., Carter, W. G., Deutzmann, R., Edgar, D., Ekblom, P., Engel, J., Engvall, E., Hohenester, E., Jones, J. C. et al. (2005). A simplified laminin nomenclature. *Matrix Biol* **24**, 326-32.

Baker, K. E. and Condon, C. (2004). Under the Tucson sun: a meeting in the desert on mRNA decay. *Rna* **10**, 1680-91.

Ball, E. H. and Singer, S. J. (1981). Association of microtubules and intermediate filaments in normal fibroblasts and its disruption upon transformation by a temperature-sensitive mutant of Rous sarcoma virus. *Proc Natl Acad Sci U S A* **78**, 6986-90.

Bauer, J. W., Rouan, F., Kofler, B., Rezniczek, G. A., Kornacker, I., Muss, W., Hametner, R., Klausegger, A., Huber, A., Pohla-Gubo, G. et al. (2001). A compound heterozygous one amino-acid insertion/nonsense mutation in the plectin gene causes epidermolysis bullosa simplex with plectin deficiency. *Am J Pathol* **158**, 617-25.

Beil, M., Micoulet, A., von Wichert, G., Paschke, S., Walther, P., Omary, M. B., Van Veldhoven, P. P., Gern, U., Wolff-Hieber, E., Eggermann, J. et al. (2003). Sphingosylphosphorylcholine regulates keratin network architecture and visco-elastic properties of human cancer cells. *Nat Cell Biol* **5**, 803-11.

Benitah, S. A., Frye, M., Glogauer, M. and Watt, F. M. (2005). Stem cell depletion through epidermal deletion of Rac1. *Science* **309**, 933-5.

Boczonadi, V., McInroy, L. and Maatta, A. (2007). Cytolinker cross-talk: Periplakin N-terminus interacts with plectin to regulate keratin organisation and epithelial migration. *Exp Cell Res* **313**, 3579-91.

Bonifas, J. M., Rothman, A. L. and Epstein, E. H., Jr. (1991). Epidermolysis bullosa simplex: evidence in two families for keratin gene abnormalities. *Science* **254**, 1202-5.

Bonne, G., Di Barletta, M. R., Varnous, S., Becane, H. M., Hammouda, E. H., Merlini, L., Muntoni, F., Greenberg, C. R., Gary, F., Urtizberea, J. A. et al. (1999). Mutations in the gene encoding lamin A/C cause autosomal dominant Emery-Dreifuss muscular dystrophy. *Nat Genet* **21**, 285-8.

Borradori, L. and Sonnenberg, A. (1999). Structure and function of hemidesmosomes: more than simple adhesion complexes. *J Invest Dermatol* **112**, 411-8.

Boukamp, P., Petrussevska, R. T., Breitkreutz, D., Hornung, J., Markham, A. and Fusenig, N. E. (1988). Normal keratinization in a spontaneously immortalized aneuploid human keratinocyte cell line. *J Cell Biol* **106**, 761-71.

Bradford, M. M. (1976). A rapid and sensitive method for the quantitation of microgram quantities of protein utilizing the principle of protein-dye binding. *Anal Biochem* **72**, 248-54.

Brocard, J., Warot, X., Wendling, O., Messaddeq, N., Vonesch, J. L., Chambon, P. and Metzger, D. (1997). Spatio-temporally controlled site-specific somatic mutagenesis in the mouse. *Proc Natl Acad Sci U S A* **94**, 14559-63.

Brown, M. J., Hallam, J. A., Liu, Y., Yamada, K. M. and Shaw, S. (2001). Cutting edge: integration of human T lymphocyte cytoskeleton by the cytolinker plectin. *J Immunol* **167**, 641-5.

Burridge, K., Turner, C. E. and Romer, L. H. (1992). Tyrosine phosphorylation of paxillin and pp125FAK accompanies cell adhesion to extracellular matrix: a role in cytoskeletal assembly. *J Cell Biol* **119**, 893-903.

Byrne, C. and Fuchs, E. (1993). Probing keratinocyte and differentiation specificity of the human K5 promoter in vitro and in transgenic mice. *Mol Cell Biol* **13**, 3176-90.

Calautti, E., Missero, C., Stein, P. L., Ezzell, R. M. and Dotto, G. P. (1995). fyn tyrosine kinase is involved in keratinocyte differentiation control. *Genes Dev* **9**, 2279-91.

Caldelari, R., Suter, M. M., Baumann, D., De Bruin, A. and Muller, E. (2000). Long-term culture of murine epidermal keratinocytes. *J Invest Dermatol* **114**, 1064-5.

Candi, E., Schmidt, R. and Melino, G. (2005). The cornified envelope: a model of cell death in the skin. *Nat Rev Mol Cell Biol* **6**, 328-40.

Cano, A., Gamallo, C., Kemp, C. J., Benito, N., Palacios, J., Quintanilla, M. and Balmain, A. (1996). Expression pattern of the cell adhesion molecules. E-cadherin, P-cadherin and alpha 6 beta 4 intergrin is altered in pre-malignant skin tumors of p53-deficient mice. *Int J Cancer* **65**, 254-62.

Capell, B. C. and Collins, F. S. (2006). Human laminopathies: nuclei gone genetically awry. *Nat Rev Genet* **7**, 940-52.

Carter, W. G., Kaur, P., Gil, S. G., Gahr, P. J. and Wayner, E. A. (1990). Distinct functions for integrins alpha 3 beta 1 in focal adhesions and alpha 6 beta 4/bullous pemphigoid antigen in a new stable anchoring contact (SAC) of keratinocytes: relation to hemidesmosomes. *J Cell Biol* **111**, 3141-54.

Ceccarelli, S., Cardinali, G., Aspite, N., Picardo, M., Marchese, C., Torrisi, M. R. and Mancini, P. (2007). Cortactin involvement in the keratinocyte growth factor and

fibroblast growth factor 10 promotion of migration and cortical actin assembly in human keratinocytes. *Exp Cell Res* **313**, 1758-77.

Chakrabarty, A. and Geisse, J. K. (2004). Medical therapies for non-melanoma skin cancer. *Clin Dermatol* **22**, 183-8.

Chang, B. Y., Chiang, M. and Cartwright, C. A. (2001). The interaction of Src and RACK1 is enhanced by activation of protein kinase C and tyrosine phosphorylation of RACK1. *J Biol Chem* **276**, 20346-56.

Chang, B. Y., Conroy, K. B., Machleder, E. M. and Cartwright, C. A. (1998). RACK1, a receptor for activated C kinase and a homolog of the beta subunit of G proteins, inhibits activity of src tyrosine kinases and growth of NIH 3T3 cells. *Mol Cell Biol* **18**, 3245-56.

Chang, B. Y., Harte, R. A. and Cartwright, C. A. (2002). RACK1: a novel substrate for the Src protein-tyrosine kinase. *Oncogene* **21**, 7619-29.

Chang, L., Shav-Tal, Y., Trcek, T., Singer, R. H. and Goldman, R. D. (2006). Assembling an intermediate filament network by dynamic cotranslation. *J Cell Biol* **172**, 747-58.

Charlesworth, A., Gagnoux-Palacios, L., Bonduelle, M., Ortonne, J. P., De Raeve, L. and Meneguzzi, G. (2003). Identification of a lethal form of epidermolysis bullosa simplex associated with a homozygous genetic mutation in plectin. *J Invest Dermatol* **121**, 1344-8.

Chavanas, S., Pulkkinen, L., Gache, Y., Smith, F. J., McLean, W. H., Uitto, J., Ortonne, J. P. and Meneguzzi, G. (1996). A homozygous nonsense mutation in the PLEC1 gene in patients with epidermolysis bullosa simplex with muscular dystrophy. *J Clin Invest* **98**, 2196-200.

Chen, H. J., Lin, C. M., Lin, C. S., Perez-Olle, R., Leung, C. L. and Liem, R. K. (2006). The role of microtubule actin cross-linking factor 1 (MACF1) in the Wnt signaling pathway. *Genes Dev* **20**, 1933-45.

Cheng, C. C., Liu, Y. H., Ho, C. C., Chao, W. T., Pei, R. J., Hsu, Y. H., Yeh, K. T., Ho, L. C., Tsai, M. C. and Lai, Y. S. (2007). The influence of plectin deficiency on stability of cytokeratin18 in hepatocellular carcinoma. *J Mol Histol*.

Chidgey, M., Brakebusch, C., Gustafsson, E., Cruchley, A., Hail, C., Kirk, S., Merritt, A., North, A., Tselepis, C., Hewitt, J. et al. (2001). Mice lacking desmocollin 1 show epidermal fragility accompanied by barrier defects and abnormal differentiation. *J Cell Biol* **155**, 821-32.

Choma, D. P., Milano, V., Pumiglia, K. M. and DiPersio, C. M. (2007). Integrin alpha3beta1-dependent activation of FAK/Src regulates Rac1-mediated keratinocyte polarization on laminin-5. *J Invest Dermatol* **127**, 31-40.

Choma, D. P., Pumiglia, K. and DiPersio, C. M. (2004). Integrin alpha3beta1 directs the stabilization of a polarized lamellipodium in epithelial cells through activation of Rac1. *J Cell Sci* **117**, 3947-59.

Chow, C. W., Woodside, M., Demaurex, N., Yu, F. H., Plant, P., Rotin, D., Grinstein, S. and Orlowski, J. (1999). Proline-rich motifs of the Na+/H+ exchanger 2 isoform. Binding of Src homology domain 3 and role in apical targeting in epithelia. *J Biol Chem* **274**, 10481-8.

Cole, J., Tsou, R., Wallace, K., Gibran, N. and Isik, F. (2001). Early gene expression profile of human skin to injury using high-density cDNA microarrays. *Wound Repair Regen* **9**, 360-70.

Corbit, K. C., Trakul, N., Eves, E. M., Diaz, B., Marshall, M. and Rosner, M. R. (2003). Activation of Raf-1 signaling by protein kinase C through a mechanism involving Raf kinase inhibitory protein. *J Biol Chem* **278**, 13061-8.

Coulombe, P. A., Hutton, M. E., Vassar, R. and Fuchs, E. (1991). A function for keratins and a common thread among different types of epidermolysis bullosa simplex diseases. *J Cell Biol* **115**, 1661-74.

Coulombe, P. A. and Omary, M. B. (2002). 'Hard' and 'soft' principles defining the structure, function and regulation of keratin intermediate filaments. *Curr Opin Cell Biol* **14**, 110-22.

Coulombe, P. A., Tong, X., Mazzalupo, S., Wang, Z. and Wong, P. (2004). Great promises yet to be fulfilled: defining keratin intermediate filament function in vivo. *Eur J Cell Biol* **83**, 735-46.

Coulombe, P. A. and Wong, P. (2004). Cytoplasmic intermediate filaments revealed as dynamic and multipurpose scaffolds. *Nat Cell Biol* **6**, 699-706.

D'Alessandro, M., Russell, D., Morley, S. M., Davies, A. M. and Lane, E. B. (2002). Keratin mutations of epidermolysis bullosa simplex alter the kinetics of stress response to osmotic shock. *J Cell Sci* **115**, 4341-51.

Dajee, M., Lazarov, M., Zhang, J. Y., Cai, T., Green, C. L., Russell, A. J., Marinkovich, M. P., Tao, S., Lin, Q., Kubo, Y. et al. (2003). NF-kappaB blockade and oncogenic Ras trigger invasive human epidermal neoplasia. *Nature* **421**, 639-43.

Danielian, P. S., Muccino, D., Rowitch, D. H., Michael, S. K. and McMahon, A. P. (1998). Modification of gene activity in mouse embryos in utero by a tamoxifen-inducible form of Cre recombinase. *Curr Biol* **8**, 1323-6.

Davies, M., Robinson, M., Smith, E., Huntley, S., Prime, S. and Paterson, I. (2005). Induction of an epithelial to mesenchymal transition in human immortal and malignant keratinocytes by TGF-beta1 involves MAPK, Smad and AP-1 signalling pathways. *J Cell Biochem* **95**, 918-31.

Dehmelt, L. and Halpain, S. (2005). The MAP2/Tau family of microtubule-associated proteins. *Genome Biol* **6**, 204.

Desai, A. and Mitchison, T. J. (1997). Microtubule polymerization dynamics. *Annu Rev Cell Dev Biol* **13**, 83-117.

DiColandrea, T., Karashima, T., Maatta, A. and Watt, F. M. (2000). Subcellular distribution of envoplakin and periplakin: insights into their role as precursors of the epidermal cornified envelope. *J Cell Biol* **151**, 573-86.

DiPersio, C. M., van der Neut, R., Georges-Labouesse, E., Kreidberg, J. A., Sonnenberg, A. and Hynes, R. O. (2000). alpha3beta1 and alpha6beta4 integrin receptors for laminin-5 are not essential for epidermal morphogenesis and homeostasis during skin development. *J Cell Sci* **113 (Pt 17)**, 3051-62.

Dowling, J., Yu, Q. C. and Fuchs, E. (1996). Beta4 integrin is required for hemidesmosome formation, cell adhesion and cell survival. *J Cell Biol* **134**, 559-72.

Eger, A., Stockinger, A., Wiche, G. and Foisner, R. (1997). Polarisation-dependent association of plectin with desmoplakin and the lateral submembrane skeleton in MDCK cells. *J Cell Sci* **110 (Pt 11)**, 1307-16.

Elliott, C. E., Becker, B., Oehler, S., Castanon, M. J., Hauptmann, R. and Wiche, G. (1997). Plectin transcript diversity: identification and tissue distribution of variants with distinct first coding exons and rodless isoforms. *Genomics* **42**, 115-25.

Eming, S. A., Krieg, T. and Davidson, J. M. (2007). Inflammation in wound repair: molecular and cellular mechanisms. *J Invest Dermatol* **127**, 514-25.

Errante, L. D., Wiche, G. and Shaw, G. (1994). Distribution of plectin, an intermediate filament-associated protein, in the adult rat central nervous system. *J Neurosci Res* **37**, 515-28.

Fabre-Jonca, N., Viard, I., French, L. E. and Masson, D. (1999). Upregulation and redistribution of E-MAP-115 (epithelial microtubule-associated protein of 115 kDa) in

terminally differentiating keratinocytes is coincident with the formation of intercellular contacts. *J Invest Dermatol* **112**, 216-25.

Faire, K., Waterman-Storer, C., Gruber, D., Masson, D., Salmon, E. and Bulinski, J. C. (1999). E-MAP-115 (Ensconsin) associates dynamically with microtubules in vivo and does not modulate their dynamics. *J. Cell Science* **112**, 4243-4255.

Faix, J. and Rottner, K. (2006). The making of filopodia. *Curr Opin Cell Biol* **18**, 18-25.

Fan, J., Guan, S., Cheng, C. F., Cho, M., Fields, J. W., Chen, M., Denning, M. F., Woodley, D. T. and Li, W. (2006). PKCdelta clustering at the leading edge and mediating growth factor-enhanced, but not ecm-initiated, dermal fibroblast migration. *J Invest Dermatol* **126**, 1233-43.

Faraldo, M. L., Rodrigo, I., Behrens, J., Birchmeier, W. and Cano, A. (1997). Analysis of the E-cadherin and P-cadherin promoters in murine keratinocyte cell lines from different stages of mouse skin carcinogenesis. *Mol Carcinog* **20**, 33-47.

Feil, R., Brocard, J., Mascrez, B., LeMeur, M., Metzger, D. and Chambon, P. (1996). Ligand-activated site-specific recombination in mice. *Proc Natl Acad Sci U S A* **93**, 10887-90.

Feil, R., Wagner, J., Metzger, D. and Chambon, P. (1997). Regulation of Cre recombinase activity by mutated estrogen receptor ligand-binding domains. *Biochem Biophys Res Commun* **237**, 752-7.

Fitsialos, G., Chassot, A. A., Turchi, L., Dayem, M. A., LeBrigand, K., Moreilhon, C., Meneguzzi, G., Busca, R., Mari, B., Barbry, P. et al. (2007). Transcriptional signature of epidermal keratinocytes subjected to in vitro scratch wounding reveals selective roles for ERK1/2, p38, and phosphatidylinositol 3-kinase signaling pathways. *J Biol Chem* **282**, 15090-102.

Foisner, R., Leichtfried, F. E., Herrmann, H., Small, J. V., Lawson, D. and Wiche, G. (1988). Cytoskeleton-associated plectin: in situ localization, in vitro reconstitution, and binding to immobilized intermediate filament proteins. *J Cell Biol* **106**, 723-33.

Foisner, R., Malecz, N., Dressel, N., Stadler, C. and Wiche, G. (1996). M-phase-specific phosphorylation and structural rearrangement of the cytoplasmic cross-linking protein plectin involve p34cdc2 kinase. *Mol. Biol. Cell* **7**, 273-288.

Foisner, R. and Wiche, G. (1987). Structure and hydrodynamic properties of plectin molecules. *J Mol Biol* **198**, 515-31.

Frank, D. E. and Carter, W. G. (2004). Laminin 5 deposition regulates keratinocyte polarization and persistent migration. *J Cell Sci* **117**, 1351-63.

Fuchs, E. and Cleveland, D. W. (1998). A structural scaffolding of intermediate filaments in health and disease. *Science* **279**, 514-9.

Fuchs, E. and Raghavan, S. (2002). Getting under the skin of epidermal morphogenesis. *Nat Rev Genet* **3**, 199-209.

Fuchs, E. and Weber, K. (1994). Intermediate filaments: structure, dynamics, function, and disease. *Annu Rev Biochem* **63**, 345-82.

Fuchs, P., Zorer, M., Rezniczek, G. A., Spazierer, D., Oehler, S., Castanon, M. J., Hauptmann, R. and Wiche, G. (1999). Unusual 5' transcript complexity of plectin isoforms: novel tissue-specific exons modulate actin binding activity. *Hum Mol Genet* **8**, 2461-72.

Gache, Y., Chavanas, S., Lacour, J. P., Wiche, G., Owaribe, K., Meneguzzi, G. and Ortonne, J. P. (1996). Defective expression of plectin/HD1 in epidermolysis bullosa simplex with muscular dystrophy. *J Clin Invest* **97**, 2289-98.

Gagnoux-Palacios, L., Dans, M., van't Hof, W., Mariotti, A., Pepe, A., Meneguzzi, G., Resh, M. D. and Giancotti, F. G. (2003). Compartmentalization of integrin alpha6beta4 signaling in lipid rafts. *J Cell Biol* **162**, 1189-96.

Gallicano, G. I., Bauer, C. and Fuchs, E. (2001). Rescuing desmoplakin function in extra-embryonic ectoderm reveals the importance of this protein in embryonic heart, neuroepithelium, skin and vasculature. *Development* **128**, 929-41.

Garrod, D. R., Merritt, A. J. and Nie, Z. (2002). Desmosomal cadherins. *Curr Opin Cell Biol* **14**, 537-45.

Geerts, D., Fontao, L., Nievers, M. G., Schaapveld, R. Q., Purkis, P. E., Wheeler, G. N., Lane, E. B., Leigh, I. M. and Sonnenberg, A. (1999). Binding of integrin alpha6beta4 to plectin prevents plectin association with F-actin but does not interfere with intermediate filament binding. *J Cell Biol* **147**, 417-34.

Geuijen, C. A. and Sonnenberg, A. (2002). Dynamics of the alpha6beta4 integrin in keratinocytes. *Mol Biol Cell* **13**, 3845-58.

Godsel, L. M., Hsieh, S. N., Amargo, E. V., Bass, A. E., Pascoe-McGillicuddy, L. T., Huen, A. C., Thorne, M. E., Gaudry, C. A., Park, J. K., Myung, K. et al. (2005). Desmoplakin assembly dynamics in four dimensions: multiple phases differentially regulated by intermediate filaments and actin. *J Cell Biol* **171**, 1045-59.

Goldfarb, L. G., Vicart, P., Goebel, H. H. and Dalakas, M. C. (2004). Desmin myopathy. *Brain* **127**, 723-34.

Goldfinger, L. E., Hopkinson, S. B., deHart, G. W., Collawn, S., Couchman, J. R. and Jones, J. C. (1999). The alpha3 laminin subunit, alpha6beta4 and alpha3beta1 integrin coordinately regulate wound healing in cultured epithelial cells and in the skin. *J Cell Sci* **112 (Pt 16)**, 2615-29.

Goldsmith, S. C., Pokala, N., Shen, W., Fedorov, A. A., Matsudaira, P. and Almo, S. C. (1997). The structure of an actin-crosslinking domain from human fimbrin. *Nat Struct Biol* **4**, 708-12.

Goley, E. D. and Welch, M. D. (2006). The ARP2/3 complex: an actin nucleator comes of age. *Nat Rev Mol Cell Biol* **7**, 713-26.

Green, K. J., Bohringer, M., Gocken, T. and Jones, J. C. (2005). Intermediate filament associated proteins. *Adv Protein Chem* **70**, 143-202.

Green, K. J. and Gaudry, C. A. (2000). Are desmosomes more than tethers for intermediate filaments? *Nat Rev Mol Cell Biol* **1**, 208-16.

Green, K. J., Geiger, B., Jones, J. C., Talian, J. C. and Goldman, R. D. (1987). The relationship between intermediate filaments and microfilaments before and during the formation of desmosomes and adherens-type junctions in mouse epidermal keratinocytes. *J Cell Biol* **104**, 1389-402.

Gregor, M., Zeold, A., Oehler, S., Marobela, K. A., Fuchs, P., Weigel, G., Hardie, D. G. and Wiche, G. (2006). Plectin scaffolds recruit energy-controlling AMP-activated protein kinase (AMPK) in differentiated myofibres. *J Cell Sci* **119**, 1864-75.

Grindley, N. D., Whiteson, K. L. and Rice, P. A. (2006). Mechanisms of Site-Specific Recombination. *Annu Rev Biochem.*

Gu, H., Marth, J. D., Orban, P. C., Mossmann, H. and Rajewsky, K. (1994). Deletion of a DNA polymerase beta gene segment in T cells using cell type-specific gene targeting. *Science* **265**, 103-6.

Gu, L. H. and Coulombe, P. A. (2007). Keratin function in skin epithelia: a broadening palette with surprising shades. *Curr Opin Cell Biol* **19**, 13-23.

Guo, L., Degenstein, L., Dowling, J., Yu, Q. C., Wollmann, R., Perman, B. and Fuchs, E. (1995). Gene targeting of BPAG1: abnormalities in mechanical strength and cell migration in stratified epithelia and neurologic degeneration. *Cell* **81**, 233-43.

Hager, B., Bickenbach, J. R. and Fleckman, P. (1999). Long-term culture of murine epidermal keratinocytes. *J Invest Dermatol* **112**, 971-6.

Hakkinen, L., Hildebrand, H. C., Berndt, A., Kosmehl, H. and Larjava, H. (2000). Immunolocalization of tenascin-C, alpha9 integrin subunit, and alphavbeta6 integrin during wound healing in human oral mucosa. *J Histochem Cytochem* **48**, 985-98.

Hamelers, I. H., Olivo, C., Mertens, A. E., Pegtel, D. M., van der Kammen, R. A., Sonnenberg, A. and Collard, J. G. (2005). The Rac activator Tiam1 is required for (alpha)3(beta)1-mediated laminin-5 deposition, cell spreading, and cell migration. *J Cell Biol* **171**, 871-81.

Hardman, M. J., Sisi, P., Banbury, D. N. and Byrne, C. (1998). Patterned acquisition of skin barrier function during development. *Development* **125**, 1541-52.

Hatzfeld, M. (2007). Plakophilins: Multifunctional proteins or just regulators of desmosomal adhesion? *Biochim Biophys Acta* **1773**, 69-77.

Hatzfeld, M., Haffner, C., Schulze, K. and Vinzens, U. (2000). The function of plakophilin 1 in desmosome assembly and actin filament organization. *J Cell Biol* **149**, 209-22.

Helfand, B. T., Chang, L. and Goldman, R. D. (2004). Intermediate filaments are dynamic and motile elements of cellular architecture. *J Cell Sci* **117**, 133-41.

Hennings, H., Michael, D., Cheng, C., Steinert, P., Holbrook, K. and Yuspa, S. H. (1980). Calcium regulation of growth and differentiation of mouse epidermal cells in culture. *Cell* **19**, 245-54.

Herold-Mende, C., Kartenbeck, J., Tomakidi, P. and Bosch, F. X. (2001). Metastatic growth of squamous cell carcinomas is correlated with upregulation and redistribution of hemidesmosomal components. *Cell Tissue Res* **306**, 399-408.

Herrmann, H., Bar, H., Kreplak, L., Strelkov, S. V. and Aebi, U. (2007). Intermediate filaments: from cell architecture to nanomechanics. *Nat Rev Mol Cell Biol* **8**, 562-73.

Herrmann, H. and Wiche, G. (1987). Plectin and IFAP-300K are homologous proteins binding to microtubule-associated proteins 1 and 2 and to the 240-kilodalton subunit of spectrin. *J Biol Chem* **262**, 1320-5.

Hintermann, E., Bilban, M., Sharabi, A. and Quaranta, V. (2001). Inhibitory role of alpha 6 beta 4-associated erbB-2 and phosphoinositide 3-kinase in keratinocyte haptotactic migration dependent on alpha 3 beta 1 integrin. *J Cell Biol* **153**, 465-78.

Ho, C. L., Martys, J. L., Mikhailov, A., Gundersen, G. G. and Liem, R. K. (1998). Novel features of intermediate filament dynamics revealed by green fluorescent protein chimeras. *J Cell Sci* **111 (Pt 13)**, 1767-78.

Hoess, R., Abremski, K., Irwin, S., Kendall, M. and Mack, A. (1990). DNA specificity of the Cre recombinase resides in the 25 kDa carboxyl domain of the protein. *J Mol Biol* **216**, 873-82.

Hofmann, M., Zaper, J., Bernd, A., Bereiter-Hahn, J., Kaufmann, R. and Kippenberger, S. (2004). Mechanical pressure-induced phosphorylation of p38 mitogen-activated protein kinase in epithelial cells via Src and protein kinase C. *Biochem Biophys Res Commun* **316**, 673-9.

Holmes, D. S. and Quigley, M. (1981). A rapid boiling method for the preparation of bacterial plasmids. *Anal Biochem* **114**, 193-7.

Honma, M., Benitah, S. A. and Watt, F. M. (2006). Role of LIM kinases in normal and psoriatic human epidermis. *Mol Biol Cell* **17**, 1888-96.

Huang, C., Jacobson, K. and Schaller, M. D. (2004). MAP kinases and cell migration. *J Cell Sci* **117**, 4619-28.

Hunt, D. M., Rickman, L., Whittock, N. V., Eady, R. A., Simrak, D., Dopping-Hepenstal, P. J., Stevens, H. P., Armstrong, D. K., Hennies, H. C., Kuster, W. et al.

(2001). Spectrum of dominant mutations in the desmosomal cadherin desmoglein 1, causing the skin disease striate palmoplantar keratoderma. *Eur J Hum Genet* **9**, 197-203.

Indra, A. K., Warot, X., Brocard, J., Bornert, J. M., Xiao, J. H., Chambon, P. and Metzger, D. (1999). Temporally-controlled site-specific mutagenesis in the basal layer of the epidermis: comparison of the recombinase activity of the tamoxifen-inducible Cre-ER(T) and Cre-ER(T2) recombinases. *Nucleic Acids Res* **27**, 4324-7.

Irvine, A. D. and McLean, W. H. (1999). Human keratin diseases: the increasing spectrum of disease and subtlety of the phenotype-genotype correlation. *Br J Dermatol* **140**, 815-28.

Isaacs, W. B., Cook, R. K., Van Atta, J. C., Redmond, C. M. and Fulton, A. B. (1989). Assembly of vimentin in cultured cells varies with cell type. *J Biol Chem* **264**, 17953-60.

Izawa, I. and Inagaki, M. (2006). Regulatory mechanisms and functions of intermediate filaments: a study using site- and phosphorylation state-specific antibodies. *Cancer Sci* **97**, 167-74.

Jamora, C. and Fuchs, E. (2002). Intercellular adhesion, signalling and the cytoskeleton. *Nat Cell Biol* **4**, E101-8.

Janes, S. M. and Watt, F. M. (2006). New roles for integrins in squamous-cell carcinoma. *Nat Rev Cancer* **6**, 175-83.

Jefferson, J. J., Ciatto, C., Shapiro, L. and Liem, R. K. (2007). Structural analysis of the plakin domain of bullous pemphigoid antigen1 (BPAG1) suggests that plakins are members of the spectrin superfamily. *J Mol Biol* **366**, 244-57.

Jefferson, J. J., Leung, C. L. and Liem, R. K. (2004). Plakins: goliaths that link cell junctions and the cytoskeleton. *Nat Rev Mol Cell Biol* **5**, 542-53.

Jefferson, J. J., Leung, C. L. and Liem, R. K. (2006). Dissecting the sequence specific functions of alternative N-terminal isoforms of mouse bullous pemphigoid antigen 1. *Exp Cell Res* **312**, 2712-25.

Jones, J. C., Hopkinson, S. B. and Goldfinger, L. E. (1998). Structure and assembly of hemidesmosomes. *Bioessays* **20**, 488-94.

Kalinin, A. E., Kajava, A. V. and Steinert, P. M. (2002). Epithelial barrier function: assembly and structural features of the cornified cell envelope. *Bioessays* **24**, 789-800.

Karakesisoglou, I., Yang, Y. and Fuchs, E. (2000). An epidermal plakin that integrates actin and microtubule networks at cellular junctions. *J Cell Biol* **149**, 195-208.

Karashima, T. and Watt, F. M. (2002). Interaction of periplakin and envoplakin with intermediate filaments. *J Cell Sci* **115**, 5027-37.

Karr, T. L., White, H. D. and Purich, D. L. (1979). Characterization of brain microtubule proteins prepared by selective removal of mitochondrial and synaptosomal components. *J Biol Chem.* **254**, 6107-11.

Kellendonk, C., Tronche, F., Casanova, E., Anlag, K., Opherk, C. and Schutz, G. (1999). Inducible site-specific recombination in the brain. *J Mol Biol* **285**, 175-82.

Kim, S. and Coulombe, P. A. (2007). Intermediate filament scaffolds fulfill mechanical, organizational, and signaling functions in the cytoplasm. *Genes Dev* **21**, 1581-97.

Kim, S., Wong, P. and Coulombe, P. A. (2006). A keratin cytoskeletal protein regulates protein synthesis and epithelial cell growth. *Nature* **441**, 362-5.

Kimura, T. E., Merritt, A. J. and Garrod, D. R. (2007). Calcium-independent desmosomes of keratinocytes are hyper-adhesive. *J Invest Dermatol* **127**, 775-81.

Kippenberger, S., Loitsch, S., Muller, J., Guschel, M., Kaufmann, R. and Bernd, A. (2004). Ligation of the beta4 integrin triggers adhesion behavior of human keratinocytes by an "inside-out" mechanism. *J Invest Dermatol* **123**, 444-51.

Kitajima, Y., Inoue, S. and Yaoita, H. (1986). Reorganization of keratin intermediate filaments by the drug-induced disruption of microfilaments in cultured human keratinocytes. *J Invest Dermatol* **87**, 565-9.

Kligys, K., Claiborne, J. N., Debiase, P. J., Hopkinson, S. B., Wu, Y., Mizuno, K. and Jones, J. C. (2007). The slingshot family of phosphatases mediates Rac1 regulation of cofilin phosphorylation, laminin-332 organization and motility behavior of keratinocytes. *J Biol Chem*.

Koch, P. J., Mahoney, M. G., Ishikawa, H., Pulkkinen, L., Uitto, J., Shultz, L., Murphy, G. F., Whitaker-Menezes, D. and Stanley, J. R. (1997). Targeted disruption of the pemphigus vulgaris antigen (desmoglein 3) gene in mice causes loss of keratinocyte cell adhesion with a phenotype similar to pemphigus vulgaris. *J Cell Biol* **137**, 1091-102.

Kodama, A., Karakesisoglou, I., Wong, E., Vaezi, A. and Fuchs, E. (2003). ACF7: an essential integrator of microtubule dynamics. *Cell* **115**, 343-54.

Koss-Harnes, D., Høyheim, B., Anton-Lamprecht, I., Gjest, A., Jørgensen, R. S., Jahnsen, F. L., Olaisen, B., Wiche, G. and Gedde-Dahl, T. (2001). A site-specific plectin mutation causes dominant Epidermolysis bullosa simplex Ogna. Two identical *de novo* mutations. *Submitted for publication*.

Koss-Harnes, D., Jahnsen, F. L., Wiche, G., Soyland, E., Brandtzaeg, P. and Gedde-Dahl, T., Jr. (1997). Plectin abnormality in epidermolysis bullosa simplex Ogna: non- responsiveness of basal keratinocytes to some anti-rat plectin antibodies. *Exp Dermatol* **6**, 41-8.

Koster, J., Geerts, D., Favre, B., Borradori, L. and Sonnenberg, A. (2003). Analysis of the interactions between BP180, BP230, plectin and the integrin alpha6beta4 important for hemidesmosome assembly. *J Cell Sci* **116**, 387-99.

Koster, J., van Wilpe, S., Kuikman, I., Litjens, S. H. and Sonnenberg, A. (2004). Role of binding of plectin to the integrin beta4 subunit in the assembly of hemidesmosomes. *Mol Biol Cell* **15**, 1211-23.

Kottke, M. D., Delva, E. and Kowalczyk, A. P. (2006). The desmosome: cell science lessons from human diseases. *J Cell Sci* **119**, 797-806.

Kowalczyk, A. P., Hatzfeld, M., Bornslaeger, E. A., Kopp, D. S., Borgwardt, J. E., Corcoran, C. M., Settler, A. and Green, K. J. (1999). The head domain of plakophilin-1 binds to desmoplakin and enhances its recruitment to desmosomes. Implications for cutaneous disease. *J Biol Chem* **274**, 18145-8.

Kremer, B. E., Haystead, T. and Macara, I. G. (2005). Mammalian septins regulate microtubule stability through interaction with the microtubule-binding protein MAP4. *Mol Biol Cell* **16**, 4648-59.

Ku, N. O. and Omary, M. B. (2000). Keratins turn over by ubiquitination in a phosphorylation-modulated fashion. *J Cell Biol* **149**, 547-52.

Kühnel, W. (2002). Taschenatlas der Zytologie, Histologie und mikroskopischen Anatomie: Thieme.

Kulesz-Martin, M., Kilkenny, A. E., Holbrook, K. A., Digernes, V. and Yuspa, S. H. (1983). Properties of carcinogen altered mouse epidermal cells resistant to calcium-induced terminal differentiation. *Carcinogenesis* **4**, 1367-77.

Kunz, M., Rouan, F., Pulkkinen, L., Hamm, H., Jeschke, R., Bruckner-Tuderman, L., Brocker, E. B., Wiche, G., Uitto, J. and Zillikens, D. (2000). Mutation reports: epidermolysis bullosa simplex associated with severe mucous membrane involvement and novel mutations in the plectin gene. *J Invest Dermatol* **114**, 376-80.

Laemmli, U. K. (1970). Cleavage of structural proteins during the assembly of the head of bacteriophage T4. *Nature* **227**, 680-5.

Lai Cheong, J. E., Wessagowit, V. and McGrath, J. A. (2005). Molecular abnormalities of the desmosomal protein desmoplakin in human disease. *Clin Exp Dermatol* **30**, 261-6.

Lane, E. B., Rugg, E. L., Navsaria, H., Leigh, I. M., Heagerty, A. H., Ishida-Yamamoto, A. and Eady, R. A. (1992). A mutation in the conserved helix termination peptide of keratin 5 in hereditary skin blistering. *Nature* **356**, 244-6.

Lariviere, R. C. and Julien, J. P. (2004). Functions of intermediate filaments in neuronal development and disease. *J Neurobiol* **58**, 131-48.

Lechler, T. and Fuchs, E. (2007). Desmoplakin: an unexpected regulator of microtubule organization in the epidermis. *J Cell Biol* **176**, 147-54.

Lee, S., Harris, K. L., Whitington, P. M. and Kolodziej, P. A. (2000). short stop is allelic to kakapo, and encodes rod-like cytoskeletal-associated proteins required for axon extension. *J Neurosci* **20**, 1096-108.

Lee, S. and Kolodziej, P. A. (2002). The plakin Short Stop and the RhoA GTPase are required for E-cadherin-dependent apical surface remodeling during tracheal tube fusion. *Development* **129**, 1509-20.

Lee S, K. P. A. (2002). Short stop provides an essential link between F-actin and microtubules during axon extension. *Development* **129**, 1195-1204.

Leone, D. P., Genoud, S., Atanasoski, S., Grausenburger, R., Berger, P., Metzger, D., Macklin, W. B., Chambon, P. and Suter, U. (2003). Tamoxifen-inducible glia-specific Cre mice for somatic mutagenesis in oligodendrocytes and Schwann cells. *Mol Cell Neurosci* **22**, 430-40.

Leung, C. L., Green, K. J. and Liem, R. K. (2002). Plakins: a family of versatile cytolinker proteins. *Trends Cell Biol* **12**, 37-45.

Lewis, L., Barrandon, Y., Green, H. and Albrecht-Buehler, G. (1987). The reorganization of microtubules and microfilaments in differentiating keratinocytes. *Differentiation* **36**, 228-33.

Li, R., Messing, A., Goldman, J. E. and Brenner, M. (2002a). GFAP mutations in Alexander disease. *Int J Dev Neurosci* **20**, 259-68.

Li, S. S. (2005). Specificity and versatility of SH3 and other proline-recognition domains: structural basis and implications for cellular signal transduction. *Biochem J* **390**, 641-53.

Li, W., Henry, G., Fan, J., Bandyopadhyay, B., Pang, K., Garner, W., Chen, M. and Woodley, D. T. (2004). Signals that initiate, augment, and provide directionality for human keratinocyte motility. *J Invest Dermatol* **123**, 622-33.

Li, W., Nadelman, C., Gratch, N. S., Li, W., Chen, M., Kasahara, N. and Woodley, D. T. (2002b). An important role for protein kinase C-delta in human keratinocyte migration on dermal collagen. *Exp Cell Res* **273**, 219-28.

Liao, J. and Omary, M. B. (1996). 14-3-3 proteins associate with phosphorylated simple epithelial keratins during cell cycle progression and act as a solubility cofactor. *J Cell Biol* **133**, 345-57.

Litjens, S. H., de Pereda, J. M. and Sonnenberg, A. (2006). Current insights into the formation and breakdown of hemidesmosomes. *Trends Cell Biol* **16**, 376-83.

Litjens, S. H., Koster, J., Kuikman, I., van Wilpe, S., de Pereda, J. M. and Sonnenberg, A. (2003). Specificity of binding of the plectin actin-binding domain to beta4 integrin. *Mol Biol Cell* **14**, 4039-50.

Litjens, S. H., Wilhelmsen, K., de Pereda, J. M., Perrakis, A. and Sonnenberg, A. (2005). Modeling and experimental validation of the binary complex of the plectin actin-binding domain and the first pair of fibronectin type III (FNIII) domains of the beta4 integrin. *J Biol Chem* **280**, 22270-7.

Liu, C. G., Maercker, C., Castanon, M. J., Hauptmann, R. and Wiche, G. (1996). Human plectin: organization of the gene, sequence analysis, and chromosome localization (8q24). *Proc Natl Acad Sci U S A* **93**, 4278-83.

Lloyd, C., Yu, Q. C., Cheng, J., Turksen, K., Degenstein, L., Hutton, E. and Fuchs, E. (1995). The basal keratin network of stratified squamous epithelia: defining K15 function in the absence of K14. *J Cell Biol* **129**, 1329-44.

Long, H. A., Boczonadi, V., McInroy, L., Goldberg, M. and Maatta, A. (2006). Periplakin-dependent re-organisation of keratin cytoskeleton and loss of collective migration in keratin-8-downregulated epithelial sheets. *J Cell Sci* **119**, 5147-59.

Lopez-Rovira, T., Silva-Vargas, V. and Watt, F. M. (2005). Different consequences of beta1 integrin deletion in neonatal and adult mouse epidermis reveal a context-dependent role of integrins in regulating proliferation, differentiation, and intercellular communication. *J Invest Dermatol* **125**, 1215-27.

Lotz, M. M., Rabinovitz, I. and Mercurio, A. M. (2000). Intestinal restitution: progression of actin cytoskeleton rearrangements and integrin function in a model of epithelial wound healing. *Am J Pathol* **156**, 985-96.

Lu, H., Chen, J., Planko, L., Zigrino, P., Klein-Hitpass, L. and Magin, T. M. (2007). Induction of Inflammatory Cytokines by a Keratin Mutation and their Repression by a Small Molecule in a Mouse Model for EBS. *J Invest Dermatol*.

Lu, H., Hesse, M., Peters, B. and Magin, T. M. (2005). Type II keratins precede type I keratins during early embryonic development. *Eur J Cell Biol* **84**, 709-18.

Lunter, P. C. and Wiche, G. (2002). Direct binding of plectin to Fer kinase and negative regulation of its catalytic activity. *Biochem Biophys Res Commun* **296**, 904-10.

Mahrle, G., Schulze, H. J., Kuhn, A. and Wevers, A. (1989). Immunostaining of keratin and vimentin in epidermis: comparison of different post-embedding immunogold techniques for electron microscopy. *J Histochem Cytochem* **37**, 863-8.

Mainiero, F., Murgia, C., Wary, K. K., Curatola, A. M., Pepe, A., Blumemberg, M., Westwick, J. K., Der, C. J. and Giancotti, F. G. (1997). The coupling of alpha6beta4 integrin to Ras-MAP kinase pathways mediated by Shc controls keratinocyte proliferation. *Embo J* **16**, 2365-75.

Mainiero, F., Pepe, A., Wary, K. K., Spinardi, L., Mohammadi, M., Schlessinger, J. and Giancotti, F. G. (1995). Signal transduction by the alpha 6 beta 4 integrin: distinct beta 4 subunit sites mediate recruitment of Shc/Grb2 and association with the cytoskeleton of hemidesmosomes. *Embo J* **14**, 4470-81.

Malecz, N., Foisner, R., Stadler, C. and Wiche, G. (1996). Identification of plectin as a substrate of p34cdc2 kinase and mapping of a single phosphorylation site. *J Biol Chem* **271**, 8203-8.

Mansbridge, J. N. and Knapp, A. M. (1987). Changes in keratinocyte maturation during wound healing. *J Invest Dermatol* **89**, 253-63.

Mariotti, A., Kedeshian, P. A., Dans, M., Curatola, A. M., Gagnoux-Palacios, L. and Giancotti, F. G. (2001). EGF-R signaling through Fyn kinase disrupts the function of integrin alpha6beta4 at hemidesmosomes: role in epithelial cell migration and carcinoma invasion. *J Cell Biol* **155**, 447-58.

Martin, P. (1997). Wound healing--aiming for perfect skin regeneration. *Science* **276**, 75-81.

Matsubayashi, Y., Ebisuya, M., Honjoh, S. and Nishida, E. (2004). ERK activation propagates in epithelial cell sheets and regulates their migration during wound healing. *Curr Biol* **14**, 731-5.

McGrath, J. A., McMillan, J. R., Shemanko, C. S., Runswick, S. K., Leigh, I. M., Lane, E. B., Garrod, D. R. and Eady, R. A. (1997). Mutations in the plakophilin 1 gene result in ectodermal dysplasia/skin fragility syndrome. *Nat Genet* **17**, 240-4.

McKoy, G., Protonotarios, N., Crosby, A., Tsatsopoulou, A., Anastasakis, A., Coonar, A., Norman, M., Baboonian, C., Jeffery, S. and McKenna, W. J. (2000). Identification of a deletion in plakoglobin in arrhythmogenic right ventricular cardiomyopathy with palmoplantar keratoderma and woolly hair (Naxos disease). *Lancet* **355**, 2119-24.

McLean, G. W., Komiyama, N. H., Serrels, B., Asano, H., Reynolds, L., Conti, F., Hodivala-Dilke, K., Metzger, D., Chambon, P., Grant, S. G. et al. (2004). Specific deletion of focal adhesion kinase suppresses tumor formation and blocks malignant progression. *Genes Dev* **18**, 2998-3003.

McLean, W. H., Pulkkinen, L., Smith, F. J., Rugg, E. L., Lane, E. B., Bullrich, F., Burgeson, R. E., Amano, S., Hudson, D. L., Owaribe, K. et al. (1996). Loss of plectin causes epidermolysis bullosa with muscular dystrophy: cDNA cloning and genomic organization. *Genes Dev* **10**, 1724-35.

McMillan, J. R., McGrath, J. A., Tidman, M. J. and Eady, R. A. (1998). Hemidesmosomes show abnormal association with the keratin filament network in junctional forms of epidermolysis bullosa. *J Invest Dermatol* **110**, 132-7.

Menon, G. K. (2002). New insights into skin structure: scratching the surface. *Adv Drug Deliv Rev* **54 Suppl 1**, S3-17.

Merdek, K. D., Yang, X., Taglienti, C. A., Shaw, L. M. and Mercurio, A. M. (2007). Intrinsic signaling functions of the beta 4 integrin intracellular domain. *J Biol Chem*.

Metzger, D. and Chambon, P. (2001). Site- and time-specific gene targeting in the mouse. *Methods* **24**, 71-80.

Metzger, D., Clifford, J., Chiba, H. and Chambon, P. (1995). Conditional site-specific recombination in mammalian cells using a ligand-dependent chimeric Cre recombinase. *Proc Natl Acad Sci U S A* **92**, 6991-5.

Michel, S., Schmidt, R., Shroot, B. and Reichert, U. (1988). Morphological and biochemical characterization of the cornified envelopes from human epidermal keratinocytes of different origin. *J Invest Dermatol* **91**, 11-5.

Miranti, C. K., Ohno, S. and Brugge, J. S. (1999). Protein kinase C regulates integrin-induced activation of the extracellular regulated kinase pathway upstream of Shc. *J Biol Chem* **274**, 10571-81.

Misra, R. P. and Duncan, S. A. (2002). Gene targeting in the mouse: advances in introduction of transgenes into the genome by homologous recombination. *Endocrine* **19**, 229-38.

Montezin, M., Simon, M., Guerrin, M. and Serre, G. (1997). Corneodesmosin, a corneodesmosome-specific basic protein, is expressed in the cornified epithelia of the pig, guinea pig, rat, and mouse. *Exp Cell Res* **231**, 132-40.

Morley, S. M., D'Alessandro, M., Sexton, C., Rugg, E. L., Navsaria, H., Shemanko, C. S., Huber, M., Hohl, D., Heagerty, A. I., Leigh, I. M. et al. (2003). Generation and characterization of epidermolysis bullosa simplex cell lines: scratch assays show faster migration with disruptive keratin mutations. *Br J Dermatol* **149**, 46-58.

Morrison, E. E. (2007). Action and interactions at microtubule ends. *Cell Mol Life Sci* **64**, 307-17.

Muller, M. B. and Keck, M. E. (2002). Genetically engineered mice for studies of stress-related clinical conditions. *J Psychiatr Res* **36**, 53-76.

Nedrelow, J. H., Cianci, C. D. and Morrow, J. S. (2003). c-Src binds alpha II spectrin's Src homology 3 (SH3) domain and blocks calpain susceptibility by phosphorylating Tyr1176. *J Biol Chem* **278**, 7735-41.

Nguyen, B. P., Gil, S. G. and Carter, W. G. (2000a). Deposition of laminin 5 by keratinocytes regulates integrin adhesion and signaling. *J Biol Chem* **275**, 31896-907.

Nguyen, B. P., Ren, X. D., Schwartz, M. A. and Carter, W. G. (2001). Ligation of integrin alpha 3beta 1 by laminin 5 at the wound edge activates Rho-dependent adhesion of leading keratinocytes on collagen. *J Biol Chem* **276**, 43860-70.

Nguyen, B. P., Ryan, M. C., Gil, S. G. and Carter, W. G. (2000b). Deposition of laminin 5 in epidermal wounds regulates integrin signaling and adhesion. *Curr Opin Cell Biol* **12**, 554-62.

Nievers, M. G., Kuikman, I., Geerts, D., Leigh, I. M. and Sonnenberg, A. (2000). Formation of hemidesmosome-like structures in the absence of ligand binding by the (alpha)6(beta)4 integrin requires binding of HD1/plectin to the cytoplasmic domain of the (beta)4 integrin subunit. *J Cell Sci* **113 (Pt 6)**, 963-73.

Nikolic, B., Mac Nulty, E., Mir, B. and Wiche, G. (1996). Basic amino acid residue cluster within nuclear targeting sequence motif is essential for cytoplasmic plectin-vimentin network junctions. *J. Cell Biol.* **134**, 1455-1467.

Norgett, E. E., Hatsell, S. J., Carvajal-Huerta, L., Cabezas, J. C., Common, J., Purkis, P. E., Whittock, N., Leigh, I. M., Stevens, H. P. and Kelsell, D. P. (2000). Recessive mutation in desmoplakin disrupts desmoplakin-intermediate filament interactions and causes dilated cardiomyopathy, woolly hair and keratoderma. *Hum Mol Genet* **9**, 2761-6.

O'Keefe, E. J., Briggaman, R. A. and Herman, B. (1987). Calcium-induced assembly of adherens junctions in keratinocytes. *J Cell Biol* **105**, 807-17.

O'Toole, E. A. (2001). Extracellular matrix and keratinocyte migration. *Clin Exp Dermatol* **26**, 525-30.

Odland, G. and Ross, R. (1968). Human wound repair. I. Epidermal regeneration. *J Cell Biol* **39**, 135-51.

Omary, M. B., Coulombe, P. A. and McLean, W. H. (2004). Intermediate filament proteins and their associated diseases. *N Engl J Med* **351**, 2087-100.

Omary, M. B., Ku, N. O. and Toivola, D. M. (2002). Keratins: guardians of the liver. *Hepatology* **35**, 251-7.

Ono, S. (2007). Mechanism of depolymerization and severing of actin filaments and its significance in cytoskeletal dynamics. *Int Rev Cytol* **258**, 1-82.

Osmanagic-Myers, S., Gregor, M., Walko, G., Burgstaller, G., Reipert, S. and Wiche, G. (2006). Plectin-controlled keratin cytoarchitecture affects MAP kinases involved in cellular stress response and migration. *J Cell Biol* **174**, 557-68.

Osmanagic-Myers, S. and Wiche, G. (2004). Plectin-RACK1 (receptor for activated C kinase 1) scaffolding: a novel mechanism to regulate protein kinase C activity. *J Biol Chem* **279**, 18701-10.

Owens, D. M., Romero, M. R., Gardner, C. and Watt, F. M. (2003). Suprabasal alpha6beta4 integrin expression in epidermis results in enhanced tumourigenesis and disruption of TGFbeta signalling. *J Cell Sci* **116**, 3783-91.

Paladini, R. D., Takahashi, K., Bravo, N. S. and Coulombe, P. A. (1996). Onset of re-epithelialization after skin injury correlates with a reorganization of keratin filaments in wound edge keratinocytes: defining a potential role for keratin 16. *J Cell Biol* **132**, 381-97.

Pankow, S., Bamberger, C., Klippel, A. and Werner, S. (2006). Regulation of epidermal homeostasis and repair by phosphoinositide 3-kinase. *J Cell Sci* **119**, 4033-46.

Pei, X. F., Leigh, I. M. and Watt, F. M. (1992). Changes in type I keratin expression associated with HPV16 transformation of human epidermal keratinocytes. *Epithelial Cell Biol* **1**, 84-9.

Pekny, M. and Lane, E. B. (2007). Intermediate filaments and stress. *Exp Cell Res* **313**, 2244-54.

Peters, B., Kirfel, J., Bussow, H., Vidal, M. and Magin, T. M. (2001). Complete cytolysis and neonatal lethality in keratin 5 knockout mice reveal its fundamental role in skin integrity and in epidermolysis bullosa simplex. *Mol Biol Cell* **12**, 1775-89.

Pfendner, E., Rouan, F. and Uitto, J. (2005). Progress in epidermolysis bullosa: the phenotypic spectrum of plectin mutations. *Exp Dermatol* **14**, 241-9.

Pfendner, E. and Uitto, J. (2005). Plectin gene mutations can cause epidermolysis bullosa with pyloric atresia. *J Invest Dermatol* **124**, 111-5.

Pollard, T. D. and Borisy, G. G. (2003). Cellular motility driven by assembly and disassembly of actin filaments. *Cell* **112**, 453-65.

Pulkkinen, L., Smith, F. J., Shimizu, H., Murata, S., Yaoita, H., Hachisuka, H., Nishikawa, T., McLean, W. H. and Uitto, J. (1996). Homozygous deletion mutations in the plectin gene (PLEC1) in patients with epidermolysis bullosa simplex associated with late-onset muscular dystrophy. *Hum Mol Genet* **5**, 1539-46.

Pulkkinen, L. and Uitto, J. (1999). Mutation analysis and molecular genetics of epidermolysis bullosa. *Matrix Biol* **18**, 29-42.

Pytela, R. and Wiche, G. (1980). High molecular weight polypeptides (270,000-340,000) from cultured cells are related to hog brain microtubule-associated proteins but copurify with intermediate filaments. *Proc Natl Acad Sci U S A* **77**, 4808-12.

Rabinovitz, I. and Mercurio, A. M. (1997). The integrin alpha6beta4 functions in carcinoma cell migration on laminin-1 by mediating the formation and stabilization of actin-containing motility structures. *J Cell Biol* **139**, 1873-84.

Rabinovitz, I., Toker, A. and Mercurio, A. M. (1999). Protein kinase C-dependent mobilization of the alpha6beta4 integrin from hemidesmosomes and its association with actin-rich cell protrusions drive the chemotactic migration of carcinoma cells. *J Cell Biol* **146**, 1147-60.

Rabinovitz, I., Tsomo, L. and Mercurio, A. M. (2004). Protein kinase C-alpha phosphorylation of specific serines in the connecting segment of the beta 4 integrin regulates the dynamics of type II hemidesmosomes. *Mol Cell Biol* **24**, 4351-60.

Raymond, K., Kreft, M., Janssen, H., Calafat, J. and Sonnenberg, A. (2005). Keratinocytes display normal proliferation, survival and differentiation in conditional beta4-integrin knockout mice. *J Cell Sci* **118**, 1045-60.

Raymond, K., Kreft, M., Song, J. Y., Janssen, H. and Sonnenberg, A. (2007). Dual Role of {alpha}6{beta}4 Integrin in Epidermal Tumor Growth: Tumor-suppressive Versus Tumor-promoting Function. *Mol Biol Cell*.

Reipert, S., Fischer, I. and Wiche, G. (2004). High-pressure cryoimmobilization of murine skin reveals novel structural features and prevents extraction artifacts. *Exp Dermatol* **13**, 419-25.

Reipert, S., Steinböck, F., Fischer, I., Bittner, R. E., Zeöld, A. and Wiche, G. (1999). Association of mitochondria with plectin and desmin intermediate filaments in striated muscle. *Exp. Cell Res.* **252**, 479-491.

Revenu, C., Athman, R., Robine, S. and Louvard, D. (2004). The co-workers of actin filaments: from cell structures to signals. *Nat Rev Mol Cell Biol* **5**, 635-46.

Rezniczek, G. A., Abrahamsberg, C., Fuchs, P., Spazierer, D. and Wiche, G. (2003). Plectin 5'-transcript diversity: short alternative sequences determine stability of gene

products, initiation of translation and subcellular localization of isoforms. *Hum Mol Genet.* **12**, 3181-3194.

Rezniczek, G. A., de Pereda, J. M., Reipert, S. and Wiche, G. (1998). Linking integrin alpha6beta4-based cell adhesion to the intermediate filament cytoskeleton: direct interaction between the beta4 subunit and plectin at multiple molecular sites. *J Cell Biol* **141**, 209-25.

Rossen, K., Dahlstrom, K. K., Mercurio, A. M. and Wewer, U. M. (1994). Expression of the alpha 6 beta 4 integrin by squamous cell carcinomas and basal cell carcinomas: possible relation to invasive potential? *Acta Derm Venereol* **74**, 101-5.

Ruhrberg, C., Hajibagheri, M. A., Simon, M., Dooley, T. P. and Watt, F. M. (1996). Envoplakin, a novel precursor of the cornified envelope that has homology to desmoplakin. *J Cell Biol* **134**, 715-29.

Russell, D., Andrews, P. D., James, J. and Lane, E. B. (2004). Mechanical stress induces profound remodelling of keratin filaments and cell junctions in epidermolysis bullosa simplex keratinocytes. *J Cell Sci* **117**, 5233-43.

Sadowski, T., Dietrich, S., Koschinsky, F., Ludwig, A., Proksch, E., Titz, B. and Sedlacek, R. (2005). Matrix metalloproteinase 19 processes the laminin 5 gamma 2 chain and induces epithelial cell migration. *Cell Mol Life Sci* **62**, 870-80.

Santoro, M. M. and Gaudino, G. (2005). Cellular and molecular facets of keratinocyte reepithelization during wound healing. *Exp Cell Res* **304**, 274-86.

Santoro, M. M., Gaudino, G. and Marchisio, P. C. (2003). The MSP receptor regulates alpha6beta4 and alpha3beta1 integrins via 14-3-3 proteins in keratinocyte migration. *Dev Cell* **5**, 257-71.

Sato, H., Nagai, T., Kuppuswamy, D., Narishige, T., Koide, M., Menick, D. R. and Cooper, G. t. (1997). Microtubule stabilization in pressure overload cardiac hypertrophy. *J Cell Biol* **139**, 963-73.

Sauer, B. (1996). Multiplex Cre/lox recombination permits selective site-specific DNA targeting to both a natural and an engineered site in the yeast genome. *Nucleic Acids Res* **24**, 4608-13.

Sauer, B. (1998). Inducible gene targeting in mice using the Cre/lox system. *Methods* **14**, 381-92.

Sauer, B. and Henderson, N. (1989). Cre-stimulated recombination at loxP-containing DNA sequences placed into the mammalian genome. *Nucleic Acids Res* **17**, 147-61.

Schaapveld, R. Q., Borradori, L., Geerts, D., van Leusden, M. R., Kuikman, I., Nievers, M. G., Niessen, C. M., Steenbergen, R. D., Snijders, P. J. and Sonnenberg, A. (1998). Hemidesmosome formation is initiated by the beta4 integrin subunit, requires complex formation of beta4 and HD1/plectin, and involves a direct interaction between beta4 and the bullous pemphigoid antigen 180. *J Cell Biol* **142**, 271-84.

Schara, U., Tucke, J., Mortier, W., Nusslein, T., Rouan, F., Pfendner, E., Zillikens, D., Bruckner-Tuderman, L., Uitto, J., Wiche, G. et al. (2004). Severe mucous membrane involvement in epidermolysis bullosa simplex with muscular dystrophy due to a novel plectin gene mutation. *Eur J Pediatr* **163**, 218-22.

Schlaepfer, D. D., Broome, M. A. and Hunter, T. (1997). Fibronectin-stimulated signaling from a focal adhesion kinase-c-Src complex: involvement of the Grb2, p130cas, and Nck adaptor proteins. *Mol Cell Biol* **17**, 1702-13.

Schluter, C., Duchrow, M., Wohlenberg, C., Becker, M. H., Key, G., Flad, H. D. and Gerdes, J. (1993). The cell proliferation-associated antigen of antibody Ki-67: a very large, ubiquitous nuclear protein with numerous repeated elements, representing a new kind of cell cycle-maintaining proteins. *J Cell Biol* **123**, 513-22.

Schober, M., Raghavan, S., Nikolova, M., Polak, L., Pasolli, H. A., Beggs, H. E., Reichardt, L. F. and Fuchs, E. (2007). Focal adhesion kinase modulates tension signaling to control actin and focal adhesion dynamics. *J Cell Biol* **176**, 667-80.

Schoch, K. G., Lori, A., Burns, K. A., Eldred, T., Olsen, J. C. and Randell, S. H. (2004). A subset of mouse tracheal epithelial basal cells generates large colonies in vitro. *Am J Physiol Lung Cell Mol Physiol* **286**, L631-42.

Schwenk, F., Kuhn, R., Angrand, P. O., Rajewsky, K. and Stewart, A. F. (1998). Temporally and spatially regulated somatic mutagenesis in mice. *Nucleic Acids Res* **26**, 1427-32.

Sedman, S. A., Hubbert, N. L., Vass, W. C., Lowy, D. R. and Schiller, J. T. (1992). Mutant p53 can substitute for human papillomavirus type 16 E6 in immortalization of human keratinocytes but does not have E6-associated trans-activation or transforming activity. *J Virol* **66**, 4201-8.

Sehgal, B. U., DeBiase, P. J., Matzno, S., Chew, T. L., Claiborne, J. N., Hopkinson, S. B., Russell, A., Marinkovich, M. P. and Jones, J. C. (2006). Integrin beta4 regulates migratory behavior of keratinocytes by determining laminin-332 organization. *J Biol Chem* **281**, 35487-98.

Seifert, G. J., Lawson, D. and Wiche, G. (1992). Immunolocalization of the intermediate filament-associated protein plectin at focal contacts and actin stress fibers. *Eur J Cell Biol* **59**, 138-47.

Sevcik, J., Urbanikova, L., Kost'an, J., Janda, L. and Wiche, G. (2004). Actin-binding domain of mouse plectin. Crystal structure and binding to vimentin. *Eur J Biochem* **271**, 1873-84.

Shah, K. and Vincent, F. (2005). Divergent roles of c-Src in controlling platelet-derived growth factor-dependent signaling in fibroblasts. *Mol Biol Cell* **16**, 5418-32.

Skalli, O., Jones, J. C., Gagescu, R. and Goldman, R. D. (1994). IFAP 300 is common to desmosomes and hemidesmosomes and is a possible linker of intermediate filaments to these junctions. *J Cell Biol* **125**, 159-70.

Slep, K. C., Rogers, S. L., Elliott, S. L., Ohkura, H., Kolodziej, P. A. and Vale, R. D. (2005). Structural determinants for EB1-mediated recruitment of APC and spectraplakins to the microtubule plus end. *J Cell Biol* **168**, 587-98.

Small, J. V. (1994). Lamellipodia architecture: actin filament turnover and the lateral flow of actin filaments during motility. *Semin Cell Biol* **5**, 157-63.

Small, J. V., Stradal, T., Vignal, E. and Rottner, K. (2002). The lamellipodium: where motility begins. *Trends Cell Biol* **12**, 112-20.

Smith, F. J., Eady, R. A., Leigh, I. M., McMillan, J. R., Rugg, E. L., Kelsell, D. P., Bryant, S. P., Spurr, N. K., Geddes, J. F., Kirtschig, G. et al. (1996). Plectin deficiency results in muscular dystrophy with epidermolysis bullosa. *Nat Genet* **13**, 450-7.

Sonnenberg, A. and Liem, R. K. (2007). Plakins in development and disease. *Exp Cell Res* **313**, 2189-203.

Sonnenberg, A., Rojas, A. M. and de Pereda, J. M. (2007). The structure of a tandem pair of spectrin repeats of plectin reveals a modular organization of the plakin domain. *J Mol Biol* **368**, 1379-91.

South, A. P., Wan, H., Stone, M. G., Dopping-Hepenstal, P. J., Purkis, P. E., Marshall, J. F., Leigh, I. M., Eady, R. A., Hart, I. R. and McGrath, J. A. (2003). Lack of plakophilin 1 increases keratinocyte migration and reduces desmosome stability. *J Cell Sci* **116**, 3303-14.

Spazierer, D., Fuchs, P., Proll, V., Janda, L., Oehler, S., Fischer, I., Hauptmann, R. and Wiche, G. (2003). Epiplakin gene analysis in mouse reveals a single exon encoding a 725-kDa protein with expression restricted to epithelial tissues. *J Biol Chem* **278**, 31657-66.

Steinberg, M. L. and Defendi, V. (1983). Transformation and immortalization of human keratinocytes by SV40. *J Invest Dermatol* **81**, 131s-6s.

Steinbock, F. A., Nikolic, B., Coulombe, P. A., Fuchs, E., Traub, P. and Wiche, G. (2000). Dose-dependent linkage, assembly inhibition and disassembly of vimentin and cytokeratin 5/14 filaments through plectin's intermediate filament-binding domain. *J Cell Sci* **113 (Pt 3)**, 483-91.

Steinert, P. M. and Marekov, L. N. (1995). The proteins elafin, filaggrin, keratin intermediate filaments, loricrin, and small proline-rich proteins 1 and 2 are isodipeptide cross-linked components of the human epidermal cornified cell envelope. *J Biol Chem* **270**, 17702-11.

Sternberg, N., Sauer, B., Hoess, R. and Abremski, K. (1986). Bacteriophage P1 cre gene and its regulatory region. Evidence for multiple promoters and for regulation by DNA methylation. *J Mol Biol* **187**, 197-212.

Stratis, A., Pasparakis, M., Markur, D., Knaup, R., Pofahl, R., Metzger, D., Chambon, P., Krieg, T. and Haase, I. (2006). Localized inflammatory skin disease following inducible ablation of I kappa B kinase 2 in murine epidermis. *J Invest Dermatol* **126**, 614-20.

Sun, D., Leung, C. L. and Liem, R. K. (2001). Characterization of the microtubule binding domain of microtubule actin crosslinking factor (MACF): identification of a novel group of microtubule associated proteins. *J Cell Sci* **114**, 161-172.

Svitkina, T. M., Verkhovsky, A. B. and Borisy, G. G. (1996). Plectin sidearms mediate interaction of intermediate filaments with microtubules and other components of the cytoskeleton. *J Cell Biol* **135**, 991-1007.

Swensson, O., Langbein, L., McMillan, J. R., Stevens, H. P., Leigh, I. M., McLean, W. H., Lane, E. B. and Eady, R. A. (1998). Specialized keratin expression pattern in human ridged skin as an adaptation to high physical stress. *Br J Dermatol* **139**, 767-75.

Taki, M., Kamata, N., Yokoyama, K., Fujimoto, R., Tsutsumi, S. and Nagayama, M. (2003). Down-regulation of Wnt-4 and up-regulation of Wnt-5a expression by epithelial-mesenchymal transition in human squamous carcinoma cells. *Cancer Sci* **94**, 593-7.

Tarutani, M., Itami, S., Okabe, M., Ikawa, M., Tezuka, T., Yoshikawa, K., Kinoshita, T. and Takeda, J. (1997). Tissue-specific knockout of the mouse Pig-a gene reveals important roles for GPI-anchored proteins in skin development. *Proc Natl Acad Sci U S A* **94**, 7400-5.

Tehrani, S., Tomasevic, N., Weed, S., Sakowicz, R. and Cooper, J. A. (2007). Src phosphorylation of cortactin enhances actin assembly. *Proc Natl Acad Sci U S A* **104**, 11933-8.

Tennenbaum, T., Li, L., Belanger, A. J., De Luca, L. M. and Yuspa, S. H. (1996). Selective changes in laminin adhesion and alpha 6 beta 4 integrin regulation are associated with the initial steps in keratinocyte maturation. *Cell Growth Differ* **7**, 615-28.

Tian, R., Gregor, M., Wiche, G. and Goldman, J. E. (2006). Plectin regulates the organization of glial fibrillary acidic protein in Alexander disease. *Am J Pathol* **168**, 888-97.

Tilghman, R. W., Slack-Davis, J. K., Sergina, N., Martin, K. H., Iwanicki, M., Hershey, E. D., Beggs, H. E., Reichardt, L. F. and Parsons, J. T. (2005). Focal adhesion kinase is required for the spatial organization of the leading edge in migrating cells. *J Cell Sci* **118**, 2613-23.

Toivola, D. M., Tao, G. Z., Habtezion, A., Liao, J. and Omary, M. B. (2005). Cellular integrity plus: organelle-related and protein-targeting functions of intermediate filaments. *Trends Cell Biol* **15**, 608-17.

Tran, N. H. and Frost, J. A. (2003). Phosphorylation of Raf-1 by p21-activated kinase 1 and Src regulates Raf-1 autoinhibition. *J Biol Chem* **278**, 11221-6.

Troy, T. C. and Turksen, K. (1999). In vitro characteristics of early epidermal progenitors isolated from keratin 14 (K14)-deficient mice: insights into the role of keratin 17 in mouse keratinocytes. *J Cell Physiol* **180**, 409-21.

Trusolino, L., Bertotti, A. and Comoglio, P. M. (2001). A signaling adapter function for alpha6beta4 integrin in the control of HGF-dependent invasive growth. *Cell* **107**, 643-54.

Tscharntke, M., Pofahl, R., Chrostek-Grashoff, A., Smyth, N., Niessen, C., Niemann, C., Hartwig, B., Herzog, V., Klein, H. W., Krieg, T. et al. (2007). Impaired epidermal wound healing in vivo upon inhibition or deletion of Rac1. *J Cell Sci* **120**, 1480-90.

Tsuruta, D., Hopkinson, S. B. and Jones, J. C. (2003). Hemidesmosome protein dynamics in live epithelial cells. *Cell Motil Cytoskeleton* **54**, 122-34.

Uitto, J., Richard, G. and McGrath, J. A. (2007). Diseases of epidermal keratins and their linker proteins. *Exp Cell Res* **313**, 1995-2009.

Vaezi, A., Bauer, C., Vasioukhin, V. and Fuchs, E. (2002). Actin cable dynamics and Rho/Rock orchestrate a polarized cytoskeletal architecture in the early steps of assembling a stratified epithelium. *Dev Cell* **3**, 367-81.

Van Aelst, L. and D'Souza-Schorey, C. (1997). Rho GTPases and signaling networks. *Genes Dev* **11**, 2295-322.

Vasioukhin, V., Bauer, C., Yin, M. and Fuchs, E. (2000). Directed actin polymerization is the driving force for epithelial cell-cell adhesion. *Cell* **100**, 209-19.

Vasioukhin, V., Degenstein, L., Wise, B. and Fuchs, E. (1999). The magical touch: genome targeting in epidermal stem cells induced by tamoxifen application to mouse skin. *Proc Natl Acad Sci U S A* **96**, 8551-6.

Vooijs, M., Jonkers, J. and Berns, A. (2001). A highly efficient ligand-regulated Cre recombinase mouse line shows that LoxP recombination is position dependent. *EMBO Rep* **2**, 292-7.

Walko, G. (2002). Plectin 1a and 1c: cellular expression, subcellular localization and signaling functions: University of Vienna.

Watt, F. M., Mattey, D. L. and Garrod, D. R. (1984). Calcium-induced reorganization of desmosomal components in cultured human keratinocytes. *J Cell Biol* **99**, 2211-5.

Werner, S. and Grose, R. (2003). Regulation of wound healing by growth factors and cytokines. *Physiol Rev* **83**, 835-70.

Whittock, N. V., Wan, H., Morley, S. M., Garzon, M. C., Kristal, L., Hyde, P., McLean, W. H., Pulkkinen, L., Uitto, J., Christiano, A. M. et al. (2002). Compound heterozygosity for non-sense and mis-sense mutations in desmoplakin underlies skin fragility/woolly hair syndrome. *J Invest Dermatol* **118**, 232-8.

Wiche, G. (1989). Plectin: general overview and appraisal of its potential role as a subunit protein of the cytomatrix. *Crit. Rev. Biochem. Mol. Biol.* **24**, 41-67.

Wiche, G. (1998). Role of plectin in cytoskeleton organization and dynamics. *J Cell Sci* **111 (Pt 17)**, 2477-86.

Wiche, G., Becker, B., Luber, K., Weitzer, G., Castañón, M. J., Hauptmann, R., Stratowa, C. and Stewart, M. (1991). Cloning and sequencing of rat plectin indicates a 466-kD polypeptide chain with a three-domain structure based on a central alpha-helical coiled coil. *J. Cell Biol.* **114**, 83-99.

Wiche, G., Krepler, R., Artlieb, U., Pytela, R. and Aberer, W. (1984). Identification of plectin in different human cell types and immunolocalization at epithelial basal cell surface membranes. *Exp. Cell Res.* **155**, 43-49.

Wiche, G., Krepler, R., Artlieb, U., Pytela, R. and Denk, H. (1983). Occurrence and immunolocalization of plectin in tissues. *J Cell Biol* **97**, 887-901.

Wilding, J., Vousden, K. H., Soutter, W. P., McCrea, P. D., Del Buono, R. and Pignatelli, M. (1996). E-cadherin transfection down-regulates the epidermal growth factor receptor and reverses the invasive phenotype of human papilloma virus-transfected keratinocytes. *Cancer Res* **56**, 5285-92.

Wilhelmsen, K., Litjens, S. H., Kuikman, I., Margadant, C., van Rheenen, J. and Sonnenberg, A. (2007). Serine Phosphorylation of the Integrin beta4 Subunit Is Necessary for Epidermal Growth Factor Receptor induced Hemidesmosome Disruption. *Mol Biol Cell* **18**, 3512-22.

Wilhelmsen, K., Litjens, S. H., Kuikman, I., Tshimbalanga, N., Janssen, H., van den Bout, I., Raymond, K. and Sonnenberg, A. (2005). Nesprin-3, a novel outer nuclear membrane protein, associates with the cytoskeletal linker protein plectin. *J Cell Biol* **171**, 799-810.

Windoffer, R., Kolsch, A., Woll, S. and Leube, R. E. (2006). Focal adhesions are hotspots for keratin filament precursor formation. *J Cell Biol* **173**, 341-8.

Windoffer, R. and Leube, R. E. (1999). Detection of cytokeratin dynamics by time-lapse fluorescence microscopy in living cells. *J Cell Sci* **112 (Pt 24)**, 4521-34.

Windoffer, R. and Leube, R. E. (2004). Imaging of keratin dynamics during the cell cycle and in response to phosphatase inhibition. *Methods Cell Biol* **78**, 321-52.

Windoffer, R., Woll, S., Strnad, P. and Leube, R. E. (2004). Identification of novel principles of keratin filament network turnover in living cells. *Mol Biol Cell* **15**, 2436-48.

Witkowski, C. M., Bowden, G. T., Nagle, R. B. and Cress, A. E. (2000). Altered surface expression and increased turnover of the alpha6beta4 integrin in an undifferentiated carcinoma. *Carcinogenesis* **21**, 325-30.

Woll, S., Windoffer, R. and Leube, R. E. (2005). Dissection of keratin dynamics: different contributions of the actin and microtubule systems. *Eur J Cell Biol* **84**, 311-28.

Wong, P., Colucci-Guyon, E., Takahashi, K., Gu, C., Babinet, C. and Coulombe, P. A. (2000). Introducing a null mutation in the mouse K6alpha and K6beta genes reveals their essential structural role in the oral mucosa. *J Cell Biol* **150**, 921-8.

Wong, P. and Coulombe, P. A. (2003). Loss of keratin 6 (K6) proteins reveals a function for intermediate filaments during wound repair. *J Cell Biol* **163**, 327-37.

Wood, W. and Martin, P. (2002). Structures in focus--filopodia. *Int J Biochem Cell Biol* **34**, 726-30.

Yamada, T., Aoyama, Y., Owada, M. K., Kawakatsu, H. and Kitajima, Y. (2000). Scraped-wounding causes activation and association of C-Src tyrosine kinase with microtubules in cultured keratinocytes. *Cell Struct Funct* **25**, 351-9.

Yang, Y., Bauer, C., Strasser, G., Wollman, R., Julien, J. P. and Fuchs, E. (1999). Integrators of the cytoskeleton that stabilize microtubules. *Cell* **98**, 229-38.

Yin, T., Getsios, S., Caldelari, R., Godsel, L. M., Kowalczyk, A. P., Muller, E. J. and Green, K. J. (2005). Mechanisms of plakoglobin-dependent adhesion: desmosome-specific functions in assembly and regulation by epidermal growth factor receptor. *J Biol Chem* **280**, 40355-63.

Yin, T. and Green, K. J. (2004). Regulation of desmosome assembly and adhesion. *Semin Cell Dev Biol* **15**, 665-77.

Yoon, M., Moir, R. D., Prahlad, V. and Goldman, R. D. (1998). Motile properties of vimentin intermediate filament networks in living cells. *J Cell Biol* **143**, 147-57.

Zaidel-Bar, R., Milo, R., Kam, Z. and Geiger, B. (2007). A paxillin tyrosine phosphorylation switch regulates the assembly and form of cell-matrix adhesions. *J Cell Sci* **120**, 137-48.

Zhang, T., Haws, P. and Wu, Q. (2004). Multiple variable first exons: a mechanism for cell- and tissue-specific gene regulation. *Genome Res* **14**, 79-89.

Zillikens, D. (1999). Acquired skin disease of hemidesmosomes. *J Dermatol Sci* **20**, 134-54.

CURRICULUM VITAE

Personal Data

Name:	Gernot Walko
Academic title:	Magister rerum naturalium
Address:	Rückertgasse 26/11, 1160 Vienna, Austria
Date of Birth:	26.05.1978
Place of Birth:	Linz, Oberösterreich
Marital status:	partnership
Citizenship:	Austria

Education

10/2003- 01/2007(planed)	Ph.D. studies of cell biology at the Department of Molecular Cell Biology, Max. F. Perutz Laboratories GmbH., Center of Molecular Biology, Campus Vienna Biocenter, University of Vienna, Dr. Bohrgasse 9, A-1030, Supervision by Univ.-Prof. Dr. Gerhard Wiche and Dr. Kerstin Andrä-Marobela, Doctoral thesis: *"Functions of plectin and its isoforms assessed in mouse stratified epithelia and keratinocyte cultures"*
26/06/2002	Graduation with excellence and attainment of masters degree in natural sciences
12/2001-06/2002	Master thesis at the Department of Molecular Cell Biology, Max. F. Perutz Laboratories GmbH., Center of Molecular Biology, Campus Vienna Biocenter, University of Vienna, Dr. Bohrgasse 9, A-1030, Supervision by Univ.-Prof. Dr. Gerhard Wiche and Dr. Kerstin Andrä-Marobela: "*Plectin 1a and 1c: cellular expression, subcellular localization and signaling functions"*

02/2000-06/2000	Educational stay (European Union "Sokrates" Program), at the Department of Molecular and Structural Biology, University of Aarhus, Denmark, Project work, *Nucleic Acids as Drugs Targets: Evaluation of the Effects of Ru- and Pt-Based Anticancer Drugs on the Translation through Interaction with UTRs of Wnt-5a mRNA,* Supervision by Prof. Just Justesen and Ph.D. Rune Hartmann
04/1999-06/2002	Master studies of biology, specialization in microbiology with subsidiary subject biochemistry at the former Faculty of Natural Sciences (now Faculty of Life Sciences), University of Vienna
10/1996-04/1999	Master studies of biology at the former Faculty of Natural Sciences (now Faculty of Life Sciences), University of Vienna
10/06/1996	School leaving examination (Matura)
10/1988-06/1996	Grammar school (Bundesgymnasium BG and BRG Völkermarkterring 27), Klagenfurt, Kärnten
10/1884-07/1988	Primary school, Klagenfurt, Kärnten

Teaching activities at the University of Vienna

2001-2007	Assignments as tutor for the biochemical courses for biologists, chemists and for the proseminar in cell biology
2003-2005	Assignments as course instructor for the biochemical courses for biologists and for chemists

Language skills

German (native), English (fluent), French (basic), Swedish (basic)

Software skills

Microsoft Office, Adobe Illustrator, Adobe Photoshop

Memberships

ÖGGGT (Austrian Association for Genetics and Genetic Engineering)
ÖGBM (Austrian Association for Biochemistry and Molecular Biology)

Publications

Ackerl R, **Walko G**, Fuchs P, Fischer I, Schmuth M, Wiche G.
Conditional targeting of plectin in prenatal and adult mouse stratified epithelia causes keratinocyte fragility and lesional epidermal barrier defects.
J Cell Sci. 2007 Jul 15;**120(Pt 14):**2435-43.

Osmanagic-Myers S, Gregor M, **Walko G**, Burgstaller G, Reipert S. Wiche G.
Plectin-controlled keratin cytoarchitecture affects MAP kinases involved in cellular stress response and migration.
J Cell Biol. 2006 Aug 14;**174(4**):557-68.

Hartmann R, **Walko G**, Justesen J.
Inhibition of 2'-5' oligoadenylate synthetase by divalent metal ions.
FEBS Lett. 2001 Oct 19;**507(1**):54-8.

APPENDIX

Manuscript copy 1

Conditional targeting of plectin in prenatal and adult mouse stratified epithelia causes keratinocyte fragility and lesional epidermal barrier defects

Reinhard Ackerl, **Gernot Walko**, Peter Fuchs, Irmgard Fischer, Matthias Schmuth and Gerhard Wiche.

The Journal of Cell Science, Vol. 120, 2435-2443

Manuscript copy 2

Plectin-controlled keratin cytoarchitecture affects MAP kinases involved in cellular stress respone and migration

Selma Osmanagic-Myers, Martin Gregor, **Gernot Walko**, Gerald Burgstaller, Siegfried Reipert, and Gerhard Wiche.

The Journal of Cell Biology, Vol. 174, 557–568